

Principles of Lightning Physics

Vladislav Mazur



Principles of Lightning Physics

Principles of Lightning Physics

Vladislav Mazur

National Severe Storms Laboratory, Norman, Oklahoma, USA



Courtesy of T A Warner

IOP Publishing, Bristol, UK

© IOP Publishing Ltd 2016

All rights reserved. No part of this publication may be reproduced, stored in a retrieval system or transmitted in any form or by any means, electronic, mechanical, photocopying, recording or otherwise, without the prior permission of the publisher, or as expressly permitted by law or under terms agreed with the appropriate rights organization. Multiple copying is permitted in accordance with the terms of licences issued by the Copyright Licensing Agency, the Copyright Clearance Centre and other reproduction rights organisations.

Permission to make use of IOP Publishing content other than as set out above may be sought at permissions@iop.org.

Vladislav Mazur has asserted his right to be identified as the author of this work in accordance with sections 77 and 78 of the Copyright, Designs and Patents Act 1988.

Video content is available from the book information online: <https://doi.org/10.1088/978-0-7503-1152-6>.

ISBN 978-0-7503-1152-6 (ebook)

ISBN 978-0-7503-1153-3 (print)

ISBN 978-0-7503-1154-0 (mobi)

DOI 10.1088/978-0-7503-1152-6

Version: 20161201

IOP Expanding Physics

ISSN 2053-2563 (online)

ISSN 2054-7315 (print)

British Library Cataloguing-in-Publication Data: A catalogue record for this book is available from the British Library.

Published by IOP Publishing, wholly owned by The Institute of Physics, London

IOP Publishing, Temple Circus, Temple Way, Bristol, BS1 6HG, UK

US Office: IOP Publishing, Inc., 190 North Independence Mall West, Suite 601, Philadelphia, PA 19106, USA

Cover image: Summer lightning storm near Tucson, Arizona, USA. Credit: Keith Kent/Science Photo Library

*To Marijo, my beloved wife,
without whose encouragement and support
this book would not have been possible*

Contents

Preface	xi
Acknowledgements	xiv
Author biography	xv
1 The components of lightning	1-1
1.1 Features of lightning plasma	1-1
1.2 Lightning is more than a spark	1-2
1.2.1 Corona glow	1-2
1.2.2 Corona streamers	1-3
1.2.3 Transition from corona streamers to a positive leader	1-5
1.2.4 Transition from corona streamers to a negative leader	1-6
1.3 Conditions for leader propagation	1-8
1.4 Lightning leaders in nature	1-12
References	1-15
2 Lightning leaders versus free-burning arcs	2-1
2.1 Similarities and differences	2-1
2.2 The $E-I$ relationship, from the results of laboratory measurements and the modeling of free-burning arcs	2-2
2.3 The $E-I$ relationship and the luminosity of leader channels	2-7
References	2-9
3 Physical concepts of a lightning leader model	3-1
3.1 The space charge leader concept based on cloud charge collection	3-1
3.2 The bi-directional, uncharged leader concept based on induced charges	3-3
3.3 Comparing the outputs of the two leader models	3-5
References	3-8
4 Verifying the concept of the bidirectional leader	4-1
4.1 How studying lightning strikes to aircraft has helped to solve the puzzle of lightning development	4-1
4.1.1 Lightning radar echo	4-2
4.2 How does an aircraft trigger lightning?	4-5

4.3	Environmental conditions that lead to aircraft-triggered lightning	4-9
4.3.1	Hypothesis of a natural lightning-triggering mechanism in thunderstorms	4-11
	References	4-13
5	Defining the types of lightning	5-1
5.1	The visible features of lightning flashes	5-1
5.2	Defining the types of lightning using the bidirectional, bipolar leader concept	5-7
5.2.1	Intra-cloud flashes	5-7
5.2.2	Cloud-to-ground flashes	5-11
	References	5-14
6	The electrostatic theory of lightning discharges	6-1
6.1	Cloud potential and induced charges of lightning	6-1
6.2	The relationship between the electric fields produced by leaders and return strokes	6-2
6.3	The relationship between lightning processes and space charges in thunderstorms	6-4
6.3.1	Thunderstorm model	6-4
6.3.2	Development of the cloud-to-ground leader	6-6
6.3.3	Return stroke	6-11
6.3.4	Electric field changes produced by CG flashes	6-12
6.3.5	Development of the intra-cloud leader	6-13
6.4	Applications and limitations of the electrostatic model	6-14
	References	6-17
7	Lightning triggered by rockets with wire and by tall structures	7-1
7.1	The idea of artificially triggered lightning	7-1
7.2	Concept and features of the classic rocket-triggered lightning technique	7-2
7.2.1	Processes related to melting of the trailing wire	7-3
7.3	Concept and features of the altitude-triggered lightning technique	7-6
7.4	Conditions required for triggering lightning with rocket-and-wire techniques	7-7
7.5	On leaders and return strokes in rocket-triggered lightning	7-8
7.6	Upward lightning triggered by tall ground structures	7-9
7.6.1	Conditions for upward lightning initiation	7-9

7.6.2	Understanding luminosity variations in the upward-lightning channel	7-12
7.7	Features of positive and negative leaders determined from studies of triggered lightning	7-15
	References	7-18
8	Understanding current cutoff in lightning	8-1
8.1	Definition and manifestation of current cutoff in different lightning events	8-1
8.2	The death of the leader in unbranched lightning channels	8-2
8.3	Current cutoff in branched leaders	8-3
8.3.1	The screening effect in single and branched channels	8-3
8.3.2	The role of branch-screening in current cutoff	8-4
8.4	Arc instability and current cutoff	8-8
	References	8-9
9	The phenomenon of recoil leaders	9-1
9.1	The nature of recoil and dart leaders	9-1
9.2	The relationship between recoil leaders and M-events: cause and effect	9-5
9.3	The electrostatic model of an M-event that produces an M-component	9-9
9.3.1	The electrostatic model of a dart leader–return stroke sequence in CG flashes	9-10
9.3.2	The electrostatic model of an M-event	9-12
9.4	The universal nature of M-events in lightning	9-14
	References	9-15
10	The physical concept of recoil leader formation	10-1
10.1	The relationship between the internal electric field and current in lightning leaders	10-1
10.2	Current cutoff prior to the occurrence of recoil leaders	10-2
10.3	The development of recoil leaders	10-3
10.4	A proposed conceptual model of recoil leader formation	10-5
10.4.1	Recoil leader formation and polarity asymmetry in branched leaders	10-8
10.5	Conclusion	10-10
	References	10-10

11 Some lightning protection issues viewed through the lens of lightning physics	11-1
11.1 Striking distance versus the parameters of downward leaders in lightning protection of ground installations	11-1
11.2 A physical model of leader interaction with a ground structure	11-4
11.3 On the hazardous effects of upward lightning to tall structures	11-8
11.4 Sharp-tipped versus blunt-tipped lightning rods	11-8
11.5 Lightning protection of aircraft	11-9
References	11-11
12 Lightning initiation—the most difficult issue of lightning physics	12-1
12.1 Hydrometeor theory of lightning initiation	12-1
12.2 The runaway theory of lightning initiation	12-4
12.3 Evidence supporting the hydrometeor theory of lightning initiation	12-5
References	12-8
Appendix	A-1

Preface

Lightning, for the average person, remains a puzzling mystery and, to some degree, this is also true for the scientists who study it. For a long time, researchers observed and described some of the physical characteristics of lightning as they were manifested in the behavior of its luminous channels and the changes in the electromagnetic field that lightning produces. However, these efforts were able to extract from this information only a few pieces of the giant jigsaw puzzle that we call the ‘lightning phenomenon’. The literature available on lightning has reflected almost exclusively this predominantly ‘descriptive’ approach to lightning studies, focusing either on individual, sometimes anomalous, lightning cases, or on comparing the various characteristics of lightning flashes that occur in different geographic regions.

The field of lightning research is a rather narrow one in comparison, for example, with that of meteorology. The lightning research community, similarly, is relatively small. The horizon of unexplored issues and unanswered questions, on the other hand, is still very broad—as are the possibilities of making some major discoveries. In my adopted country, the United States of America, and in several other countries, the past 30 years have proven to be among the most exciting and productive ever in the field of lightning studies. Aided by newly developed observational tools, significant progress has been made in our understanding of lightning’s essential processes. I have been fortunate to be an active participant in, and contributor to, many of the major advances achieved during this period. The search for the physical features common to all kinds of lightning discharges has been the strongest motivation in my long career as a lightning researcher. Most of my published papers, as well as those written together with my long-term collaborator, Dr Lothar H Ruhnke, have been devoted to uncovering the key physical processes that govern the different aspects of the lightning phenomenon.

Until now, there has been no book available in the literature on lightning that sought to present the newest discoveries in lightning research, based on valid physical concepts. A recent book on lightning by Rakov and Uman¹ serves as an excellent reference, presenting data obtained through the last three decades from the entire field of lightning research. However, that book does not include any of the newer physical concepts of lightning development. An advanced-level book written by two world-famous experts in the field of gas discharges in long gaps, Eduard Bazelyan and Yuri Raizer², is aimed at readers with strong physics backgrounds. Long-gap gas discharges and lightning leaders share a common feature: the streamer-leader process. This commonality has allowed the book by Bazelyan and Raizer to become a valuable contribution to the lightning literature.

¹ Rakov V A and Uman M A 2003 *Lightning: Physics and Effects* (Cambridge: Cambridge University Press)

² Bazelyan E M and Raizer Yu P 2000 *Lightning Physics and Lightning Protection* (Bristol: Institute of Physics Publishing)

Unfortunately, the ambiguities and fallacies in the interpretations of lightning processes that have held sway and been unchallenged throughout the past several decades have continued to mislead lightning researchers. Historically, most of the terminology found in the lightning literature was created with little consideration (and perhaps a poor understanding) of the physical nature of the events this terminology identified. A dramatic change occurred with the acceptance, finally, of the concept of the bidirectional, bipolar and uncharged leader, put forward since 1950 by the brilliant German physicist, Heinz-Wolfram Kasemir (1910–2007). This theory had been considered controversial, and ignored, for many years. As often happens in science and nature, however, the solutions to some difficult problems frequently turn out to be beautifully simple and elegant; this is the case with Kasemir's theory of the bidirectional and uncharged leader, as it is applied to lightning physics.

This book seeks to correct the glaring deficiency that exists in lightning research, specifically, the lack of an accessible presentation of the basic physics of lightning discharges, with a focus on leaders as the key components. The challenge for research scientists, as I see it, is to assemble the pieces of the lightning puzzle, so that not only do they fit, but they also produce a coherent picture of the features present in other manifestations of the lightning phenomenon. As a product of the electrical environment in thunderstorms, lightning processes are interpreted in this book, first and foremost, by using the laws of electrostatics. This approach works well for the development of the majority of lightning processes in intra-cloud and cloud-to-ground flashes, and is supported by a multitude of convincing observations and measurements. The exception is the mechanism of recoil-leader formation, which has been interpreted by using electrodynamics and an analogy to a free burning arc. In addition, the relevance of some of the results of lightning research to the practice of lightning protection is discussed in chapter 11.

With the recent advances in lightning physics, the need has become apparent for correct terminology to implement the interpretation of lightning processes. Accordingly, the terminology, used widely until just recently in the lightning literature, and still influenced by Schonland's outdated 1947 concept, has been corrected in this book to agree with Kasemir's concept.

Publications concerned with atmospheric electricity have typically been required to declare which of the two sign conventions is being used—that of ‘physics’ or ‘atmospheric electricity’—to represent the electric field. The difference between the two is that they assign opposite polarities to ground-based electric field measurements, a practice always confusing to the reader. At the 2014 International Conference on Atmospheric Electricity in Norman, Oklahoma, the lightning research community decided unanimously to standardize usage of the so-called ‘physics’ sign convention in the lightning literature. That convention is used in this book. When records from other, earlier publications made using the atmospheric electricity sign convention are included in the book, a comment will be added to the figure caption.

What is not in this book? In order to avoid redundancy with the literature that currently exists, this book does not present all the published data about lightning;

that information may be readily found in Uman³, and in Rakov and Uman¹. Neither does this book address the separate topic of thunder; for this, interested readers can refer to chapter 12 in Uman⁴, where this subject is well, and exhaustively, described. Nor does this book cover the topics of such high-energy atmospheric phenomena as blue jets, red sprites, etc, at high altitudes above thunderstorms, because these often appear subsequent to the occurrence of lightning in thunderstorms, not as part of it. These topics are thoroughly covered by Dwyer and Uman⁵. Furthermore, because my book is a monograph, presenting primarily my own research, rather than a reference book, I have been selective in referring to only those publications essential to the material I have intended to cover.

Although, admittedly, this book is somewhat specialized, one may find it useful as supplementary reading in a university course on atmospheric electricity and lightning. It is intended to introduce lightning physics to readers of different backgrounds, levels of experience, and knowledge, including graduate students, lightning enthusiasts, and researchers in the field of atmospheric electricity.

³ Uman M A 1987 *The Lightning Discharge* (New York: Academic)

⁴ Uman M A 1986 *All About Lightning* (New York: Dover)

⁵ Dwyer J R and Uman M A 2014 The physics of lightning *Phys. Rep.* **534** 147–241

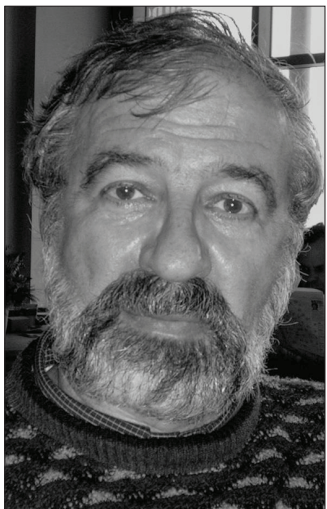
Acknowledgements

Writing this book has been an enormous undertaking for which I have received great support and encouragement from the National Severe Storms Laboratory in Norman, Oklahoma, and its Director, Dr Steve Koch, who have made the writing of this book possible. I would also like to acknowledge the many helpful colleagues, too numerous to mention, from the lightning research community who have graciously contributed their results to this book. Many thanks to T A Warner for his generous permission to use his exceptional video images of lightning events for this book. I am also extremely grateful for the more than 25 years of friendship and scientific collaboration with Dr Lothar H Ruhnke.

Finally, special gratitude goes to my dear wife, Marijo Hennagin-Mazur, the best editor anyone could hope for, who has spent countless hours tirelessly improving this manuscript.

Author biography

Vladislav Mazur



Vladislav Mazur was born in 1941 in Leningrad (now St Petersburg), Russia, in the former USSR, during the Second World War. His higher education includes an MS degree in Mechanical Engineering from the Leningrad Shipbuilding Institute in 1964, and an MS degree in Electrical Engineering from the Leningrad Institute of Precise Mechanics and Optics in 1967.

Dr Mazur began his career as a lightning researcher in 1969, in the Department of Experimental Atmospheric Physics at the Leningrad Hydrometeorological Institute, where he joined a very small group of enthusiasts who intended to study lightning features using long-wave radars. He later entered the PhD program in Geophysics at the same institute. By 1977, Dr Mazur had completed his dissertation on the subject of lightning studies using long-wave radars, but was not allowed to defend it because of his plans to emigrate from the USSR.

In 1978 Dr Mazur immigrated to the United States. In the same year, he began his long association with the Storm Electricity Group at the National Severe Storms Laboratory (NSSL) in Norman, Oklahoma, and worked as a Graduate Research Assistant at the University of Oklahoma. He received his PhD from the University of Oklahoma, this time in Electrical Engineering, in 1981.

From 1981 until 1984 he was a Fellow at the Cooperative Institute for Mesoscale Meteorological Studies (CIMMS) at the University of Oklahoma. In 1984 he joined the permanent staff at NSSL, where he still works. The experience and knowledge that Dr Mazur had gained from studying lightning with radars led to his participation in the NASA Storm Hazards Program (1982–6). This program was investigating lightning interaction with aircraft. The use of UHF radar for guiding the NASA research aircraft into thunderstorms was an approach that proved to be extremely successful in achieving the program's objectives. During the 1980s, with the goal of confirming the conclusions obtained in the NASA program, Dr Mazur also collaborated closely with two other programs that were studying lightning-aircraft interaction: the US Air Force/FAA Lightning Characterization Program (1985–7) and the ONERA Transall Program in France (1988–9). He then extended his efforts and interest into the interpretation of the records of the numerous sensors on board the research aircraft, in an attempt to understand the physical mechanism of the aircraft-triggered lightning.

In 1988, recognizing the essential role Dr Mazur had played in the research programs that addressed lightning–aircraft interaction, he was awarded the coveted US Department of Commerce Gold Medal.

Understanding the processes involved in lightning initiation on a flying aircraft provided a key to the interpretation of other features of lightning, which has become the central focus of Dr Mazur’s research efforts from the 1980s onward. His scientific collaboration with Dr Lothar H Ruhnke, a talented physicist and experimenter, which began in the late 1980s and continued for the next 25 years, resulted in some groundbreaking discoveries, as well as the confirmation of a fundamental, but controversial theory of lightning development—the concept of the bidirectional, bipolar leader advanced by Heinz-Wolfram Kasemir. This theory is now accepted as the starting point for a full understanding of the phenomenon of lightning. During the past 30 years, Dr Mazur has promoted and applied this concept in his research, revising and changing outdated dogmas, and building a new foundation for lightning physics.

Dr Mazur has applied his expertise in lightning physics to assist with lightning protection for the National Weather Service’s (NWS) weather-radar network, and the Federal Aviation Administration (FAA) radar installations and air traffic control towers at several major airports in the United States.

Dr Mazur lives in Norman, Oklahoma with his wife of 33 years, Marijo, and his two beloved collies.

Principles of Lightning Physics

Vladislav Mazur

Chapter 1

The components of lightning

1.1 Features of lightning plasma

Plasma is an ionized gas composed of a mixture of free electrons, positive ions, and neutral atoms or molecules. *Ionization* is the process by which the separation of electrons from atoms occurs through the application of certain external forces, which transforms the atoms into ions and frees electrons. Literally the production of ions (and, thus, free electrons), ionization can be achieved through two very common processes: heat (thermal ionization) and electric field (electrical ionization). Electrical breakdown ‘is commonly understood as an act of fast formation of a strong ionized state under the action of applied electric or electromagnetic field’ (Bazelyan and Raizer 1998, p 12). The visible result of a gas electrical breakdown is a *spark*, with the stage of its plasma similar to arc plasma. In addition to sparks, other examples of plasma produced by electrical ionization are neon and fluorescent lights, and welding arcs, among others.

The presence of free electrons in plasma makes the plasma capable of carrying *electric current*, which is the directed motion of charged particles (electrons and ions) under the force of an electric field. The collisions between electrons and ions produce heat; the heating of the plasma produces additional *thermal ionization*, which also makes the plasma luminous and visible.

In lightning channels that carry an electric current of more than several tens of amperes, the number of free electrons per unit of volume, called *plasma density*, can reach 10^{19} electrons or higher, per cubic meter. A density of this value is high enough to *backscatter*, i.e. reflect, the electromagnetic waves of a radar beam from a lightning channel, as if the channel were made of metal. In principle, this is what makes lightning ‘visible’ by radar. Very high frequency (VHF, 30 to 300 MHz, wavelength 10 to 1 m), ultra high frequency (UHF, 300 MHz to 3 GHz, wavelength 1 m to 1 dm), and L-band (1 to 2 GHz, wavelength 30 to 15 cm) radars were used in the 1970s and 1980s as tools for studying various aspects of lightning and lightning’s relationship to storm structures (e.g. Mazur and Rust 1983, Williams *et al* 1990).

UHF radar also played a pivotal role in the investigations into the nature of lightning-aircraft interactions. The results of these studies profoundly affected our understanding of the physical processes involved in lightning development (Mazur 1989). More about this topic can be found in chapter 4.

Other manifestations of the lightning process, such as *luminosity, acoustic waves* (thunder), and *electric and magnetic fields* are all the results of the flow of electric current through a lightning-plasma channel.

1.2 Lightning is more than a spark

Both in the lightning literature and in various other media, lightning is often referred to as a spark discharge, e.g. quoting from Bazelyan and Raizer (1998): ‘Lightning is, in itself, a tremendous spark discharge’ and ‘Lightning is justly believed to be the longest spark discharge observable’. An electrical discharge in the air, lightning shares many common features with spark discharges produced in a gap in a high-voltage laboratory. There, electrical breakdown is achieved by applying high voltage in a gap (of up to several meters) between two electrodes, usually one pointed and one flat. There are, however, significant differences between what happens in nature as a lightning discharge, and what we can reproduce in a laboratory as a long spark in a gap between electrodes. First of all, there are no electrodes in a thunderstorm where intra-cloud (IC) and cloud-to-ground (CG) lightning initiates, so lightning is an electrodeless discharge. Second, there is at least a three-orders-of-magnitude difference in the dimensions of these two phenomena: meters, in the case of long sparks, versus kilometers, in the case of lightning. Third, there are differences between the environmental and electrical conditions of a thunderstorm and those found in a laboratory. It would be extremely complicated, as well as prohibitively expensive, to reproduce inside a high-voltage chamber the humidity, temperature, pressure, and precipitation particles that characterize thunderstorms.

These differences, however, should not dissuade us from pursuing laboratory studies that use long sparks as surrogates for lightning. Such studies provide us with the only means currently available to look closely into the micro-processes that occur during lightning formation, so that we may model them. An entire branch of physics, called the physics of gas discharges, is based on refined experiments in high-voltage chambers. From the studies of long sparks we may derive a truer understanding, based on sound physics, of many of the features of lightning.

1.2.1 Corona glow

In the laboratory, electrical discharges start from a pointed electrode of one polarity connected to a high-voltage generator; the electrode of the opposite polarity is usually a flat, grounded plate. There are two possible scenarios for the development of a discharge, depending upon the speed with which the high voltage is applied to the electrode.

In the first scenario, a discharge occurs when the voltage to the pointed electrode is applied slowly, when the electric field near the tip of the electrode exceeds the electrical breakdown threshold (3 MV m^{-1} in normal atmospheric conditions), and when a small area near the tip becomes ionized, producing a glowing cone that fans

out. This type of discharge is called a *corona discharge*. When a pointed electrode is of positive polarity (in the case of a positive corona) the electrons in the corona current move toward the electrode, while the positive ions remaining near the electrode tip constitute a positive *space charge*. When the pointed electrode is of negative polarity, the current of the negative corona is ionic, and electrons attach to neutral molecules, forming the negative ions of the space charge. The corona current in the corona is weak (usually measured in microamperes), which causes the plasma to be cold and barely luminous. Both the corona current and corona glow may last for several seconds. It should be noted here that a corona discharge of this type bears no resemblance to a spark.

The presence of the space charge diminishes ("chokes off") the electric field near the tip of the electrode, which causes the electric field there to fall below the breakdown value, and the corona current to stop. If the space charge is moved away from the electrode, however, (by wind, or by moving the electrode, as examples) and the electric field is still present, the corona reappears.

Corona discharges are very common phenomena during thunderstorms. They emanate from objects with pointed shapes, such as branches of trees, or even blades of grass, because the electric field's magnitude is greatly enhanced by any sharp edge, or point, in a structure. In fact, most of the ground vegetation affected by the strong electric field under a thunderstorm produces coronas, but they usually remain invisible due to their low luminosity. Space charges from ground vegetation create a charge layer above the ground that may be as thick as a few hundred meters. This charge layer significantly diminishes the ambient electric field near the ground.

Apart from coronas from ground vegetation, there is another example of coronas that many of us have observed: sometimes, from an aircraft window while flying at night, we may see a blue corona glowing at the tip of the wings. Multiple short rods, not thicker than a pencil, with little brushes at the tip are installed at the edges of the wings of commercial airliners, and serve as *corona dischargers*. The aircraft in flight is electrically charged as a result of the friction of its metallic skin against the cloud and precipitation particles (the *triboelectric effect*). The electrically charged body of a flying aircraft produces an electric field. When this electric field is magnified at the sharp extremities of the aircraft (e.g. at the tip, or at an edge of the wing), and the field reaches the threshold value, a corona starts there. Excessive charges on the aircraft 'leak out' through the wing-tip corona dischargers, in the form of corona current. Because of the aircraft's forward motion, the space charges near the wing-tips are constantly left behind, so they cannot choke off the electric field near the dischargers. The aircraft's movement away from the space charges allows the corona current to continually reduce the electrical charges accumulating on the aircraft, until the electric field near the corona dischargers falls below the threshold value.

1.2.2 Corona streamers

In the second scenario, where high voltage is applied very quickly in the form of a voltage impulse, a different type of corona discharge occurs. Rather than a corona glow, a thin corona filament emerges from the electrode for a fraction of a millisecond and then disappears; this filament is a spark known as a *corona streamer*.

Two features of multiple corona streamers are (1) that they have a common stem at a high-voltage electrode, and (2) that they are not continuous, either in space or time. A corona streamer is usually much longer than the length of a corona-glow cone. It may be as long as several meters, but it is still made up of cold plasma of low conductivity, and carries a small current, which is measured in microamperes. In long sparks in a high-voltage laboratory, ‘depending on the voltage, streamers can cross a larger or a smaller portion of the gap space, or reach the opposite electrode, but they never cause a gap breakdown because of low conductivity’ (Bazelyan and Raizer 1998).

The higher the amplitude of the high-voltage pulse, the greater the number of corona streamers, all attached to the tip of the electrode. Streamers increase in number so much (by hundreds and thousands) that they create a densely packed, fan-shaped *corona region* ahead of the electrode. As in the case of a corona glow, the corona-streamer region contains a space charge of the same polarity as the starting electrode. An example of the corona region is shown in figure 1.1, and also in figure 1.2, at time t_1 .

It has been established experimentally that the extent of corona streamer development, i.e. its length, is determined by a critical value of the electric field ahead of it, E_{cr} , which is the lowest electric field necessary to support streamer propagation (Bazelyan and Raizer 2000). The values of E_{cr} are $\sim 450\text{--}500 \text{ kV m}^{-1}$ for positive, and $\sim 750\text{--}1000 \text{ kV m}^{-1}$ for negative corona streamers.

We may experience a corona streamer ourselves if we walk on a carpeted floor in a heated room during the winter, wearing shoes with leather soles. Through the friction between the carpet and our shoes, we are charging our bodies to a voltage of

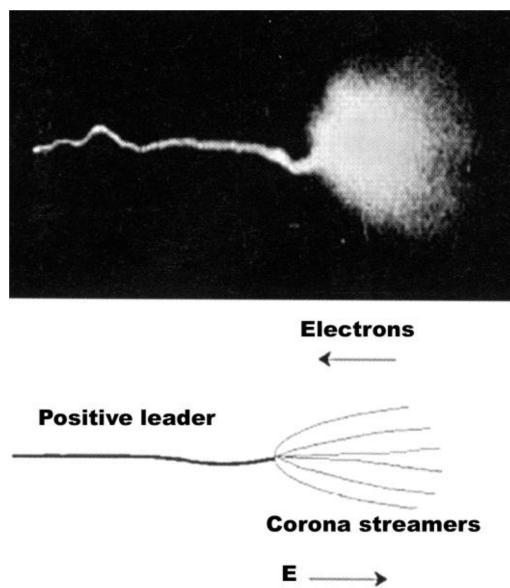


Figure 1.1. Region of corona streamers (right) and positive leader (left), started from a pointed electrode in a high-voltage chamber. Reprinted with permission from Gallimberti *et al* (2002). Copyright 2002 Elsevier Masson SAS. All rights reserved.

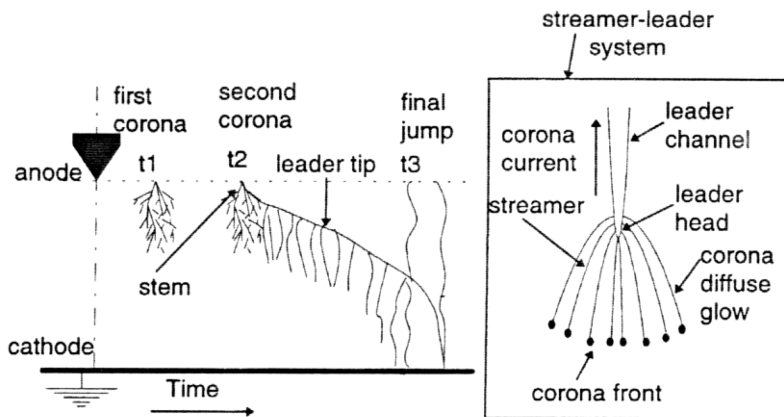


Figure 1.2. Development of a positive leader from a pointed electrode. t_1 = inception of first coronas; t_2 = occurrence of second coronas, formation of stem, and starting of leader; t_3 = attachment to cathode and final jump up to anode. Note the continuous path of the leader toward the cathode. Reprinted with permission from Goelani *et al* (1997). Copyright 1997 IOP Publishing.

tens of kilovolts (the same triboelectric effect as that which takes place on an aircraft flying through clouds). Then, at the instant we touch a metal doorknob with our hand we may experience a spark between our fingers and the knob. This spark is a corona streamer. Another example of a corona streamer in nature is known as *St Elmo's fire*, which emanates from sharp or pointed objects on tall ships during thunderstorms.

The leader process is the next phase of corona-streamer transformation that follows an increasing voltage applied to an electrode. This process occurs differently for voltages of both polarities; therefore, it is described separately in the sections that follow.

1.2.3 Transition from corona streamers to a positive leader

As the voltage on the pointed electrode of positive polarity (*anode*) increases, the appearance of numerous corona streamers there will be followed by the birth of a short, thin, hot plasma stem called a *leader*, attached to the electrode's tip (figure 1.2). This transformation from multiple streamers to a leader is called the *streamer-leader transition*. The transition occurs as follows. Thousands of corona streamers originating from, and focused in, the small area near the tip (the coronas' common root) heat the area (by their combined currents) to a very high temperature, of 5000–6000 K. The intensity of this heat turns the air into hot plasma at time t_2 (figure 1.2). The entire process is analogous to focusing the rays of the Sun onto a small spot with a magnifying glass and heating this spot to a temperature sufficient to ignite a fire. The pause between the first and second corona is a result of the 'choking' effect of the space charge of the first corona on the external electric field.

The newly created hot plasma at the electrode tip serves as a highly conductive addition to the metallic electrode, and becomes a portion of the leader. Formation of

the positive leader is a continuous process of elongation that ends with the leader's attachment to the opposite electrode (*cathode*) and a final jump between electrodes, also called a *flash-over*. The repeated bursts of corona streamers originating from the leader tip, seen in figure 1.2, occur during the entire duration of leader development, from time t_2 to t_3 .

1.2.4 Transition from corona streamers to a negative leader

The sequential stages of the streamer-leader transition near the tip of the negative electrode are very different from and more complicated than those for the positive electrode. The dynamics of negative-leader formation from a pointed electrode are depicted in figure 1.3.

The first burst of negative corona streamers (marked CN) starts at time t_i . However, the streamer-leader transition begins at time t_1 , not at the tip of the electrode, but *at an inception point ahead of the electrode*, and at a distance from the electrode equal to the length of the first corona streamers that precede them, at time t_i . The initial stage of the transition is an electrodeless discharge made up of corona streamers of opposite polarity: the positive one pointing toward the high-voltage electrode (marked CP), and the negative one pointing toward the ground plate (marked CN). Consecutive cycles of these bipolar and bidirectional coronas, also called a 'pilot system' (marked PL), begin at time t_1 and continue at times t_1' and t_1'' , with relaxation processes separating them, each time developing from the tip of the preceding PL system. A negative main leader (LN) emerges from the negative electrode, at time t_2 . Very shortly, with the number of corona streamers of both polarities in the pilot system drastically increasing, and (as a result) causing temperatures at the starting point of the pilot system to rise above 1500 K, a small blob of hot plasma (a *stem*) starts to form at the focal point of the bipolar corona streamers of the pilot system, at time t_3 (figure 1.4).

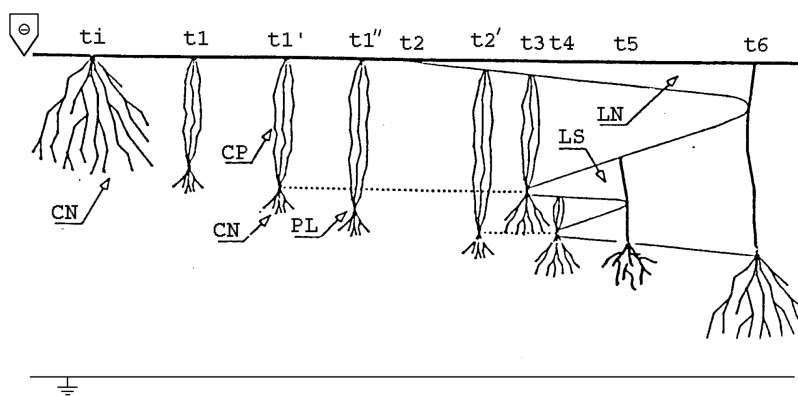


Figure 1.3. Simplified scheme of inter-step processes in a negative stepped leader starting from a pointed negative electrode (cathode), reflecting experimental observations in a high-voltage laboratory. CN = negative corona streamers; CP = positive corona streamers; PL = pilot system; LS = space leader; LN = negative leader. Reprinted from Bacchigia *et al* (1994).

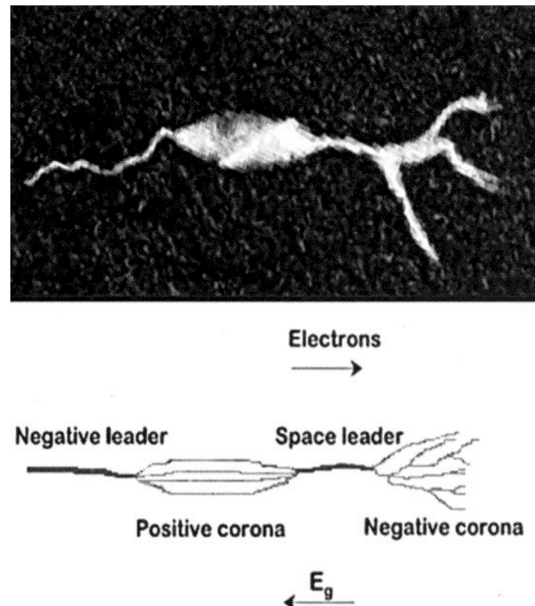


Figure 1.4. Corona streamers, a space leader, and a negative leader from a pointed electrode in a high-voltage chamber. Reprinted with permission from Gallimberti *et al* (2002). Copyright 2002 Elsevier Masson SAS. All rights reserved.

The space leader LS—an electrodeless discharge—develops from the plasma stem by extending bidirectionally (towards, and away from, the electrode) in a continuous fashion, at times t_3 and t_4 . The speed of the space leader LS moving towards the negative electrode is twice that of the one moving away from it (Bacchigia *et al* 1994). On a ‘collision course’, the continuous growth of the space and main leaders ends with their junction, at time t_6 . It is important to state here that the potential of the space leader is different from that of the high-voltage electrode, which causes their mismatched voltages, brought together as a short circuit, to create an arc-type spark at the moment of junction. The bright illumination of the whole channel by a strong current pulse is perceived visually as an instant elongation, and as a discrete *step* forward of the main-leader channel. The image in figure 1.4, of a negative leader in a high-voltage laboratory, depicts all the elements of the negative leader at this phase. The process described, of negative leader formation, repeats itself from the tip of the extended leader at time t_6 as another step before reaching the grounded electrode, when the flash-over occurs in the gap.

This step-like development of a negative leader is very different from the continuous development of a positive leader. The luminous steps, typically one microsecond each in duration, are separated by periods of 10–20 μs , during which the new cycles of development of the bipolar coronas and space leader take place. The strong current pulses that accompany the steps in a negative-leader progression are sources of powerful radiation, especially in VHF–UHF bands. Positive leaders, on the other hand, do not produce particularly noticeable radiation signals. More about positive leaders can be found in chapter 6.

The streamer-leader transition is what creates the leader. This mechanism is equivalent to a plasma-making machine, which, by converting the energy of the ambient electric field into leader current, leaves a trail of hot plasma behind it. By the continuous elongation of this plasma channel through the streamer-leader transition, the leader becomes a *propagating discharge*.

1.3 Conditions for leader propagation

The two stages of negative-leader development leading to formation of the bidirectional corona streamers of the pilot system (depicted at times t_i and t_1 , in figure 1.3) may be better understood by using the results of both the theoretical modeling of negative leaders and those of laboratory measurements in experiments on long sparks (Le Rénardières Group 1981, Bacchiega *et al* 1994, Bondiou and Gallimberti 1994). These results are presented in graphic form in figure 1.5, showing a plot of the potential profile changes that take place during these two stages.

The streamer-leader transition of a negative leader begins with corona streamers that emanate from the tip of the cathode, when the electric field there exceeds the breakdown value ($>3.0 \text{ MV m}^{-1}$ at normal atmospheric pressure). The region of corona streamers contains a net negative charge that fans out from the tip of the negative leader. As mentioned in section 1.2.2, the critical value of the electric field ahead of the leader needed to support propagation of negative corona streamers is $\sim 750 \text{ kV m}^{-1}$. Because of the low conductivity of very thin corona streamers, they do not disturb the surrounding electric field, and approximately the same electric

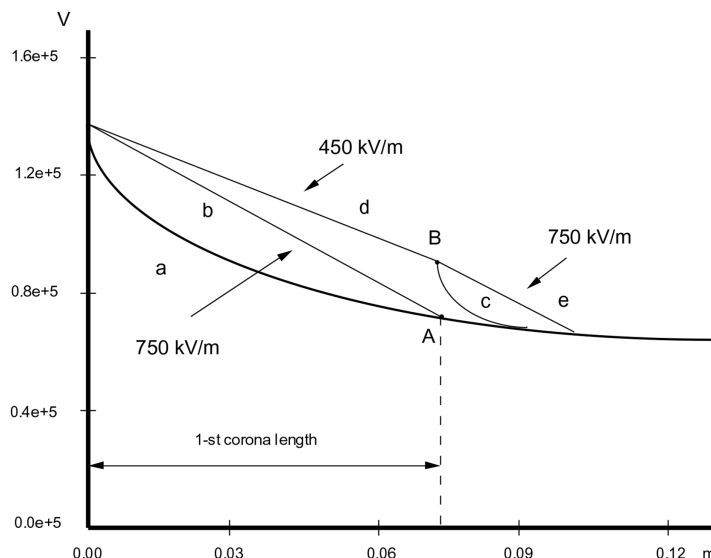


Figure 1.5. Potential profile ahead of the negative leader tip at different stages of the corona process. *a* = prior to development of first corona streamers; *b* = first negative-corona region with an internal field of 750 kV m^{-1} and extending to point *A*; *c* and *d* = during the relaxation process. The bidirectional ‘pilot’ forms at point *B*, with a linear potential drop of 750 kV m^{-1} (line *e*), and of 450 kV m^{-1} (line *d*), corresponding to the negative and positive corona streamers, respectively. Reprinted from Bacchiega *et al* (1994).

field value is maintained both inside and outside the established corona region. Therefore, the shape of the ambient potential profile ahead of the leader (line *a*), and the line of the potential drop for the constant electric field of 750 kV m^{-1} maintained inside the established corona region (line *b*), are the two factors that affect the length of the negative streamers. This length is the distance to point A, in figure 1.5, which is the point of intersection of lines *a* and *b*, corresponding to the front edge of the corona-region boundary.

During the pause that occurs after the appearance of the first corona streamers, the space charges begin to redistribute themselves in a *relaxation process* that takes place according to the conductivity and the dielectric constant within the corona region. A small current also flows from the leader tip into the corona region because of the low conductivity and electric field that exist there. The outcome of this relaxation process is an increasing potential at the front edge of the corona boundary, from point A upward to point B. This change causes (1) the potential gradient beyond the end of the corona region, i.e. from point B forward (line *e*), to increase and to reach a renewed breakdown condition (750 kV m^{-1}) for the negative corona streamers, and (2) the potential gradient behind point B (from line *b* to line *d*) to decrease to a breakdown condition for the positive corona streamers (450 kV m^{-1}), which would develop from point B backwards, towards the negative electrode. The change described, in the potential gradient near point B, leads to the occurrence of the pilot system ahead of the negative leader.

The relationship between the external electrical conditions and the characteristics of leader channels has been studied in the laboratory. The findings of these studies have been applied, in Lalande *et al* (2002), to the simplified electrostatic modeling of a non-time-dependent extension of a straight-leader channel in a constant ambient electric field. The model does not depend on the mechanism of leader initiation and, thus, may be applied to a straight leader of any polarity.

The following is a list of the variables that describe the electrical conditions governing the development of a leader (some of these variables are a function of altitude, *z*):

- $\Phi_{\text{atm}}(z)$ —ambient potential, assumed to be distributed linearly;
- $\Phi_{\text{extr}}(z)$ —potential at the leader tip;
- $\Phi_{\text{ce}}(z)$ —potential produced by a space charge of corona streamers;
- $\Delta\Phi_T$ —potential difference ahead of the tip of the leader, also called ‘potential drop’;
- E_0 —ambient electric field, constant when the potential distribution is linear;
- E_{int} —internal electric field in the leader channel, due to its finite resistance;
- E_{cr} —electric field inside the streamer zone, assumed to be 450 kV m^{-1} and 750 kV m^{-1} , for positive and negative leaders, respectively;
- q_{ce} —space charge per unit length, generated by the streamer-leader transition (C m^{-1}).

The variables for the physical dimensions of the leader are as follows:

- H —height of the structure, from which the leader is initiated;
- L —length of the developing leader;

- L_c —length of the streamer zone ahead of the leader;
- a_{ce} —radius of the space-charge envelope surrounding the leader.

Electrical discharges are sensitive to air-density variation, such as that which is described by Paschen's law of the relationship between breakdown voltage, gas pressure, and gap length. Therefore, for lightning leaders, the ambient field $E_0(z)$ must be corrected by the factor $1/\rho(z)$, in order to take into account the air-density variation with altitude.

The variables that describe the atmospheric conditions along the leader's path, and those that change with altitude, z , are:

- $P(z)$ —ambient pressure;
- $T(z)$ —ambient temperature;
- $\rho(z)$ —air density, calculated using the following expression: $\rho(z) = [P(z)T_0]/[P_0T(z)]$ (P_0 is the atmospheric pressure at ground level, and $T_0 = 300$ K is the normal temperature at ground level).

Figure 1.6, which depicts Lalande's model, has two parts: the upper part shows the leader structure with a space-charge envelope made by corona streamers; the lower part shows the potential distribution ahead of, and along, the leader path.

The structure from which the leader initiates is assumed to be a perfect conductor and, thus, is on zero ground potential. The magenta line indicates the potential

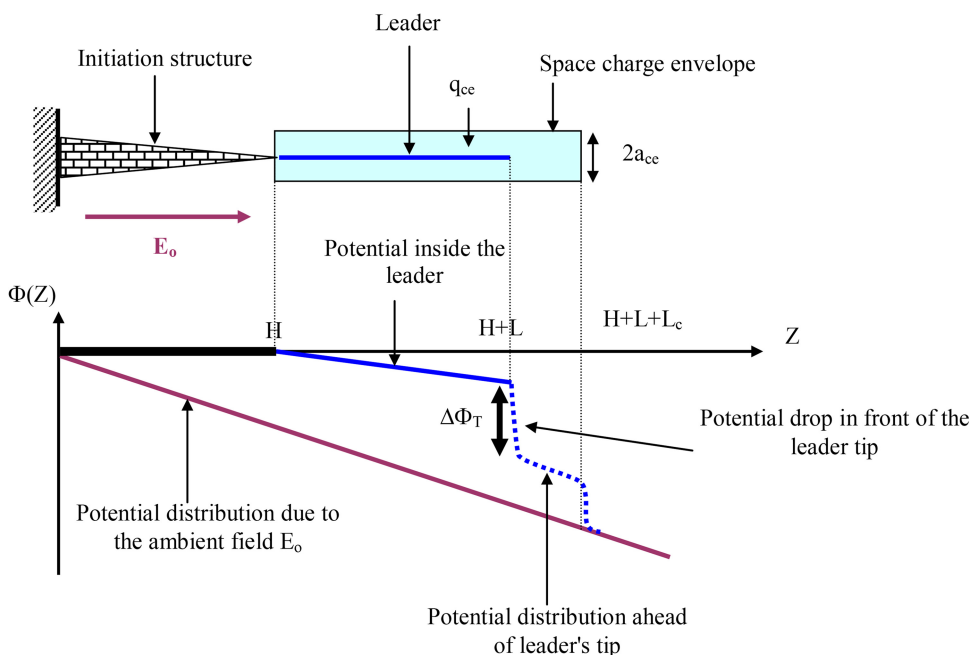


Figure 1.6. Longitudinal potential distribution along the path of an upward positive leader developing from a tall ground structure. Reprinted with permission from Lalande *et al* (2002). Copyright 2002 Elsevier Masson SAS. All rights reserved.

distribution from the ambient electric field E_0 . The resistance of the conductive leader channel explains the line of the potential drop along the channel from the internal field E_{int} , which is assumed to be constant. Because the conductive leader channel possesses electrical capacitance, it carries electrical charges that are distributed along the channel.

During the leader's development, its thin, hot, highly conductive channel penetrates the volume occupied by the corona streamers ahead of the leader tip. This happens because the speed of the leader's propagation (in the range of 10^4 – 10^6 m s $^{-1}$) is much faster than the speed of the space charge's dissipation. Thus, the leader channel becomes surrounded by space charges in a form assumed in the model to be a cylindrically shaped corona envelope. The space charges are considered to be stationary, and remain so much longer than the lifetime of the lightning flash.

The dotted-blue curve in figure 1.6 indicates the potential distribution from the leader tip to the outer boundary of the space-charge region. It appears from the shape of this distribution that, by reducing the potential drop at the leader tip to the value of $\Delta\Phi_T$, the space-charge region ahead of the leader negatively affects the longitudinal propagation of the leader. The potential difference available to sustain leader propagation is the potential drop $\Delta\Phi_T$ at the leader tip, defined by equations (1.1)–(1.4):

$$\Delta\Phi_T = \Phi_{\text{extr}}(H + L) - [\Phi_{\text{atm}}(H + L) + \Phi_{\text{ce}}(H + L)], \quad (1.1)$$

where

$$\Phi_{\text{atm}}(H + L) = -E_0(H + L) \quad (1.2)$$

$$\Phi_{\text{extr}}(H + L) = -E_{\text{int}}L. \quad (1.3)$$

In this simplified model, the space charge is in the form of a cylinder with a radius of a_{ce} , and a length of $L + L_c$, with a uniform charge of linear density q_{ce} . The potential caused by the space charge, Φ_{ce} , was derived from laboratory measurements for the space-charge envelope of the radius, a_{ce} , of 0.5 m (Lalande *et al* 2002).

Equation (1.1), for the potential drop $\Delta\Phi_T$, may be presented in a form that separates contributions to it from the ambient electric field E_0 , the internal field of the leader E_{int} , and the space charge from the corona envelope, Φ_{ce} :

$$\Delta\Phi_T = E_0H + (E_0 - E_{\text{int}})L - \Phi_{\text{ce}}. \quad (1.4)$$

In order for the leader to propagate, the potential drop $\Delta\Phi_T$ should be positive and above a certain critical value that varies, based on environmental conditions. This requirement can be achieved only if the internal electric field E_{int} is significantly less than the ambient field E_0 .

The corona-streamer length, L_c , is inferred in equation (1.5) from the potential drop, $\Delta\Phi_T$, and the critical field, E_{cr} , which is needed for streamer propagation, and which is maintained inside the corona streamer zone:

$$L_c = \Delta\Phi_T/E_{\text{cr}}. \quad (1.5)$$

1.4 Lightning leaders in nature

After learning about the properties of leaders through experiments in a high-voltage laboratory, a legitimate question arises: how applicable is this knowledge to natural leaders in lightning? Bazelyan and Raizer (2000) concluded that the experimental data obtained in studies of sparks may be ‘extended to lightning only qualitatively’. Only through observations of natural-leader progression at close range, using a high-speed video system, are we able to confirm the qualitative similarities between long sparks and lightning leaders, as well as to register the quantitative differences between them. These differences are obvious: they reside in the dimensions and magnitudes of their electrical characteristics (potential, charges, and currents).

Traditionally, natural leaders are identified first by their polarity, i.e. by the charge they carry, in the same way as leaders in long laboratory sparks. The polarity of natural leaders is recognizable by the signatures of their electric-field changes (in the physics sign convention) as they approach an electric-field sensor; a positive or negative change corresponds to a positive or negative leader, respectively.

The confirmation that lightning flashes that originate in thunderstorms are always bidirectional and bipolar leaders (Mazur 1989; see also chapter 3) brought into question their proper nomenclature. Because the bidirectional, bipolar leader is made of two parts—one carrying negative and another carrying positive charges—it would be appropriate to name these parts from now on as *positively and negatively charged leaders*. As in long sparks, positively charged leaders in natural lightning have a conically shaped corona-streamer region ahead of the leader’s tip (figure 1.7) and, in the cases of unbranched leaders, the same continuing path of leader progression as seen in figure 1.8.

Also, leaders are visually identified by the types of leader-propagation paths: stepped and continuous. *Stepping* is a feature characterized by a discontinuity in the direction of propagation, and by impulse-like changes (produced by stepping) in current, luminosity, and electric- and magnetic-field records. Stepping is an attribute of negatively charged leaders in nature. Positively charged leaders generally propagate continuously, and have a slowly varying current and luminosity.

Recently obtained high-speed video observations of natural negatively charged stepped leaders reveal a complex filamentary structure of corona streamers at the

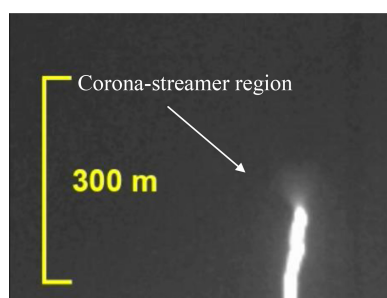


Figure 1.7. An image of the tip of an unbranched upward positively charged leader, with a conically shaped corona-streamer region ahead of it. Courtesy of T A Warner.



Figure 1.8. Development of a downward positively charged leader of a positive CG flash at a distance of 3.4 km from the observation site, recorded at the speed of 9000 fps. The return-stroke current is ~ 180 kA. The length of the corona-streamer region ahead of the leader is ~ 100 m. Reproduced from Petersen and Beasley (2013). Copyright 2013 by John Wiley & Sons, Inc. Reprinted by permission of John Wiley & Sons, Inc.

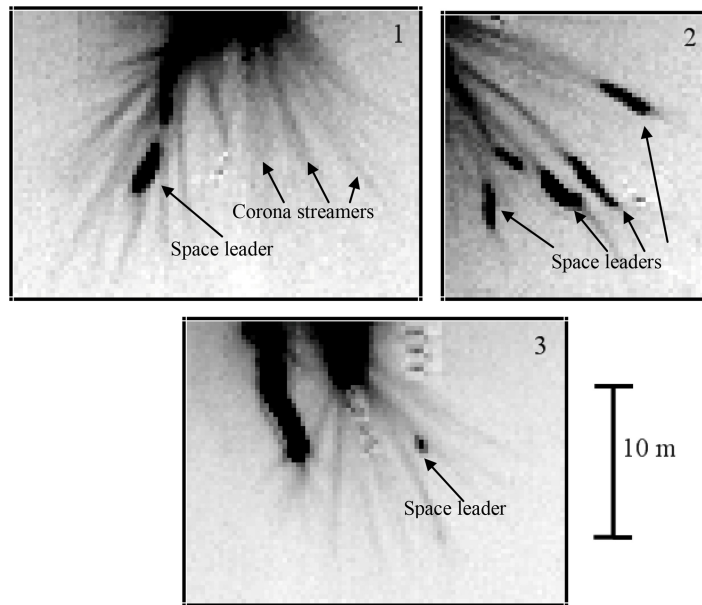


Figure 1.9. Inverted (negative) images of the tips of downward stepped leaders of a negative CG flash, showing the different stages in step formation ahead of the main leader made of corona streamers and space leaders. Reproduced from Petersen and Beasley (2013). Copyright 2013 by John Wiley & Sons, Inc. Reprinted by permission of John Wiley & Sons, Inc.

leader tip, with multiple, embedded space leaders; this makes them different from long sparks (see figure 1.9). An analysis of the video records shows that a leader step occurs when one of several existing space leaders reaches the tip of the main leader.

Branching occurs only in natural leaders, and cannot be replicated in long sparks in a high-voltage laboratory. With the use of high-speed video observations, it has

been determined that branching starts from the tip of the leader as the ‘splitting’ of a single channel into two branches, or as the appearance of a new branch from the side of the main leader, following the usual sequence of step formation (e.g. figure 1.10, the area marked *b*).

Another apparent similarity between leaders in a laboratory and in natural lightning is the final jump, which occurs when a laboratory-produced leader reaches the opposite electrode. This final jump is similar to a *return stroke* in a natural CG lightning flash upon contact with the ground, and is also called a *return stroke of a long spark* (Bazelyan and Raizer 1998).

In spite of the many qualitative similarities between long sparks and natural leaders, there are certain types of lightning leaders that simply cannot be replicated in a high-voltage chamber; these are known as *recoil* and *dart leaders*. Both propagate along the previously established paths of positive leaders. Close-up images of a dart-leader tip obtained with a high-speed video system (figure 1.11) show that, ahead of the leader (zone *a*), there is a low-luminosity zone (*b*), and an even weaker luminosity zone (*c*) ahead of that. See chapter 9 for more about what we have learned from these very important and informative images.

High-speed video recordings of the development of positively and negatively charged downward leaders can be found in the appendix (figures A.1 and A.2).

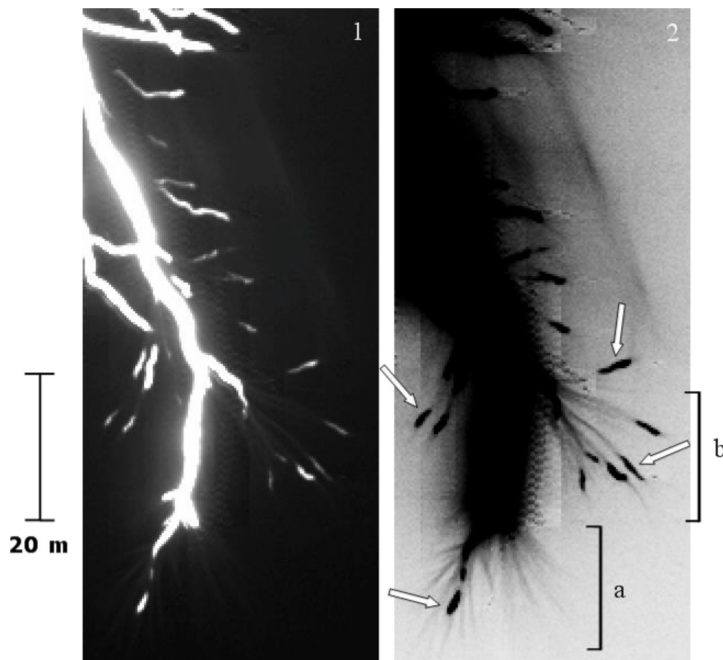


Figure 1.10. Positive and inverted (negative) images of downward stepped leaders of a negative CG flash, showing the stages in step and branch formation. The arrows point to space leaders within the corona-streamer region ahead of the tip of the leader (*a*) and on both sides of the leader channel (*b*). Like an envelope, the low-luminosity filamentary structure of corona streamers surrounds the core plasma channel of the leader, and is particularly noticeable in the negative image on the right. Reproduced from Petersen and Beasley (2013). Copyright 2013 by John Wiley & Sons, Inc. Reprinted by permission of John Wiley & Sons, Inc.

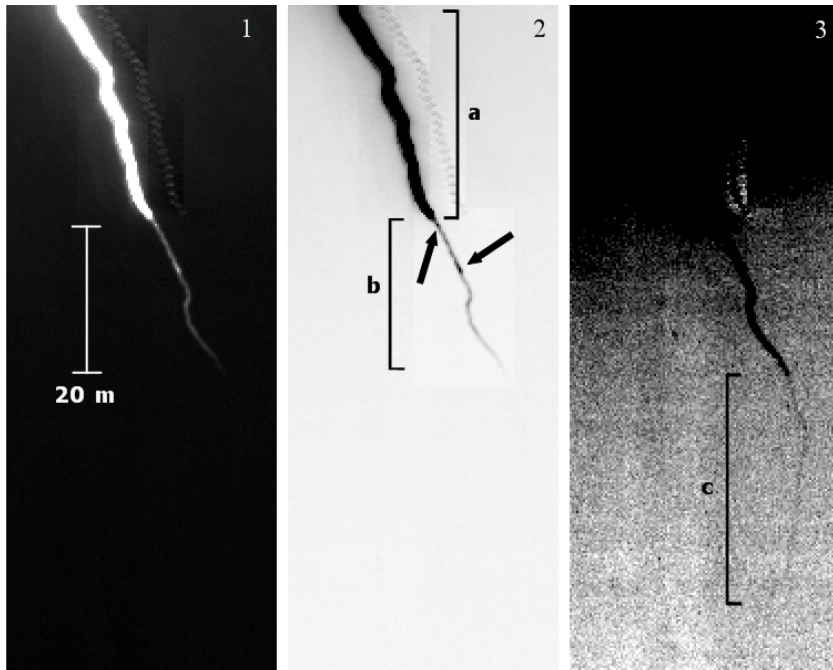


Figure 1.11. Close-up positive and inverted (negative) images of a descending negative dart leader. *a* = a highly luminous leader channel; *b* and *c* = low-luminosity zones ahead of the leader tip, along the path of the previously existing positive leader. Reproduced from Petersen and Beasley (2013). Copyright 2013 by John Wiley & Sons, Inc. Reprinted by permission of John Wiley & Sons, Inc.

As shown in this chapter, the comparison of lightning and its components to an electric spark is, indeed, purely qualitative. What is most important to understand is that the essential parts of lightning—natural leaders, which are initiated as electro-deless discharges in thunderstorms—have many features that cannot be reproduced in a laboratory. A natural leader is much more than a momentary electric spark; rather, it is a propagating discharge on the same great scale as the thunderstorm's dimensions.

References

- Bacchigella G L, Gazzani A, Bernardi M, Gallimberti I and Bondiou A 1994 Theoretical modeling of the laboratory negative stepped leader *Proc. Int. Aerospace Ground Conf. Lightning and Static Electricity* (Mannheim, Germany) pp 13–22
- Bazelyan E M and Raizer Yu P 1998 *Spark Discharge* (New York: CRC)
- Bazelyan E M and Raizer Yu P 2000 *Lightning Physics and Lightning Protection* (Bristol: Institute of Physics Publishing)
- Bondiou A and Gallimberti I 1994 Theoretical modeling of the development of the positive spark in long gaps *J. Phys. D: Appl. Phys.* **27** 1252–66

- Gallimberti I, Bacchegna G, Bondiou-Clergerie A and Lalande P 2002 Fundamental processes in long air gap discharges *CR Phys.* **3** 1335–59
- Goelian N, Lalande P, Bondiou-Clergerie A, Bacchegna G L, Gazzani A and Gallimberti I 1997 A simplified model for the simulation of the positive spark development in long air gaps *J. Phys. D: Appl. Phys.* **30** 2441–52
- Lalande P, Bondiou-Clergerie A, Bacchegna G and Gallimberti I 2002 Observations and modeling of lightning leaders *CR Phys.* **3** 1375–92
- Le Rénardières Group 1981 L'amorçage en polarité négative des grands intervalles d'air aux Rénardières; résultats de 1979 *Electra* **74**
- Mazur V and Rust W D 1983 Lightning propagation and flash density in squall lines as determined with radar *J. Geophys. Res.* **88** 495–502
- Mazur V 1989 Triggered lightning strikes to aircraft and natural intracloud discharges *J. Geophys. Res.* **94** 3311–25
- Petersen D A and Beasley W H 2013 High speed video observations of a natural negative stepped leader and subsequent dart leader *J. Geophys. Res.* **118** 12, 110–12, 119
- Williams E, Mazur V and Geotis S 1990 Lightning investigation with radar *Radar in Meteorology, The Battan Memorial and 40th Anniversary Radar Meteorology Volume* (Boston, MA: American Meteorological Society) pp 143–50

Principles of Lightning Physics

Vladislav Mazur

Chapter 2

Lightning leaders versus free-burning arcs

2.1 Similarities and differences

In chapter 1 we addressed the principal similarities between lightning leaders and sparks. Because the physics of gas discharges teaches that, ‘Even in a short-lived spark, the plasma is generally similar to arc plasma, so that the final spark stage can be regarded as an arc flash’ (Bazelyan and Raizer 1998, p 13), this brings us naturally to a consideration of the similarities between lightning leaders and electric arcs. It is important to realize that leaders produced in a high-voltage laboratory and free-burning arcs are both steady-state discharges, meaning that their properties are unchanging with time. While the properties of lightning leaders, however, are not exactly steady in time, they are nearly unchanging in response to the changing ambient potential along the leader’s propagation path.

It is commonly accepted in the literature that lightning is an analog of an electric arc, which possesses a descending current–voltage characteristic, and is capable of passing high currents. The description of an arc discharge in the *Encyclopedia Britannica* is: ‘Electric arc, continuous, high-density electric current between two separated conductors in a gas or vapor with a relatively low potential difference or voltage, across the conductors.’

This definition, while pointing to some similarities between arcs and leaders, also refers to an important difference between them, in the ways both of these phenomena start and progress. A free-burning arc starts as a short-circuit by two touching electrodes, while a leader in the laboratory starts from a single electrode and, by reaching the opposite electrode, ends in a flash-over that is an analog of a short-circuit. Upward unipolar leaders from tall ground structures or rockets with trailing grounded wires also start from single ‘electrodes’, which are both the tall ground structure and the ascending rocket with a conducting wire. The return-stroke phenomenon in CG flashes is an analog of the short-circuit effect of a flash-over in leaders in the laboratory.

There are other differences, as well. An arc discharge occurs between two electrodes connected to a current or a voltage source, while a lightning leader, when started inside the cloud, is an electrodeless discharge. Also a leader's plasma channel is created through the process of streamer-leader transition, which forms a corona envelope surrounding the propagating leader channel. Arcs do not have this corona envelope.

An important similarity, which engenders great interest in the physics of a free-burning arc, is the relationship between its current and the internal electric field. This relationship is difficult to ascertain either from measurements of laboratory leaders, or, most certainly, from observations of lightning leaders.

The numerical simulation of plasma-channel behavior (Gallimberti *et al* 2002), which came from studies of leaders in a high-voltage laboratory, shows that, for low currents (a few milliamperes), the internal electric field is primarily driven by electron-neutral collisions, and remains higher than 100 kV m^{-1} . With current values above several amperes, the leader's plasma channel is heated to temperatures above 5000 K, and the plasma becomes thermalized (Gallimberti *et al* 2002, Popov 2003). This means that the plasma is in a state of thermodynamic equilibrium: all types of particles (neutral atoms, molecules, ions, and electrons) from the volume are at the same temperature, and the ionization is essentially due to thermal collisions between molecules, depending only on the gas temperature (Gallimberti *et al* 2002). Thermal ionization leads to a sharp decrease in the internal electric field, down to a few hundred V m^{-1} , which is emblematic of the so-called *negative relationship between the internal electric field (voltage gradient) and current*, also a feature of a free-burning arc.

2.2 The E - I relationship, from the results of laboratory measurements and the modeling of free-burning arcs

Under laboratory conditions, a stationary arc is produced in the gap between electrodes, the length of which ranges from a few centimeters to a few meters, making it possible to measure both current and voltage at the electrodes (e.g. King 1961, Tanaka *et al* 2003). However, in these laboratory arcs, an unavoidable contamination of the arc plasma also exists, caused by metal vapors during arc ignition with a metal wire, and by the emission of metal particles from the electrodes at the high current of hundreds of amperes (King 1961). There is no evidence that such contamination exists in natural lightning leaders, however, probably because none of the numerous measurements of light spectra from lightning have ever shown any metal vapors in the spectra of lightning channels situated above 20 m from the ground (Salaneve 1980). The same is true for IC lightning channels.

The voltage gradient-current curve (identified hereafter as the E - I curve) seen in figure 2.1, obtained by King (1961) for a stationary arc in a 5 cm gap, has a negative slope only for currents lower than 100 A. The positive slope in the curve, for currents above 100 A, is explained by King as being the result of metal contamination from the electrode effect. King identified three main E - I curve regions: the glow-corona region of current below 0.1 A, the stationary arc region of current from 0.1 to 100 A, and a contaminated (by metal vapors) arc region of current above 100 A.

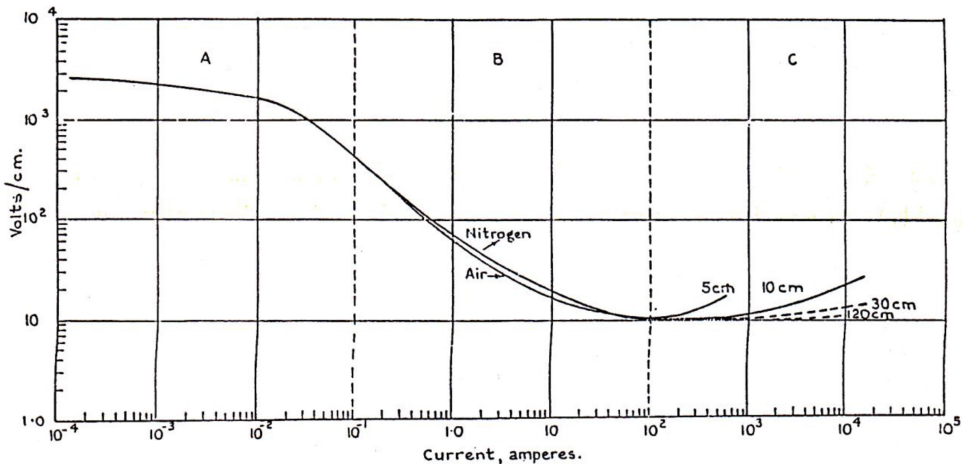


Figure 2.1. Characteristic E - I curve of a free-burning arc in nitrogen and in air. The curve can be divided into three main regions: $A < 0.1$ A; $B = 0.1$ – 100 A; and $C > 100$ A. Reprinted with permission from King (1961). Copyright 1961 Elsevier.

The contaminating electrode effect decreases in arcs that occur within longer gaps, so the reverse of the E - I curve slope, from negative to positive (observed in figure 2.1, starting approximately at 100 A), would occur at much higher currents in longer gaps. King infers from his study, and also from studies of arcs in 30 cm and 120 cm gaps, that in longer gaps the voltage gradient remains reasonably constant, about 1 kV m^{-1} , for very high currents in the range of 100 to 1000 A.

Modeling of the physical processes that govern arc-channel behavior, such as expansion of the channel's length and its radius, and the change of the internal voltage gradient after application of the current (Chemartin *et al* 2009), employed the gas-dynamic approach and the resistive magnetohydrodynamics method for imperfectly conducting fluids, such as plasma. The results of modeling for a leader channel, after applying 100 A current, were compared with the measurements of a free-burning arc of 1.6 and 3.2 m length that had been subjected to a steady current of 100 A during a period of 100 ms (Tanaka *et al* 2003). The results of the measurements and modeling depicted in figure 2.2 show a similar gradual decrease with time in the voltage gradient, after a step-like current application and approximately the same values of voltage gradient at time 80 ms. The noticeable difference between the measurements and computations visible in the first 50 ms in figure 2.2 is explained by metal-vapor contamination in the experiment caused by the copper wire used for ignition of the arc (Tanaka *et al* 2003). (The copper vapor increases the arc-column conductance, reducing the channel resistance, and thus reducing the voltage gradient.)

The results of the studies depicted in figure 2.2 describe the phenomenon of transition from the initial to steady-state condition, after application of the current. During this transition, the voltage gradient decreases significantly within the first 200 ms, starting (for models) at 3500 V m^{-1} at current ignition, and ending, for both the models and the experiment, at $\sim 300\text{ V m}^{-1}$. The time constant of this evolution

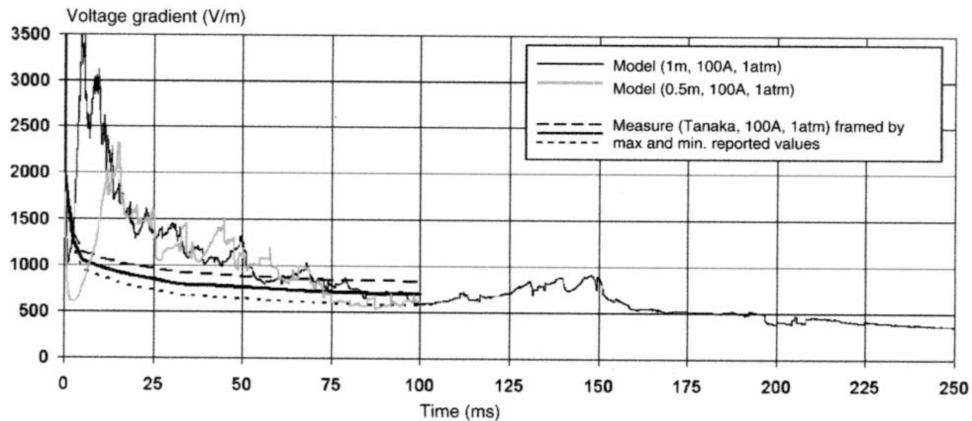


Figure 2.2. Evolution of the measured and computed internal voltage gradient in a free-burning arc. Two leader channels, of 0.5 m and 1 m length, are modeled. Reprinted with permission from Chemartin *et al* (2009). Copyright 2009 Elsevier.

is ~ 25 ms. The transition to the steady-state condition takes place as the radius of the plasma channel increases by a factor of five, which, in turn, causes the ‘domino effect’ of the lowering of the channel resistance and, thus, a lowering of the voltage gradient (Chemartin *et al* 2009). The time-lag of the voltage gradient behind the application of current in the arc column indicates that the timing of the event’s development significantly affects the actual value of the voltage gradient along the arc column. This phenomenon also points to a potentially problematic issue with the integrity of the voltage-gradient measurements in arcs, if measurements are performed prior to the arc’s reaching the steady-state condition.

The time-lag of the voltage gradient behind the current in arc channels explains the hysteresis-type relationship between leader current and its luminosity (see section 2.3 for more details).

The studies we review next extended the scope and scale of voltage and current measurements in the laboratory and through modeling far beyond the modest efforts by King (1961). The expressions for the E - I relationship in the steady-state arc condition, all of them negative relationships, have come either from modeling, or from elaborate experiments with free-burning arcs. We will review these expressions with the purpose of defining the character of the E - I relationship for the range of currents typical of lightning leaders.

Bazelyan *et al* (2008), in their calculation of the length of a ground conductor that would be sufficient for the initiation of a viable upward leader, assumed a simplified relationship (2.1) between an average internal electric field, E , and a leader’s current, I .

$$E = bI^{-1.0}, \quad b = 3 \times 10^4 \text{ Vm}^{-1} \text{ A}^{-1} \quad (2.1)$$

Earlier, Pellerin *et al* (2000) investigated the influence of buoyancy and convection on current and potential gradient along the channel of a DC gliding arc discharge (glidarc) in laboratory experiments, and compared the measurements with their

proposed model. They arrived at the relationship (2.2) of an internal electric field, E , to the current, I , and the relative air velocity to that of the arc (lifting velocity), v , in glidars with currents of a few amperes,

$$E = A v^{1-\alpha} I^{-\alpha} \quad (2.2)$$

where the coefficients A and α are 5300 and 0.52, respectively, determined from measurements.

Measurements of an arc in inter-electrode distances of 60 to 300 cm, with currents of 50–10 000 A (Sunabe and Inaba 1999), produced a slightly negative relationship between the internal electric field and the current. It is essential to state here that the length of the arc in this study was equal to the inter-electrode distance,

$$E = 13.8 I^{-0.068} \quad (2.3)$$

By considering the length of the arc *as fixed and equal to the distance between electrodes*, the relationship in formula (2.3) does not count the effects of buoyancy, local looping (meandering) due to the effect of electromagnetic forces, or upward and downward displacements of the arc column from the central axis of the electrodes. However, the meandering of both the arc column and the lightning channel, and their displacements, are common features for them, as depicted in the images in figure 2.3. These factors, when taken into account, will increase the actual length of the arc column and, thus, will affect the character of the E – I curve.

Using high-speed photography, Sunabe and Inaba (1999) ascertained the relationship (2.4) between the lifting velocity of a DC arc column, v , and the arc current, I , considering only the buoyancy effect, and also the relationship (2.5) that considers the effects of buoyancy, meandering, and arc-column displacements.

$$v = 0.37 I^{-0.29} \quad (2.4)$$

$$v = 0.081 I^{-0.71} \quad (2.5)$$

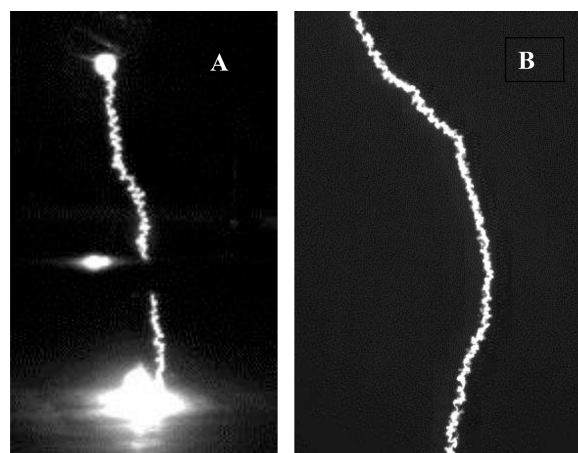


Figure 2.3. Meandering channels of an arc column produced in a high-voltage laboratory (A), and of a lightning channel in nature at close range (B). Courtesy of Dan Petersen.

Larsson *et al* (2005) applied the relationship (2.5) to (2.2) for a glidarc, and arrived at (2.6), which they applied for currents in the range of 10^2 – 10^4 A,

$$E = bI^{-0.18} \quad (2.6)$$

The E – I relationships obtained in the studies already reviewed here are applicable to a range of arc lengths and arc currents outside the scope of the laboratory study by King (1961). In order to determine the general trend in the E – I relationship in DC free-burning arcs, we have produced in figure 2.4 a composite of the part of the curve from King (1961, figure 2.1) for an arc current lower than 10 A, and the line elements (dotted and dashed lines) of the E – I relationships for larger arc currents from (2.3) and (2.6), respectively, as well as data points from measurements of a 3 m long arc in Tanaka *et al* (2003, table 2). We should take some comfort from the close consistency of the voltage gradient obtained with (2.6) and the voltage gradient measured in long-gap DC free-burning arcs with currents in the range of 100 to 2000 A (data points marked with stars in figure 2.4). A solid horizontal line corresponds to King's postulation of the constant voltage gradient of 1000 V m⁻¹ for currents above 10 A.

The dotted and dashed lines and data points in figure 2.4 reflect the influence of buoyancy on the E – I relationship, as well as buoyancy-plus-electromagnetic forces, which actually affect arc columns with currents greater than 10 A. Use of the low-current part of King's curve in figure 2.4 is justified, because arcs with currents less than 10 A are not affected by buoyancy or electromagnetic forces. The postulation in King (1961) of a constant voltage gradient for arc columns with currents greater than 100 A contradicts results in other studies that show a negative trend in the E – I relationship for this range of current. However, this may be explained by the following fact: King did not consider the actual, much-longer length of the free-burning arc column, which is a

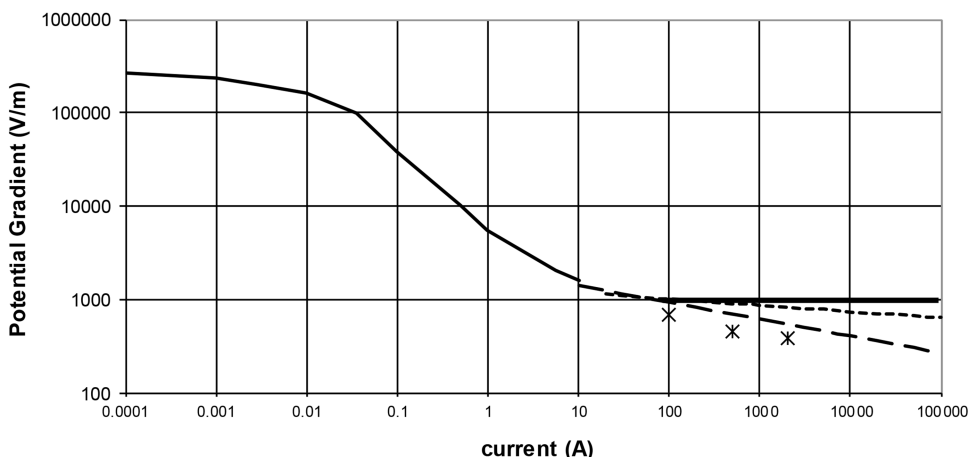


Figure 2.4. Relationship between current and voltage gradient in arc columns: a composite of results from previous studies. Solid line: currents less than 10 A, from King (1961); dotted line: using (2.5), from Sunabe and Inaba (1999); dashed line: using (2.8), from Larsson *et al* (2005); stars: data points from measurements for a 3 m long arc column, in Tanaka *et al* (2003). Reproduced from Mazur and Ruhnke (2014). Copyright 2014 by John Wiley Sons, Inc. Reprinted by permission of John Wiley & Sons, Inc.

result of buoyancy and electromagnetic forces; instead, he used the shorter length of an inter-electrode gap for the arc's length.

The clear conclusion to be drawn from our analysis of these reviewed studies is that the E - I relationship in the steady-state condition of a free-burning arc is *negative* in the entire range of current values typical for continuing currents in lightning leaders, i.e. from the few tens of amperes needed to initiate a sustained formation of the leader to the few hundreds of amperes in a developing leader.

Needless to say, the findings from studies of free-burning arcs are also applicable to interpretations of the physical processes in lightning leaders. In particular, the relationship between the leader's current and its internal electric field is critical for establishing the conditions necessary to sustain leader propagation. As discussed in chapter 1, in order for a leader channel to elongate, the internal electric field of the leader must be much less than the ambient electric field. In reference to the E - I relationship for the leader's plasma channel, this means that the current in the channel should be above a certain minimum value that corresponds to a sufficiently low internal field. As an example, in the E - I curve in figure 2.1 a stationary arc with a 10 A current will have a longitudinal electric field of $\sim 2 \text{ kV m}^{-1}$. A field such as this is comparable to the values of the ambient electric field of a thundercloud near the ground and, thus, is not low enough to start and maintain leader formation on short ground objects.

The following observation of a self-initiated upward positive leader at the 160 m high Peissenberg Tower in Germany confirms the conditions for leader initiation found in the E - I relationship. A rough estimate of the lowest current at the very beginning of an upward leader from the Peissenberg tower is $\sim 30 \text{ A}$ (Heidler 2012). The internal electric field in the leader, $\sim 1 \text{ kV m}^{-1}$, as found from the E - I curve in figure 2.4 for an arc current of 30 A, is much smaller than the ambient electric field near the tip of the tower, which is, possibly, a few tens of kV m^{-1} .

2.3 The E - I relationship and the luminosity of leader channels

We have shown that, by using the E - I relationship, we can better understand the conditions necessary for leader propagation. Actual remote measurement of the current in natural leaders is a challenging task; however, this current can be measured in upward leaders that ascend either from a ground structure, or from a rocket with a trailing grounded wire. Most meaningful would be current measurements of a single unbranched leader channel, which is very similar to an arc channel. Unfortunately, however, since no possibility exists to measure the internal field E , we cannot quantitatively verify the E - I relationship for lightning leaders. We are able, nonetheless, to find a confirmation of this relationship in the records of lightning-channel luminosity versus its current for a lightning leader in a steady-state condition.

To start with, it is reasonable to assume that the channel's luminosity is proportional to the power per unit length, $P = EI$. Then, from an analysis of the light-current relationship, we can determine the trend in the changes of the internal electric field, E . The records of current and light intensity variation in time, in Wang *et al* (2005), for the first 90 μs of a return-stroke channel in a rocket-triggered negative cloud-to-ground flash, provide us with a good example for such an analysis (see figure 2.5). Because the

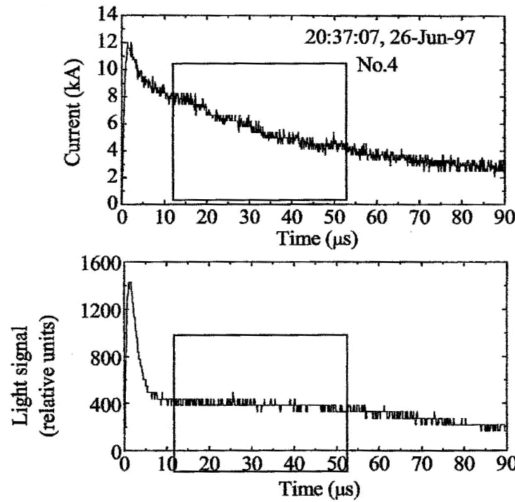


Figure 2.5. Correlated current and light records of a return stroke of a negative cloud-to-ground flash produced by a classic rocket-triggered lightning technique. Reprinted with permission from Wang *et al* (2005). Copyright 2005 Elsevier.

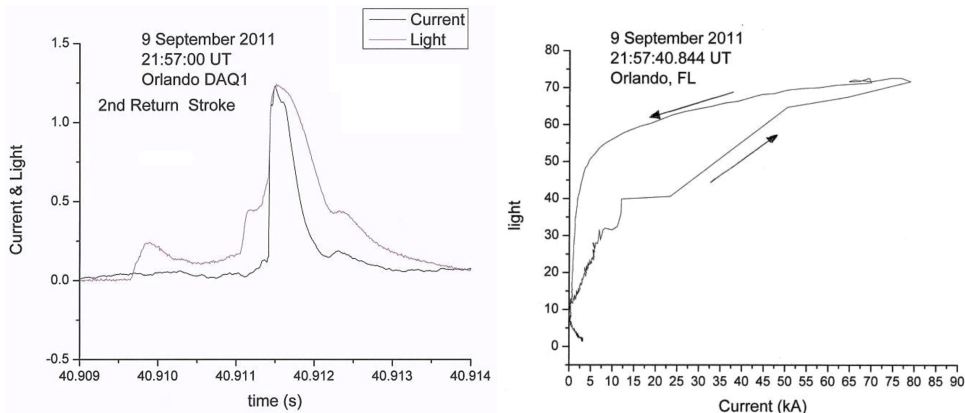


Figure 2.6. (A) Light and current waveforms (in relative scale) of a 45 kA return stroke. (B) Light-current relationship for the same return stroke. Reprinted from Ruhnke (2014).

plasma channel of the return stroke is in the near-steady-state condition within 50 μ s from initiation, the constant luminosity of its channel during a period of 40 μ s, when the current steadily declines, is evidence of an increasing longitudinal electric field E and, thus, of the negative E - I relationship in the plasma channel.

Most of the records of the light-current relationship in the lightning literature clearly show a strong positive correlation between them, in general, but with differences between the rising and decreasing phases. The hysteresis in the light-current curves was reported by Zhou *et al* (2013) from their observations of segments of leader channels with continuing current. A similar hysteresis effect takes place in

the light–current relationship of a return stroke (figure 2.6) in Ruhnke (2014). The hysteresis effect is related to the lagging of the voltage gradient behind an applied current in arc channels (see section 2.2), which would affect the power per unit length $P = EI$ and, thus, the luminosity of the lightning channel.

References

- Bazelyan E M, Raizer Y P and Aleksandrov N L 2008 Corona initiated from grounded objects under thunderstorm conditions and its influence on lightning attachment *Plasma Sources Sci. Technol.* **17** 024015
- Bazelyan E and Raizer Yu 1998 *Spark Discharge* (New York: CRC)
- Chemartin L, Lalande P, Montreuil E, Delalondre C, Chern B G and Lago F 2009 Three-dimensional simulation of a DC free-burning arc. Application to lightning physics *Atmos. Res.* **91** 371–80
- Gallimberti I, Bacchigia G, Bondiou-Clergerie A and Lalande P 2002 Fundamental processes in long air gap discharges *C.R. Phys.* **3** 1335–59
- Heidler F 2012 Personal communication
- King L A 1961 The voltage gradient of the free burning arc in air and nitrogen *Proc. 5th Int. Conf. Ionization Phenomena in Gases* **2** 871–7
- Larsson A, Delannoy A and Lalande P 2005 Voltage drop along a lightning channel during strikes to aircraft *Atmos. Res.* **76** 377–85
- Mazur V and Ruhnke L H 2014 The physical processes of current cutoff in lightning leaders *J. Geophys. Res. Atmos.* **119** 2796–810
- Popov N A 2003 Formation and development of a leader channel in air *Plasma Phys. Rep.* **29** 695–708
- Pelerin S, Richard F, Chapelle J, Cormier J-M and Musiol K 2000 Heat string model of bi-dimensional dc Glidarc *J. Phys. D.: Appl. Phys.* **33** 2407–19
- Ruhnke L H 2014 Analysis of electric fields and potentials on lightning channels *Ground'2014 and LPE Conf. (Manaus, Brazil)*
- Salaneve L E 1980 *Lightning and its Spectrum, An Atlas of Photographs* (Tucson, AZ: University of Arizona Press) p 85
- Sunabe K and Inaba T 1999 Electric and moving characteristics of DC kilo ampere high-current arcs in atmospheric air *Electr. Eng. Japan* **110** 9–20
- Tanaka S, Sunabe K-Y and Goda Y 2003 Internal voltage gradient and behavior of column on long-gap dc free arc *Electr. Eng. Japan* **144** 8–16
- Wang D, Takagi N, Watanabe T, Rakov V, Uman M A, Rambo K J and Stapleton M V 2005 A comparison of channel-base currents and optical signals for rocket-triggered lightning strokes *Atmos. Res.* **7** 412–422
- Zhou E, Lu W, Zhang Y, Zhu B, Zheng D and Zhang Y 2013 Correlation analysis between the channel current and luminosity of initial continuous and continuing current processes in an artificially triggered lightning flash *Atmos. Res.* **129–130** 79–89

Principles of Lightning Physics

Vladislav Mazur

Chapter 3

Physical concepts of a lightning leader model

3.1 The space charge leader concept based on cloud charge collection

The most precise characterization of Schonland's concept (1938) of 'the space charge leader' is found in Kasemir (1983), who identified it as 'the mechanism of a lightning discharge ... analogous to a spark discharge between two metallic electrodes'. For CG flashes, one of the two 'electrodes' is the charged cloud volume; the other is the ground. For IC flashes, the two 'electrodes' are the two oppositely charged cloud volumes. In view of this similarity to discharges between two electrodes, Kasemir called Schonland's leader concept 'the uni-directional or charged leader theory'.

Schonland's model suggests that, during the negative leader stage in CG flashes, 'the negative charge is progressively removed from the cloud, and becomes distributed along the whole leader channel' (Malan 1963, p 47), as illustrated in figure 3.1. The figure depicts the 'space charge leader' advancing from the cloud towards the ground (CG flashes), and leaders developing within the cloud (IC flashes). Quoting from Kasemir (1983), in his description of the leader to ground in figures 3.1(a) and 3.1(b): 'The leader has collected negative charge from the cloud and stored it along its channel with a *constant* charge per unit length of about $q = 1 \text{ C km}^{-1}$. If contact with the ground is made, the negative charge flows into the ground in the return stroke, completely discharging the leader channel.' Figures 3.1(c) and 3.1(d) depict the same discharging mechanism, but for the space charge leader in an IC flash. In the case of an upward-moving leader, the space-charge leader collects negative charges from the lower part of the cloud, and moves them to the upper, positive part of the cloud, whereas in the case of a downward-moving leader, it collects positive charges from the upper part of the cloud and moves them to the lower, negative part of the cloud.

When applied to calculations based on electric field measurements on the ground, the process of the space charge leader's development is described as the emergence of a leader from an imagined center of the cloud space charges, Q , and the progression of the leader channel with uniformly distributed charges of density, q , that issue from

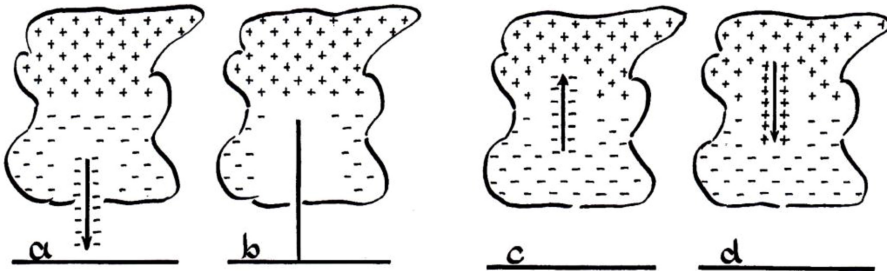


Figure 3.1. The concept of charge distribution in a space charge leader. (a) Stepped leader, (b) after the return stroke, (c) cloud discharge advancing upward, and (d) cloud discharge advancing downward. Reproduced from Kasemir (1983). Copyright 1983 by John Wiley Sons, Inc. Reprinted by permission of John Wiley & Sons, Inc.

the cloud space charges. The electric field changes on the ground, in this scenario, are affected by the motion of the leader charges and the decreasing space charges from which the leader emerged.

Neither Schonland nor Malan tried to explain the nature of the physical mechanism that removes charges from the cloud, forces them into the leader channel, and distributes them uniformly along the leader channel. Since ‘there is no physical law which makes even mobile negative (or positive) cloud charges concentrate in a lightning channel’ (Kasemir 1983), one may only wonder why such an important question, about the validity of Schonland’s model, was not debated in the lightning literature many years ago.

Another reason that the assumption of evenly distributed charges in the leader cannot be justified by the laws of physics lies in the relationship between the charges on a conductor suspended in an ambient electric field E and the ambient potential distribution ϕ . The *induced* charges on a conductor (leader), in their distribution along the leader, *mirror* the ambient potential distribution ϕ (Kasemir 1986). It follows, from the definition of the electric field vector as $E = -\text{grad}\phi$, that a constant electric field would be the result of a linearly changing cloud potential ϕ . This means that, even in the idealized case of a constant ambient electric field, the induced charges are distributed linearly. Thus, there are no known ambient electrical conditions in which the charges on a conductor could be uniformly distributed, as assumed in the ‘space charge leader’ concept.

The ‘space charge leader’ model should, therefore, be treated as an empirical model inspired by a misperception: that of the similarity between lightning leaders and sparks between electrodes connected to a charge source. Supporting this misperception was also, perhaps, the fact of the similarity between waveforms in the records of electric field changes produced using both the space charge leader model and those of natural lightning leaders. Needless to say, neither charge sources similar to a battery in the cloud, nor electrodes connected to such a charge source exist, and there are no electrical conditions in nature that produce uniformly distributed charges on the leader. Therefore, Schonland’s entire model of ‘the space charge leader’ cannot be physically valid.

3.2 The bi-directional, uncharged leader concept based on induced charges

The concept of the lightning leader, introduced by Heinz-Wolfram Kasemir (1950), considers a leader to be the result of an electrodeless discharge that produces a plasma channel (a conductor) in an ambient electric field of cloud charges. The same ambient electric field, which leads to the formation of the leader through the streamer-leader transition process, influences the distribution of charges in the leader channel by electrostatic induction. The induced charges on a suspended conductor are in the form of an electrical dipole, with the maximum value of those charges at the tips of the conductor, and the net charge always equal to zero. Kasemir's concept of 'the uncharged leader' completely obviates any need for a mechanism that collects cloud charge into a leader channel, which was the foundation of Schonland's 'space charge leader' model, and which mechanism does not exist in nature.

Figure 3.2 illustrates Kasemir's concept of 'the bidirectional uncharged leader' for the same types of lightning flashes as those in figure 3.1, for the 'space charge leader'. The charge distribution on the suspended leader channel (figure 3.2(a)) and on the lightning channel after the return stroke (figure 3.2(b)), is quite different from that in figure 3.1, of the 'space charge leader'. The return stroke channel carries a positive charge flowing from the ground, rather than being fully discharged. The bidirectional development of a zero-net-charge leader in an IC flash is illustrated in figures 3.2(c) and 3.2(d). The cloud charges in Kasemir's concept are uninvolved and unmoving at every stage of lightning development; the cloud charges remain in their places, both in the case of a downward leader to ground, and in an IC flash.

The profound difference between the two leader concepts is also reflected in the different meanings of two terms, commonly used in the lightning literature: 'discharge' and 'neutralization' of cloud charges by lightning. Kasemir (1983) stated that neither IC nor CG flashes actually discharge the cloud, i.e. remove cloud charges. What they do, in fact, is to transport the charges that reside on the bipolar parts of the bidirectional leader dipole into the cloud volume; in other words, the negative leader charges move into a cloud volume with positive space charges, and

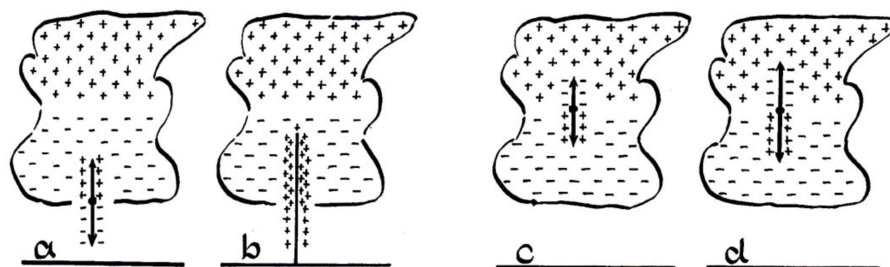


Figure 3.2. The concept of charge distribution on a bidirectional uncharged leader in cases of (a) a stepped leader, (b) after the return stroke, (c) cloud discharge advancing upward, and (d) cloud discharge advancing downward. Reproduced from Kasemir (1983). Copyright 1983 by John Wiley Sons, Inc. Reprinted by permission of John Wiley & Sons, Inc.

the positive leader charges move into a cloud volume with negative space charges. During the lifetime of the lightning flash, these charges are still confined within the lightning channel. In contrast to the very rapid deposit of these bipolar leader charges into the cloud, the actual neutralization of the leader's charges, which begins after lightning progression stops, may last (quoting from Kasemir) 'a minute or more, rather than a second or less'. During the process of neutralization, free electrons and air ions of lightning plasma 'will disperse in the neighborhood of the channel, neutralize oppositely-charged cloud elements, or attach themselves to neutral cloud elements or precipitation particles' within a cloud volume nearby. The net effect of depositing into a cloud the induced charges of the bidirectional leader is to decrease the electrical energy of the cloud without removing the cloud charges.

Another use of the term 'neutralization' is found in the description of the return stroke process in CG flashes when applying the space charge leader concept. According to this concept, a return stroke (1) carries a uniformly distributed charge of polarity opposite to that of the downward leader, but equal to it in magnitude; and (2) 'neutralizes' the leader's charges, leaving the return-stroke channel with a zero net charge (see the sketch in figure 3.1(b)). However, this process cannot take place in nature: the plasma channel of a return stroke is conductive, and the conducting channel in the ambient electric field should possess induced charges that are distributed in accordance with the ambient potential distribution.

Kasemir (1983) validated his concept of a bidirectional, uncharged leader by analyzing the energy balance of a conductor in an ambient electric field. He quoted J A Stratton (1941, section 2.13) who introduced, in his classic textbook *Electromagnetic Theory*, a theorem on the energy of uncharged conductors in an ambient electric field, which reads: 'The introduction of an uncharged conductor into the field of a fixed set of charges diminishes the total energy of the field.' This theorem is expressed in the following mathematical formula:

$$U - U' = \frac{1}{2} \int_{V_0} \epsilon E^2 dv + \frac{1}{2} \int_{V_1} \epsilon (E - E')^2 dv \quad (3.1)$$

Here, U is the energy before and U' is the energy after the introduction of the conductive lightning leader. E and E' are the electric field vectors before and after the uncharged body is brought into the ambient field. V_0 is a volume with an electric field that surrounds the conductor, and V_1 is a volume occupied with a conductor, so $V_0 + V_1 = V$ is the total volume of electrical charges. Stratton's expression, 'uncharged conductor', means that the net charge on the conductor is zero.

Because the difference, $U - U'$, in the expression (3.1), is positive, the uncharged bidirectional leader channel, carrying only induced charges, draws the energy for its growth and related energy-consuming phenomena (e.g. ionizing, heating the channel, and producing electromagnetic radiation) from the energy stored in the electric field of a thunderstorm. In Kasemir's words, 'we may consider the lightning discharge as an energy converter'.

A comparison of the two leader models leaves no further doubts about the sound physical foundation on which Kasemir's bidirectional, uncharged leader model is built.

3.3 Comparing the outputs of the two leader models

Using an invalid model of a lightning leader will very likely produce results that contradict those derived from actual lightning observations; conversely, the use of a physically sound model of a lightning leader is essential for the correct interpretation of remote lightning measurements, as well as for determining the structure of space charges in a thunderstorm. In order to demonstrate the models' respective usefulness, one should compare the results of applying the two models to actual lightning observations.

Perhaps it has been comforting to supporters of Schonland's space charge model to realize that the waveforms of the E field changes calculated using this model are similar to those of natural lightning leaders; but so are the waveforms of the E field changes of the bidirectional uncharged leader. All this tells us is that waveforms similar to those of natural leaders may occur in models that are built on totally different physical grounds.

Mazur and Ruhnke (1993) calculated the electric field changes on the ground produced by a unidirectional 'space charge leader' (Schonland's concept), as well as a bidirectional, bipolar, uncharged leader (Kasemir's concept) for a simple case of a uniform ambient E -field. In each case, the leader that propagated downward with the same speed started at the same height above the ground, and at the same ground distance to an E -field sensor (see figure 3.3). In this study, the 'space charge leader' has its charges uniformly distributed, with the charge per unit length ρ_L . The charge

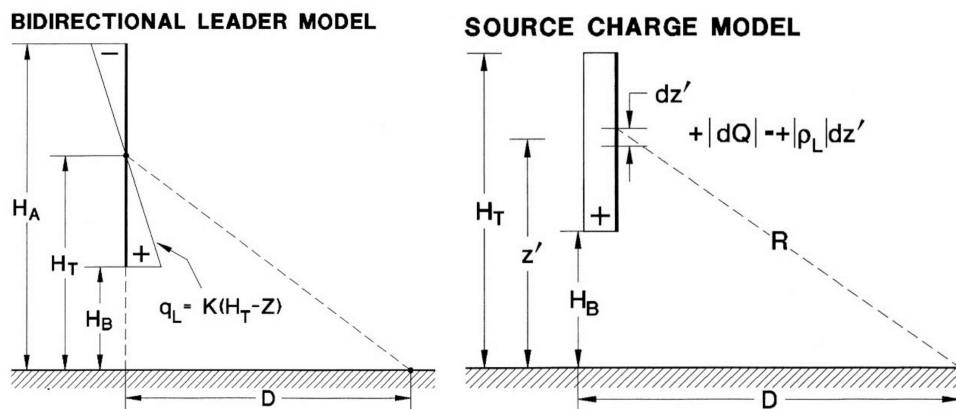


Figure 3.3. Conceptual sketches of a bidirectional leader model and a space charge leader model in a uniform ambient E -field. In both models, H_T is the leader's starting height, and D is the distance from the ground E -field sensor; H_A and H_B are the heights above the ground of the positively charged and the negatively charged tips of the bidirectional leader, respectively. Reproduced from Mazur and Ruhnke (1993). Copyright 1993 by John Wiley Sons, Inc. Reprinted by permission of John Wiley & Sons, Inc.

per unit length of the bidirectional leader in a uniform ambient E -field, $q_L(z)$, changes linearly, with zero at the point of leader-initiation height, H_T , and the slope, k , mirroring the slope of the ambient potential, so that $q_L(z) = k(H_T - z)$.

Assuming the same speed of propagation for both the positively and negatively charged tips of a bidirectional leader, the electric field change is

$$\Delta E = \int_{H_B}^{H_A} 2k(H_T - z) \frac{z dz}{4\pi\epsilon_0(z^2 + D^2)^{1.5}} \quad (3.2)$$

After integration, the electric field change is

$$\begin{aligned} \Delta E = \frac{k}{2\pi\epsilon_0} & \left\{ \frac{H_A - H_T}{(H_A^2 + D^2)^{0.5}} + \frac{H_T - H_B}{(H_B^2 + D^2)^{0.5}} - \ln \left[H_A + (H_A^2 + D^2)^{0.5} \right] \right. \\ & \left. + \ln \left[H_B + (H_B^2 + D^2)^{0.5} \right] \right\} \end{aligned} \quad (3.3)$$

When the downward part of the leader channel reaches the ground, then $H_B = 0$, $H_A = 2H_T$, $E = E_0$, and (3.3) becomes

$$\Delta E_0 = \frac{k}{2\pi\epsilon_0} \left[\frac{H_T}{(H_T^2 + D^2)^{0.5}} + \frac{H_T}{D} - \ln \left[2H_T + (4H_T^2 + D^2)^{0.5} \right] + \ln D \right] \quad (3.4)$$

The electric field change produced by the positively charged space charge leader is

$$\Delta E = \frac{\rho}{2\pi\epsilon_0} \left[\frac{1}{(D^2 + H_B^2)^{0.5}} - \frac{1}{(D^2 + H_T^2)^{0.5}} - \frac{(H_T - H_B)H_T}{(D^2 + H_T^2)^{1.5}} \right] \quad (3.5)$$

Here, as in (3.2), H_B is the height of the lower tip of the space charge leader; H_T is the height of the source charge center, as well as the starting altitude of the leader; and ρ is the constant charge per unit length on the leader. The first two members in brackets represent contributions from the uniformly charged and downward-moving leader, and the last member represents the contribution, due to depletion, of the source charge resulting from formation of the leader.

In order to quantitatively compare the expressions for electric field changes from the two leader models, we assume that, in both cases, the same amount of charge Q is flowing from the ground into the leader's channel during the return stroke. In the bidirectional leader model, the return stroke deposits, along the leader channel of length $2H_T$, a uniformly distributed charge, with a polarity opposite to that of the leader, and with a charge density equal to that of the leader at the ground level at the moment of ground attachment, i.e. $q_L = kH_T$. (This requirement comes from the need to satisfy a zero charge condition of induced charges on a conductor at the ground point.) Thus, the total charge flowing in the return stroke channel is $Q = 2kH_T^2$.

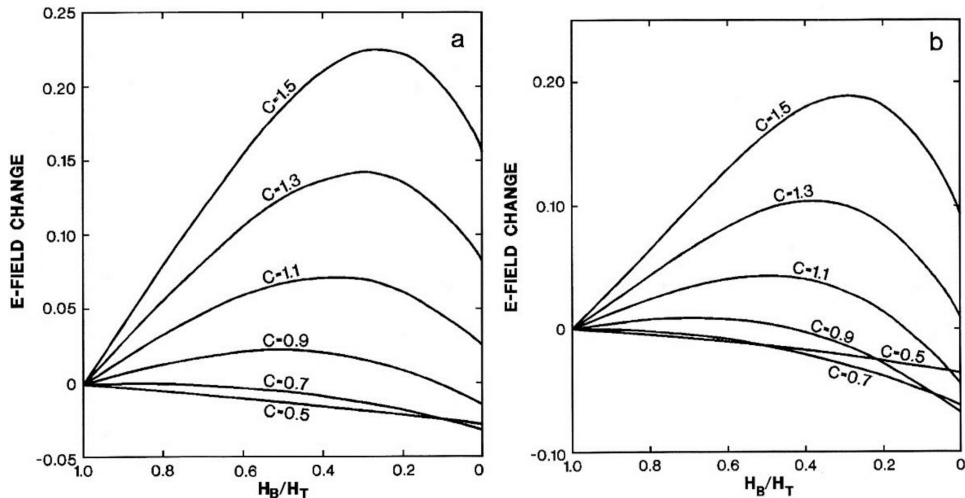


Figure 3.4. Electric field change per unit charge for (a) the bidirectional leader model and (b) the space charge model, with a positive leader moving downward. H_T is the height of the leader initiation point, H_B is the height of the lower tip of the leader, and ratio c is equal to D/H_T , where D is the distance from the leader to an observer (sensor). Reproduced from Mazur and Ruhnke (1993). Copyright 1993 by John Wiley Sons, Inc. Reprinted by permission of John Wiley & Sons, Inc.

For the space charge leader, the return stroke deposits a uniformly distributed charge equal to that of the downward leader, $Q = \rho H_T$. This is commonly described as the process of ‘neutralizing’ the leader’s charges by the return stroke. Expressing the variables k and q (in (3.4) and (3.5)) as a function of Q , we plot in figure 3.4 the electric field changes per unit charge as a function of the ratio H_B/H_T and for the varying ratio of the distance from the flash to the origin height, $c = D/H_T$. Again, as in the case of the electric field changes, the similarity in the curves for the two models in figure 3.4 is apparent.

A convenient parameter for the quantitative comparison of the models is the value of ratio $c = D/H_T$, which corresponds to the electric field change $\Delta E_0 = 0$ at some point on the ground. This value is found by the graphical solution of (3.4), and is 1.27 for the space charge model, and 0.98 for the bidirectional leader model. What this means is that, to produce the same electric field change, $\Delta E_0 = 0$, at the same ground distance D from the flash, the space charge model must place the starting altitude of the leader, H_T , approximately 30% higher than the bidirectional leader model. These results are relevant to, and have been used by, researchers to determine the locations of the lightning-initiation origins in thunderstorms.

It should be also mentioned that the location of the lightning’s origin has a different meaning in the two models: in the space charge leader model, the lightning origin is at the center of the space charge region; the electric field there is close to zero, and at maximum value at the outer boundary of the charge region. In view of these conditions, however, it is inconceivable that the initiation point of the leader is at the center of the space charge region. The bidirectional uncharged leader, on the

other hand, starts at the place with highest ambient electric field, which would be between the space charge regions of opposite polarities.

Direct measurement of lightning radiation source locations with a VHF mapping system (Proctor *et al* 1988, Proctor 1991), with an accuracy of within 140–250 m, identified the heights of the origin of lightning leaders for hundreds of CG flashes to be at a mean value of 5.3 km above mean sea level and an ambient temperature of –3.3 °C. From multiple-station measurements of electric field changes on the ground, and by applying the space charge model, Krehbiel *et al* (1979; 1984), Krehbiel (1981), Jacobson and Krider (1976), and Krider (1989) calculated the heights of the CG flash origins to be at a mean value of 7.4 km and an average temperature of about –14 °C, or almost 40% higher than Proctor's 5.3 km, and more than 10 °C lower than his ambient temperature estimated. Proctor (1991), who compared his results with those based on the space charge leader model, was unable to explain this discrepancy.

The heights of lightning origins calculated using the bidirectional leader model closely match those determined from VHF mapping. This fact reinforces the conclusion that the contradiction between the results of direct measurements and interpolations using the space charge leader model can be explained by the fact of having used an empirical, rather than a physical, model. We will show, in chapter 5, that recent results of field observations using the time of arrival lightning-mapping technique have fully confirmed this conclusion.

The critical advantage of the bidirectional leader model over the space charge model is that it provides a physically sound concept and solid foundation for interpreting the sometimes-fragmented *in situ* or remote observations of natural and artificially triggered lightning. In light of these strong arguments, there would seem to be little reason to continue to retain the empirical space charge leader model in lightning studies. This model may have had some utility in the past, but it has long since exhausted its usefulness, now confusing, rather than clarifying, our understanding of lightning physics.

References

- Jacobson E A and Krider E P 1976 Electrostatic field changes produced by Florida lightning *J. Atmos. Sci.* **33** 113–6
- Kasimir H W 1950 Qualitative Uebersicht ueber Potential-, Feld-, und Ladungsverhaltnisse bei einer Blitzentladung in der Gewitterwolke *Das Gewitter* ed H Israel (Leipzig: Akademische Verlagsgesellschaft)
- Mazur V and Ruhnke L H (ed) 2013 *Heinz Wolfram Kasimir: His Collected Works* (New York: Wiley) pp 398–411 (Engl. transl.)
- Kasimir H W 1983 Static discharge and triggered lightning *Proc. 8th Int. Aerospace and Ground Conf. on Lightning and Static Electricity* (Fort Worth, TX, June 21–23) DOTIFAA/CT-83125,24.1 24.11
- Mazur V and Ruhnke L H (ed) 2013 *Heinz Wolfram Kasimir: His Collected Works* (New York: Wiley) pp 418–28 (Engl. transl.)

- Kasemir H W 1986 Electrostatic model of lightning flashes triggered from the ground *Proc. Int. Conf. on Lightning and Static Electricity* (Dayton, OH)
- Mazur V and Ruhnke L H (ed) 2013 *Heinz Wolfram Kasemir: His Collected Works* (New York: Wiley) pp 547–55 (Engl. transl.)
- Krehbiel P R 1981 An analysis of the electric field-change produced by lightning *PhD Thesis* New Mexico Institute of Mining and Technology, Socorro
- Krehbiel P R, Brook M and McCrory R A 1979 An analysis of the charge structure of lightning discharges to ground *J. Geophys. Res.* **84** 2432–456
- Krehbiel P R, Tennis R, Brook M, Holmes E W and Comes R 1984 A comparative study of the initial sequence of lightning in a small Florida thunderstorm *Proc. 8th Int. Conf. on Atmospheric Electricity (Albany, NY, June)* pp 279–85
- Krider E P 1989 Electric field changes and cloud electrical structure *J. Geophys. Res.* **94** 13145–9
- Malan D J 1963 *Physics of Lightning* (London: English University Press) pp 46–56
- Mazur V and Ruhnke L H 1993 Common physical processes in natural and artificially triggered lightning *J. Geophys. Res.* **98** 12913–30
- Proctor D E, Uytenbogaardt R and Meredith B M 1988 VHF radio pictures of lightning flashes to ground *J. Geophys. Res.* **93** 12683–727
- Proctor D E 1991 Regions where lightning flashes began *J. Geophys. Res.* **96** 5099–112
- Schonland B F J 1938 Progressive lightning. IV. The discharge mechanism *Proc. R. Soc. London A* **164** 132–50
- Stratton J A 1941 *Electromagnetic Theory* (New York: McGraw-Hill)
- Uman M 1987 *The Lightning Discharge* (San Diego, CA: Academic)

Principles of Lightning Physics

Vladislav Mazur

Chapter 4

Verifying the concept of the bidirectional leader

4.1 How studying lightning strikes to aircraft has helped to solve the puzzle of lightning development

The study of lightning–aircraft interaction was a case when the need to find an engineering solution to a problem that involved natural phenomena led to the opening of new horizons in basic research. In the early 1980s, revolutionary developments in the field of materials science made it possible to design and build lighter commercial and military aircraft, by utilizing composite materials for parts of the fuselage. Similarly, major advances in computer technology led to the incorporation of sophisticated computer-driven components into the aircraft’s navigational, control, and weapons systems, using low-voltage microchips. The expectation, however, was that both trends would make the aircraft susceptible to serious direct and indirect lightning hazards, either by the penetration of lightning current during lightning attachment to it, or through the induced effects from the electromagnetic field transients produced by a nearby lightning flash. Lightning strikes to a flying aircraft, though rarely fatal, can be quite debilitating, making it difficult or impossible for the aircraft to continue its mission, because of the devastating effects on its vital systems.

The problems associated with the triggering of lightning by rockets were addressed, beginning in 1960, by Heinz-Wolfram Kasemir, in technical reports and conference presentations (Kasemir 2013). The speculation that an aircraft might trigger lightning was based on observed cases of such strikes that occurred during penetrations of an electrified cloud without detectable lightning activity (Fitzgerald 1967, Cobb and Holitzka 1968). However, the evidence was purely circumstantial. The then-prevailing explanation of lightning strikes to aircraft was that the aircraft attracted the IC lightning flash that was occurring nearby, similarly to the way in which a lightning rod draws the lightning to itself (e.g. Rustan *et al* 1985). The need to evaluate all aspects of lightning–aircraft interaction, and to design effective lightning protection for both the aircraft’s frame and its electronics, became the objective of three important research



Figure 4.1. NASA F-106B research aircraft conducted thunderstorm penetrations as part of the NASA Storm Hazards program (1980–6), with a total of 620 triggered lightning strikes obtained. Courtesy of NASA.

programs, two in the United States and one in France, during the course of eight years (1980–8) (Mazur 1993).

In each research program, special lightning-hardened aircraft (the NASA F-106B (figure 4.1)), the French C-160, and the USAF/FAA CV 580), with sophisticated observational and recording systems aboard, flew through thunderstorms in attempts to draw a lightning strike. The NASA Storm Hazards Program (1980–6) implemented the most successful strategy for obtaining lightning strikes to aircraft; this strategy involved guiding the aircraft into the region of the storm where lightning flashes had been detected by UHF radar, and monitoring the radar returns in the vicinity of the aircraft with the lightning-detecting UHF-band radar.

4.1.1 Lightning radar echo

As a research tool for the study of lightning, radar was first used in the 1950s (Ligda 1956), and later in the 1970s and 80s (Williams *et al* 1990). How does radar detect lightning? It was mentioned, in chapter 2, that lightning channels made of plasma, with a high density of free electrons, would backscatter the electromagnetic waves transmitted by radars, and that the backscattering signal (also called a *radar echo*) can be as strong as if the lightning channels were made of metal. There are several factors that affect the strength of a radar echo from any object, besides its material properties. The most obvious factor is the power transmitted by the radar (the greater the power, the stronger the radar echo). The strength of the lightning radar echo would depend on the radar's wavelength, and also on the plasma density and the dimensions and orientation of the lightning channels that together constitute the so-called *radar cross-section*. We can imagine a lightning channel as the equivalent of a metal wire a couple of centimeters in diameter (approximately that of the current-carrying core), and hundreds of meters long in the branching structure. Considering the size of the radar beam and the possible length of the lightning channels, the radar cross-section of lightning could be from several to tens of square meters. This is comparable to, or even greater than, the radar cross-section values

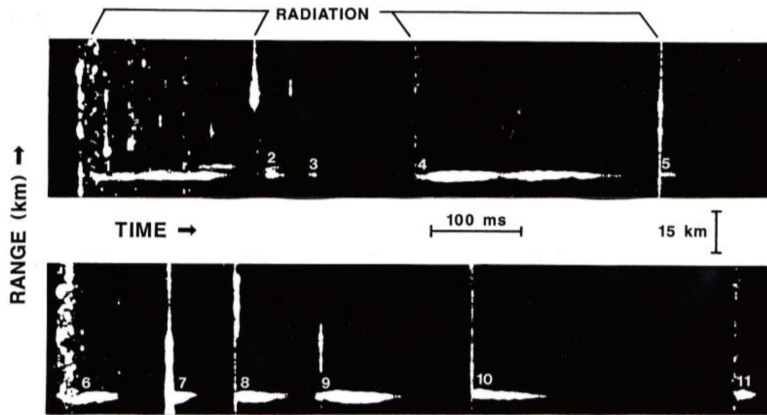


Figure 4.2. Lightning echo of a multi-stroke (presumably CG) flash obtained with a VHF-band radar (wavelength of 2 m). The image, made by a camera with continuous film movement, is from an A-scope of the radar using Z-axis modulation. Numbers mark echoes of the sequence of leader-return strokes. Radiation produced by a stepped or dart leader accompanies the lightning echoes, and coincides with echo onset. Reproduced from Mazur and Rust (1983). Copyright 1983 by John Wiley Sons, Inc. Reprinted by permission of John Wiley & Sons, Inc.

for modern aircraft. The lower the plasma density, the longer the wavelength of the incoming wave must be to produce a noticeable radar echo. Therefore, lightning channels carrying currents of hundreds of amperes, and having plasma density greater than 10^{19} electrons per m^3 , may be easily detected by radars of all ranges of wavelengths, from millimeters to meters (figure 4.2). After the current flow stops, the plasma density of a lightning channel, along with its backscattering signal, rapidly decreases.

The next question is: how can the radar ‘see’ lightning inside a thundercloud that is composed of water vapor and precipitation particles of various sizes? Because the transmitted electromagnetic waves are scattered by objects with dimensions that approximate or exceed the radar’s wavelength, there is an advantage to using radars with longer wavelengths (of decimeters and meters), which are much longer than the dimensions of the precipitation particles, to detect lightning channels that may be hidden inside a cloud. Long-wavelength radar can ‘see’ through the cloud with the ability to detect lightning—the proverbial ‘needle in a haystack’—while radars with much shorter wavelengths obtain mostly echoes composed of those from both the cloud particles and the lightning plasma channels. These combined returns can be very convoluted and, thus, quite difficult to separate into two distinct types of signals.

During storm penetrations by the NASA F-106B research aircraft, a ground C-band radar tracked its transponder’s signal, and the azimuth and elevation of the C-band antenna was synchronized (‘slaved’) with those of the UHF-band radar (figure 4.3). This arrangement allowed the radar beam of the UHF-band radar to remain ‘glued’ to the aircraft throughout the storm penetration and—this is

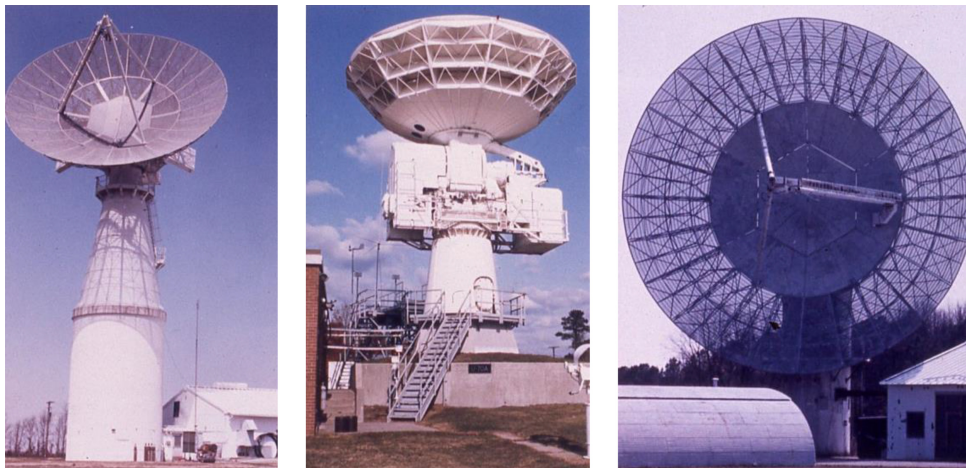


Figure 4.3. Three radars at the NASA Wallops Flight Facility, Wallops Island, Virginia, used for directing (S-band radar, left), tracking (C-band radar, center), and guiding (UHF radar, right) the NASA F-106B research aircraft in thunderstorm penetrations. Courtesy of NASA.

crucial—also to observe echo signals from the lightning channels in the close vicinity of the aircraft, all within the radar beam.

Each time the aircraft was struck by lightning, the radar obtained a combined echo signal from both the aircraft and the lightning (figure 4.4); however, not every case of the overlapping aircraft and lightning echoes corresponded to a confirmed lightning strike to the aircraft.

In the absolute majority of the cases (~80%) of lightning attachment to the research aircraft, the time sequences of the radar returns of the UHF radar showed the buildup of the lightning echo above the echo from the airplane. What followed was either the development of the lightning echo bidirectionally from the location of the aircraft echo (as in case 1 in figure 4.4), or unidirectionally (as in case 2 in figure 4.4). These dynamics are indicative of lightning initiated (triggered) by the aircraft itself. In the cases of a lightning flash passing near the aircraft, its radar echo first appears at some distance away from the aircraft's echo, moves toward it, and then passes by.

Records of the UHF-band radar returns, like those in figure 4.4, provided the first direct and indisputable evidence of aircraft-triggered lightning strikes (Mazur *et al* 1984). With the installation of conventional and high-speed video cameras on the NASA F-106B and French C-160 research aircraft, respectively, it became possible to confirm lightning initiation on an aircraft visually, as a process of the bidirectional development of bipolar leaders from an aircraft's extremities (Mazur, 1989, Moreau *et al* 1992) (see the example in figure 4.5). Video images showing the development of a lightning flash triggered by the NASA F-106B aircraft can be found in the appendix, figures A.3–A6.

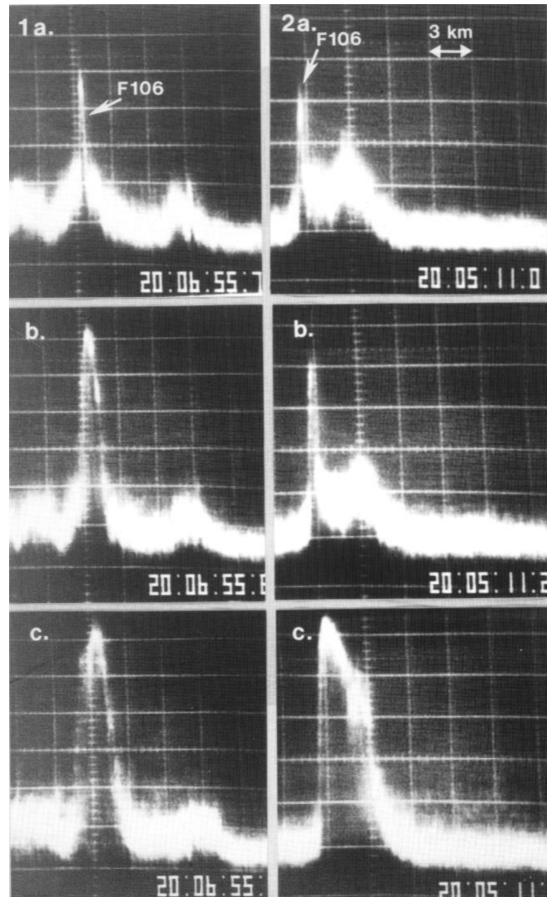


Figure 4.4. Examples of UHF radar echo time sequences, from the NASA F-106B airplane triggering a lightning flash during a thunderstorm penetration. The radar echoes of the airplane and lightning are seen on a background of the much weaker radar return from the penetrated cloud. Time is shown in h:min:s. Case 1: bidirectional radar echo development of a lightning flash triggered by the aircraft. Case 2: unidirectional radar echo of a lightning flash triggered by the aircraft. Reproduced from Mazur *et al* (1984). Reprinted by permission of the American Institute of Aeronautics and Astronautics, Inc.

4.2 How does an aircraft trigger lightning?

The importance of the discovery, in the 1980s, that an aircraft triggers lightning cannot be overestimated, since the prevailing hypotheses had suggested that aircraft attract nearby natural lightning in the same way that a lightning rod does. This discovery verified earlier speculations by some scientists that the nature of a lightning–aircraft interaction was not simply an occasional occurrence. So, the next logical question is: how does this happen and how is this phenomenon to be verified by airborne measurements?

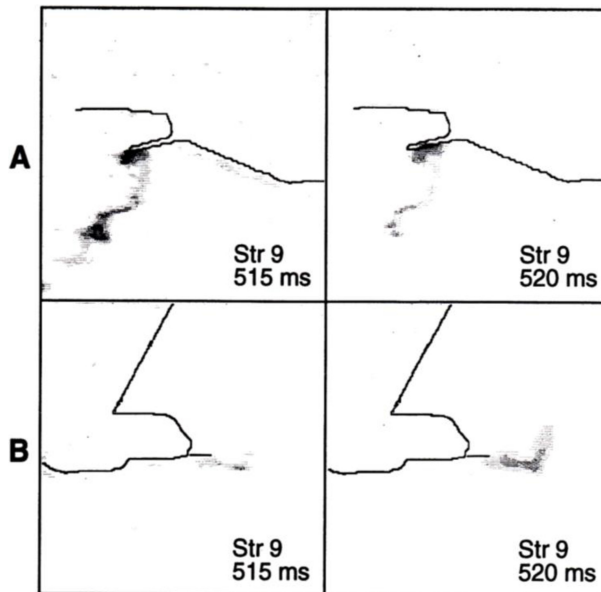


Figure 4.5. The first two video frames (images inverted) of the simultaneous development of a bidirectional leader from the extremities of the C-160 aircraft, obtained with a high-speed video camera (200 fps) installed under the right wing. (A) The view of the tail boom and tail section of the fuselage; (B) the view of the nose boom and right wing). Reproduced from Moreau *et al* (1992). Copyright 1992 by John Wiley Sons, Inc. Reprinted by permission of John Wiley & Sons, Inc.

A research aircraft presents us with the opportunity to install on board multiple sensors, to record the characteristics of currents and the electric and magnetic fields, both during initiation as well as during the development of lightning, while it is still attached to the aircraft. This is equivalent to placing sensors inside a lightning channel. Video cameras at key locations on the aircraft also allow us to obtain images of the lightning channel at very close range. This is truly a rare opportunity.

Confirmation, from the radar echo analysis, of the lightning's initiation on the aircraft provided a major clue and starting point for a physical concept to apply to the interpretation of records from the multiple sensors on board. The *correct* physical concept would allow all the airborne measurements from the variety of sensors to fit perfectly together.

That physical concept was Heinz Kasemir's (1950) proposed concept of a *bidirectional, bipolar, and uncharged leader* starting from a nucleus in an ambient electric field.

A metal aircraft penetrating a thunderstorm is an *electrically floating* conductor, which means that it is not physically connected to any external source of electric power. Outside the electric field, a conductor is either zero-charged or uniformly charged (e.g. as the result of triboelectric charging of a flying aircraft in a clear sky). Within the ambient electric field, the conductor becomes an *electrical dipole* by means of *electrostatic induction*, with the maximum positive and negative charges at the extremities of the conductor. In the case of a symmetrical conductor previously uncharged, the induced charges decrease toward its middle, and a zero-charge point

is at the exact middle. The net charge on the conductor remains unchanged after insertion into the electric field; it is simply distributed differently than before (zero charge everywhere). When a bidirectional leader emerges from the conductor, it remains an electrically floating dipole, with its charges preserved.

A bidirectional leader is composed of two leaders: the leader that carries positive charges, and starts from the extremity of the nucleus with the maximum positive charges and, therefore, the highest positive electric field; and the leader that carries negative charges, and starts from the extremity with the maximum negative charges and, therefore, the highest negative electric field.

Analyses of the airborne records of electric field changes and current on an FAA CV-580 airplane have shown that initiation of the positive leader usually starts first, followed in a few milliseconds by initiation of the negative leader (see figure 4.5). As determined from laboratory studies of leader formation (referred to in chapter 1), the magnitude of the ambient electric field required to support propagation of the positive leader ($\sim 450 \text{ kV m}^{-1}$) is lower than that for the negative leader ($\sim 750 \text{ kV m}^{-1}$). Because a flying aircraft moves away from the space charge being emitted from its own extremities, the streamer-leader transition is not inhibited ('choked') by the space charge of the corona streamers.

Each stage of bidirectional leader development on an aircraft has a distinctly different signature in its electric field and current records (figure 4.6). The positive leader exiting an aircraft's extremity produces a negative electric field change on the aircraft (marked as stage 1 in figure 4.6(A)), so as to maintain an unchanging net charge. The continuing current of the positive leader during this period is in the range of tens of amperes; it is seen in the current record in figure 4.6(B) as being much lower than the sensor's threshold of $\sim 250 \text{ A}$. A positive change in the electric field occurs next, during stage 2 in figure 4.6(A). It indicates the beginning of the formation of a negative leader that exits the aircraft from the other, opposite extremity. Shortly after the beginning of stage 2, the impulse current that characterizes development of the negative stepped leader is seen in figures 4.6 (C) and (D) superimposed on the continuing current of the positive leader, at stage 3 in figure 4.6(A). At this time, the bidirectional and bipolar leader is established. From airborne current measurements with broadband recorders, the pulses of the negative leader's current are shown to have peak amplitudes of up to 20 kA , and the duration of a fraction of microseconds (Mazur 1989).

The development of a bidirectional leader from an aircraft, seemingly simultaneous in both directions, actually occurs initially in sequential stages of extension of the bipolar leader from the oppositely charged aircraft extremities. Note, in the electric field record in figure 4.5(A), that development of the negatively charged leader started $\sim 3 \text{ ms}$ after the positively charged leader. There is an explanation for this phenomenon: the positive (or negative) part of a bipolar leader that emerges first from one aircraft extremity increases the overall length of the conductor, which is composed of the aircraft plus the newly formed part of the leader channel. To maintain the net charge of the emerging electrodeless conductor, the charges on the opposite polarity of the aircraft will grow, thus increasing the voltage there to a breakdown level, sufficient to start the leader of the opposite polarity to the one that

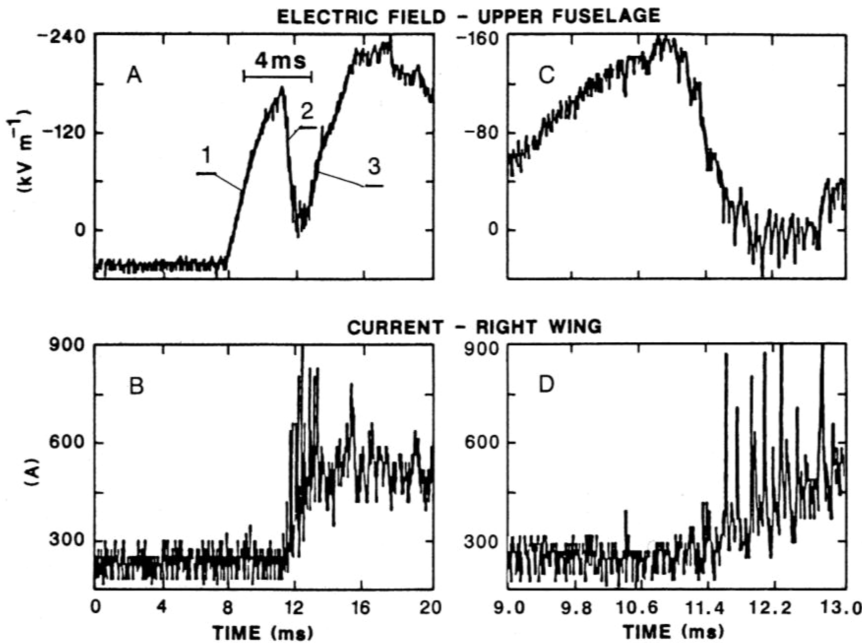


Figure 4.6. A typical example of (A) the electric field and (B) the current records during initiation of a lightning flash on an FAA CV-580 storm-penetrating aircraft. (C) and (D) are 4 ms extensions of records (A) and (B), respectively. The numbers in (A) identify three distinct stages of electric field development: (1) the positive-leader stage, (2) the negative-leader stage, and (3) the established bidirectional-leader stage. Reproduced from Mazur (1989). Copyright 1989 by John Wiley Sons, Inc. Reprinted by permission of John Wiley & Sons, Inc.

occurred earlier. This process, illustrated in figure 4.6, takes some time, due to the capacitance of the aircraft. Shortly after starting on the aircraft, this process becomes self-propagating, i.e. it is governed by the ambient electrical conditions at the tips of the bipolar leaders, even if the leader channels are still attached to the aircraft (figure 4.7).

Most lightning flashes, after starting on a flying aircraft, develop into regular IC flashes while remaining connected to the aircraft for hundreds of milliseconds, until the aircraft, which pulls the lightning channel behind it, breaks away from the lightning. (After the initiation of a flash, an aircraft has no further influence on its development.)

An aircraft-triggered lightning flash may also become CG lightning, but this can only happen when the aircraft is flying at altitudes below 7 km (Mazur *et al* 1990). A rare documented example of such an occurrence is shown in figure 4.8. The long period of lightning attachment presents a unique opportunity for researchers to study the features of lightning flashes directly ‘inside’ the lightning channel.

Among the characteristics of IC flashes recorded following lightning initiation on a research aircraft are the slowly varying DC-type continuing current of several hundreds of amperes and, superimposed on it, the occasional current pulses of up to several thousands of amperes. These are unique data, never before

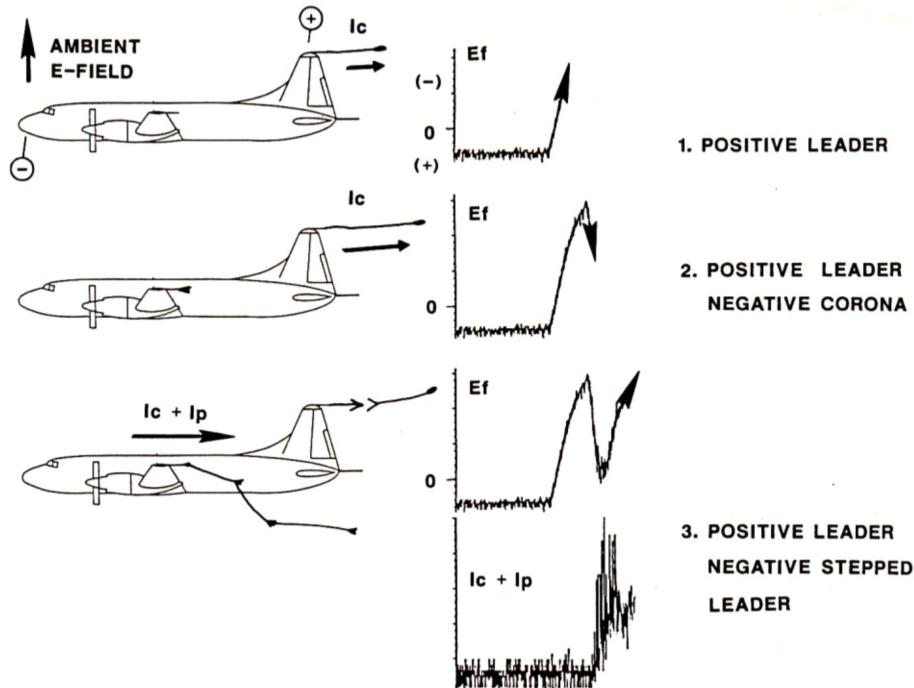


Figure 4.7. Conceptual sketches depicting the three stages of lightning initiation on the CV-580 airplane. Attachment points are the vertical stabilizer for the positive leader and the left wing-tip for the negative leader. The stages of attachment are identified in the electric field and current records in figure 4.6. Reproduced from Mazur (1989). Copyright 1989 by John Wiley Sons, Inc. Reprinted by permission of John Wiley & Sons, Inc.

available, on the current of IC flashes (figure 4.9), clearly showing that the continuing current is an indication of, and part of, the developing leader. The current pulses are associated with so-called M-events (Mazur *et al* 1995), resulting from attachment to the conducting channel of recoil leaders in the decayed branches of the positively charged part of the bidirectional leader. (See chapter 9 for more about this phenomenon.)

4.3 Environmental conditions that lead to aircraft-triggered lightning

The significant enhancement of the electric field at the extremities of an aircraft occurs because of the aircraft's dimensions and the sharpness of the tips and edges of its extremities. The aircraft's size also determines its *capacitance* to store the electric charge that feeds the initial bipolar leader. The large dimensions of an aircraft make it easier for it to become a nucleus for lightning initiation in an ambient electric field, which is lower than the breakdown electric field. We have also learned, from the analysis of the environmental conditions during storm penetrations by the NASA F-106B aircraft (Mazur *et al* 1984), that the probability of triggered lightning decreases with an increasing rate of natural lightning. In a recorded voice log from the NASA F-106B, pilots reported that during some storm penetrations the visually

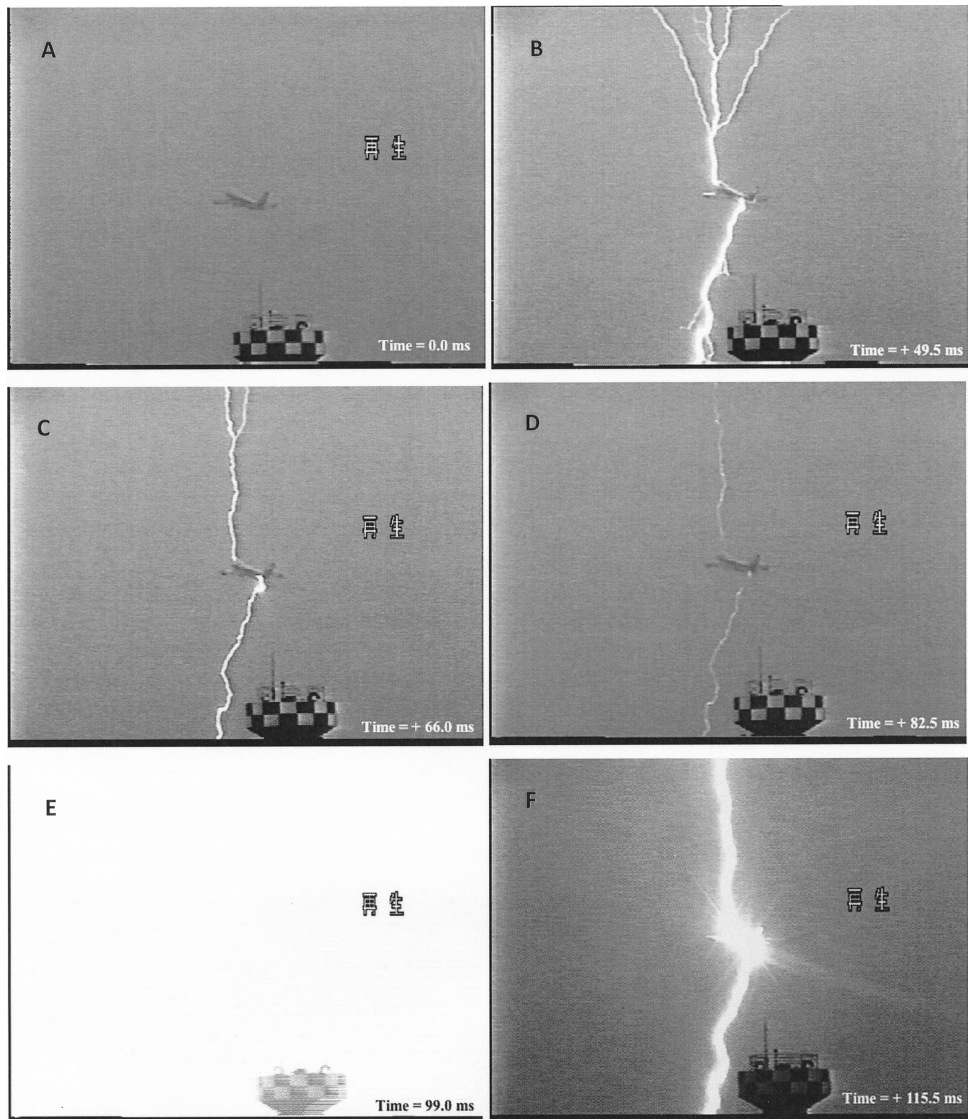


Figure 4.8. A sequence of video fields (halves of the video frames) obtained for an aircraft-triggered, multi-stroke CG flash, during a takeoff from an airport on the east coast of Japan in a decaying winter storm. The video images were recorded by a ground observer with a conventional video camera. (A) An aircraft taking off at Komatsu AFB, Japan. (B) A bidirectional lightning leader initiated by the aircraft, and the return stroke that immediately followed. The upward part is a positive and the downward part is a negative leader. The return stroke brightens parts of both leaders. (C) A continuing current in the established channel to ground. (D) A continuing current still flows in the established channel to ground. (E) The second return stroke is much more powerful than the first one. (F) A continuing current in the established channel to ground. Courtesy of Z-I Kawasaki.

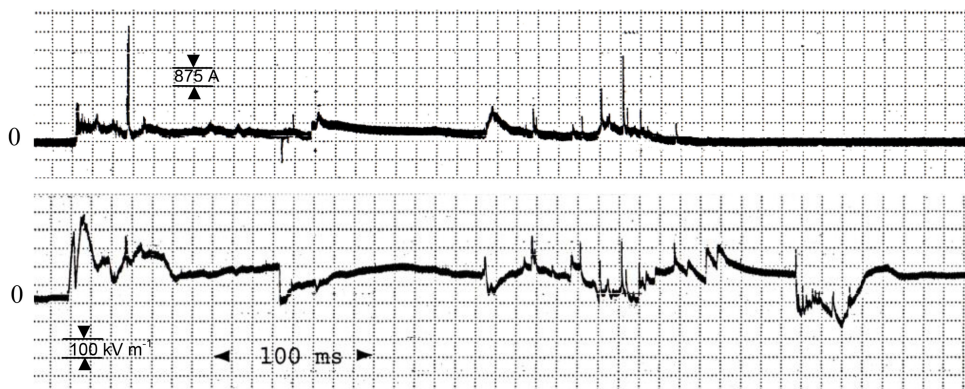


Figure 4.9. Electric field and current waveforms (lower and upper records, respectively) during development of a lightning flash triggered by the FAA CV-580 research airplane. The individual upward (negative) spikes in the electric field record after lightning initiation correspond to recoil leaders attaching to the conducting leader channel (M-events). These pulses are seen in the current record, superimposed on the continuous current. Reproduced from Mazur (1989). Copyright 1989 by John Wiley Sons, Inc. Reprinted by permission of John Wiley & Sons, Inc.

observed lightning rate around the aircraft was so high that ‘it looked like Fourth of July fireworks’, but the aircraft itself did not trigger any lightning. In contrast, penetrations by aircraft in decaying thunderstorms very frequently led to triggered lightning. These observations certainly confirm that it takes a considerably weaker ambient electric field to initiate lightning from such a sizable nucleus as an aircraft than it would to initiate natural lightning in a decaying thunderstorm that has no natural lightning activity.

4.3.1 Hypothesis of a natural lightning-triggering mechanism in thunderstorms

The seemingly paradoxical phenomenon of the lower probability of triggering lightning by an aircraft when penetrating an active, i.e. lightning-producing, thunderstorm, than when penetrating a decaying storm with no lightning activity, may be understood if we try to imagine the existence of a ‘natural lightning-triggering mechanism’ in thunderstorms. A hypothesis about such a lightning-triggering mechanism was presented in Mazur (1986). It was based on the interpretation of rapidly occurring, quasi-stationary echoes (detected by VHF-band radar) of small radar cross-sections of a few square meters, and thus the length on the order of tens of meters. They occurred in a thunderstorm characterized, otherwise, by an extremely high rate of full-length lightning flashes. The presence of almost-stationary ‘baby lightning’ echoes, appearing very frequently (up to 200 per minute), was perceived as an indication of triggering attempts for full-length lightning flashes.

The sustained propagation of a bidirectional leader in the cloud requires that certain electrical conditions (described in chapter 1) be present ahead of the leader, along its entire path. In the absence of these conditions (namely, a sufficient ambient electric field), the bidirectional leader, ignited by a still-unknown mechanism, will

terminate soon after initiation, or will produce, instead, ‘baby lightning’ flashes like those described in Mazur (1986).

Each lightning flash diminishes the electrical energy stored in the cloud and also changes the distribution of the ambient electric field, most noticeably in the close proximity of the lightning channel. It takes some ‘recovery’ time (seconds, or even tens of seconds) for the continuing process of cloud electrification to ‘restore’ this energy, and to bring the ambient electric field of the cloud to a level sufficient to support self-propagation of the next full-length lightning flash. It is reasonable to assume that, if the triggering conditions occur only in a small region of the cloud before leader-propagation conditions are in place in the much-larger cloud scale, the development of a regular lightning flash cannot occur. Thus, the formation of a full-length lightning flash may be considered as a two-phase process: (1) the phase of leader initiation in a region of a cloud with some specific electrical and microphysical conditions (required in order to be identified as a triggering mechanism); and (2) the phase of bidirectional leader development in the cloud scale after the so-called electric field recovery period.

The timing of these two phases is not synchronized. When the two stages of lightning formation are in sync, each triggering event will lead to a fully developed lightning flash. Try to imagine a situation when the conditions for the initiation of leaders occur more often than those for the restored electrical field in the larger scale, i.e. the natural lightning-triggering mechanism is very active. Then, many more small-scale ‘baby lightning’ flashes will occur than full-length lightning flashes. Thus, in the case of a high rate of natural lightning flashes, any additional source for lightning-triggering, such as an aircraft penetrating the storm, may be ‘out-of-sync’ with the electric field regeneration in the cloud, and so will be ignored. Alternatively, during the decaying stage of the storm, the cloud is still electrified; that is, the ambient electric field is still strong, but the natural lightning-triggering mechanism is either very weak, or dead (evidence of this is the lack of lightning activity). At this stage, an aircraft penetrating the storm becomes the likely source of lightning initiation, due to its conductivity and size.

A good analogy for the two stages in the development of a full-length lightning flash in a thunderstorm is a gas-filled thyratron (figure 4.10), where the gap between the cathode and the grid serves as a stage for triggering the arc discharge in the larger gap between the cathode and the anode. This arc discharge is the analog of a full-length lightning flash. Without the positive voltage applied to the anode, the arc discharge in the big gap will not occur, even if a triggering voltage is applied to the grid.

In line with this interpretation of the two-stage lightning-triggering mechanism are the observations of 620 lightning strikes to a storm-penetrating aircraft from the NASA Storm Hazards Program (1980–6), which show that the probability of aircraft-triggered lightning is at its highest during the decaying stage of a thunderstorm that includes marginally electrified clouds which did not produce natural lightning. The same conclusion comes from the commercial airline pilots’ surveys and investigations of a few cases of lightning strikes to ascending space vehicles in the United States (e.g. Christian *et al* 1989).

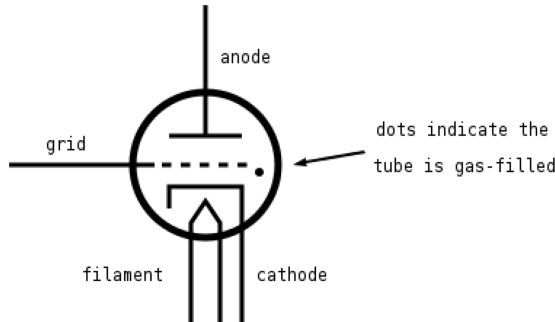


Figure 4.10. A hot-cathode thyratron, with positive voltage applied to the anode, a negative cathode, and the grid as an electrode that controls, by trigger voltage, the occurrence of an arc discharge between the cathode and the anode.

The verification of Kasemir's bidirectional uncharged leader concept, obtained in the course of the investigation of lightning-aircraft interaction, provided stimulation for the development and proliferation of a new type of rocket-triggered lightning technique, so-called 'altitude-triggered lightning', in the 1990s (Laroche *et al* 1991). This technique was in addition to the classic rocket-triggered lightning technique introduced in the 1970s (Rakov and Uman 2003). See chapter 7 for more about this issue.

References

- Christian H J, Mazur V, Fisher B D, Ruhnke L H, Crouch K and Perala R P 1989 The Atlas/centaur lightning strike incident *J. Geophys. Res.* **94** 13169–77
- Cobb W E and Holitzka F J 1968 A note on lightning strikes to aircraft *Mon. Weather Rev.* **96** 807–8
- Fitzgerald D R 1967 Probable aircraft 'triggering' of lightning in certain thunderstorms *Mon. Weather Rev.* **95** 835–42
- Kasemir H W 1950 Qualitative Uebersicht ueber Potential-, Feld-, und Ladungsverhaltnisse bei einer Blitzentladung in der Gewitterwolke *Das Gewitter* ed H Israel (Leipzig: Akademische Verlagsgesellschaft)
- Mazur V and Ruhnke L H (ed) 2013 *Heinz Wolfram Kasemir: His Collected Works* (New York: Wiley) pp 398–411 (Engl. transl.)
- Laroche P, Idone V, Eybert-Berard A and Barret L 1991 Observations of b-directional leader development in a triggered lightning flash *Proc. Int. Conf. on Lightning and Static Electricity* (Cocoa Beach, FL) pp 57/1–10
- Ligda M G H 1956 The radar observations of lightning *J. Atmos. Terr. Phys.* **9** 329–46
- Mazur V and Rust D W 1983 Lightning propagation and flash density in squall lines as determined with radar *J. Geophys. Res.* **88** 1495–502
- Mazur V, Fisher B D and Gerlach J C 1984 Lightning strikes to an airplane in a thunderstorm *J. Aircraft* **21** 607–11
- Mazur V 1986 Rapidly occurring short duration discharges in thunderstorms, as indicators of a lightning-triggering mechanism *GRL* **13** 355–8
- Mazur V 1989 A physical model of lightning initiation on aircraft in thunderstorms *J. Geophys. Res.* **94** 3326–40

- Mazur V, Fisher B D and Brown P W 1990 Multistroke cloud-to-ground strike to the NASA F-106B airplane *J. Geophys. Res.* **95** 5471–84
- Mazur V 1993 Lightning threat to aircraft: do we know all we need to know *J. Aircraft* **30** 156–9
- Mazur V, Krehbel P R and Shao X-M 1995 Correlated high-speed video and radio interferometric observations of a CG flash *J. Geophys. Res.* **100** 25731–53
- Moreau J-P, Alliot J-C and Mazur V 1992 Aircraft lightning initiation and interception from *in situ* electric measurements and fast video observations *J. Geophys. Res.* **97** 15903–13
- Rakov V A and Uman M A 2003 *Lightning Physics and Effects* (Cambridge: Cambridge University Press) ch 10
- Rustan P L, Kuhlman B and Reazer J M 1985 Airborne and ground electromagnetic field measurements of lightning *Proc. 10th Int. Aerospace and Ground Conf. on Lightning and Static Electricity (Paris, June)* pp 253–58
- Williams E R, Mazur V and Geotis S G 1990 Lightning investigation with radar *Radar in Meteorology* ed D Atlas (Boston, MA: American Meteorological Society) ch 18, pp 143–9

Principles of Lightning Physics

Vladislav Mazur

Chapter 5

Defining the types of lightning

5.1 The visible features of lightning flashes

Lightning in nature (or, as we should call it, *natural lightning*) originates in a thundercloud, and can be of two basic categories: CG and IC *flashes*, depending on whether the lightning either touches, or does not touch, the ground. The tendency to differentiate natural lightning even further, e.g. as cloud-to-cloud or cloud-to-air flashes etc, only confuses the issue. The major difference exists between the basic lightning processes that occur before and following either the attachment of a lightning leader to the ground, or the termination of a leader anywhere above the ground. In those lightning flashes that do not make contact with the ground, the physical processes are all essentially the same, and therefore belong to the same category—that of IC flashes.

Somewhat different from these two main categories of lightning flashes are those flashes that start from a structure on the ground, or from a structure suspended in the air (such as a rocket, or an aircraft). Lightning flashes triggered by a flying aircraft (see chapter 4) and lightning that starts from a tall structure (see chapter 7) belong to the same category, called *structure-triggered lightning*. Rocket-triggered lightning flashes (see chapter 7) also belong to this category. Initiation of these lightning flashes would not occur without exposure of the structure to the ambient electric field of the thunderstorm, and it is also strongly affected by the object itself. To be clear, for example: if no structure were installed at a given location, the probability that natural lightning would strike this location would be less than the probability of structure-triggered lightning starting at this location with a tower there.

The visible parts of a CG lightning flash are the luminous leader channels that extend below the bottom of the cloud and towards the ground. Most IC flashes develop inside the cloud, so their channels remain hidden, with occasional bursts of light illuminating the cloud. Sometimes, channels of IC lightning can be seen in the cloud openings, or even propagating outside the cloud. The flashes during the decaying stage of thunderstorms with visible channels below the cloud base used to



Figure 5.1. So-called spider lightning observed during the late stages of thunderstorms. Courtesy of Kevin Ambrose.

be called ‘spider lightning’, for their multiple, stratified long ‘fingers’ that resemble spiders (figure 5.1). However, they were later found to be negatively charged leaders of IC flashes, or IC parts of CG flashes, with their appearance determined by the space charge, which is different from that in the earlier, mature stage of the storm (Mazur *et al* 1998).

Traditional definitions of the types of lightning flashes in the lightning literature have been based on the direction of propagation of visible leader channels, and the polarity of charges carried by those leaders. The obvious limitations in this approach leave us only with a clear definition of CG flashes, the channels of which we can easily observe below the cloud base.

The visual impression of a downward leader emerging from a cloud fits well intuitively with the ‘space charge leader’ concept of cloud charges flowing into a leader channel. Interpretations of natural lightning based on the ‘space charge leader’ concept are still to be found today (see figure 5.2), even as recently as in a publication on the physics of lightning (Dwyer and Uman 2013), where the following quotation appears: ‘negative CG flashes … are initiated by a negatively-charged, downward-propagating leader, and result in the lowering of negative charge from the main negative charge region in the middle part of the cloud to the ground.’ A similar interpretation, from the same publication, is given for positive CG flashes, in figure 5.2.

If, instead of relying upon the naked eye, we use a camera with a high-speed shutter, or with film that moves continuously in the so-called ‘streak mode’, we will see the dynamics of a CG flash, with the direction of movement clearly identified. Furthermore, were we to use more sensitive film in the camera, we would discover

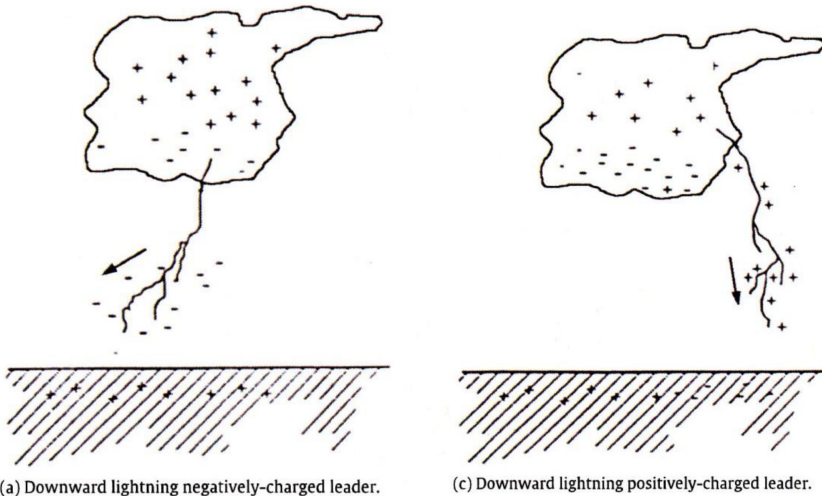


Figure 5.2. Two types of CG flashes, as defined from the direction of leader progression and the charge of the initiating leader. Adapted with permission from Dwyer and Uman (2013). Copyright 2013 Elsevier.

that a faintly luminous path of a lightning leader, often with many downward-extending branches, descends from the cloud toward the ground, prior to reaching it. As one of the branches contacts the ground, a wave of very bright luminosity travels upward along the previously visible branched leader channel, and then illuminates the cloud from inside. This wave is called the *return stroke* of the CG flash. The name itself indicates the fact of its propagation from the ground up, *returning to the origin of the flash*. This is an important fact to keep in mind.

A return stroke is similar to an arc discharge between two ‘electrodes’: an elongated electrode made of the plasma leader channel emerging from the cloud, its voltage in millions of volts, and the ground electrode, which is an object on the ground, its voltage zero. An analog of the return stroke, in the small scale of a high-voltage chamber, is the arc that occurs when the leader from a high-voltage electrode touches the ground plate. Because the path of a leader channel with downward branches is already ionized before the touchdown, it serves as a path for the return stroke as it propagates upward. In identifying the polarity of CG flashes, the polarity of the charges carried by the leader to the ground determines the polarity of the flash.

The return stroke, carrying current of tens of kiloamperes, heats and re-illuminates the branches of the preceding downward leaders on its way back upward, with the channel-to-ground illuminated most brightly, and also illuminates the portion of the cloud where the upper part of the bipolar leader channel is hidden from the eyes of the observer. In negative CG flashes return strokes carry a positive charge, and in positive CG flashes the return stroke carries upward a negative charge along the ionized path of the preceding downward leaders to ground. The speed of propagation of these return strokes approaches the speed of light.

Negative leaders, both in nature and in the laboratory, propagate in ‘steps’, or by increments of variable length and changing direction. The step lengths in a negative

leader in nature vary from tens to hundreds of meters long, depending on the potential drop at the tip of the leader $\Delta\Phi_T$ and the critical field E_{cr} needed for negative-streamer propagation (see (1.1) in chapter 1). Each new step tends to deviate from the direction of the previous step by some small angle. Positive leaders, on the other hand, typically propagate in a continuous fashion.

One may easily determine the direction of leader motion from visual observations of an illuminated lightning structure. The direction of branching away from the trunk is always that of lightning propagation. For example, a visible branching downward characterizes leaders of CG flashes, and visible upward branching characterizes those that originate on a ground structure. In the video frame in figure 5.3, one may clearly identify the upward-branching and downward-branching leaders that started on the aircraft, which means that the depicted lightning strike was aircraft-triggered.

The branching structures of positive and negative leaders are distinctly different from each other. They are more dendritic, with prevailing smaller-sized branches in negative leaders, and fewer and much-longer branches in positive leaders.

Observations of negative CG flashes with the naked eye reveal multiple re-illuminations of the channel to ground, sometimes as a flickering, sometimes as an appearance, with intervals of tens of milliseconds, of distinct time-separated channels. (The human eye can distinguish the time separation between visual events when it is longer than $1/25$ s, or 40 ms.) The phenomena we are describing here are *multiple return strokes* of a lightning flash that emerge from the same region in the cloud. We call this a *multi-stroke CG lightning flash*.

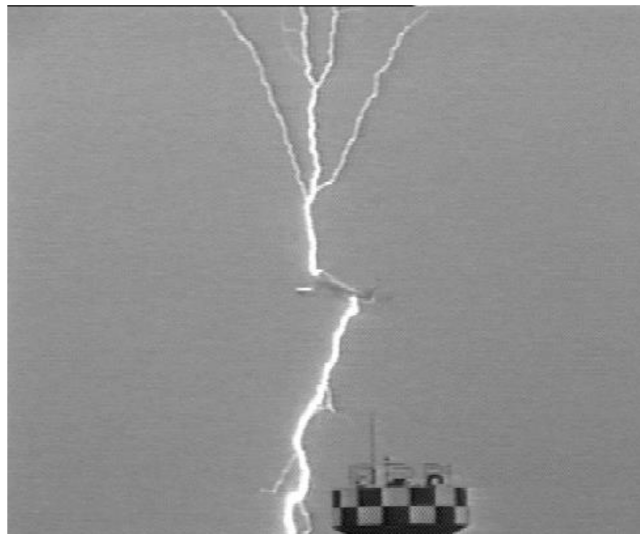


Figure 5.3. A bidirectional lightning leader initiated by an aircraft. The upward part is a positively charged and the downward part a negatively charged part of the leader. (A video frame of an aircraft-triggered CG flash, from the sequence in figure 4.7.) Courtesy of Z-I Kawasaki.

The luminosity of the return stroke channel totally ceases in the intervals between sequential return strokes, suggesting that the channel does not carry a sufficient current to keep it illuminated. This phenomenon is called *current cutoff*. The inter-stroke interval ends when a very fast, and usually non-branched and non-stepping, downward leader (called the *dart leader*) emerges from the cloud. A new return stroke starts upon the dart leader's contact with the ground. Several cycles (the number can be up to two dozen), each consisting of the downward negatively charged leader and the return stroke, may take place during development of the same multi-stroke lightning flash to the ground. The intervals between each leader-return stroke cycle vary from a few milliseconds to two hundred milliseconds—the assumed threshold value required to separate multiple cycles in the same flash from two sequential, unrelated flashes. The most important fact about multi-stroke CG flashes is that they are all of negative polarity. Overwhelming evidence exists that positive CG flashes have only a single return stroke. We will elaborate on this in chapters 9 and 10.

Similar to the first return stroke that follows along the stepped leader channel upward, a downward dart leader propagates (most of the time) along the channel of the previous return stroke, because leaders and return strokes in multi-stroke CG flashes share either a part, or the entire length, of the common ionized path produced during the previous cycle. When the interval between subsequent cycles is long, and the previously ionized path partially diffuses, or even totally disappears, the next dart leader propagates along the still-remaining old path for a while, before breaking a new path as a stepped leader. This new path is always in the lower part of the leader channel. Downward leaders that exhibit features of both the dart and stepped leader are called *dart-stepped leaders*. The stepped leader's jagged, branched path indicates propagation through virgin air, while the dart leader's path, which is non-branched, indicates the existence of the old, ionized path of the earlier lightning process. Because breaking a new path is always slower than following a path made previously, the average speed of stepped leaders, in 10^5 m s^{-1} , is slower than that of dart leaders, in 10^6 m s^{-1} .

The definitions of CG lightning types, based on their visual and polarity features, can be confusing or misleading, like Berger's (1977) definitions of CG flashes, which applied the characteristics of natural CG flashes, negative (sketched in figure 5.4(1)) and positive (sketched in figure 5.4(3)), to lightning flashes from tall ground structures (seen in figures 5.4(2) and 5.4(4)). The only difference between the natural and structure-triggered flashes in Berger's definitions lies in the direction and polarity of the leaders, marked *L*, and the return strokes, marked *R*.

Relevant to Berger's characterizations in figure 5.4 was the question, raised by Berger (1975, 1977) and Uman (1987), of whether positive CG flashes are initiated not only by downward positively charged leaders, but also by upward-moving negatively charged leaders (a concept shown in figure 5.4(4)). In his description of CG flashes, Berger (1977, p 137) stated: "The negative upward leader progresses in the form of a very long "connecting leader" into an existing IC flash which, first, caused the transient field by which the upward leader was initiated and, later, is discharged to earth through this connecting leader." Berger's definition of upward,

structure-triggered flashes in figures 5.4(2) and 5.4(4) confuses the nature of the return strokes, marked there as *R*.

In the correction offered by Mazur and Ruhnke (1993) in figure 5.5 for Berger's images in figure 5.4, the return strokes, *R*, are shown as always originating from the ground as ground potential waves that bring the entire lightning channel to zero ground potential, and that always propagate upward. Another difference between Berger's original and the corrected images is that the recoil leaders were identified as components of structure-triggered flashes (compare the images in figures 5.4(2) and 5.5(2), and figures 5.4(4) and 5.5(4)). However, the cases of positive CG flashes triggered by an upward-moving negative leader, as depicted in figure 5.5(4), are hypothetical, because their occurrences were not observed in nature. This inference is based on the experience of launching negative upward leaders using the rocket-triggered lightning technique in winter storms in Japan (Kawasaki and Mazur 1992). During the entire lifetime of this program, no downward positively charged leaders were ever observed following a rocket-triggered upward negative leader, and thus, no return strokes took place that were similar to those in positive CG flashes (Kawasaki 2001). All upward negatively charged leaders initiated with the rocket-triggered lightning technique in Japan ended by terminating in the cloud.

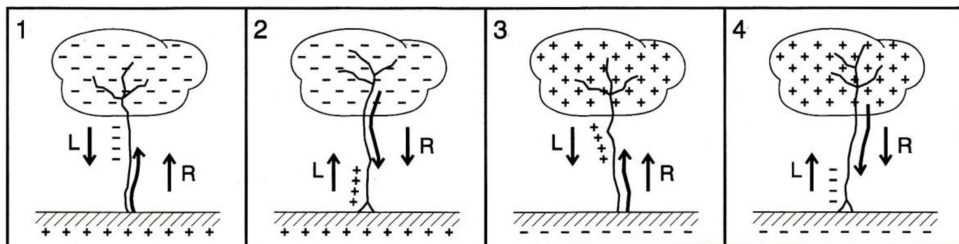


Figure 5.4. Four types of CG flashes, based on the directions and polarity of leaders and return strokes, proposed by Berger (1977). (1) Negative CG flash, (2) upward positive, structure-triggered flash, (3) positive CG flash, and (4) upward negative, structure-triggered flash. Reprinted with permission from Berger (1977). Copyright 1977 Elsevier.

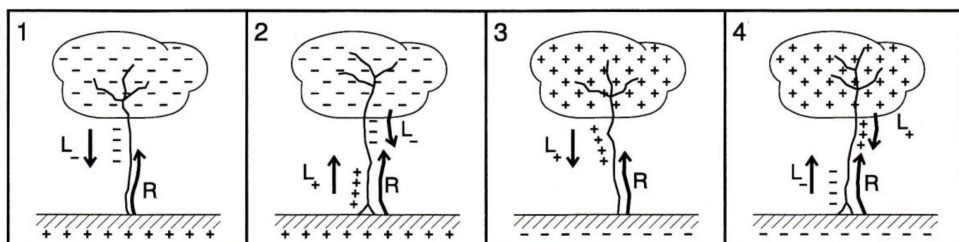


Figure 5.5. ‘Corrected’ types of CG and structure-triggered flashes presented in figure 5.4. Reproduced from Mazur and Ruhnke (1993). Copyright 1993 by John Wiley Sons, Inc. Reprinted by permission of John Wiley & Sons, Inc.

5.2 Defining the types of lightning using the bidirectional, bipolar leader concept

The processes that occur inside the cloud where the return stroke disappears, where the development of IC flashes takes place, and from where a dart leader emerges, are all visually unavailable to the observer. New techniques of mapping lightning radiation sources, using VHF interferometers and the difference time of arrival (DTOA) techniques, allow us to ‘see’ what is hidden from our eyes in the cloud, and to understand better the nature of these lightning processes.

By applying the bidirectional, bipolar leader concept, we are able to identify the stages of lightning development, common to all types of lightning flashes. Because every IC and CG flash originates inside the cloud, it seems obvious that the processes involved in leader initiation and its development, inside or outside the cloud in all natural lightning, must be similar. At the initiation stage, the difference between IC and CG flashes is, perhaps, only in the regions of the cloud where these processes occur. The return strokes, on the other hand, exist only in flashes that are attached to ground. However, both IC flashes and return strokes, which occur in the final stage of CG flashes, terminate in the air, either inside or outside the cloud, with current cutoff in the branched leaders of both polarities playing a crucial role in the termination process in all types of lightning flashes (see chapter 8 for further details).

5.2.1 Intra-cloud flashes

The interpretation of an IC flash as a bidirectional and bipolar lightning ‘tree’, made of a common trunk and branched structures on both sides, was suggested by Mazur (1989), and came out of the analysis of lightning-radiation source maps obtained with a VHF-band interferometer (Richard *et al* 1986). However, both the VHF-band interferometers implemented in lightning research in the 1980s in France (Richard and Auffray 1985) and the USA (Rhodes *et al* 1994), and the DTOA technique used in South Africa (Proctor *et al* 1988) and the USA (Lennon and Maier 1991) were able to map lightning-radiation sources only from negatively charged leaders (see figure 5.6). Besides the negatively charged leaders, as parts of the bidirectional and bipolar leader structure during and following lightning initiation, there are also so-called *recoil leaders* that occur during the later stages of lightning development, and which are results of current cutoffs of the branched channels of positive leaders. (See chapter 9 for further details.)

The term ‘recoil’ reflects the propagation of these leaders following the ionized path that remains from the previous leaders, back towards a branching point, and in the general direction of the lightning origin (figure 5.7). Recoil leaders commonly occur after the development of the negative part of the lightning tree stops. Mazur (1989) interpreted the traces of mapped recoil leaders as paths of previously existing positively charged leaders in a bipolar and bidirectional leader structure of IC flashes (figure 5.8). (See chapters 9 and 10 for more about the nature and the mechanism of recoil leaders.)

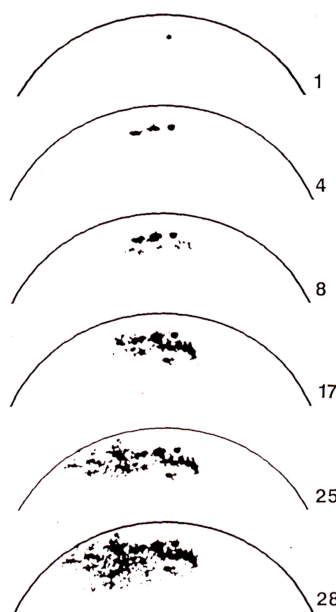


Figure 5.6. A sequence of images depicting the development of negatively charged leaders in an IC flash, from the projection on the ground of a lightning-radiation map, obtained with a VHF interferometer, and recorded with a 16 mm movie camera. Note the absence of radiation paths of recoil leaders during the same period, and highly dendritic branching structure of negatively charged leaders. Reproduced from Mazur (1989). Copyright 1989 by John Wiley Sons, Inc. Reprinted by permission of John Wiley & Sons, Inc.

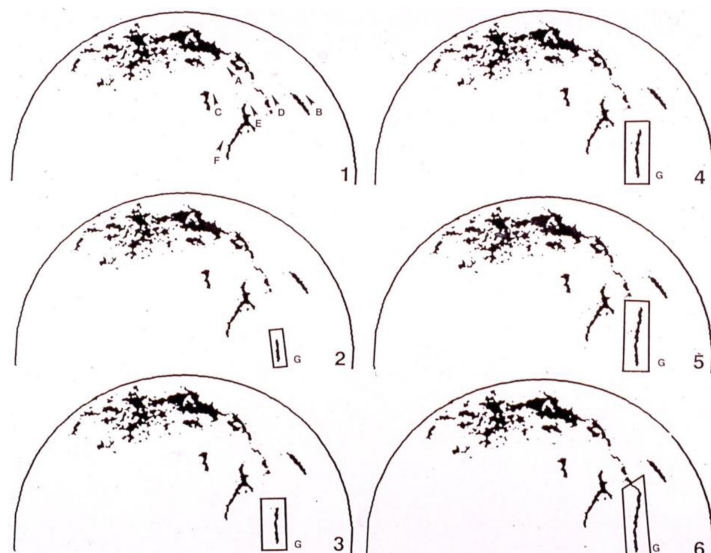


Figure 5.7. A sequence of images depicting the development of a recoil leader in an IC flash, from the projection on the ground of a lightning-radiation map, obtained with a VHF interferometer, and recorded with a 16 mm movie camera. The development of the dendritic structure of the negative part of the lightning tree ceased prior to the occurrence of channel-like recoil leaders (see figure 5.6). Reproduced from Mazur (1989). Copyright 1989 by John Wiley Sons, Inc. Reprinted by permission of John Wiley & Sons, Inc.

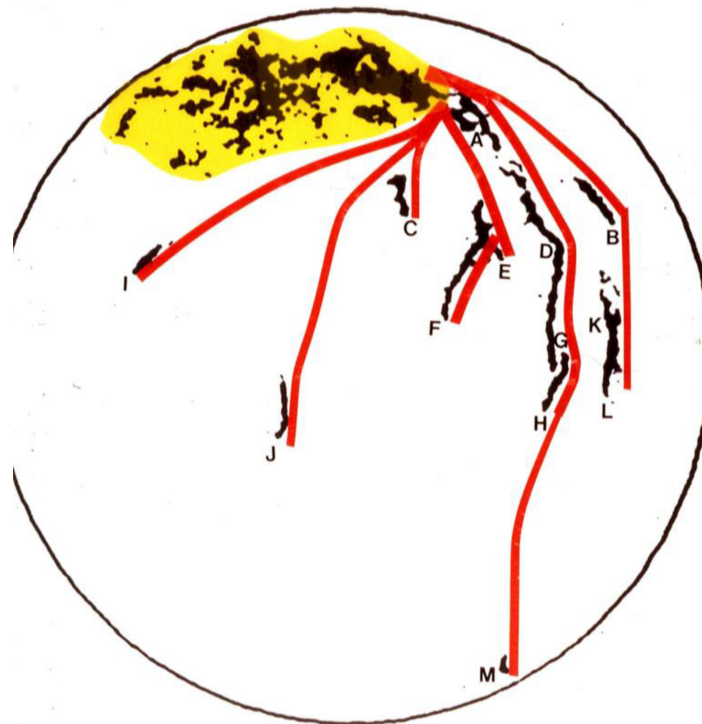


Figure 5.8. The radiation map of an IC flash, projected on a ground plate, obtained with a VHF interferometer. The region of negatively charged leaders is colored in yellow; the channel-like traces are recoil leaders; and red ribbons mark possible traces of branched positively charged leaders that preceded the occurrence of recoil leaders. The letters signify the sequential appearance of recoil leaders. Reproduced from Mazur (1989). Copyright 1989 by John Wiley Sons, Inc. Reprinted by permission of John Wiley & Sons, Inc.

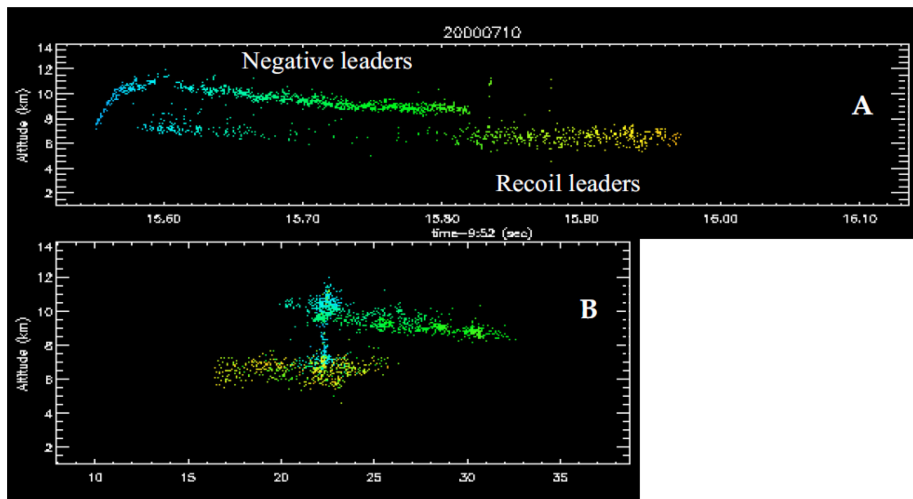


Figure 5.9. Lightning radiation map of an IC flash. (A) and (B) depict the altitude (km)–time (s) and altitude (km)–range (km) progression of the radiation sources, respectively. The recoil leaders (lower layer) have a much greater dispersion and a lesser density of sources than the initial negative leaders (upper layer). Courtesy of R Thomas.

The radiation map of a typical IC flash obtained with the DTOA system, in figure 5.9, confirms the dynamics of the development of the bidirectional lightning tree derived from the images in figures 5.6 and 5.7. This map also clearly exhibits a two-layer structure, with a vertical bridge (a ‘tree trunk’) produced by negatively charged leaders—that started at 7.8 km altitude, ascended, and then stratified between 9–11 km (the upper layer)—and recoil leaders that stratified in the 6–7 km region (the lower layer).

Because leaders that carry charges of one polarity propagate in cloud regions with space charges of the opposite polarity, the lightning-radiation map in figure 5.9 is indicative of an existing, classical tripole-charge structure in a thundercloud. In this structure, an upper positive space-charge region is at an altitude of 9–11 km, a lower negative space charge region is at an altitude of 6–7 km, and a lower positive charge region is at the cloud base.

Negative leaders in the IC flash dominate the initial stage of the discharge, as the images in figure 5.7 clearly indicate, but cease during the subsequent, so-called ‘junction stage’, indicating that the negative end of the tree is ‘dead’ during this stage. This death produces the current cutoff in the bridge that connects the two parts of the bidirectional leader structure. While bidirectional development at both ends of the lightning tree takes place during the initial stage, no new negative leaders develop at the negative end of the tree during the junction stage.

The negative-leader radiation on the map in figure 5.9 appears as a dense pattern of sources noticeably different from that of the recoil-leader radiation, which is highly dispersed, perhaps because of fewer widely separated channels. The recoil leaders in figure 5.9 briefly appear 30 ms after lightning initiation, but become dominant during the final stage of the discharge, starting at 270 ms after initiation.

There is an obvious asymmetry in the emerging pattern of bidirectional leader development during the initiation and junction stages. Because the DTOA lightning-mapping system detected only the radiation of negatively charged leaders, we cannot map the paths of positively charged leaders, or determine when these leaders may have ceased propagation, or how long after that the recoil leaders may have

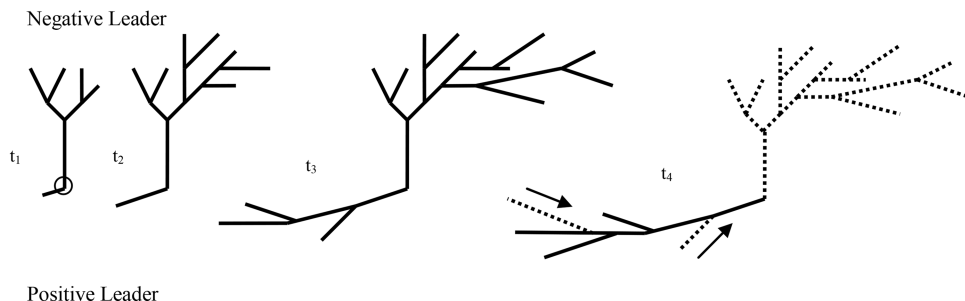


Figure 5.10. The concept of development of a bipolar lightning ‘tree’ in a typical IC flash. t_1 = initiation of a bipolar and bidirectional leader from the origin (circle); t_2-t_3 = periods of branching and progression of the bidirectional leader during the initial stage of the flash; t_4 = negatively charged parts of the lightning tree cease development, and negatively charged recoil leaders (arrows) restore the previously dead branches, shown as dashed lines, of positively charged leaders.

occurred. Recoil leaders, therefore, may trace only part of the structure of preceding positively charged leaders. However, observations of multi-stroke CG and rocket-triggered flashes suggest that unidirectional development of positive leaders could take place during the junction stage of the IC flash.

In the conceptual sketch in figure 5.10, we synthesized the stages of development of a bidirectional and bipolar lightning ‘tree’ in a typical IC, flash, as described earlier.

5.2.2 Cloud-to-ground flashes

A radiation map of a typical CG flash, obtained with the DTOA technique depicting its development in time and height, is shown in figure 5.11, and the conceptual sketch of its processes is depicted in figure 5.12.

The multi-stroke negative CG flash mapped in figure 5.11 exhibits four cycles of a downward stepped or a dart leader, followed by return strokes. Return strokes produce almost no VHF radiation by being both positively charged and traveling along the still-perfectly conducting channels of downward leaders. Dart leaders are those recoil leaders that have reached the ground.

The IC development of positive leaders (recognized by the presence of recoil leaders in a lightning-radiation map) is energized by return strokes, which, after reaching the upper tips of the bipolar lightning tree, bring the ground potential to a cloud region that has high ambient potential. The resulting positive breakdown may be accompanied by strong VHF radiation (Rhodes *et al* 1994). The lightning-radiation map of a multi-stroke negative CG flash (figure 5.11) shows the trails of positively charged leaders associated with the negative space-charge region of the cloud to be situated between 6 and 8 km of altitude.

The conceptual sketch of the development of a single-stroke negative CG flash is depicted in figure 5.12. Prior to the first stepped leader touching the ground, the stages of development of a single-stroke negative CG flash are, in principle, the same as those in IC flashes (figure 5.10). In the VHF radiation map during this period,

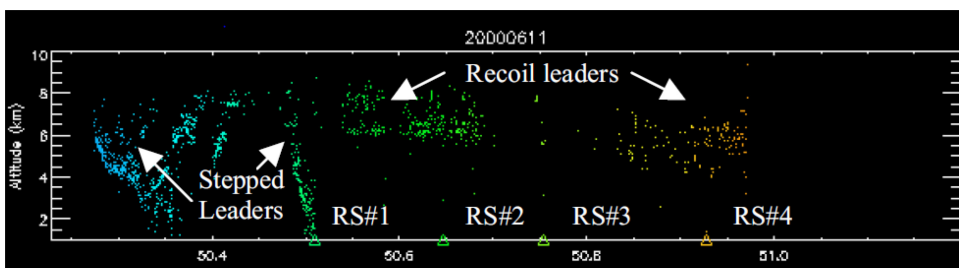


Figure 5.11. Lightning-radiation map, altitude (km)-time (s), of a multi-stroke negative CG flash. Stepped leaders started at an altitude of 6 km, first terminating in the air, and then reaching the ground at time 50.5 s. Four return strokes (RS) are marked with the symbol Δ on the time axis. Negative dart leaders are virtually invisible on the radiation map, because of their very weak radiation due to propagation along the weakly ionized channels of previous return strokes, rather than through virgin air, as in the case of stepped leaders. Courtesy of R Thomas.

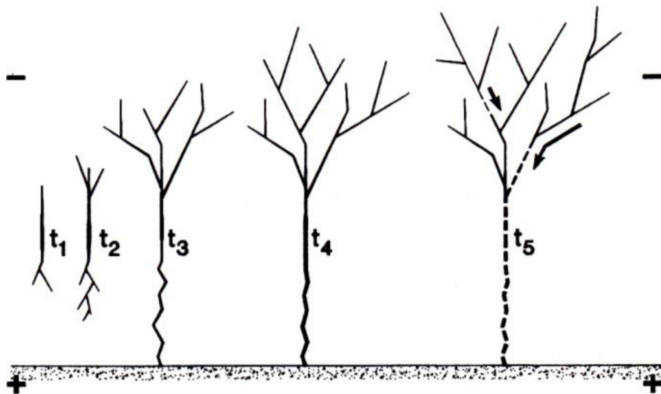


Figure 5.12. The concept of the development of a bidirectional, bipolar lightning ‘tree’ in a negative CG flash (a cycle of a single-stroke flash). t_1 = initiation of a bipolar and bidirectional leader from the lightning origin; t_2 = period of branching and progression of the bidirectional leader during the initial stage of the flash; t_3 = attachment of downward negatively charged leader to ground; t_4 = return stroke, and new unipolar development of the positively charged upward leader; t_5 = current cutoff in return-stroke channel, and negatively charged recoil leaders (arrows) propagating toward branching points of preceding positively charged leaders, shown as dashed lines.

negatively charged leaders dominate the initial stage of the bidirectional lightning-tree development, while positively charged leaders are not mapped.

In multi-stroke CG flashes, recoil leaders occur during the continuous IC development of positively charged leaders after each return stroke. There is a strong similarity between this stage in CG flashes and the junction stage of IC flashes, after the death of the negatively charged end of the lightning tree.

In the case of a positive CG flash, a VHF radiation map of which is shown in figure 5.13, the initial negative leader progression occurs within the positive space-charge region of a cloud. This region is associated with a melting layer located above 0 °C isotherm, and is recognized in a vertical radar cross-section of the cloud as a so-called ‘bright band’.

Because the trail of the radiation sources of a downward positively charged leader is hard to detect, the point of the leader’s attachment to ground can be found only by tracing the slightly more pronounced radiation path of the following return stroke, which carries a negative charge. As in negative CG flashes, the arrival of the return stroke to the upper, negatively charged branches of the lightning tree energizes new negative breakdowns there, and expands a dendritic structure of negatively charged leaders.

The conceptual sketch of the development of positive CG flashes, presented in figure 5.14, has an obvious similarity, in its stages, to those in a single-return-stroke negative CG flash. However, there is a significant difference between the CG flashes of both polarities in the multiplicity of return strokes, which is absent in positive CG flashes.

The stages of positive CG flash development, marked t_3 and t_4 in figure 5.14, are replicated in negative rocket-triggered lightning, with the sole difference being the

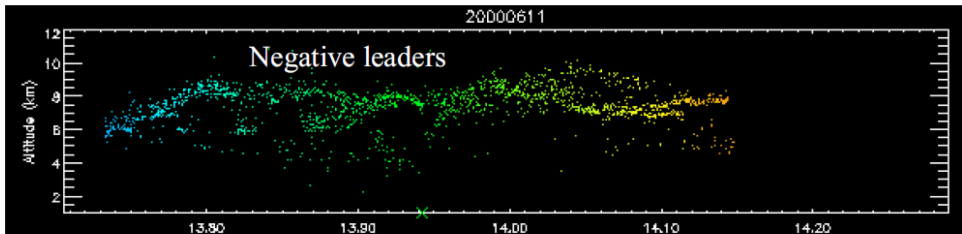


Figure 5.13. Lightning-radiation map, altitude (km)–time (s), of a positive CG flash. The panel depicts the altitude (km)–time (s) progression of the radiation sources. The return stroke is marked with the symbol X on the time axis. The positive leader is virtually invisible on the radiation map. The negative leader started at an altitude of 6 km, then developed within the positive space-charge region at around 8 km of altitude. Courtesy of R Thomas.

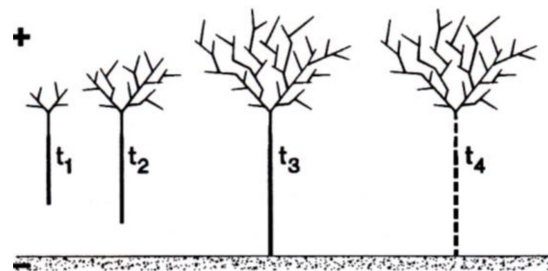


Figure 5.14. A conceptual sketch of the development of a bidirectional, bipolar lightning ‘tree’ in a positive CG flash. t_1 = initiation of a bipolar and bidirectional leader from the lightning origin; t_2 = period of branching and progression of the bidirectional leader during the initial stage of the flash; t_3 = attachment of downward positively charged leader to ground, return stroke, and new unipolar development of negatively charged upward leader; t_4 = current cutoff in return stroke channel. Note the absence of recoil leaders in the lightning tree.

fact that the return stroke is replaced by an upward negatively charged leader that started on a rocket with a grounded wire. Observations of positive CG flashes suggest that usually they have only one return stroke (Beasley 1985). The occasional claims appearing in the lightning literature regarding the existence of multiple return strokes in positive CG flashes probably refer to a case of actually *independent* positive CG flashes that have simply occurred in a succession typical of multi-stroke CG flashes. Such cases of positive CG flashes separated by distances of tens of km from each other have been observed and mapped with the DTOA system in summer thunderstorms in the USA (Thomas 2001).

Studies in winter storms in Japan of upward negatively charged leaders triggered by rockets with a trailing grounded wire have shown the absence of positively charged recoil leaders emerging from the cloud, and traveling along the remnants of the previous channel of a negatively charged leader. If such recoil leaders do exist, they would be similar in nature to recoil leaders in IC and negative CG flashes, but different from them in *polarity*.

References

- Beasley W 1985 Positive CG lightning observations *J. Geophys. Res.* **90** 6131–8
- Berger K 1975 Development and properties of positive lightning flashes at Mount San Salvadore *Culham Conf. on Atmospheric Electricity* (UK: Abingdon Berbs)
- Berger K 1977 The Earth flash *Physics of Lightning* vol 1 ed R H Golde (San Diego, CA: Academic) pp 119–90
- Dwyer J R and Uman M A 2013 The physics of lightning *Phys. Rep.* **534** 147–241
- Kawasaki Z-I 2012 Personal communication
- Kawasaki Z-I and Mazur V 1992 Common physical processes in natural and triggered lightning in winter storms in Japan *J. Geophys. Res.* **97** 12935–45
- Lennon C L and Maier L 1991 Lightning mapping system *NASA Conf. Publ.* **3106** 89.1–10
- Mazur V 1989 Triggered lightning strikes to aircraft and natural IC discharges *J. Geophys. Res.* **94** 3311–23
- Mazur V and Ruhnke L H 1993 Common physical processes in natural and artificially triggered lightning *J. Geophys. Res.* **98** 12913–30
- Mazur V, Shao X-M and Krehbiel P R 1998 ‘Spider’ lightning in intracloud and positive cloud-to-ground flashes *J. Geophys. Res.* **103** 19811–22
- Proctor D E 1981 VHF radio pictures of cloud flashes *J. Geophys. Res.* **86** 4041–75
- Proctor D E, Uytenbogaardt R and Meredith B M 1988 VHF radio pictures of lightning flashes to ground *J. Geophys. Res.* **93** 12683–727
- Rhodes C T, Shao X M, Krehbiel P R, Thomas R J and Hayenga C O 1994 Observations of lightning phenomena using radio interferometry *J. Geophys. Res.* **99** 13059–82
- Richard P and Auffray G 1985 VHF–UHF interferometric measurements, applications to lightning discharge mapping *Radio Sci.* **20** 171–92
- Richard P, Delannoy A, Labaune G and Laroche P 1986 Results of special and temporal characterization of the VHF–UHF radiation of lightning *J. Geophys. Res.* **91** 1248–60
- Thomas R J 2001 Personal communications
- Uman M 1987 *The Lightning Discharge* (San Diego, CA: Academic)

Principles of Lightning Physics

Vladislav Mazur

Chapter 6

The electrostatic theory of lightning discharges

6.1 Cloud potential and induced charges of lightning

The analysis of the electrostatic aspects of a lightning discharge first presented in Kasemir (1950, 1960) and then advanced in Kasemir (1983) is based on Kasemir's concept of a bidirectional, bipolar leader. This analysis provides the foundation on which we have built our understanding of the basic relationships between electrical potentials, ambient electric field, and induced charges on lightning leaders of different types. Therefore, we will start this section with the essence of Kasemir's analysis, expanding upon it later in the chapter.

The lightning channel, as a conductor submerged in a cloud ambient electric field of the potential ϕ , has a dipole distribution of induced charges (with net zero charges); these charges generate the secondary potential ϕ_c . Superimposition of the two potentials, ϕ_1 and ϕ_2 , results in the constant potential of a perfectly conducting lightning channel ϕ_0 :

$$\phi + \phi_c = \phi_0 \quad (6.1)$$

If we assume, for convenience, that $\phi_0 = 0$, then $\phi = -\phi_c$. This means that the potential function of the induced charges on the lightning channel ϕ_c is of the same amplitude, but of opposite polarity from the potential function of the cloud charges ϕ .

Figure 6.1 depicts cloud potentials and charge distributions on conductive channels under five different ambient electric field conditions, with the charge density shown as a shaded area, a vertical, heavy line representing the lightning channel, and a thin, solid line representing the ambient potential ϕ . The crucial feature in all cases shown in figure 6.1 is that the charge distribution is proportional to the potential function of cloud charges ϕ , but is of the opposite polarity.

In the charged channel in a zero electric field, case (a), the charges are uniformly distributed. In cases (b) and (d) of an uncharged channel in homogeneous and inhomogeneous electric fields, respectively, the charges are bipolar, with a zero net

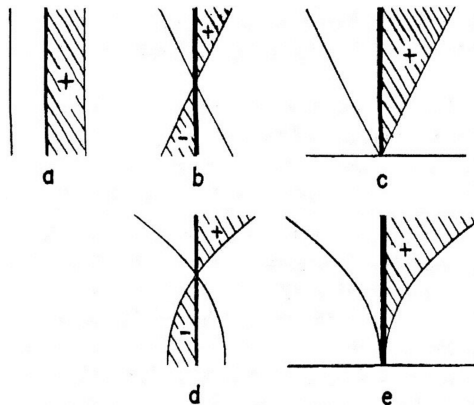


Figure 6.1. Ambient potential distribution ϕ (solid lines) and charge distribution on a lightning channel (shaded area) for (a) a charged channel in zero electric field, (b) an uncharged channel in a homogeneous electric field, (c) a charged channel connected to ground in a homogeneous electric field, (d) an uncharged channel in an inhomogeneous electric field, and (e) a charged channel connected to ground in an inhomogeneous electric field. Reproduced from Kasemir (1960). Copyright 1960 by John Wiley Sons, Inc. Reprinted by permission of John Wiley & Sons, Inc.

charge. Cases (b) and (d) represent a bidirectional, uncharged lightning leader in a thunderstorm, or a leader before it touches the ground. Cases (c) and (e) represent a unipolar and unidirectional channel of a return stroke, or an upward leader from the ground.

6.2 The relationship between the electric fields produced by leaders and return strokes

The leader and return stroke in a CG flash share the same conductive channel connected to the ground. For this reason, we expect to uncover a unique relationship between the cloud's electrical potential and the induced charges on the channels of a leader and a return stroke in CG flashes. The easiest way to find this relationship is by applying a simplified electrostatic approach to a scenario in which the atmospheric electric field is vertical and one-dimensional, and the leader-return stroke geometry is a vertical line.

The flash starts as a bidirectional, bipolar leader in an ambient electric field $E(z)$ at altitude z . The leader's induced charges in the form of an electrical dipole would have charges per unit length, $q(z)$, proportional, but opposite in sign, to the cloud potential $\phi(z)$ at that level (Kasemir 1986; Heckman and Williams 1989):

$$q(z) = -k[\phi(z) - \phi_0] \quad (6.2)$$

The constant k in (6.2) is the capacitance per unit length of the conducting leader channel, and ϕ_0 is the potential of the conducting channel. The ambient electric field $E(z)$ is defined by the potential distribution $\phi(z)$:

$$E(z) = d\phi(z)/dz \quad (6.3)$$

The bipolar leader before touching the ground has a zero net charge, i.e. the integrated charge over the length of the leader (from its lower tip at altitude z_l to its upper tip at altitude z_u) is zero:

$$\int_{z_l}^{z_u} q(z) dz = 0 \quad (6.4)$$

Because of the high conductivity of its channel, the leader is assumed to be at equal potential ϕ_0 , with its expression in (6.5) derived from (6.2) and (6.4):

$$\phi_0 = \frac{1}{z_u - z_l} \int_{z_l}^{z_u} \phi(z) dz \quad (6.5)$$

Equation (6.5) reflects an important feature of the leader in an ambient electric field, namely, that its potential ϕ_0 is equal to the average cloud potential over the leader's length. The magnitude of ϕ_0 varies with the changing leader's position during its development in the cloud. Just before touching the ground, the leader's potential ϕ_0 becomes equal to

$$\phi_r = \frac{1}{z_u} \int_0^{z_u} \phi(z) dz \quad (6.6)$$

Upon contact with the ground, the leader's potential begins to change from ϕ_r to zero ground potential, with the formation of a return-stroke channel that creates the ground potential wave that is propagating upward along the leader channel until the entire channel is at ground potential. In this process, the channel's new distribution of charge per unit length changes and becomes, according to (6.2),

$$q_{l+r} = -k\phi(z) \quad (6.7)$$

Starting at the instant the leader touches the ground, the transformation of the bipolar leader channel with zero net charge and potential ϕ_r into a return-stroke channel with zero potential is accompanied by adding to the leader channel a uniform charge Q of a constant charge per unit length, q_r :

$$q_r = -k\phi_r = -\frac{k}{z_u} \int_0^{z_u} \phi(z) dz \quad (6.8)$$

By integrating q_r over the total channel, which has the total capacitance C , we obtain the net charge Q carried by the return-stroke channel:

$$Q = -C\phi_r \quad (6.9)$$

The net charge Q is distributed over the length of the channel proportional to the capacitance per unit length. For a thin channel with a constant diameter over its length, this capacitance per unit length remains constant over the entire channel.

The quantitative relationship between the electrical parameters of the CG leader and the return stroke can be obtained from the analysis of the electric field measurements on the ground. At the distance D from an element of the vertical leader channel with charge density $q(z)$, the electrostatic field change ΔE (Uman 1987) is expressed as:

$$\Delta E = \frac{1}{2\pi\epsilon} \int_{z_l}^{z_u} \frac{q(z)z dz}{(D^2 + z^2)^{1.5}} \quad (6.10)$$

By applying to (6.10) the charge per unit length from (6.8), we obtain the electric field change produced by the return stroke alone:

$$\Delta E_r = -\frac{k\phi_r}{2\pi\epsilon} \int_0^{z_u} \frac{z dz}{(D^2 + z^2)^{1.5}} \quad (6.11)$$

The electric field change produced by the leader before it touches the ground is:

$$\Delta E_l = -\frac{k}{2\pi\epsilon} \int_0^{z_u} \frac{[\phi(z) - \phi_0]z dz}{(D^2 + z^2)^{1.5}} \quad (6.12)$$

The two unknown variables in these two equations are the ambient cloud potential distribution $\phi(z)$ and the dimensions of the channel. The general relationships expressed in (6.11) and (6.12) are applicable not only to straight, but also to branching, channels and channels with a horizontal variability of potential distribution.

6.3 The relationship between lightning processes and space charges in thunderstorms

A study of the relationship between cloud charges and lightning from *in situ* or remote measurements is an unrealistic undertaking. A better alternative is to address this issue analytically. Heinz-Wolfram Kasemir (1950, 1960) was the first to do so, by applying the ‘potential theory’ to the Wilson–Simpson thunderstorm model and by using analytical methods for solutions. The key physical concept in relating lightning features to ambient cloud charges was that of the bidirectional uncharged leader, first introduced by Kasemir (1950), and further developed by him (1983). To be maintained, the lightning discharge requires that the mechanism by which the channel extends itself into new cloud regions that contain stored electrostatic energy continues at the tips of the bidirectional, bipolar leader.

6.3.1 Thunderstorm model

Mazur and Ruhnke (1998) followed in the footsteps of the groundbreaking work by Kasemir, and applied numerical solutions to a physical model of an axisymmetric leader in a two-dimensional thunderstorm-charge model, to determine the relationship between cloud charges and lightning leaders. The primary cloud charges in their

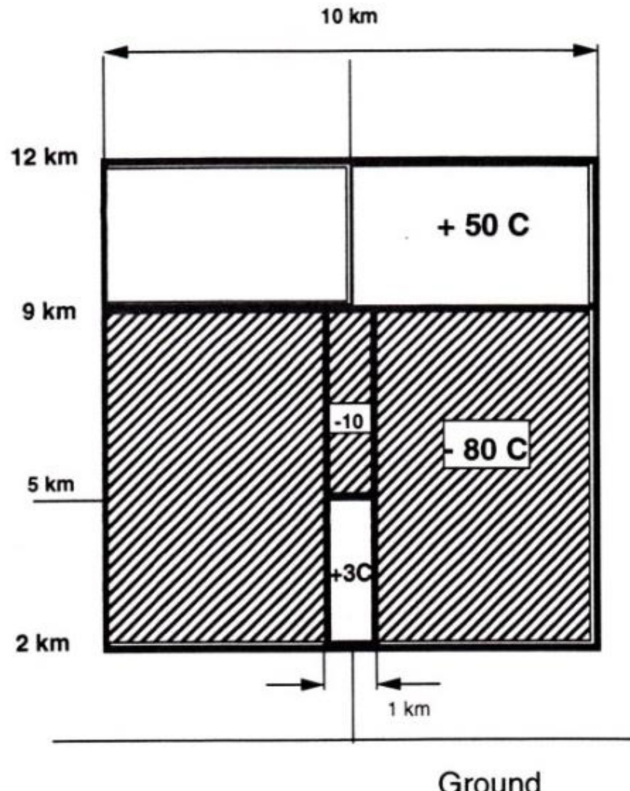


Figure 6.2. A two-dimensional axisymmetrical charge model of a thunderstorm at the mature stage. Reproduced from Mazur and Ruhnke (1998). Copyright 1998 by John Wiley Sons, Inc. Reprinted by permission of John Wiley & Sons, Inc.

model (see figure 6.2) are in an axisymmetric structure, with features representing the mature stage of a thunderstorm. The maximum electric fields in the model are at two preferred altitudes, where VHF radiation from the initial breakdown of CG and IC flashes (Proctor 1991) had been observed. The assumed radius of the charged cloud is 5 km, the typical dimension of an isolated storm in radar-reflectivity data. The estimates of cloud charges fall within the scale of those quoted in the literature (tens of coulombs), but with the main negative charge much larger than the main positive one.

The high charge-density core of 0.5 km radius in the model corresponds to an intensive updraft region, which is the primary charge-generating region of the storm (after Kuettner 1950). This core includes a small positive-charge region of 3 C, which extends from the lower cloud boundary to a 5 km altitude, and a small negative-charge region of 10 C at between 5 and 9 km altitude. The model does not take into account the corona space charges near the ground.

The numerical solution of the Poisson equation (6.13) for the potential distribution ϕ anywhere in the computation region, which is made of the electrified cloud

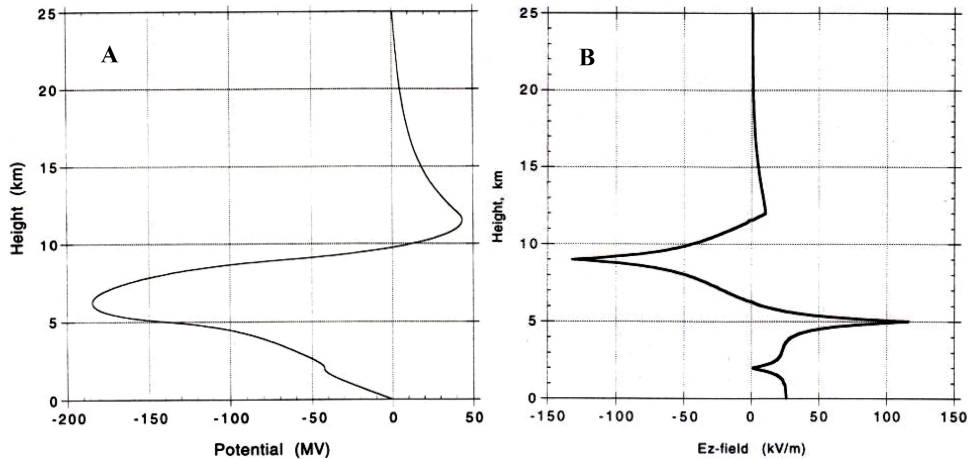


Figure 6.3. Vertical cloud potential (A) and electric field (B) profiles in the center of the storm. Reproduced from Mazur and Ruhnke (1998). Copyright 1998 by John Wiley Sons, Inc. Reprinted by permission of John Wiley & Sons, Inc.

with charge distribution q with and without lightning, was obtained with the charge-simulation method (e.g. Malik 1989):

$$\operatorname{div} \operatorname{grad} \phi = -q/\epsilon \quad (6.13)$$

The electric fields E in any direction s are:

$$E = -d\phi/ds \quad (6.14)$$

The potential distribution and, therefore, the electric fields from the cloud charges are assumed to be stationary throughout the period of lightning-channel development. The presence of the lower positive-charge region is crucial for the initiation of CG flashes (Clarance and Malan 1957, Williams 1989).

The vertical profile of the cloud potential ϕ in the center of the cloud is shown in figure 6.3(A). In the plot of the vertical electric field in figure 6.3(B), two altitudes are easily recognizable, 5 km and 9 km, where the electric fields are of maximum values, and where the lightning initiation regions are at 5 km altitude for negative CG flashes, and at about 9 km for IC flashes (Proctor 1991).

Cloud potential is the main determining factor in the derivation of induced charges on the leader channel. By using both the channel-propagation velocity and the induced-charge changes, we are able to calculate the leader's current. With the justifiable assumption that the leader is a perfect conductor, the potential of the leader channel will be constant over its length, as well as equal to the average potential from the ambient cloud charges along the leader's length (see expression 6.5).

6.3.2 Development of the cloud-to-ground leader

In the model, the CG leader originates at a 5 km altitude, and develops vertically and bidirectionally along the axis of symmetry. Ignoring the stage of lightning initiation, which we do not yet fully understand (and, thus, cannot model), the

calculation in the model of the leader's parameters begins with an already-formed leader channel of 1 km length. The assumed radius of the ionized leader channel is 1 m (Schonland 1956).

The measurements of the leader's speed, taken from video observations, show that both positively and negatively charged leaders accelerate gradually after initiation, with their final speeds increasing by five to ten times over their initial speed (Kito *et al* 1985). However, in order to simplify calculations, the bidirectional progression of the leader was assumed to be achieved with an average speed of 10^5 m s^{-1} for both the upper positively charged and the lower negatively charged leader tips. This results in the extension of the leader by 500 m in both directions every 5 ms.

Figure 6.4 shows the evolution of the potential profiles of a leader during its progression toward the ground on a background of the ambient cloud potential from the plot in figure 6.3. The greatest enhancements of the vertical potential gradient (electric field) are at both tips of the leader channel, causing breakdown conditions to persist at the tips. The channel potential ϕ_0 , which is uniform along the channel at any given moment, initially changes only very slightly, because of the fairly symmetrical distribution of ambient potentials above and below the breakdown point; but it shifts systematically toward lower values as the leader approaches the ground.

The progression of the leader stops when the potential gradient at the leader tip is close to the breakdown threshold value, and resumes if the gradient rises above this threshold value. When the leader's potential at the upper, positively charged tip of the leader channel becomes equal to the cloud potential (as seen in figure 6.4 at incremental step 7) at an altitude of 8.5 km, the leader's upward propagation stops.

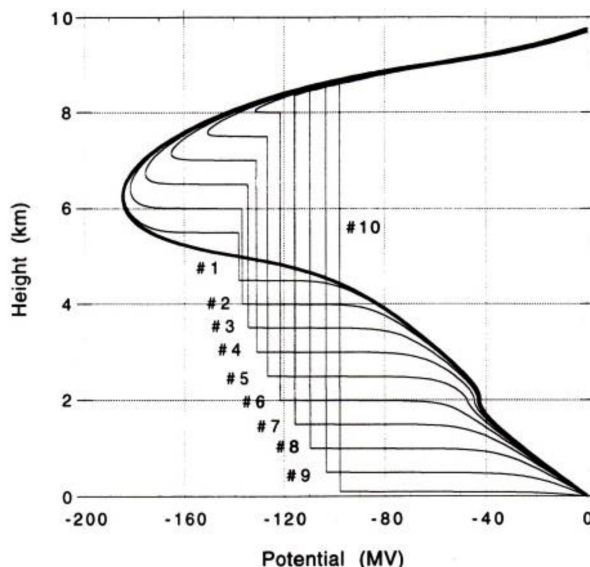


Figure 6.4. Evolution of potential profiles on the developing CG leader. Reproduced from Mazur and Ruhnke (1998). Copyright 1998 by John Wiley Sons, Inc. Reprinted by permission of John Wiley & Sons, Inc.

From then on, no upward propagation is possible, unless the potential gradient at the upper tip again reaches above the breakdown value, while the lower, negatively charged tip of the leader continues to move toward the ground until it touches it.

The induced charges on the leader channel are calculated by utilizing the numerical solution of (6.13) for determining the potential distribution anywhere in the cloud where the leader is present. Two assumptions were made for calculation of the induced leader charges: in the first, the leader channel was considered to be a very narrow, charged conductor of radius r_0 and of great length; in the second, the electric field lines on the surface of the conductor and on the coaxial surface of radius r ($r > r_0$) were assumed to be perpendicular to the coaxial surfaces of radii r and r_0 . Thus, based on the second assumption, there is the same number of electric field lines per unit length on each surface, and the relationship between their surface electric fields, $E(r)$ and E_0 , is

$$E(r) = E_0 r_0 / r \quad (6.15)$$

The potential $\phi(r)$ on the surface of radius r is obtained by the integration of (6.15), with ϕ_0 being the potential of the surface of the conductor

$$\phi(r) - \phi_0 = -E_0 r_0 \ln(r/r_0) \quad (6.16)$$

In the radial direction, the potential rapidly changes from leader potential to ambient cloud potential in the relatively short distance of a few hundred meters (figure 6.5). The potential gradient near the surface of the leader (for a significant

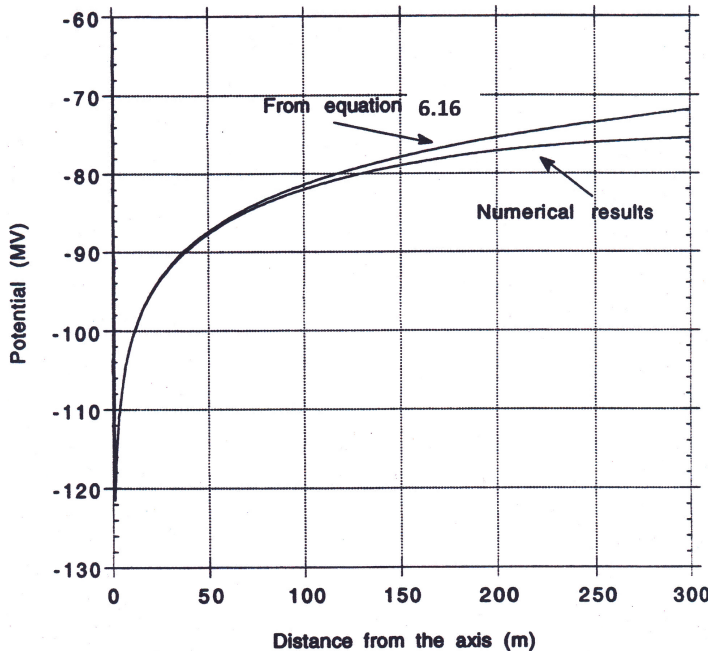


Figure 6.5. Radial transition of leader potential to cloud potential, for a section of the leader of 4 km length, and at step 6 of downward development. Reproduced from Mazur and Ruhnke (1998). Copyright 1998 by John Wiley Sons, Inc. Reprinted by permission of John Wiley & Sons, Inc.

part of the channel's length) may be sufficient to create the corona sheath. A comparison of the potential transition from the leader to the ambient cloud potential, obtained numerically with it calculated using (6.16), shows that (6.16) is valid up to a distance of 50 radii (50 m) from the leader.

The induced charge per unit length of the channel, $q_i = 2\pi\epsilon_0 E_0$, with the surface electric field, E_0 , expressed as a function of the cloud potential (see (6.16)), is

$$q_i = [\phi_0 - \phi(r)] 2\pi\epsilon_0 / \ln(r/r_0) \quad (6.17)$$

In calculations of q_i , one can use potential profiles ϕ_0 and $\phi(r)$ on the leader surface of $r_0 = 1$ m, and on the surface of $r = 3r_0 = 3$ m, respectively. A radius of 3 m was chosen, because it was well within the range of the logarithmically changing potential (6.16), and well above the limitations set by the grid-sizes in the computational scheme. Equation (6.17) indicates that the induced charges per unit length are only slightly dependent on the channel radius.

Figure 6.6 shows the evolution of the induced charges on the leader channel during its progression toward the ground, for each of the ten incremental steps. The total charge of the leader remains zero throughout, while the positive and negative charges on both parts of the bidirectional leader increase. In general, the charge density follows the cloud potential structure as its mirror image (compare the shapes of the plots in figures 6.4 and 6.6), with significant deviations only at the tips of the leader. Just prior to touching the ground, the absolute value of the positive (or negative) charge was $Q = 1.55$ C.

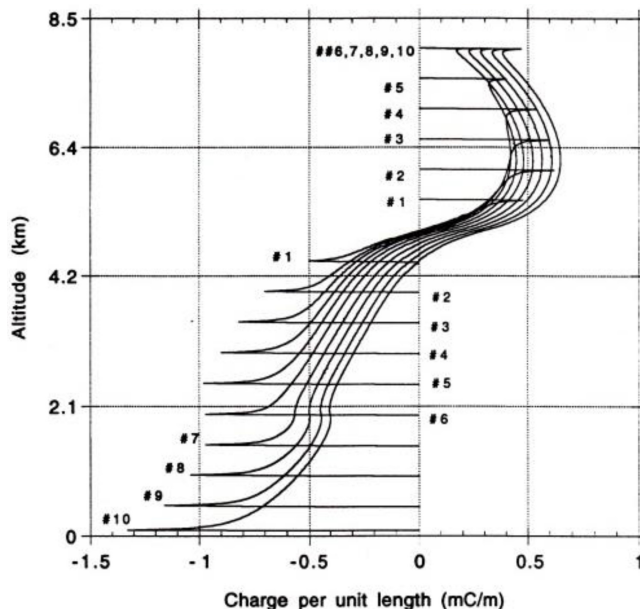


Figure 6.6. Induced charges on the CG leader with incremental steps of 5 ms. Reproduced from Mazur and Ruhnke (1998). Copyright 1998 by John Wiley Sons, Inc. Reprinted by permission of John Wiley & Sons, Inc.

With the diminishing potential gradient at the upper tip of the bidirectional leader, the distribution of the induced charges changes its shape, from initially symmetrical, with the maximum charge density at the tip, to asymmetrical, with the 'hump' of the charge in the middle and a much lower charge density at the tip. This process coincides with a slowing down of the progression of the leader and a lowering of the current at the upper tip.

Because there is some uncertainty in the literature regarding the diameter of leader channels, we tested the influence of channel diameter on the charge per unit length with our numerical model calculation. By increasing the diameter of the leader channel by a factor of 3, from 2 m to 6 m, we obtained only a 20% increase in the induced charge per unit length.

We then calculated the current flow I in the leader of length l , as the result of changes in the induced charge distribution, dq/dt , during channel development, under our assumption of a steady propagation velocity:

$$I = \int_0^l (dq/dt)dl \quad (6.18)$$

It is important to note that, during leader channel progression toward the ground, the current along the channel (see figure 6.7) is not constant, since the charge density

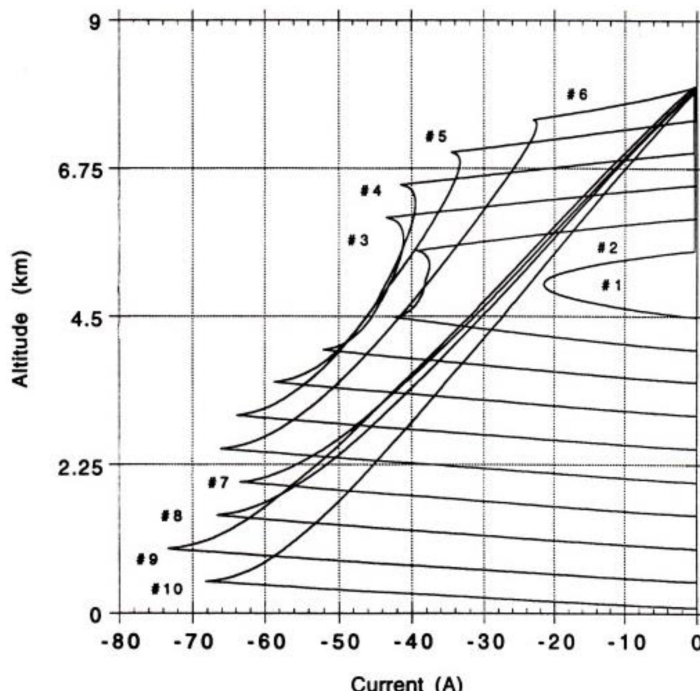


Figure 6.7. Current distribution in the progressing CG leader channel. Reproduced from Mazur and Ruhnke (1998). Copyright 1998 by John Wiley Sons, Inc. Reprinted by permission of John Wiley & Sons, Inc.

varies differently at different points along the channel's length. It should be also noted that when the upper tip of the leader stops (steps 7–10), but the lower one is still moving, the current at the upper tip only (and nowhere else) becomes zero.

6.3.3 Return stroke

On contact with the ground, the potential of the leader shifts to zero ground potential value, and an extra positive charge is deposited from the ground into the channel during the course of the return-stroke process. Figure 6.8 shows the charge distribution along the return-stroke channel, which was obtained through the numerical solution of (6.17); i.e. the return-stroke process adds charge density of a constant charge per unit length (curve 'RS' in figure 6.8). The 'end effect' (increase of capacitance per unit length at the end of a long channel) at the tip of the return stroke channel is the result of a much greater channel capacitance at the leader tip, and is responsible for the deviation from a constant charge density along the channel, observed at the upper tip.

The resulting induced charges on the return-stroke channel, after it traverses the previous leader channel, are marked 'leader+RS' in the plot. They are produced by adding the return-stroke charges ('RS') to the bipolar, zero net charges of the downward leader ('CG leader'). This process is not actually the discharging of the leader, as is frequently mentioned in the literature, but rather, the *addition and redistribution of charges* by the return-stroke process. The total charge deposited by

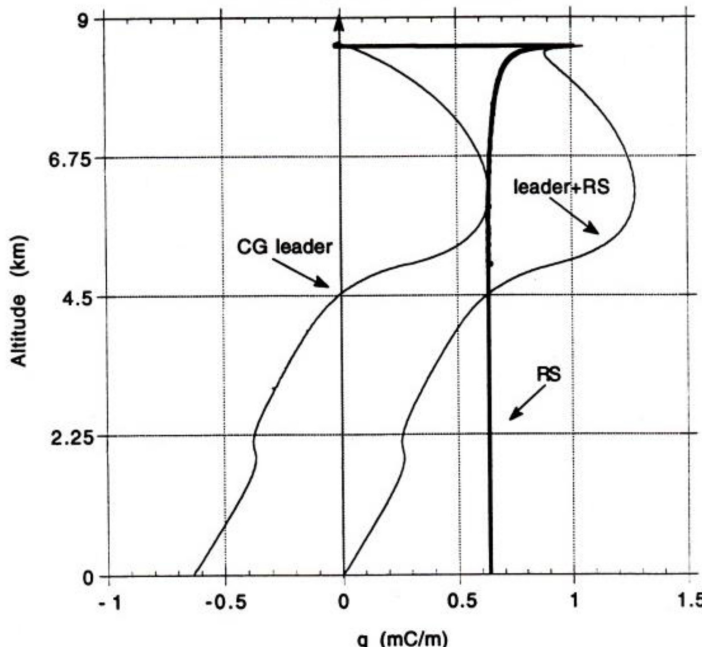


Figure 6.8. Induced charge distribution on the CG leader channel just before touching the ground, and after the return stroke. Reproduced from Mazur and Ruhnke (1998). Copyright 1998 by John Wiley Sons, Inc. Reprinted by permission of John Wiley & Sons, Inc.

the return stroke to the leader channel is 5.4 C, and is larger than the sum of the absolute values of the negative and positive charges on the bipolar CG leader, calculated as 3.1 C.

The final charge distribution on the return-stroke channel is similar to that on any ground-conducting structure in the ambient electric field, which mirrors the ambient potential distribution, and which has a zero charge on the ground (see figure 6.1).

6.3.4 Electric field changes produced by CG flashes

To compare the results of our modeling with lightning observations, we calculated the surface electric field changes at distance D from the leader during the leader/return stroke sequence, by using the computed values of induced charges on the leader q in (6.10), previously presented in section 6.2 (Uman 1987):

$$\Delta E = \frac{1}{2\pi\epsilon} \int_{z_l}^{z_u} \frac{q(z)z dz}{(D^2 + z^2)^{1.5}} \quad (6.19)$$

The waveforms and their dynamics with a changing distance D in figure 6.9 are consistent with field measurements (e.g. Beasley *et al* 1982): that is to say, at short distances, the leader's amplitude is opposite in polarity to that of the return stroke

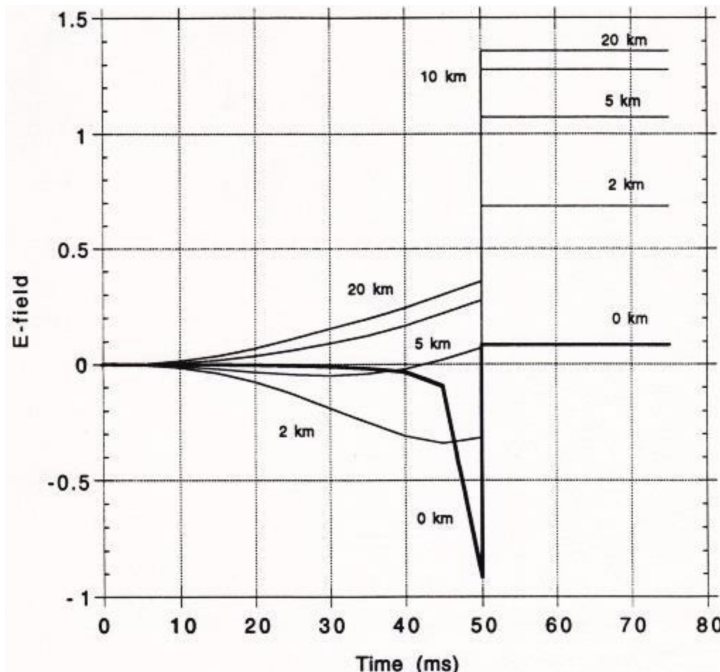


Figure 6.9. Vertical electric field changes on the ground from the CG leader and return stroke. Magnitudes are normalized to the return-stroke amplitude at a given distance from the channel (marked in kilometers). Reproduced from Mazur and Ruhnke (1998). Copyright 1998 by John Wiley Sons, Inc. Reprinted by permission of John Wiley & Sons, Inc.

amplitude; at greater distances, the leader and return stroke have the same polarity, and the ratio of leader to return stroke amplitude is approximately 0.36. This is in close agreement with the analytical estimate for a vertically developing bidirectional leader derived in Mazur *et al* (1995).

6.3.5 Development of the intra-cloud leader

The same approach used for determining the parameters of the CG leader in the cloud charge model is used in calculating the potentials, induced charges, and current of an IC leader. The IC leader originates at a 9 km altitude, where the vertical electric field distribution has a second maximum value (the first is at 5 km). It develops, similar to a CG leader, both vertically and bidirectionally along the cloud's axis of symmetry. The speed of the leader progression, in both directions, is assumed to be 10^5 m s^{-1} , applying the same rationale as for the speed of a bidirectional CG leader. Figure 6.10 shows the evolution of electrical potential profiles along the leader surface for the ten incremental steps of progression, each lasting 5 ms. The systematic shift in the leader's potential, observed in the developing CG leader, is less pronounced here. The progression of the lower positive-leader tip stops below 4 km, when its potential gradient is below the threshold value for electrical breakdown, or is close to zero. The model's calculations show that propagation of the upper negatively charged leader tip, with its huge potential gradient, is not limited by the upper boundary of the cloud at 12 km, and could

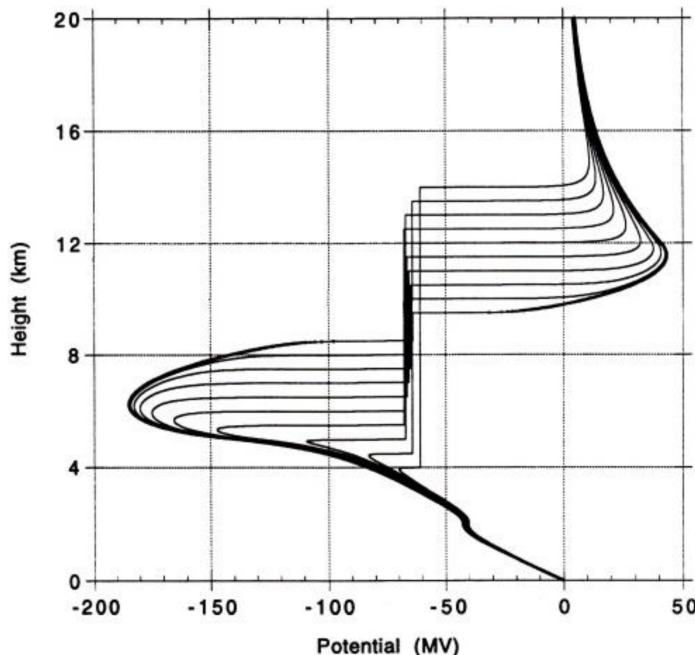


Figure 6.10. Evolution of potential profiles (1 m from the axis) of the developing IC leader. Reproduced from Mazur and Ruhnke (1998). Copyright 1998 by John Wiley Sons, Inc. Reprinted by permission of John Wiley & Sons, Inc.

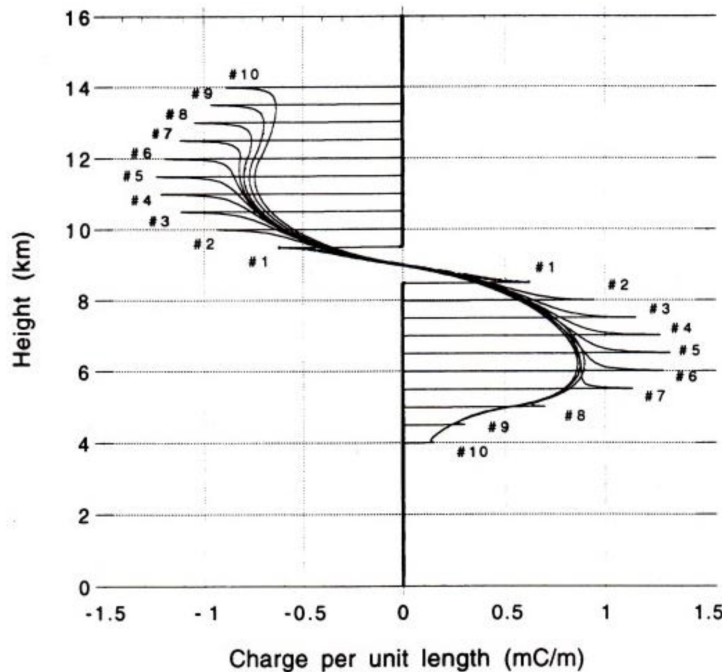


Figure 6.11. Induced charges on the IC leader developing with incremental steps of 5 ms. Reproduced from Mazur and Ruhnke (1998). Copyright 1998 by John Wiley Sons, Inc. Reprinted by permission of John Wiley & Sons, Inc.

continue up to the stratosphere, as long as the potential gradient at the tip exceeds the threshold value for the formation of negative streamers. This result is not totally surprising, because lightning channels extending from the top of the cloud into the stratosphere have been reported in the past by observers from spacecraft and high-altitude airplanes (e.g. Vonnegut 1980).

The induced charges on an IC leader (figure 6.11) have values similar to those on a CG leader (figure 6.6). With progression of the positively charged part of the IC leader ceasing at an altitude below 4 km, the induced charges at the tip diminish to zero value. Current distribution in the leader channel (figure 6.12) shows the same behavior as (and similar values to) that of a CG leader; the only difference is that of current polarity. The vertical electric-field intensity waveforms at the ground surface, resulting from the IC leader's progression (figure 6.13), have sign-reversal at the range of approximately 12 km. These waveforms exhibit the same range variation as those observed in the field (Ogawa and Brook 1964); that is, at close ranges, the waveforms are positive in polarity with slopes steeply inclined, while at greater distances, they are monotonically negative.

6.4 Applications and limitations of the electrostatic model

In the model, the quantitative relationships between the lightning processes and space charges in thunderstorms were obtained from numerical solutions of a

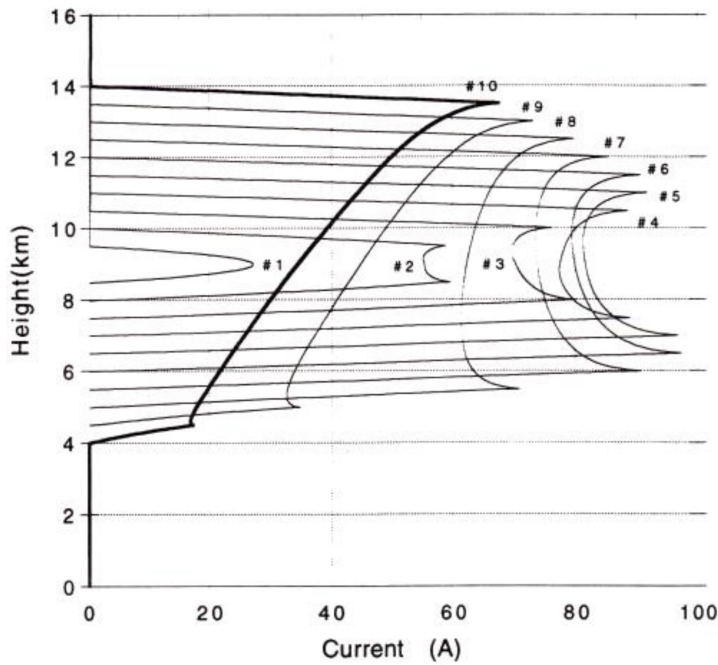


Figure 6.12. Current distribution in the progressing IC leader channel. Reproduced from Mazur and Ruhnke (1998). Copyright 1998 by John Wiley Sons, Inc. Reprinted by permission of John Wiley & Sons, Inc.

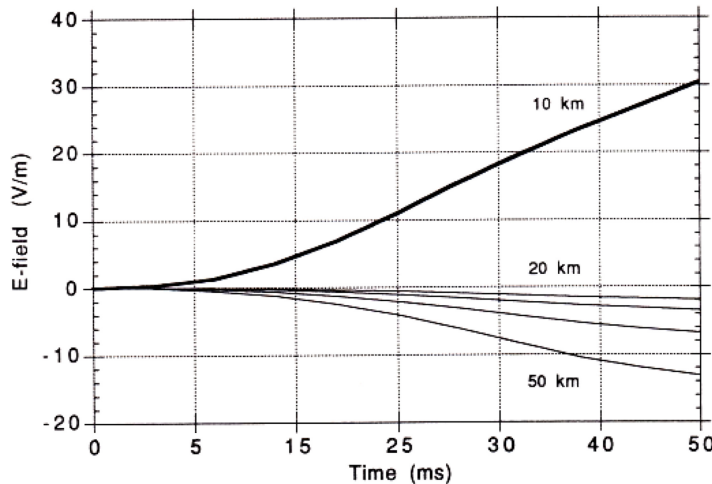


Figure 6.13. Electric field changes on the ground from the progressing IC leader. Reproduced from Mazur and Ruhnke (1998). Copyright 1998 by John Wiley Sons, Inc. Reprinted by permission of John Wiley & Sons, Inc.

simplified cloud-charge model, which should be considered a continuation of the earlier work of Kasemir (1950), identified by him as ‘a preparation for an exact mathematical analysis’. It has been shown that knowledge of the potential distribution within a thunderstorm cloud allows us to calculate the leader’s induced

charges and currents. Even with a crude two-dimensional cloud-charge model, it was possible to simulate the dynamics of the bidirectional leader process in CG and IC flashes. With the continuous streamer-to-leader transition at the leader's tip serving as the 'engine' of lightning progression, the lightning current continues to flow, both when the leader expands bidirectionally (initial stage), and when it expands unidirectionally (later stage). When the leader's tip reaches its potential inside the cloud (that is, when the potential gradient at the tip is near a threshold breakdown value), its propagation stops, and the current at the tip drops to zero. This represents the beginning of the 'current cutoff' condition (Mazur and Ruhnke 2014). When both tips cease expanding, the lightning process ends.

The reduction of propagation speed, and therefore, the reduction of current (such as that observed at the upper positive tip in the CG leader, or at the lower positive tip of the IC leader), occurs when the tip's potential is close to that of the ambient cloud potential. This is an example of how the speed of the leader is affected by the cloud potential distribution.

The model estimated the average current in the CG leader at ranges between 40 and 50 A, which is close to the 50 and 63 A measured with a magnetometer by Williams and Brook (1963). They also argued that, in general, this current should be less than 50 A. Airborne current measurements during lightning attachment to an aircraft (e.g. figure 4.9), lasting hundreds of milliseconds, provide values that fall within the same general range.

The charge transfer by negative first-return strokes, determined by integrating the current waveform over time (Berger *et al* 1975), averages 5.2 C. This is quite close to the model's estimate of 5.4 C. Charges in the return stroke are related to, and determined by, charges in the preceding leader, which we show to be below 2 C of the total positive or negative charge. The model's estimate corresponds to the low end of the range of values reported in the literature, from a few to tens of coulombs (Brook *et al* 1962; Krehbiel 1981).

In the electrostatic approximation, an external electric field is certainly critically important during lightning initiation, but should not be considered as the sole physical criterion during the propagation stage. After establishment of the conducting channel, the leader's propagation is determined by the potential gradient at the tip(s), which is changing due to two factors: (1) the ambient cloud potential near the given tip, and (2) the overall leader potential that varies with leader progression. This concept is illustrated in the electrostatic model, which shows that lightning can propagate upward to the stratosphere, where the ambient electric field is low. As long as the channel's potential is high, even if the cloud potential is zero, the potential gradient is sufficient to propel the leader even into a region of small space charges.

Further work on more complex electrostatic-type models of leader development may benefit from consideration of the following: (1) leader branching, which implies the use of a three-dimensional code for potential and field distribution, and (2) finite resistance of the leader channel leading to an average internal field of 1 kV m^{-1} for a 50 A current, instead of the zero internal field in our approximation (see King's curve in chapter 2). Considering finite resistance of the leader channel should not

make a significant difference in the results: for example, an 8 km long leader channel would have a potential change of 8 MV, which is less than 10% of the potential values shown in our leader model. Determining the consequences of commonly observed leader branching on leader current and charges with a computer-simulated electrostatic model is a very much needed, and a more challenging, task.

We know, from the kinematic numerical model of thunderstorm electrification (Ziegler and MacGorman 1994), that the electric field distribution has mostly vertical electric fields within the storm convective core, and mostly horizontal fields above the core in the region of high horizontal wind shear. Similarly, *in situ* balloon-borne measurements show that the electric field gains a significant horizontal component, starting at altitudes of 8 km and upward (Marshall and Marsh 1993, Marshall *et al* 1995). These measurements also show that, near the edge of the cloud, the field is of low magnitude, and is principally horizontal (Winn *et al* 1981). Therefore, the cloud model should reflect a horizontal heterogeneity of space charges at the upper region of the storm, so that, if the vertical IC leader is initiated at the center of the cloud's symmetry, the upper tip of the bidirectional leader will propagate horizontally within the cloud, and may be trapped inside the upper cloud boundary. The upper negative screening layer of a space charge may be an additional factor that affects the horizontal stratification of the negative part of IC leaders. The lightning structure that fits this description is observed with DTOA mapping systems (e.g. figure 5.9).

References

- Beasley W H, Uman M A and Rustan P L 1982 Electric fields preceding cloud-to-ground lightning flashes *J. Geophys. Res.* **87** 4883–902
- Berger K, Anderson R B and Kroninger H 1975 Parameters of lightning flashes *Electra* **80** 23–37
- Brook M, Kitagawa N and Workman E J 1962 Quantitative study of strokes and continuing currents in lightning discharges to ground *J. Geophys. Res.* **67** 649–59
- Clarance N D and Malan D J 1957 Preliminary discharge processes in lightning flashes to ground *QJR Meteorol. Soc.* **83** 161–72
- Heckman S and Williams E R 1989 Corona envelopes and lightning currents *J. Geophys. Res.* **94** 13287–97
- Kasemir H W 1950 *Qualitative Uebersicht ueber Potential-, Feld-, und Ladungsverhaltnisse bei einer Blitzentladung in der Gewitterwolke Das Gewitter* ed H Israel (Leipzig: Akademische Verlagsgesellschaft)
- Kasemir H W 1960 A contribution to the electrostatic theory of a lightning discharge *J. Geophys. Res.* **65** 1873–8
- Kasemir H W 1983 Static discharge and triggered lightning *Proc. 8th Int. Aerospace and Ground Conf. on Lightning and Static Electricity* (Fort Worth) pp 24.1–11
- Kasemir H W 1986 Model of lightning flashes triggered from the ground *Int. Aerospace and Ground Conf. on Lightning and Static Electricity* (Dayton, OH) p 39–1
- Kito Y, Horii K, Higashiyama Y and Nakamura K 1985 Optical aspects of winter lightning discharges triggered by the rocket-wire technique in Hokuriku district of Japan *J. Geophys. Res.* **90** 6147–57

- Krehbiel P R 1981 An analysis of the electric field change produced by lightning *PhD Thesis* University of Manchester
- Kuettner J 1950 The electrical and meteorological conditions inside thunderclouds *J. Meteorol.* **7** 322–32
- Malik N H 1989 A review of the charge simulation method and its applications *IEEE Trans. Electr. Insul.* **24** 3–20
- Marshall T C and Marsh S J 1993 Negatively-charged precipitation in a New Mexico thunderstorm *J. Geophys. Res.* **98** 14909–16
- Marshall T C, Rust W D and Stolzenburg M 1995 Electrical structure and updraft speeds in thunderstorms over the southern Great Plains *J. Geophys. Res.* **100** 1001–15
- Mazur V and Ruhnke L H 1998 Model of electric charges in thunderstorms and associated lightning *J. Geophys. Res.* **100** 23299–308
- Mazur V and Ruhnke L H 2014 The physical processes of current cutoff in lightning leaders *J. Geophys. Res.* **119** 2796–810
- Mazur V, Ruhnke L H and Laroche P 1995 The relationship of leader and return strike processes in cloud-to-ground lightning *Geophys. Res. Lett.* **22** 2613–6
- Ogawa T and Brook M 1964 The mechanism of the intracloud lightning discharge *J. Geophys. Res.* **69** 514–9
- Proctor D E 1991 Regions where lightning flashes began *J. Geophys. Res.* **96** 5099–112
- Schonland B F J 1956 The lightning discharge *Handb. Phys.* **22** 576–628
- Uman M 1987 *The Lightning Discharge* (San Diego, CA: Academic) p 317
- Vonnegut B 1980 Cloud-to-stratosphere lightning *Weather* **35** 59–60
- Williams D P and Brook M 1963 Magnetic measurements of thunderstorm currents *J. Geophys. Res.* **68** 3243–7
- Williams E 1989 The tripole structure of thunderstorms *J. Geophys. Res.* **94** 13151–67
- Winn W P, Moore C B and Holmes C R 1981 Electric field structure in an active part of a small, isolated thundercloud *J. Geophys. Res.* **86** 1187–93
- Ziegler C L and MacGorman D R 1994 Observed lightning morphology relative to modified space charge and electric field distributions in a tornadic storm *J. Atmos. Sci.* **51** 834–51

Principles of Lightning Physics

Vladislav Mazur

Chapter 7

Lightning triggered by rockets with wire and by tall structures

7.1 The idea of artificially triggered lightning

If it is possible to initiate a leader from a pointed electrode in a high-voltage laboratory, as described in chapter 2, why not try to do that in the gap between the ground and a thundercloud, using a ground structure as the pointed ignition electrode? This was the idea behind the earliest attempts to trigger lightning from the ground. Of course, there are differences between the settings in a high-voltage laboratory—with a gap of a certain, limited length between the pointed high-voltage and ground electrodes—and the settings under a thundercloud, with its ambient electric field, and a lower ground electrode alone, with no upper one. The moving ground electrode in the classic rocket-and-wire technique is an ascending small rocket pulling a thin metal wire that is connected to the ground.

The first difference between two settings is in the magnitudes of the electric fields. A field of several million volts per meter can be created in a laboratory by a high-voltage pulse generator, while the highest ambient field under a thundercloud rarely reaches even 20 kV m^{-1} . Affected by the corona layer formed above sharp-edged and pointed ground vegetation, the vertical electric field at ground level during thunderstorms is usually much less than 10 kV m^{-1} . Another difference between laboratory and nature is in the ways to overcome the corona space-charge shield near the tip of the electrode. This shield forms in a high ambient E -field, choking the corona current, and thus preventing the corona streamer-leader transition—the first stage of leader development. In a high-voltage chamber, the application of high voltage to the electrode occurs very suddenly, as a voltage impulse. This solves the problem of breaking through the corona shield. A somewhat similar effect, of overcoming the corona shield formed near the tip of the tall structure, takes place when a very fast change in the ambient electric field is produced by a fast approaching IC leader, or a return stroke of a CG flash nearby, both of which

carry charges of the polarity opposite to that of the triggered leader. The escape, or overrunning, of the corona space-charge shield may also be achieved by moving the grounded electrode (or any pointed conducting body contained within the ambient electric field) forward more rapidly than the speed with which the shield of the space charge is formed. For this reason, the speed of the rocket is critical, and should be greater than 100 m s^{-1} . The same effect explains why the blades of tall windmill towers trigger lightning more frequently when they are rotating than when they are stationary.

Most lightning events triggered using the rocket-and-wire techniques in summer thunderstorms develop as positively charged leaders, due to the presence of a dominant negative space-charge region in the lower part of most of these storms. Triggered lightning events that are negatively charged leaders are rarities, in general, particularly in summer thunderstorms. The majority of such events have been produced in winter thunderstorms, in the coastal areas of the Sea of Japan. A small number of cases of triggered upward negatively charged leaders have been observed on the Peissenberg tower in Germany, and on the Gaisberg tower in Austria, during cold seasons.

Using the rocket-and-wire technique researchers can control the placement of the triggered lightning event and, therefore, have the opportunity to pre-arrange coordinated and synchronized observations of the event with a variety of sensors. Also, by guiding a triggered lightning flash to a grounded structure, and exposing it to the hazardous effects of lightning, researchers are able to evaluate the performance of the crucially important lightning-protection systems installed at such sensitive places as storage and operations facilities for explosives, and electric power lines (e.g. Schnetzer and Fisher 1991).

7.2 Concept and features of the classic rocket-triggered lightning technique

The electric field at the tip of an elongated conductive object, composed of the rocket plus the attached grounded wire, is proportional to the ambient field value multiplied by the *form factor* of the conductor, that is, the ratio of the object's length to its diameter. The form factor, as well as the ambient electric field, increases with the increasing length of the wire above the ground. At a certain height, usually of more than 100 m, the electric field at the rocket's tip reaches the breakdown value for starting the corona streamers. These streamers first form the short-lived 'attempted leaders'—precursors of a sustainable leader (Lalande *et al* 1998). They appear as a series of current impulses of $30 \mu\text{s}$ duration, of tens of amperes in amplitude, and with intervals between them on the order of 10 ms (Willett *et al* 1999). As the rocket continues its ascent, and the ambient *E*-field becomes sufficient to support the sustainable development of the leader channel, the precursor pulses decrease in amplitude, becoming unipolar current pulses superimposed on a slowly growing DC-type current (figure 7.1).

In essence, with the rocket-and-wire technique, the grounded electrode is extended fast enough to escape the choking effect of the corona formed at the

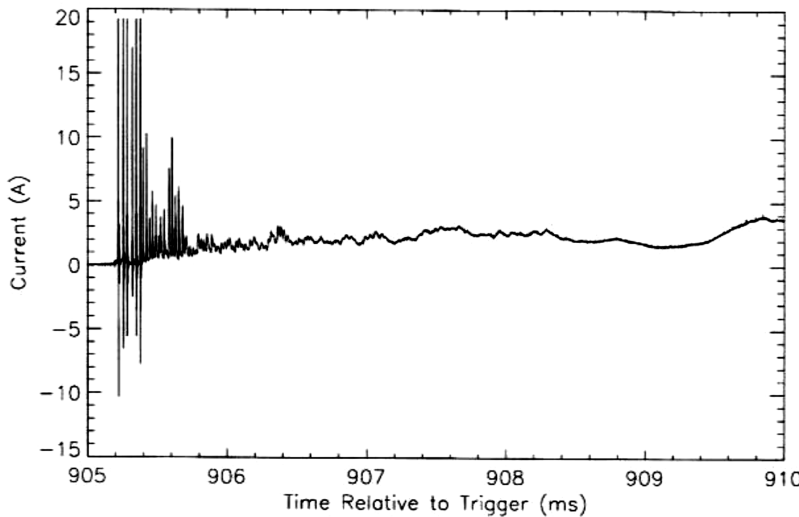


Figure 7.1. Current record of the upward positive leader triggered by the classic rocket-and-wire technique. Reprinted with permission from Willett *et al* (1999). Copyright 1999 Elsevier.

rocket tip, and far enough into the ambient electric field to reach the electrical conditions needed for leader formation. This action is in contrast to the stationary set-up in a high-voltage laboratory gap, where the same conditions (see chapter 2) are achieved by applying a high-voltage impulse to a pointed electrode.

Producing a self-propagating leader that ascends into a thundercloud is always the first stage in the triggering of a CG lightning flash with the rocket-and-wire technique. Such a flash, however, may or may not follow the leader's formation; but it is, nevertheless, the main objective of the entire exercise (see figure 7.2).

According to the *law of electrical inductance*, a grounded conductive wire spooled vertically in the ambient electric field will obtain induced charges along its length; the total charge will increase with height, and will be of zero value at ground level. The distribution of the induced charges along the wire should mirror in its shape the ambient potential distribution with height (Kasemir 1986). With the wire ascending, the total induced charge will change; this change constitutes the electrical current that flows into the wire from the ground. If the grounded wire were to remain stationary (such as a metal tower, for example), the stationary charge distribution on the wire would not produce the current flow.

7.2.1 Processes related to melting of the trailing wire

The current from the ground grows faster after the upward leader begins to develop from the tip of the wire, because the speed of the leader (initially approximately 10^4 m s^{-1}) is much greater than the speed of the ascending rocket ($\sim 200 \text{ m s}^{-1}$). When the wire current exceeds $\sim 100 \text{ A}$, the thin wire starts to melt and then evaporates; this cuts off the connection to, and the current from, the ground. The melting of the trailing grounded wire—the most common feature in upward

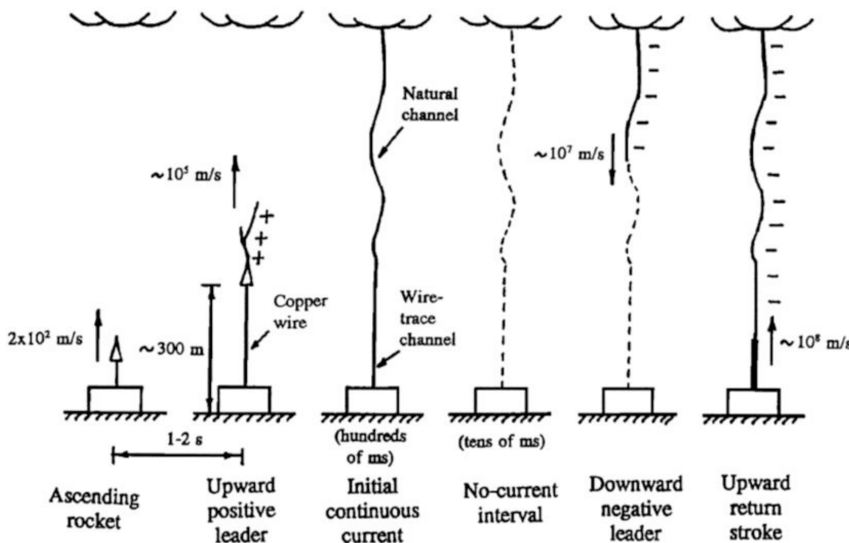


Figure 7.2. Sequence of events that occurs during the formation of a classic triggered lightning flash. The melting of the copper wire and re-establishment of the conductive leader channel are not shown in the figure. Reproduced from Rakov *et al* (1998). Copyright 1998 by John Wiley Sons, Inc. Reprinted by permission of John Wiley & Sons, Inc.

lightning triggered with the classic rocket-and-wire technique—is followed by other processes which deserve an explanation.

The effects of the melting of the triggering wire observed in current and electric-field records of a positive upward leader (see the example in figure 7.3) were carefully examined by Rakov *et al* (2003). They interpreted the bridging of the gap produced by the vaporization of the triggering wire as a type of leader/return stroke process.

There is an ‘electrostatic’ interpretation of this process. After the melting of the wire and, thus, the interruption of the current flow from the ground, the plasma channel of an upward positive leader becomes electrically floating. The potential of the leader, from its zero ground potential before wire meltdown, instantly changes towards a more negative ambient potential value. This drop in leader potential is seen as the negative slope B_1 of the V-shaped pulse in the E -field recorded in figure 7.3. The difference in potentials of the lower end of the floating leader and the path with metal vapors, still ionized and under the ground potential, is sufficient to produce an arc discharge that instantly reconnects the leader to the ground. This reconnection is seen in the electric- and magnetic-field changes that occur during the V-shape change (figure 7.4): the current pulse starts at the beginning of the recovery of the E -field (the upward slope) that happens after leader’s contact is established with the ground.

The current- and electric-field records in figure 7.3 have two distinct features: (1) the period of linear increases in both the average leader current (with pulses superimposed) and the corresponding E -field and (2) the period of decreasing current during the still-rising E -field. The feature of linear growth is well understood: it characterizes the extension of a single (non-branched) vertical channel. Indeed,

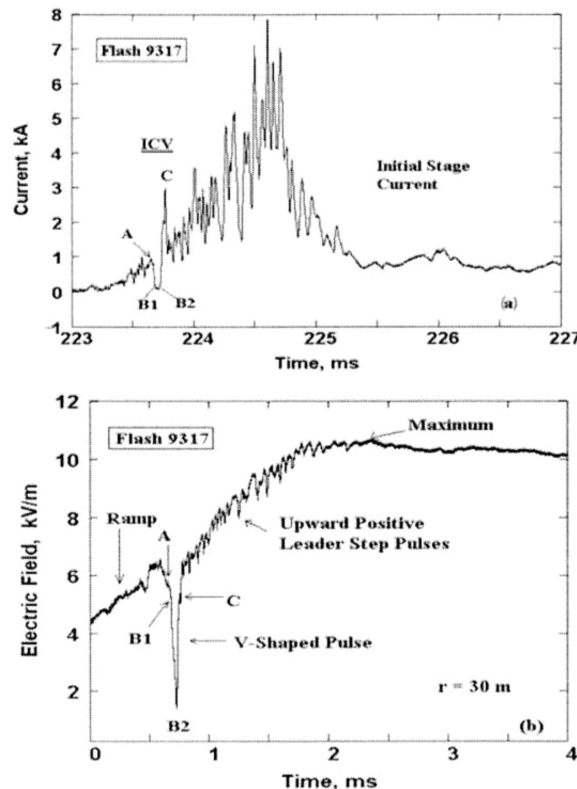


Figure 7.3. The current and the electric field from a positive leader started with the classic rocket-triggering technique. Reproduced from Rakov *et al* (2003). Copyright 2003 by John Wiley Sons, Inc. Reprinted by permission of John Wiley & Sons, Inc.

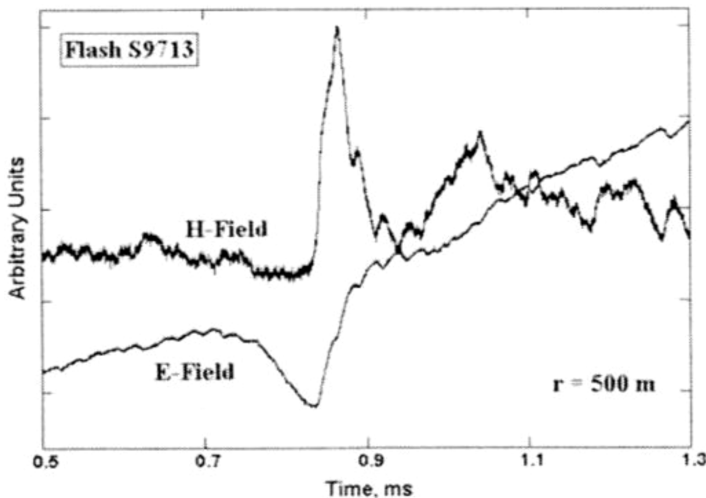


Figure 7.4. Magnetic- and electric-field records during vaporization of the triggering wire and restoration of the continuity of the positive leader. Reproduced from Rakov *et al* (2003). Copyright 2003 by John Wiley Sons, Inc. Reprinted by permission of John Wiley & Sons, Inc.

visual observations of classic-type rocket-triggered lightning after launching the rocket confirm the existence of only a single luminous channel entering the cloud. The beginning of horizontal branching that follows the upward leader as it enters the cloud was the subject of speculation by some researchers a while ago, but has only recently been verified in observations using the lightning-radiation mapping technique (e.g. Hill *et al* 2012). The period of current decline visible in the record in figure 7.3 coincides with the IC development of the upward leader, which is also accompanied by branching of the leader channel. The E -field on the ground, during progression of the upward leader (figure 7.3), reaches its maximum, while the current value drops to a steady DC level. An interpretation of the decline of the leader current after it reaches its peak to a steady value (~ 100 A in figure 7.2) is given in chapter 8.

In the classic rocket-and-wire technique, after restoration of the leader's connection to the ground, an upward leader of either polarity may continue to develop, at least until the current from the ground in the leader channel ceases to flow (the current cutoff). A second scenario takes place in upward positively charged leaders, and has not yet been observed in upward negatively charged leaders; it includes the appearance of a *dart leader* after the current cutoff in the leader channel and a pause of up to hundreds of milliseconds. The downward negatively charged dart leader travels along the ionized remnants of the preceding upward leader channel and, with the *return stroke* that follows, constitutes an artificially triggered CG lightning flash. A flash such as this has all the characteristics of the subsequent dart leader–return stroke cycle in negative multi-stroke CG flashes.

7.3 Concept and features of the altitude-triggered lightning technique

A modified classic rocket-triggering technique, called *altitude-triggering*, was introduced in the 1990s, and consisted of replacing the lower portion of the copper trailing wire attached to a rocket with a long section (~ 400 m) of insulating Kevlar cable, followed by a short (~ 50 m) section of grounded wire. In this scheme, a rocket with a trailing wire is effectively disconnected from the ground. The incentive for this modification came from studies of lightning interactions with flying aircraft, which confirmed that an electrically floating conductor (an aircraft) may trigger lightning in the ambient electric field of a thunderstorm (Laroche *et al* 1991). See chapter 4 for more details.

The dynamics of leader development in the altitude-triggering technique (figure 7.5) are different from that of the classic rocket-and-wire technique, where the current cutoff occurs during melting of the trailing wire and, for a short while, metal vapors provide a weakly ionized path to the ground. This sequence does not happen in the altitude-triggering technique, because a non-conductive Kevlar cable is inserted at the lower end of the trailing wire between it and the ground (see figure 7.5), as opposed to the direct connection of this wire to the ground in the classic rocket-and-wire technique (figure 7.2). Within a few milliseconds, after reaching an altitude of several hundred meters and the start of the positive leader at the upper tip of the rocket, a negative downward leader starts at the lower end of the trailing wire. This constitutes the development of a bidirectional, bipolar leader from an electrically floating conductor in the ambient electric field, and is similar in

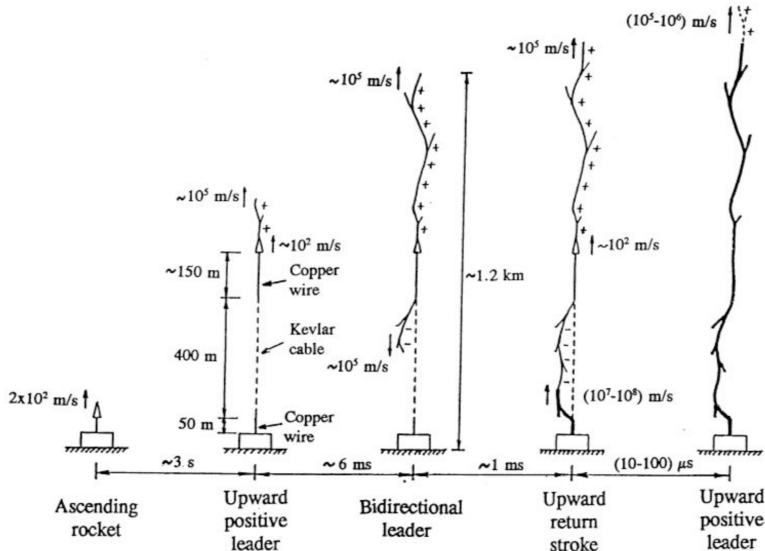


Figure 7.5. Sequence of events occurring during formation of the first return stroke in altitude-triggered lightning. Based on Laroche *et al* (1991). Courtesy of NASA.

all respects to the development of aircraft-triggered lightning. The downward leader of negative polarity is of the ‘stepped’ type, because it progresses in virgin air between the lower end of the conductive wire and the ground.

The return stroke that follows may be characterized as a ‘mini’-return stroke, because of its relatively low current. The explanation for such a low current is in the relatively small difference between the potentials of a bidirectional leader channel of altitude-triggered lightning and the ground; the channel of a triggered upward leader does not extend far enough into the thundercloud to have its potential comparable to the much greater potential of bidirectional leaders in natural lightning flashes originated in the cloud. In altitude-triggered lightning, the occurrence of a mini-return stroke is virtually guaranteed, after which the sequence of processes is the same as that found in triggering with the classic rocket-and-wire technique.

Both rocket-and-wire lightning-triggering techniques have been effective tools in studying the physics and properties of positively and negatively charged leaders, and also the nature of the sequential return strokes in negative multi-stroke CG flashes (Lalande *et al* 1998). Our ability to investigate, using the altitude-triggering technique, the processes involved in the formation of a bidirectional and bipolar leader from an electrically floating conducting wire has been a particularly valuable result of these studies.

7.4 Conditions required for triggering lightning with rocket-and-wire techniques

The successful triggering of a CG flash (not counting a mini-return stroke) using the rocket-and-wire or altitude-triggering technique is never guaranteed, and depends

on several factors, among which are the stage of the storm's evolution, the magnitude of the electric field on the ground, and even the frequency of natural lightning flashes at the time of the launch. The majority of the attempts at successful lightning-triggering by the rocket-and-wire techniques are achieved in summer thunderstorms, with a negative electric field on or above the ground and, therefore, triggered lightning started as upward leaders of positive polarity. In winter thunderstorms, prevalent in the coastal areas of the Sea of Japan, the rocket-triggered upward leaders can be of either positive or negative polarities, the latter being a rare occurrence in any other part of the world. A significant feature of triggered negative upward leaders is that they never lead to the occurrence of downward positive dart leaders after current cutoff in the channel to the ground and, consequently, do not produce a positive CG flash.

Scientists who were involved in studies of triggered lightning quickly discovered that it is nearly hopeless to try to trigger lightning by launching rockets during the active stage of a thunderstorm, a period characterized by a high rate of natural lightning flashes. They arrived at a better approach: wait for the decaying stage of the storm, when the electric field on the ground may still be high, but the rate of natural lightning is drastically lower, and launch the rocket when the ambient field reaches its maximum, provided that natural lightning does not start before the rocket launch. Artificial triggering is most successful when the natural triggering mechanism (about which we still do not know too much) is either dormant, or very slow in its development, which is typical for the decaying stage of a thunderstorm. Therefore, the intrusion of either an aircraft or rocket with a trailing wire into the ambient electric field of a thunderstorm produces a triggering mechanism, which then acts in competition with the natural lightning-triggering mechanism in the storm.

7.5 On leaders and return strokes in rocket-triggered lightning

The return stroke in a CG flash and an upward leader triggered by a rocket with a trailing grounded wire have one feature in common: both carry a charge of the same polarity, i.e. both are ‘unipolar’, with a zero charge at the ground end, and a growing induced charge with increasing height. The difference between the return stroke and the upward leader lies in the nature of their propagation paths. The path of the return stroke is the channel of the preceding downward bidirectional, bipolar leader, a highly ionized plasma channel that serves as a ‘high-speed highway’ for the return stroke. The path of the upward leader, on the other hand, is through virgin air on a newly forged pathway that slows down the propagation speed. The different nature of the pathways results in a huge difference between the speeds of the upward leader and the return stroke and, thus, the magnitudes of their currents.

The return stroke, after it reaches the top of the preceding bipolar leader channel, produces a vigorous breakdown due to the huge difference between the near-ground potential of the return-stroke channel and the high cloud potential. This vigorous breakdown may initiate a new leader of the same polarity as that of the return stroke. Progression of this new leader can be recognized in the presence of the

continuing current that flows in the return-stroke channel, as long as the new leader continues its propagation.

The current cutoff in the upward-leader channel, commonly observed in rocket-triggered lightning in summer thunderstorms, may be a result of two possible outputs: the first is the termination of development of a single, unbranched leader channel, which occurs when the potential drop at the tip of the leader reaches the minimum threshold needed for leader extension; the second output is the current cutoff in the trunk of the branched upward leader channel, which is followed by a dart leader that retraces the decaying channel of the preceding positively charged upward leader. The mechanism of this current cutoff is discussed in chapter 8.

The unusual events of downward dart leaders that follow along the conducting channel of upward leaders without a preceding current cutoff have been observed in rocket-triggered flashes in the mountains of New Mexico (Eack 2015). The following hypothesis may explain this phenomenon: thunderstorms in the mountains have a low cloud base, so straight upward-leader channels between ground and the cloud base are shorter than those in thunderstorms over the flat terrain. The total induced charges on the ascending leader channel and the speed of the accelerating leader will not result in a melting current prior to the leader entering the cloud where leader branching begins. In this scenario, a recoil leader that occurs in a branching structure of the leader reaches the grounded leader trunk in the manner of an M-event. See chapter 9 for further details of this phenomenon.

7.6 Upward lightning triggered by tall ground structures

The most common types of structure-triggered lightning are the upward leaders that emanate from the tops of skyscrapers, tall TV and radio towers, and transmission-line towers at high elevations. Observation of these triggered events has provided unique opportunities for the lightning research described in the next two sections.

7.6.1 Conditions for upward lightning initiation

The majority of lightning strikes to tall structures of more than 100 m in height fall into the category of so-called ‘upward lightning’, as opposed to downward CG flashes, for the simple fact of their development from the top of tall structures, upward. Heidler (2002) reported that during a period of six years (1992/93–98) the 160 m tall Peissenberg telecommunications tower in Bavaria, Germany, received 117 lightning strikes, of which all but one were upward lightning events. Diendorfer *et al* (2005) reported that upward lightning represented 236 out of 242 recorded strikes to an instrumented 100 m tall tower in the Austrian Alps during the 2000–3 storm seasons.

The dynamics of an upward lightning event from a tall structure are similar to those of a classic-type rocket-and-wire triggered lightning, except for the melting of the ground wire and, thus, the mini-return-stroke occurrence. Sustained upward leaders from tall structures are different from short-lived leaders, which appear in response to an approaching downward leader of the opposite polarity, but which terminate when the downward leader reaches the ground. As in the cases of

rocket-triggered lightning, not every upward leader is followed by a dart leader–return stroke cycle of a CG flash. For example, only 50% of the upward lightning from the Empire State Building and 27% of the upward lightning from the Ostankino TV tower exhibited the dart leader–return stroke cycle, according to Rakov (2015).

The presence of a ground corona layer under the thunderstorm, up to several hundred meters high, should be considered when one evaluates the possibility of initiation of upward lightning from tall structures. A rocket with a trailing wire, by reaching cloud regions at altitudes beyond the heights of most tall structures, is much more likely to produce sustainable formation of an upward leader than a stationary tall structure. The exceptions would be a few buildings and towers with heights above 300 m, such as the Empire State Building (443 m) in the USA, the Toronto CNT tower (553 m) in Canada, the Ostankino TV tower (540 m) in Russia (see figure 7.6), and the Tokyo Skytree (634 m) in Japan, or towers of lesser heights, but installed very high above the surrounding terrain, such as the Gaisberg Tower (Austria) (100 m high + 800 m above sea level (ASL)) and the Peissenberg Tower, Germany (160 m high + 250 m ASL) (see figure 7.7). The tops of these tall towers are above the ground corona layer and are already exposed to high ambient E -fields. The ground corona layer provides a sort of height boundary, below which triggering by the tall structure may not occur, even if the corona shield at the top is removed. This boundary height is approximately 150 m above the ground. Towers shorter than this boundary height may experience lightning strikes by natural CG flashes.

There are important similarities between a tall ground structure and a rocket with a trailing wire: the significant enhancement of the ambient E -field, due to the height of a structure, or the altitude of the tip of an ascending rocket above the ground, and their connections to the ground. The differences between them become evident in the way they each overcome the effect of the current-choking corona shield in order to reach a high ambient E -field at the tip of the structure. A fast-moving rocket escapes the slowly forming corona shield at its tip, however, at the top of a tall structure, the corona shield develops in a stationary ambient E -field. This corona shield can be removed by a strong wind, or can be overpowered by a pulse-like ambient E -field



Figure 7.6. Upward lightning triggered from various very tall ground structures.



Figure 7.7. Communication towers in Austria (Gaisberg Tower) and Germany (Peissenberg Tower), instrumented for observations of upward lightning initiated by the tower.

change of the polarity opposite to that of the corona-shield charge. This change, in the case of the positive corona-shield charge, may be produced by an approaching negatively charged leader of an IC flash, or the return stroke of a positive CG flash nearby that carries a negative charge. These circumstances take place in the majority of triggered upward lightning events from tall structures with heights above 150 m, during summer thunderstorms (Mazur and Ruhnke 2011).

The dynamics of the occurrence of an upward positive leader from the 295 m tall CBS tower in Kansas City, triggered by an approaching negative leader, are illustrated in figure 7.8. The shape of the current record during upward leader initiation from the top of the tower is seen in the shape of the dE/dt record in figure 7.8, and is very similar to the shape of current records during the initial period of classic rocket-triggered lightning (see figure 7.2).

Upward leaders from tall structures triggered by passing in-cloud leaders of the opposite polarity (an interpretation first suggested by Berger and Vogelsander 1969), or by return strokes carrying charges of the opposite polarity, may be considered to be examples of *associated or sympathetic discharges* (Mazur 1982, Vaughan and Vonnegut 1989), so-called because one lightning process produces the conditions for starting the other in the space of a few milliseconds, some distance away, and without evidence of any physical connection between the two discharges. Kitterman (1981), who observed upward lightning from two TV towers (324 m and 295 m tall) in Kansas City, Missouri, separated by a distance of 1.1 km, reported (from analysis of photographs with a streak camera array) the occurrence of ‘concurrent’ upward lightning at the towers, with an average time separation of 40 ms. Kitterman speculated that ‘the first flash of concurrent pairs may be significantly responsible for triggering the second’. If this were true, we have to assume the possibility of the two sequential flashes being of opposite polarity; this can be proven only with

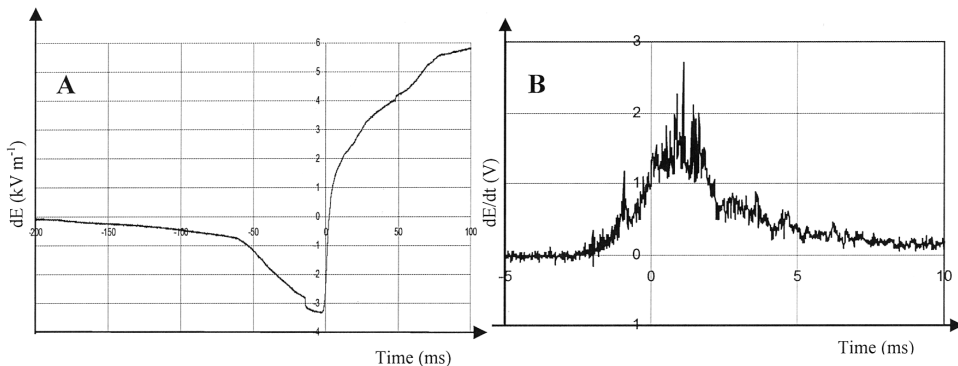


Figure 7.8. (A) Record of electric-field changes indicating an approaching negatively charged leader (negative change in dE) prior to the zero time mark, and the occurrence of a triggered upward positively charged leader from the tower (positive change in dE), started at about the zero time mark. (B) The dE/dt record of the initial period of an upward positive leader from a tall tower triggered by the approaching negative leader of an IC flash. The zero-time corresponds to the time of triggering of the high-speed video system. Reprinted with permission from Mazur and Ruhnke (2011). Copyright 2011 Elsevier.

electric-field measurements, which were not available to Kitterman. The evidence of such an occurrence was presented by Lu *et al* (2009), from observations during a winter storm in Japan of upward lightning from two tall towers in close proximity to each other. The incident of the ‘concurrent’ or, rather, rapidly sequential occurrence of upward leaders from two or more towers triggered by the same external source was also reported in Warner *et al* (2008); however, in this instance, the towers involved were widely separated.

The initiation conditions for upward leaders from tall structures without the presence of such triggering factors as in-cloud leaders or return strokes, are still poorly understood. Wang *et al* (2008) identified such a category of cases from the analysis of upward lightning strikes to a wind turbine and a protective mast (both about 100 m tall) during winter storms in coastal areas of the Sea of Japan. Earlier evidence of upward positive leaders initiated without apparent in-cloud lightning flashes preceding them, also observed in Japan, have been reported by Takagi *et al* (2006). In the data presented by Wang *et al* (2008), there is an indication of a strong wind near the top of the mast at the time of upward-leader initiation. This wind may have caused the removal of the corona shield, thus exposing the mast to the very high electric field typical of winter storms in Japan. A strong wind, not uncommon at the tops of very tall structures, can remove the corona shield there, thus clearing the way for initiation of an upward leader. This is the most probable explanation (still in need of verification) for the upward-lightning statistics that list cases of triggered upward lightning from tall structures that occurred in the absence of the preceding nearby lightning flashes.

7.6.2 Understanding luminosity variations in the upward-lightning channel

Ascending upward leaders from tall towers appear as continuously luminous single channels, prior to entering the cloud. The luminosity of these channels may persist

for hundreds of milliseconds, always exhibiting slow variations in brightness, and also occasional pulse-type bursts of re-illumination. These slow variations in luminosity last a few milliseconds (figure 7.9). The physical concept illustrated in figure 7.10 interprets this luminous variation as being the result of propagation of the conducting channel through a region of varying ambient potential.

If the vertical profile of ambient potential distribution is represented by the curve ϕ , then the induced charges, q , on the ascending conducting channel will be distributed along a profile which is the mirror image of curve ϕ (Kasemir 1986). The current in the leader channel, I , is the result of the changing induced charges during the ascent of the leader (e.g. between times t_1 and t_2 in the sketch). Thus, although the current remains constant along the channel at any given moment, the current amplitude changes with time (see current curve in figure 7.10), and so does the channel's luminosity. A similar relationship between the vertical charge distribution and the current in an ascending upward leader triggered with a rocket-and-wire technique was deduced from electric field measurements at three distances (0.5 km, 2.2 km, and 9.6 km) from a launching site at the Kennedy Space

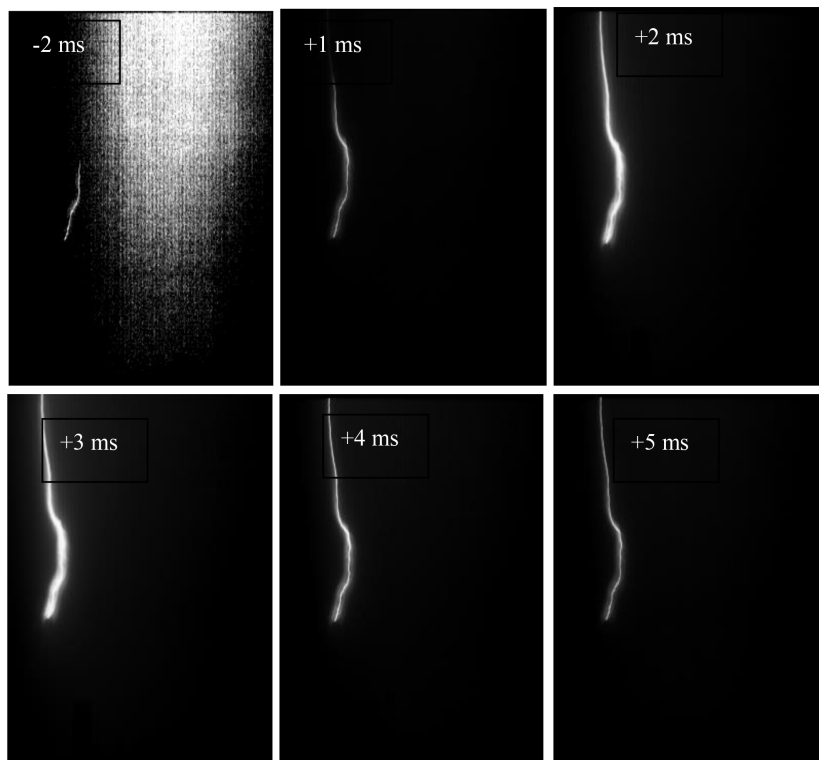


Figure 7.9. Video frames of the slowly changing luminosity of an upward leader following its initiation from a tower (video recording speed 1000 fps). Timing of the video frames is relative to the time of the triggering of the video system. Reprinted with permission from Mazur and Ruhnke (2011). Copyright 2011 Elsevier.

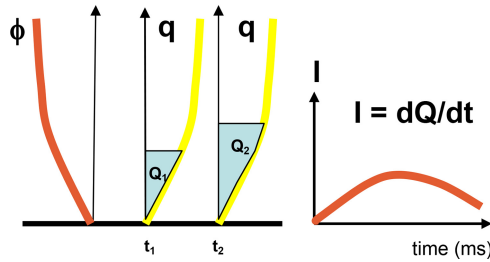


Figure 7.10. Conceptual sketch explaining the slowly varying luminosity of an ascending leader channel. Depicted are a vertical ambient potential profile (ϕ); induced charges per unit length (q) on a vertical conducting channel at times t_1 and t_2 ; and the current (I) in the ascending channel, as a function of time and the induced charge Q . Reprinted with permission from Mazur and Ruhnke (2011). Copyright 2011 Elsevier.

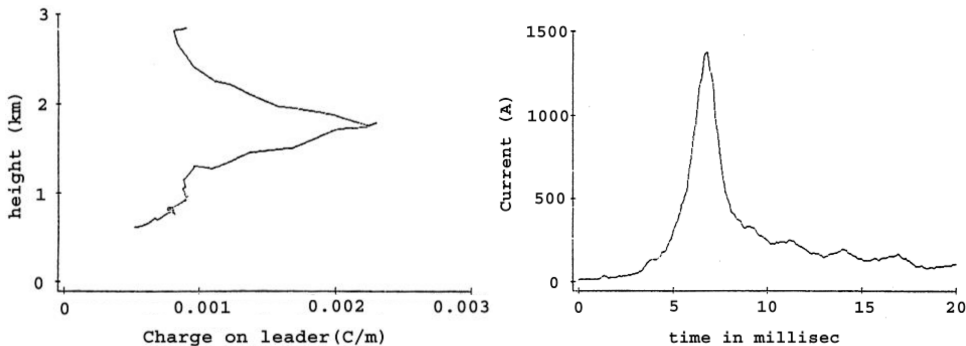


Figure 7.11. Vertical distribution of induced charges on an ascending rocket-triggered leader and the corresponding current in the leader channel, calculated from electric-field measurements at multiple distances from the launching site. Reproduced from Ruhnke and Kasemir (1988). Copyright 1988 by John Wiley Sons, Inc. Reprinted by permission of John Wiley & Sons, Inc.

Center in Florida (Ruhnke and Kasemir 1988) (see figure 7.11). Again, note the similarity between the current records in figures 7.2, 7.8, and 7.11.

In addition to a slowly changing luminosity, the pulse-type brightening phenomenon has been observed in the trunks of upward leaders, but only after they entered and disappeared in the cloud, and also in the trunks of visibly branched upward leaders. Therefore, it is reasonable to associate this type of luminosity with branching processes. The luminosity pulse appears in a single frame of the high-speed video recording, with a speed of 1000 fps (see example in figure 7.12). The dE/dt and dE records in figure 7.13, corresponding to this event, indicate the actual duration of the luminosity pulse to be only a fraction of a millisecond.

Events that produce the pulse-type brightening of an upward-leader channel have an electric-field change with a ‘hook’-shaped signature, which fits the definition in the lightning literature of the M-component (Malan and Schonland 1947, Rakov and Uman 2003). The phenomenon of the M-component, and its mechanism, are the subjects of chapter 9.

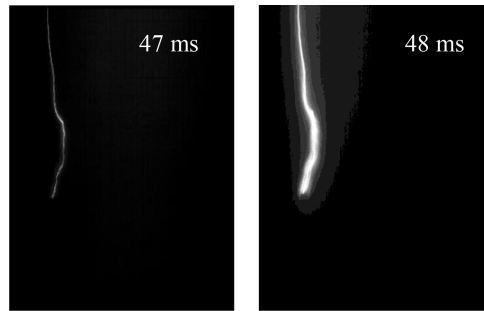


Figure 7.12. The pulse-type brightening, at 48 ms, of the upward-leader channel, that had maintained weak luminosity until 47 ms, and after 48 ms. Reprinted with permission from Mazur and Ruhnke (2011). Copyright 2011 Elsevier.

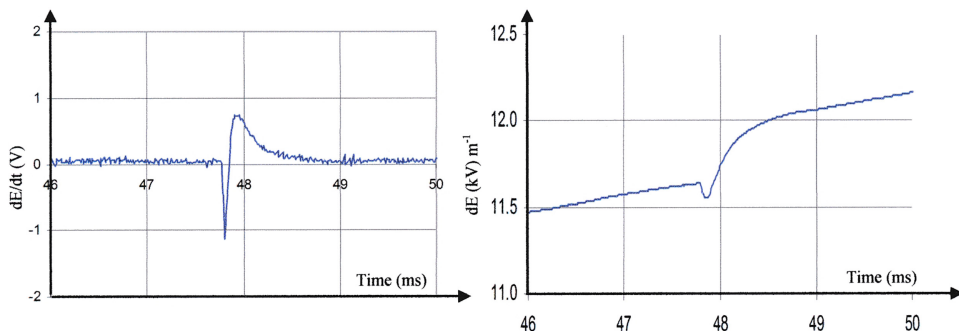


Figure 7.13. The raw dE/dt and dE records of the pulse-type brightening event in an upward positive leader, seen in video images at 48 ms in figure 7.12. Reprinted with permission from Mazur and Ruhnke (2011). Copyright 2011 Elsevier.

7.7 Features of positive and negative leaders determined from studies of triggered lightning

The majority of data obtained with the rocket-and-wire lightning-triggering techniques are from upward positively charged leaders and the dart leader-return stroke sequences in multi-stroke negative CG flashes. The characterization of upward positive leaders is based mainly on analysis of their current records, a typical example of which is in figure 7.14 (Miki *et al* 2005). The upward leader lasts for hundreds of milliseconds, on average ~ 300 ms, with a maximum duration of ~ 700 ms, while the range of its current values is between 15 A and 2.1 kA. The impulsive currents, superimposed on continuous current in figure 7.14, are the results of M-events, and their amplitude is in the range of those in the weak return strokes of negative CG flashes (Heidler 2002, Flashe *et al* 2011).

It is, perhaps, appropriate to comment here on the inadequate terminology applied to descriptions of the phases of leader development. The terms ‘initial stage’, ‘initial continuous current’, and ‘initial continuous current pulses’, frequently used to describe the beginning of upward lightning development, actually reflect only

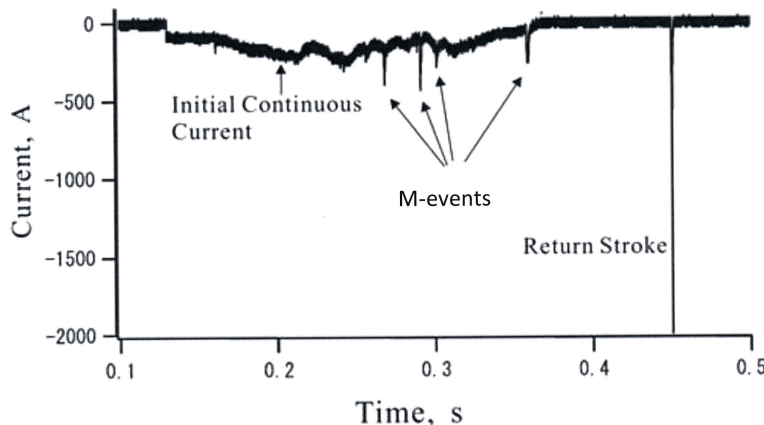


Figure 7.14. Current record of a rocket-triggered upward positive leader followed by multiple cycles of dart leader–return strokes (in the box). (Note that the record is in the atmospheric electricity sign convention.) The identity of the current pulses superimposed on the current of the positive leader was changed from the original ‘initial continuous current pulses’ to ‘M-events’, in agreement with the interpretation of these pulses in chapter 9, as being of the same nature as the M-events that follow return strokes. Reproduced from Miki *et al* (2005). Copyright 2005 by John Wiley Sons, Inc. Reprinted by permission of John Wiley & Sons, Inc.

their timing, not the nature of the processes involved. The term ‘continuing current’ describes only the *type* of the current’s variability in time (e.g. continuing versus pulsing), but not its *nature*. Rakov and Uman (2003, p 173) stated that the continuing current ‘can be viewed as a quasi-stationary arc between the cloud charge source and ground along the path created by the preceding leader–return stroke sequence.’ However, the physics of lightning leaders clearly shows that the continuing current is an inseparable part of any leader process, regardless of polarity. The presence of continuing current is an indication of a developing (growing) leader in the flash (Mazur 2002). The continuing current is not a quasi-stationary arc, because this current will exist as long as the leader (an arc) propagates. Moreover, as an attribute of any leader process, the continuing current occurs not only in CG flashes, but rather, in all types of lightning flashes; thus, the continuing current is the leader current.

No representative sample of data of triggered upward lightning carrying negative charges, which are rather rare events even in winter storms, is available from observations of rocket-triggered lightning. These data have been obtained only from current measurements on tall instrumented towers (e.g. Heidler 2002).

The duration of the negative upward-leader current (see figure 7.15) is usually much shorter (measured in milliseconds) than that of positive leaders (measured in hundreds of milliseconds). Other noticeable differences from the current of positive leaders are the absence of the distinct impulsive current, which is associated with M-events, and the much-higher amplitude of the leader current (on average ~10 times higher), in the kilo-ampere range (see figure 7.16). With much shorter duration and much greater current amplitude, negative upward leaders triggered by

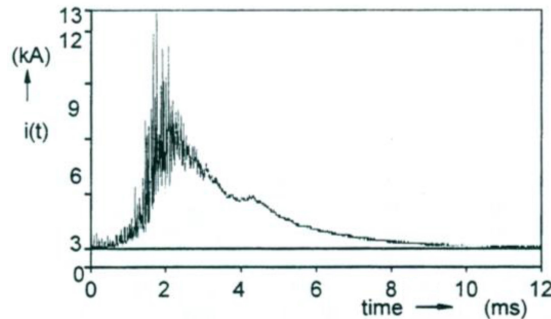


Figure 7.15. Current record of an upward negative leader triggered by a tall tower. Note that the record is in the atmospheric electricity sign convention. Reprinted from Heidler *et al* 2002.

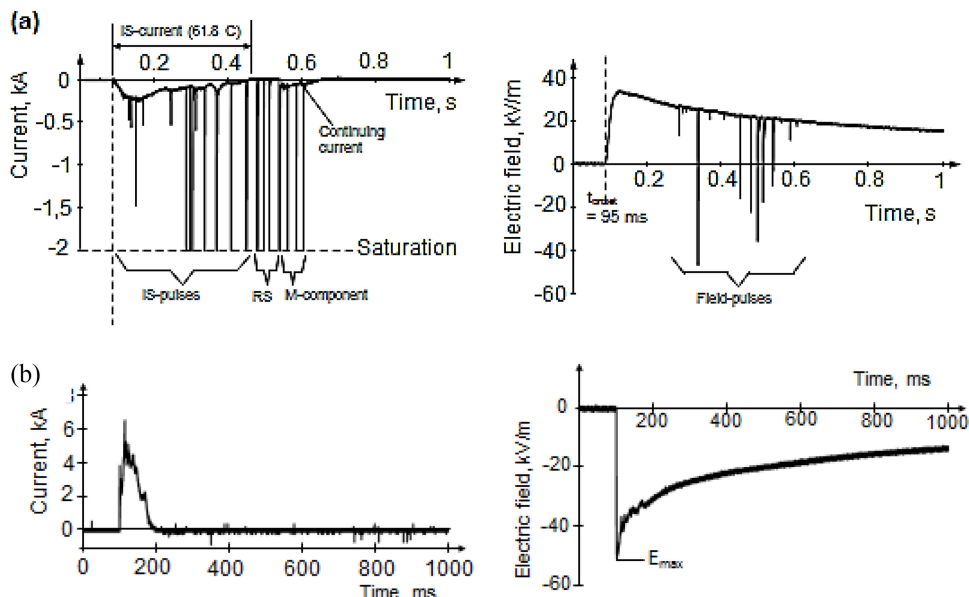


Figure 7.16. Comparison of the current and electric-field records of upward leaders of positive (a) and negative (b) polarities from the Peissenberg tower. Note: the plots were created using the atmospheric electricity sign convention. Courtesy of F Heidler.

tall structures transfer approximately the same amount of charge as upward positive leaders triggered by the same structures.

The profound difference in the current waveforms of positively and negatively charged upward leaders suggests that major differences exist between them in the physical processes during their development, assuming that such external factors as the ambient potential distribution in the space-charge regions affect leaders of different polarity in the same way. However, the similarity in waveforms of the E -field of the two leaders indicates the presence of long-lasting residual charges in the leader structure of both leaders after current cutoff at the main trunk connected to ground.

References

- Berger K and Vogelsander E 1969 New results of lightning observations *Planetary Electrodynamics* ed S C Coronti and J Highes (New York: Gordon and Breach) pp 489–510
- Diendorfer G, Pichler H and Mair M 2005 Characteristics of positive upward lightning measured on an instrumented tower *Geophys. Res. Abstracts* **7** 10175
- Eack K 2015 Personal communication
- Flashe D, Rakov V, Heidler F H, Zischank W J and Thottappillil R 2011 On the origin of two types of current pulses observed during the initial stage of upward lightning *Proc. 7th Asia-Pacific Intern. Conf. on Lightning (Chengdu, China)*
- Heidler F 2002 Lightning current measurements at the Peissenberg telecommunication tower *Proc. Int. Conf. on Grounding and Earthing GROUND'2002 (Rio de Janeiro, Brazil)* pp 117–22
- Hill J D, Pilkey J, Uman M A, Jordan D M, Biggerstaff M I, Hyland P, Rison W, Krehbiel P R and Blackeslee R 2012 Correlated lightning mapping array (LMA) and radar observations of the initial stages of florida triggered lightning *Geophys. Res. Lett.* **39** L09807
- Kasemir H W 1986 Model of lightning flashes triggered from the ground *Proc. Int. Aerospace Ground Conf. on Lightning and Static Electricity* (Dayton, OH) pp 39–1
- Mazur V and Ruhnke L H (ed) 2013 *Heinz Wolfram Kasemir: His Collected Works* (New York: Wiley) pp 547–55 (Engl. transl.)
- Kitterman C G 1981 Concurrent lightning flashes on two television transmission towers *J. Geophys. Res.* **86** 5378–80
- Lalande P, Bondiou-Clergerie A, Laroche P, Eybert-Berard A, Berlandis J-P, Bador B, Bonamy A, Uman M A and Rakov V A 1998 Leader properties determined with triggered lightning techniques *J. Geophys. Res.* **103** 14109–15
- Laroche P, Idone V, Eybert-Berard A and Barret L 1991 Observations of bidirectional leader development in triggered lightning *Proc. Int. Conf. on Lightning and Static Electricity, NASA (Cocoa Beach, FL)*
- Lu W, Wang D, Zhang Y and Takagi N 2009 Two associated upward lightning flashes that produced opposite polarity electric field changes *Geophys. Res. Lett.* **36** L05801
- Malan D J and Schonland B F J 1947 Progressive lightning. Part 7. Directly correlated photographic and electrical studies of lightning from near thunderstorms *Proc. R. Soc. A* **191** 485–503
- Mazur V 1982 Associated lightning discharges *Geophys. Res. Lett.* **9** 1227–30
- Mazur V 2002 Physical Processes during development of lightning flashes *C. R. Phys.* **3** 1393–409
- Mazur V and Ruhnke L H 2011 Physical processes during development of upward leaders from tall structures *J. Electrostat.* **69** 97–110
- Miki M, Rakov V A, Shindo T, Diendorfer G, Mair M, Heidler F, Zischank W, Uman M A, Thottappillil R and Wang D 2005 Initial stage in lightning initiated from tall objects and in rocket-triggered lightning *J. Geophys. Res.* **110** D02109
- Rakov V A 2015 Personal communication
- Rakov V A and Uman M A 2003 *Lightning Physics and Effects* (Cambridge: Cambridge University Press)
- Rakov V A, Crawford D E, Kodali V, Idone V P, Uman M A, Schnetzer G H and Rambo K J 2003 Cutoff and reestablishment of current in rocket-triggered lightning *J. Geophys. Res.* **108** 4747
- Rakov V A *et al* 1998 New insights into lightning processes seined from triggered-lightning experiments in Florida and Alabama *J. Geophys. Res.* **103** 14117–30

- Ruhnke L H and Kasemir H W 1988 Electrostatic fields of ground triggered lightning *Proc. 8th Int. Conf. on Atmospheric Electricity (Uppsala, Sweden)* 377–82
- Schnetzer G H and Fisher R J 1991 Rocket-triggered lightning test of the DoD security operations test site munitions storage bunker Ft McClellan, Alabama vol 1 *Sandia Report SAN91-2343 UC-706*
- Takagi N, Wang D and Watanabe T 2006 A study of upward positive leaders based on simultaneous observations of *E*-field and high-speed images *Trans. Inst. Electr. Eng. Japan* **126** 256–9
- Vaughan O H and Vonnegut B 1989 Recent observations of lightning discharges from the top of a thundercloud into the clear air above *J. Geophys. Res.* **94** 13179–82
- Wang D, Takagi N, Watanabe T, Sakurano H and Hashimoto M 2008 Observed characteristics of upward leaders that are initiated from a windmill and its lightning protection tower *Geophys. Res. Lett.* **35** L02803
- Warner T A, Mazur V and Ruhnke L H 2008 High-speed video observations of upward leaders from tall towers *EOS Trans. AGU Fall Meet. Suppl.* **89** abstract AE21A-08
- Willett J C, Davis D A and Laroche P 1999 An experimental study of positive leaders initiating rocket-triggered lightning *Atmos. Res.* **51** 189–219

Principles of Lightning Physics

Vladislav Mazur

Chapter 8

Understanding current cutoff in lightning

8.1 Definition and manifestation of current cutoff in different lightning events

The expression ‘current cutoff’ is defined as the disconnection of the current flow from its source. Historically, this term has described a feature in multi-stroke CG flashes that consists of the cessation of return strokes, which precedes the occurrence of a new sequence of the dart leader–return stroke process, after some pause in the current record. More recently, this term has been used to describe any cessation of current that takes place in lightning channels, not only in multi-stroke CG flashes, but in the bidirectional leaders of IC and CG flashes, and also in unidirectional upward leaders triggered by rocket-and-wire techniques and by tall ground structures. However, while we may have a reasonable description for current cutoff, its mechanism is still not fully understood.

A search for the cause of current cessation in lightning leaders should begin with a review of the nature of the leader current, I , which is produced as a result of the changing of induced charges, Q , on a conducting leader channel during its propagation in an ambient electric field. The expression for this relationship is $I = dQ/dt$. Because the induced charges are stationary, the change in the total charge, Q , occurs only with the changing length of the leader channel, with its speed directly affecting the magnitude of the leader current.

The propagation of a straight and unipolar leader requires (1) the internal electric field in the leader channel (E_i) to be much less than the ambient electric field (E_0) and (2) the magnitude of the ambient field to be sufficient for the formation of corona streamers of a given polarity. In a straight leader, these conditions establish the necessity for the potential drop, $\Delta\Phi_T$, at the leader tip to be positive and greater than the minimum threshold value; below this, the leader stops propagating (Lalande *et al* 2002). The potential drop $\Delta\Phi_T$ has several components, shown in (8.1), and illustrated in figure 1.6 for an upward leader from a ground structure in a constant ambient electric field: L is the length of a straight leader, Φ_{in} is the initial potential of

the leader, which is zero in grounded structures; E_0L is the ambient potential; and E_iL is the potential at the tip of the leader; and $\Delta\Phi_c$ is the potential drop generated by the space-charge envelope at the leader tip:

$$\Delta\Phi_T = \Phi_{in} + (E_0 - E_i)L - \Delta\Phi_c \quad (8.1)$$

It follows from (8.1) that the decrease in the potential drop $\Delta\Phi_T$ could be achieved either by decreasing the ambient electric field E_0 , or by increasing the internal electric field of the leader E_i . Changing the potential drop $\Delta\Phi_T$ affects the speed of propagation, which is proportional to $\Delta\Phi_T$ and, thus, the magnitude of the leader current.

8.2 The death of the leader in unbranched lightning channels

Current flow ceases when the charge distribution on a leader channel stops changing, which occurs when the potential drop at the leader tip reaches a level below the threshold $\Delta\Phi_{min}$ necessary for its propagation. Therefore, current cutoff is, in essence, a consequence of unmet conditions for leader-channel propagation in an ambient electric field. This type of current cessation has been identified as ‘the death of the leader’ in Mazur and Ruhnke (2014), and occurs in channels of unbranched leaders (see figure 8.1).

Leaders that remain unbranched for their entire life cycles are quite rare phenomena; more often, the unbranched part of the leader is observed in upward leaders from tall structures and in rocket-triggered lightning prior to the leader’s entrance into the cloud where branching most often occurs (Warner 2012, Hill *et al* 2012).

In branching bidirectional, bipolar leaders, current cutoff is often manifested in the ceasing propagation of a leader of one polarity, while a leader of the opposite polarity continues its propagation. An event such as this occurs in bidirectional leaders of both CG and IC flashes, as inferred from observations made with the

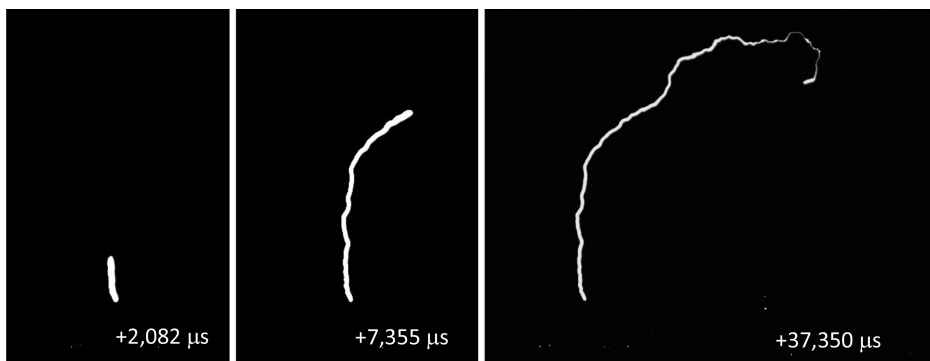


Figure 8.1. Images of an unbranched positive leader from a tall tower, obtained with a high-speed video camera with a recording speed of 7200 fr s^{-1} . Time in μs is counted from the time of initiation of the leader. The high-speed video showing the development of this leader is figure A.8 in the appendix. Courtesy of T A Warner.

lightning-radiation mapping technique, and in recoil leaders, as observed with a high-speed video system (Mazur *et al* 2013).

8.3 Current cutoff in branched leaders

Branching is common in all natural lightning flashes, as well as in the majority of upward lightning that emanates from tall ground structures, or triggered using the rocket-and-wire technique. Observations of lightning development outside the cloud with high-speed video systems, and inside the cloud by the lightning-radiation mapping system, show that branching is more extensive in negatively charged leaders than in positively charged ones. This difference is not only apparent in the degree of branching density, greater in negative leaders, but also in the length of the individual branches, which is much shorter in negative leaders than in positive ones (see figures 10.4 and 10.5 in chapter 10).

8.3.1 The screening effect in single and branched channels

Any branched structure is made of a multitude of single channels of different lengths; therefore, the criterion of ‘the death of the leader’ is applicable to each individual channel of this structure. There is a difference, however, between the development of a branching structure and that of a single, isolated channel. This difference is caused by the so-called ‘screening effect’ that exists in closely packed branches, when one branch affects the development of another branch located close by. The screening effect is well-known and recognized in nature, most noticeably in the branches of trees.

The essence of this screening mechanism is explainable by the electrostatic induction, according to which the induced charges on a conductor in an ambient E -field produce their own field that diminishes the external E -field. Thus, one conductor may diminish the ambient E -field affecting another conductor located nearby, and possibly even arrest its development. Of course, the screening effect is most pronounced in leaders with branching structures of high density and with short branches.

Kasemir (1986) found that the induced charges of the straight leader channel decreased by up to ten per cent on the lower part of the leader during its vertical ascent. The decreasing of charges is the result of the decreasing ambient potential at lower levels of the extending leader. This is another manifestation of the screening effect, produced, in this case, by the induced charges on the upper part of the conductor screening the ambient electric field for the lower part of the leader channel. This screening effect is particularly noticeable in records of the E -field on the ground in close proximity to the vertical channel of the ascending leader (figure 8.2).

In negative leaders, branching starts when a single channel splits in two; a feature observed in high-speed video recordings of negative leaders (Petersen 2012). The size of this initial angle at the splitting affects the spacing between the developing branches, while a close proximity of the branches causes ‘electrostatic interference’ between them. As the result of such interference, some branches continue to

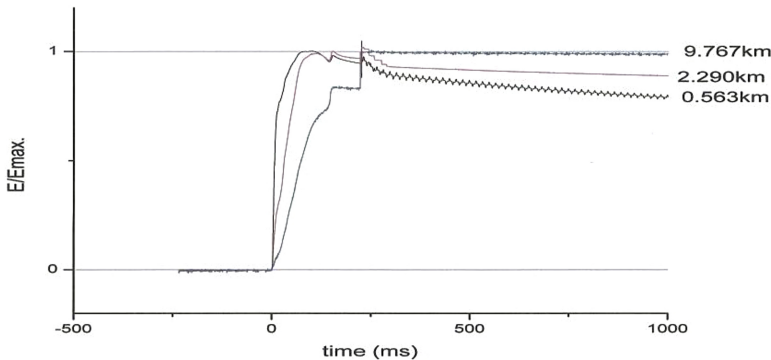


Figure 8.2. E-field records of the upward leader of a rocket-triggered lightning at various distances from a launching site at the Kennedy Space Center, Florida. Reproduced from Mazur and Ruhnke (2014). Copyright 2014 by John Wiley Sons, Inc. Reprinted by permission of John Wiley & Sons, Inc.

propagate, while some are arrested in their development, and, thus, die. In the electrostatic model of leader development as the three-dimensional propagation of a branching upward leader, Lalande and Mazur (2012) demonstrated how the space charge around the leaders regulates the total number of active branches, by reducing the ambient potential available for their propagation.

8.3.2 The role of branch-screening in current cutoff

The concept that explains the effect of branch-screening on the current cutoff process is presented using the example of an ascending upward leader from a ground structure that is developing in a uniform ambient E -field. The sketch in figure 8.4 depicts the leader with two layers of horizontal branches, the early, lower layer and the later, upper layer. The induced charges, Q , of each growing branch are produced in the streamer zone ahead of the channel's tip, and reside in the corona envelope that forms around the conducting core of the moving channel. These charges are stationary, and their vertical distribution mirrors the vertical distribution of the ambient potential (Kasemir 1960).

Any conducting leader channel starting from the ground structure is on the ground (zero) potential. The leader current, I , is produced by the adding of new induced charges at the tip of the branching leader during its development, and is initially constant along the straight channel, due to the constant speed of ascent. In figure 8.3(A), the current's values during the initial stage of the leader are shown as the red column.

The screening effect by the low branches would be manifested by a reduction in the ambient electric field below the branching point, changing the ambient potential distribution with the height and, thus, changing the charge distribution along the straight vertical channel (see the E -field lines in figure 8.3(B)). However, because the induced charges are stationary, the only way to bring them into accordance with the changed ambient potential is to add negative charges that will flow into the trunk of the leader from the ground. This 'negative' current will deposit negative charges

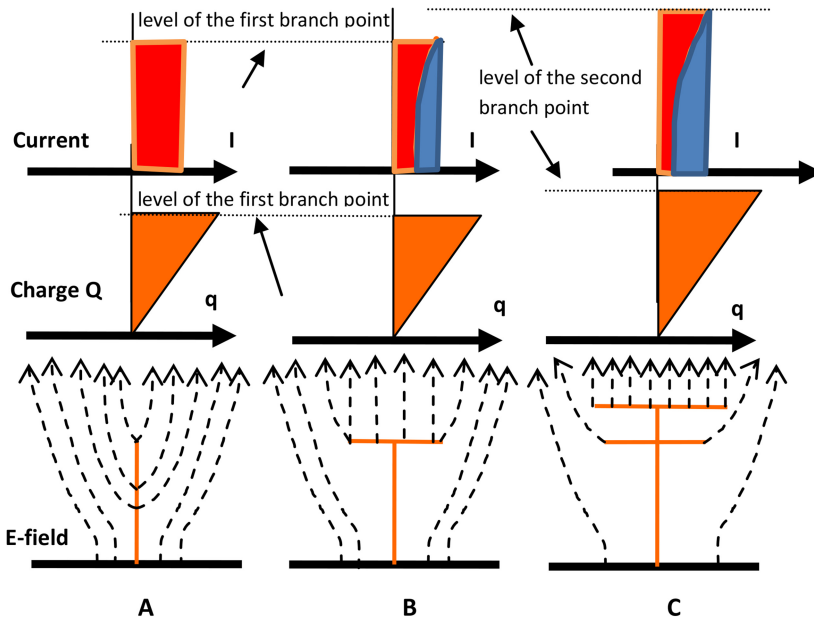


Figure 8.3. A conceptual sketch of the three stages of a branching upward leader: (A) before branching, (B) at initial branching, and (C) at advancing branching. The lower row of sketches depicts changes in the number and density of the electric field lines after the appearance of first branches, and then the next layer of branches. The middle row of sketches shows the stationary induced positive charges on the vertical trunk of the leader. The upper row of sketches depicts the current distribution along the vertical trunk of the leader: the total base current (red) and the negative current flowing from the ground, which is produced by the effects of screening (blue). Reproduced from Mazur and Ruhnke (2014). Copyright 2014 by John Wiley Sons, Inc. Reprinted by permission of John Wiley & Sons, Inc.

only at the section of the channel between the ground and the branching point, i.e. the region where the screening effect is most pronounced. The negative current value will be highest at ground level, and zero at the branching points, where the screening effect is minimal (see the current values marked in blue in figures 8.3(B) and (C)). As a result of this addition of the negative current, the total base current in the trunk of the leader (made of contributing positive and negative currents) decreases, but remains positive in value (shown in red in figure 8.3(B) and (C)), as long as development of the upper branches continues. A greater change in the total base current will occur at ground level. Thus, as long as the development of new branches continues at the top of the branched leader, and screening of the lower branches continues to take place, there will be two competing currents.

The illustration of the concept of two competing currents in branched leaders is found in the base current and *E*-field records of the upward positively charged leader from a tall tower (figure 8.4) and in the base current record of an upward leader triggered by the rocket-and-wire technique (figure 8.5).

The records in figure 8.4 show that the current is increasing, as expected, for ~ 100 ms after initiation of the leader, during its ascent to the cloud, and then decreasing to zero. The electric field nearby, however, reaches its maximum much

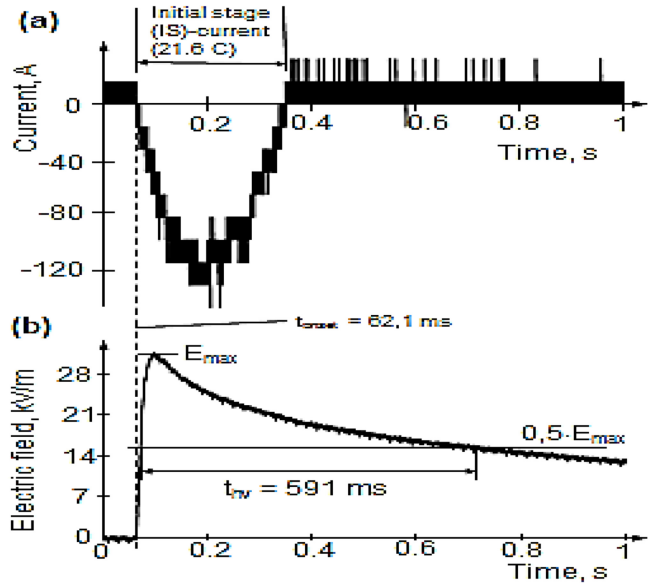


Figure 8.4. (a) Base current of an upward positively charged leader from the Peissenberg tower and (b) the electric field at 190 m away from the tower, for the same event. Note that the records are in the atmospheric electricity sign convention. Courtesy of F Heidler.

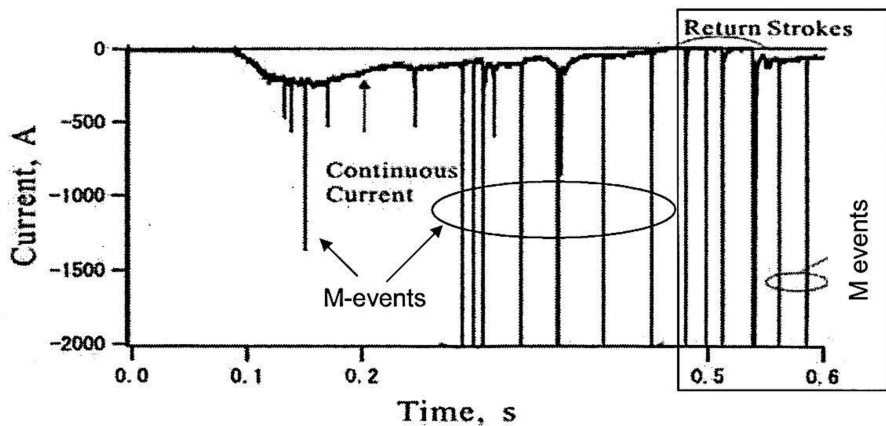


Figure 8.5. The base-current record of an upward positively charged leader on the Peissenberg tower followed by four return strokes. The rectangular frame outlines the record of the dart leader–return stroke phase. Note that the record is in the atmospheric electricity sign convention. Reproduced from Miki *et al* (2005). Copyright 2005 by John Wiley Sons, Inc. Reprinted by permission of John Wiley & Sons, Inc.

sooner than the current does; it then starts slowly declining, while the base current of the leader still continues to grow. The long-lasting E -field record after the base current comes to zero indicates the presence of residual charges in the branches of the leader inside the cloud.

In the base current records of positively charged upward leaders triggered either by a tall structure (figure 8.4), or with the rocket-and-wire technique (figure 8.5), there is a period of initial, and almost linear, growth lasting tens of milliseconds. We know, from visual observations of upward leaders, that the initial period of current growth is associated with the development of a single vertical channel. The current level almost stabilizes after the period of linear growth and then decreases to zero during the next hundreds of milliseconds (more noticeably in the current record in figure 8.6).

What explains the change in leader current from its linear growth to its leveling-off and then to its gradual decrease? The leader undergoes a transformation, from a single channel to one with branches, usually when a straight channel approaches the cloud base and enters the cloud. This dynamic is confirmed by video observations of upward leaders triggered by tall structures, and also from lightning-radiation maps of rocket-triggered leaders (Hill *et al* 2012). Moreover, the presence of the current pulses of M-events superimposed on the continuing current of a positively charged upward leader, when it levels off, indicates the occurrence of branching after the leader enters the cloud (see figure 8.5). We will show, in chapter 9, that M-events are closely associated with branching.

It is logical to assume, therefore, that the leveling-off of current, rather than its continuing growth, as shown in records such as figures 8.4 and 8.5, is the effect of screening by branching (Mazur and Ruhnke 2014). This interpretation has been tested by analyzing the time-variation of the base-current record simultaneously with the development of leader branches in the three-dimensional lightning mapping of the upward positively charged leader that was obtained with the Lightning Mapping Array (LMA) system in Hill *et al* (2012). To quote from this study of the initial stages of rocket-triggered lightning: ‘The first branching of the initial stage was observed in eight of the nine events at altitudes ranging from about 580 m to about 5.2 km. No significant change in the current at ground was observed at the time of branching.’ This statement, about the unchanging current to ground when a

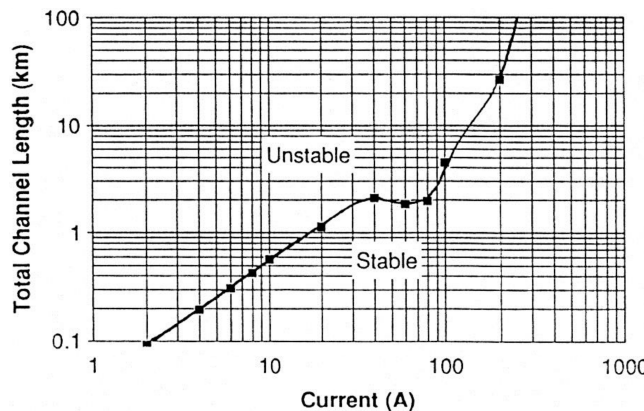


Figure 8.6. Minimum stable continuing current as a function of channel length. Reprinted from Heckman (1992). Courtesy of S Heckman.

branching leader continues to develop, confirms the anticipated screening effect of branching, as providing a negative current simultaneously with the positive current supplied by new branches. A leveling-off of the base current occurs when the contributions from the positive current are comparable to those from the negative current.

Current cutoff is not an instantaneous act, such as cutting a cord, but rather the process of the current's demise. The decrease in the base current to ground during the cutoff process will coincide with the decrease in the number of new branches at the top of the positively charged leader, or the slowing of their development, which will also affect the positive current. As this trend continues, the total current in the flash may arrive at zero, but only when the upper branches stop propagating.

In multi-stroke negative CG flashes, however, the base-current cutoff most likely takes place before development of the upper branches fully ceases. The occurrence of a dart leader–return stroke sequence (see figure 8.5) is an indication of this. There is abundant evidence, in radiation maps of these flashes, that confirms the development of the upper part of the branched leaders during inter-stroke intervals, after current cutoff is registered at the ground, which is followed by a dart leader to ground. What actually happens with the current in the lightning channel during the current cutoff process will be discussed in chapter 10.

The screening effect of branching on the cutoff process takes place in any type of flash that has branching channels, either inside or outside an electrified cloud. However, the net result of the negative current from the screened, old branches may vary, because of differences in the dynamics of branching (the density and the speed of branching development) in leaders of two polarities.

8.4 Arc instability and current cutoff

A hypothesis of current cutoff proposed by Heckman (1992) suggested the phenomenon of the instability of the free-burning arc as a mechanism for current cutoff in both straight and branched lightning channels. An alternative hypothesis, of the screening effect on the base current in branched leader channels, was first introduced in Mazur and Ruhnke (1993), and re-examined and refined in Mazur and Ruhnke (2014).

The criterion for lightning instability was derived from a consideration of the critical value of current in the lightning channel of a certain length (see figure 8.6). If the lightning channel's current is in excess of this critical value, which is different for different lengths of the channel, then the channel is stable, and will be carrying continuing current. If the channel's current is less than this critical value, the channel is unstable, which would lead to current cutoff and the possibility of ‘discrete’ strokes in CG flashes. The criterion for arc instability in Heckman (1992) was drawn from his assumption that equated a lightning channel to an equivalent circuit consisting of the resistance of the lightning channel, its capacitance, and an independent current source—all three components connected in parallel. The variable that Heckman defined as ‘negative differential resistance’ reflected the negative E – I relationship in stable free-burning arcs.

The validity of this ‘lightning-instability’ concept, which divides stable from unstable lightning channels by a required minimum current for a given channel length, has been challenged in Mazur and Ruhnke (2014). They have shown that the primary assertion on which this concept was built (the equivalent electric circuit) is invalid for lightning channels. The second assertion of Heckman’s concept, suggesting that the existence of negative differential resistance influences the specific conditions for the occurrence of current cutoff, is also invalid, because this is a feature of arcs and leader channels of all ranges of currents and lengths. These two objections, taken together, have invalidated the concept of ‘lightning instability’ in its entirety.

If we identify the continuous development of a lightning channel as its ‘stable’ state, then ‘instability’ is the state when the lightning channel ceases to propagate, and starts the process of current diminishment (current cutoff). At that point, the transition from a stable to an unstable state is determined by the changing potential drop at the tip of the leader channel (see (8.1)). The length of the leader L and the internal field E_i are variables in this equation. Also, because of the negative E - I relationship that exists in plasma channels (see chapter 2), the internal electric field E_i in leader channels increases with the decreasing current I . Through these relationships among the three variables in (8.1), the leader current and the length of the leader channel are certainly involved in the conditions for leader propagation and, thus, in current cutoff. However, these two variables, I and L , are not the only factors that determine the occurrence of current cutoff, contrary to the criterion for ‘lightning instability’ illustrated in figure 8.6. The other factors that influence the conditions for current cutoff in (8.1) are the initial potential of the leader, Φ_{in} , the ambient E -field, E_0 , and the potential drop generated by the space-charge envelope at the leader tip, $\Delta\Phi_c$. These variables represent the parameters determined by the electrical environment, in which lightning leaders originate and develop.

In summary, the conditions that actually govern the ‘instability’ of the leader, identified here as current cutoff, include not only those that characterize the leader’s plasma channel (its length, current, and internal E -field), but also those that are determined by the external electrical environment.

References

- Heckman S 1992 *PhD Thesis* Massachusetts Institute of Technology
- Hill J D, Pilkey J, Uman M A, Jordan D M, Rison W and Krehbiel P R 2012 Geometrical and electrical characteristics of the initial stages Florida triggered lightning *Geophys. Res. Lett.* **39** doi:10.1029/2012GL051932
- Kasemir H W 1960 A contribution to the electrostatic theory of a lightning discharge *J. Geophys. Res.* **65** 1873–978
- Kasemir H W 1986 Model of lightning flashes triggered from the ground *Proc. Int. Aerospace Ground Conf. on Lightning and Static Electricity* (Dayton, OH) pp 39–1
- Lalande P, Bondiou-Clergerie A, Bachiega G and Gallimberti I 2002 Observations and modeling of lightning leaders *C.R. Phys.* **3** 1375–92
- Lalande P and Mazur V 2012 A physical model of branching in upward leaders *Aerospace Lab J.* **5** AL05-07

- Mazur V and Ruhnke L H 1993 Common physical processes in natural and artificially triggered lightning *J. Geophys. Res.* **98** 12913–30
- Mazur V, Ruhnke L H, Warner T A and Orville R E 2013 Recoil leader formation and development *J. Electrostat.* **71** 763–8
- Mazur V and Ruhnke L H 2014 The physical processes of current cutoff in lightning leaders *J. Geophys. Res.* **119** 2796–810
- Miki M, Rakov V A, Shindo T, Diendorfer G, Mair M, Heidler F, Zischank W, Uman M A, Thottappillil R and Wang D 2005 Initial stage in lightning initiated from tall objects and in rocket-triggered lightning *J. Geophys. Res.* **110** D02109
- Petersen D 2012 Personal communication
- Warner T A 2012 Observations of simultaneous upward lightning leaders from multiple tall structures *Atmos. Res.* **117** 45–54

Principles of Lightning Physics

Vladislav Mazur

Chapter 9

The phenomenon of recoil leaders

9.1 The nature of recoil and dart leaders

One of the remaining challenging issues in the physics of lightning is the mechanism of recoil leaders in branched positive leader channels or in multi-stroke negative CG flashes during periods between sequential return strokes. Recoil leaders originate somewhere along the decaying traces of the preceding channels, and propagate along the remnants of these channels towards either a branching point of a positive leader, or the ground. Historically, the phenomenon of the recoil leader, under the name ‘K-changes’, was identified as being associated with a rapid electric-field variation of negative polarity during the so-called ‘junction process’, the time interval between the return strokes of multi-stroke negative CG flashes. K-changes were later observed also in IC flashes. Ogawa and Brook (1964) suggested that K-changes are actually *negative ‘recoil streamers’* that occur when a positive leader, during the junction stage, reaches a cloud region of concentrated negative charge. This interpretation made K-changes the equivalent of ‘mini-return strokes’, in accordance with Schonland’s ‘source-charge’ leader model; however, this model assumed the possibility of a direct charge transfer from a space charge to a conducting leader—a mechanism that does not exist in nature.

The word ‘recoil’, as used by Ogawa and Brook (1964), which means the return to a starting point or source (by definition in the Webster New World Dictionary), correctly reflects the reality of the process, i.e. propagation along remnants of the channels of the positive leaders which preceded them, towards the origins of the leaders. However, the term ‘streamer’ misrepresents the nature of the phenomenon and should be replaced by the correct physical term, *recoil leader*, which matches all the attributes of K-changes (Mazur 2002). Streamers are cold corona filaments of the length of a few meters, with currents in the range of milliamperes, and of very low luminosity. Leaders, on the other hand, are self-propagating discharges made of hot, luminous plasma channels of various lengths, with zones of *streamer filaments*

of limited length ahead of the tip of the channel, and with currents in the tens to hundreds of amperes.

A new term, introduced in Edens *et al* (2012) for this phenomenon, is *retrograde leader*, i.e. going backwards, which neither changes nor adds anything to the meaning of the term ‘recoil leader’. In the view of the author, this new term merely contributes to the existing confusion in lightning terminology.

The interpretation by Ogawa and Brook (1964) of the nature of K-changes was elaborated on and advanced by Mazur (1989), based on analyses of lightning-radiation maps of IC flashes obtained with a VHF interferometer (see figure 9.1). These maps clearly indicated that recoil leaders occur in the positively charged part of the bipolar lightning ‘tree’ after the cessation of development in the negatively charged part of the ‘tree’, and then move toward the origin of an IC flash.

Because the radiation maps of VHF interferometers do not trace the paths of positive leaders, the location of the starting point of recoil leaders is still unknown. In the hypothesis of recoil leaders by Ogawa and Brook (1964), the starting point of the recoil leader would be the tip of the decaying positive leader channel. This issue is discussed further in chapter 10.

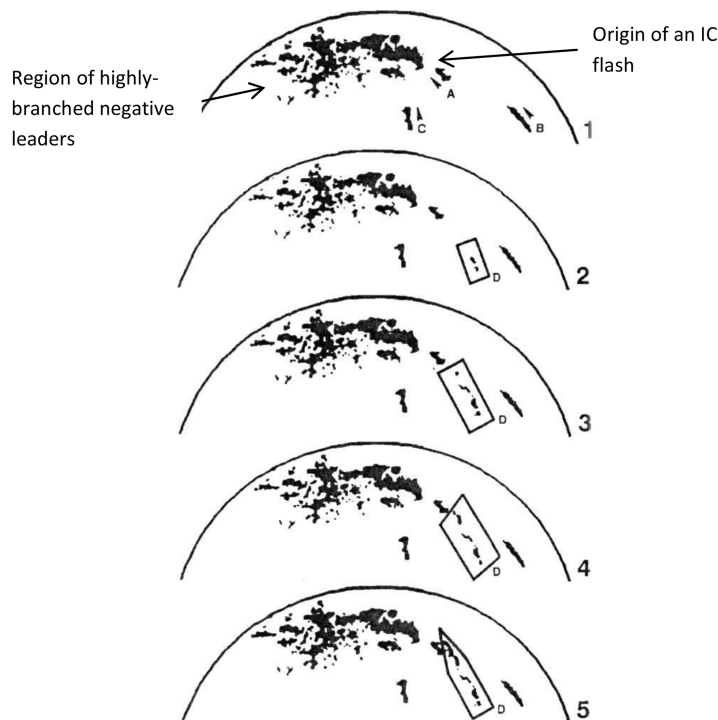


Figure 9.1. Radiation map (interferometric images) of an IC flash. Sequential development of the recoil leader D is shown in the enclosed areas in images 2–5. The numbers correspond to subsequent frames of the 16 mm movie. Reproduced from Mazur (1989). Copyright 1989 by John Wiley Sons, Inc. Reprinted by permission of John Wiley & Sons, Inc.



Figure 9.2. Composite image of all recoil-leader channels coming from the periphery toward the flash origin in an IC flash from a video sequence obtained with a high-speed video system (7200 fps^{-1}). Courtesy of T A Warner.

Visual observations that confirmed the inference about the nature of recoil leaders as propagating along previously visible paths of a positive leader back to a flash origin (see figure 9.2) or to a branching point of this leader were only obtained with the use of high-speed video systems (Saba *et al* 2008, Mazur and Ruhnke 2011).

Both the E -field change signature of recoil leaders and their radiation signature obtained by a VHF interferometer, which predominantly maps the radiation from negative breakdown (Stock *et al* 2013), indicated that they are negatively charged leaders—an interpretation that has persisted in the lightning literature until just recently. However, this interpretation contradicts the very nature of recoil leaders as being electrodeless discharges—which means that they *cannot* be unipolar and unidirectional, but rather, must be bipolar and bidirectional. The confirmation of this true nature of recoil leaders is found in the high-speed video observation (see figure 9.3) of a recoil leader forming along the path of the preceding positive leader branch (figure 9.4), about 10 ms after current cutoff there (Mazur *et al* 2013).

The first image of a recoil leader appeared on a trace of the decayed branch (frame 1, figure 9.3), at a point also marked by the white arrow in figure 9.4 of the preceding positive leader branch. The video images in frames 1–7 of figure 9.3 show the bidirectional development of a floating bipolar leader. However, in frames 8–10, the leader progression becomes unidirectional, toward the main trunk of the preceding leader branch.

During the entire video sequence, the E -field change sensor registers the negative field changes produced by the negative charge moving towards the sensor, i.e. towards the main leader trunk. The E -field sensor does not register the development of the positively charged part of the bipolar leader in frames 1–7, because it moves away from the E -field sensor simultaneously to the movement towards the sensor of the negatively charged part of the leader. Two features clearly noticeable in this video sequence are: (1) the origin of the recoil leader that is not at the tip of the preceding positively charged branch, but below it (marked by arrows in figures 9.3 and 9.4);

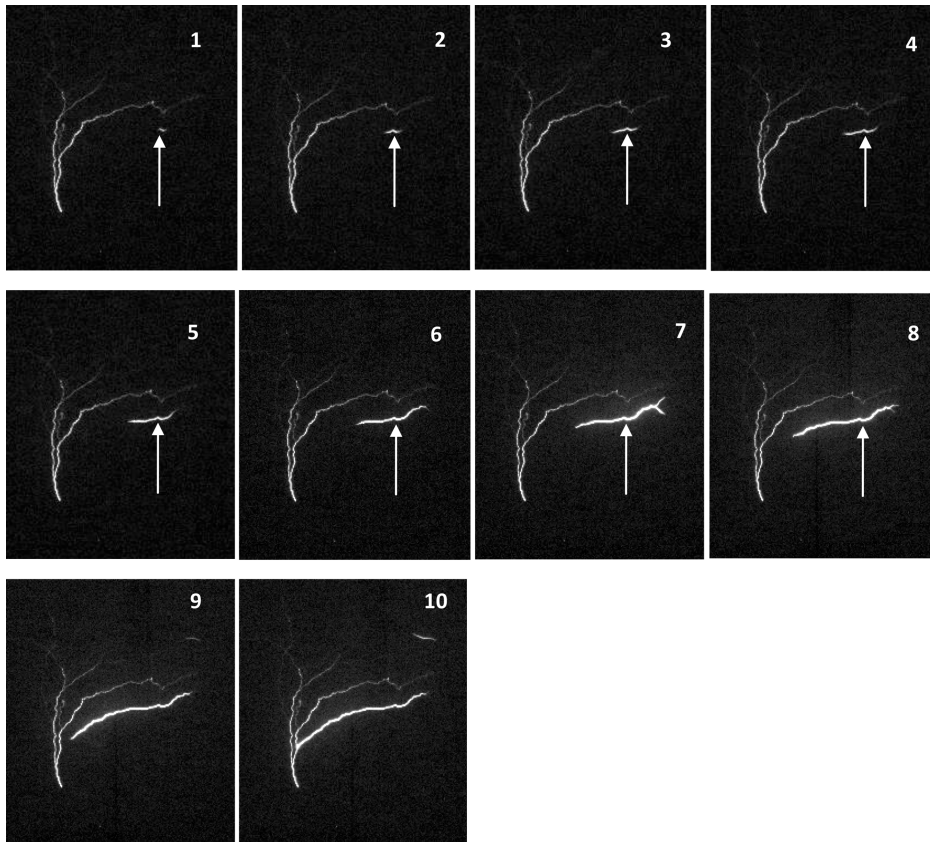


Figure 9.3. Development of a recoil leader recorded with the speed of 54 000 fps, and a frame exposure of $18.12 \mu\text{s}$. The vertical arrow points to the location of the starting point of the recoil leader. The entire sequence of recoil leader development depicted in the video series lasted $185.2 \mu\text{s}$, until attachment to the conducting main trunk at the old branching point. Reprinted with permission from Mazur *et al* (2013). Copyright 2013 Elsevier.

and (2) the progression of the positively charged part of the recoil leader that stops (see frames 8–10) near the location of the tip of the preceding positively charged branch (compare frame 9, in figure 9.3, with figure 9.4). We will look again at these two features from high-speed video images in our discussion of the physics of recoil leaders, in chapter 10.

Both the positively charged part of the recoil leader, and the positively charged branch before the appearance of the recoil leader, ended their propagations at the same place, because the potential difference at their tips reached a minimum threshold there. Meanwhile, the negatively charged part of the recoil leader continued to move toward the branching point, because the potential drop at its tip was sufficiently high to support the continuous formation of the recoil leader's plasma channel. A computer-simulated model of bidirectional leaders produced similar behavior in CG and IC flashes (Mazur and Ruhnke 1998).

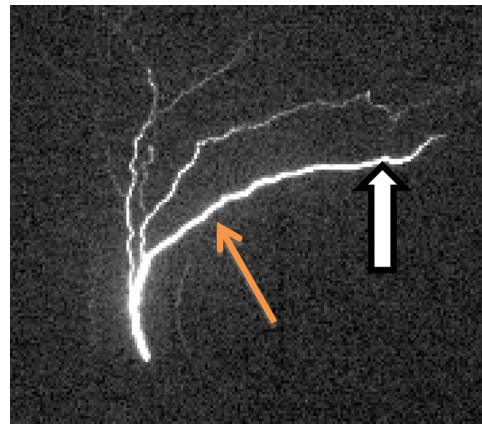


Figure 9.4. An upward positive leader from a 163 m tall tower, triggered by a passing negative leader. The green arrow points to the branch that, after the current cutoff, was a path for a developing recoil leader. The white arrow points to the region where the recoil leader later starts. Reprinted with permission from Mazur *et al* (2013). Copyright 2013 Elsevier.

The conclusion that recoil and dart leaders are similar phenomena was based on analysis of the time-resolved VHF images of lightning processes obtained with an interferometer (Mazur *et al* 1995, Shao *et al* 1995). A difference between them, however, lies in the points of their attachment: for recoil leaders, it is at the branching point; for dart leaders, it is at the ground. Thus, dart leaders in CG flashes are actually recoil leaders that reach the ground.

9.2 The relationship between recoil leaders and M-events: cause and effect

The M-component phenomenon was first identified by Malan and Schonland (1947), as current surges (pulses) superimposed on a DC-type continuing current that re-illuminate the channel-to-ground during inter-stroke intervals in multi-stroke negative CG flashes. M-components also have distinctive ‘hook’-type signatures in records of electric-field changes (see the example in figure 9.5) that indicate the negative polarity of the charge transferred to ground.

Rakov *et al* (1995) proposed a model of the M-component as ‘a guided-wave process that involves a downward-progressing incident wave (the analog of a leader) and an upward-progressing wave that is a reflection of the incident wave from the ground (the analog of a return stroke).’ This concept, depicted in the boxed part in figure 9.6, interprets the M-component as a superimposition of two guided waves, each propagating in opposite directions in the same channel with continuing current.

The assumption of similarity with the guided electromagnetic or current wave, in the model by Rakov *et al* (1995), requires a symmetrical shape for the reflected wave, which is not the case for the M-component signatures in electric-field records (see figure 9.7). Also, the speed of guided-wave propagation should be equal to the speed of light, which is also not the case for an M-component. Furthermore, if a

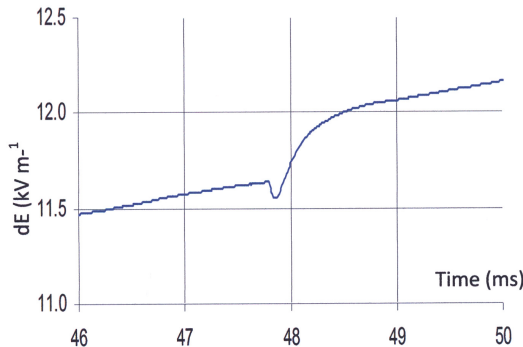


Figure 9.5. The dE record of the pulse-type brightening event in an upward positive leader produced by an M-event. Note the characteristic ‘hook’-type shape of the signature. Reprinted with permission from Mazur and Ruhnke (2011). Copyright 2011 Elsevier.

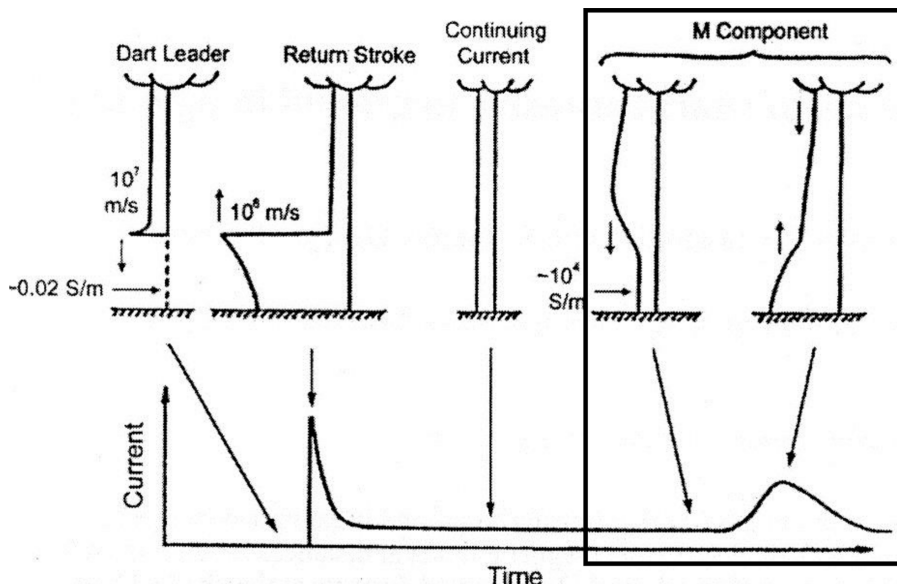


Figure 9.6. Sketch of the physical mechanisms of charge transfer and current profiles. The boxed part of the sketch illustrates the ‘guided-wave’ mechanism of the M-component. Reproduced from Rakov *et al* (2001). Copyright 2001 by John Wiley Sons, Inc. Reprinted by permission of John Wiley & Sons, Inc.

guided electromagnetic wave could propagate in plasma channels, we would observe both the reflections from each end of the lightning channel and also the resonance phenomenon; neither of these was ever observed, due to attenuation in the plasma channels.

The negative slope in the E -field records of the M-component in figure 9.7 is identical to the typical signature of an electric-field change of a negatively charged leader approaching the conducting channel to ground. The surge in current and electric field occur at the time of the attachment of the negative-charge carrier to the grounded channel with continuing current; and the upward jump in the E -field

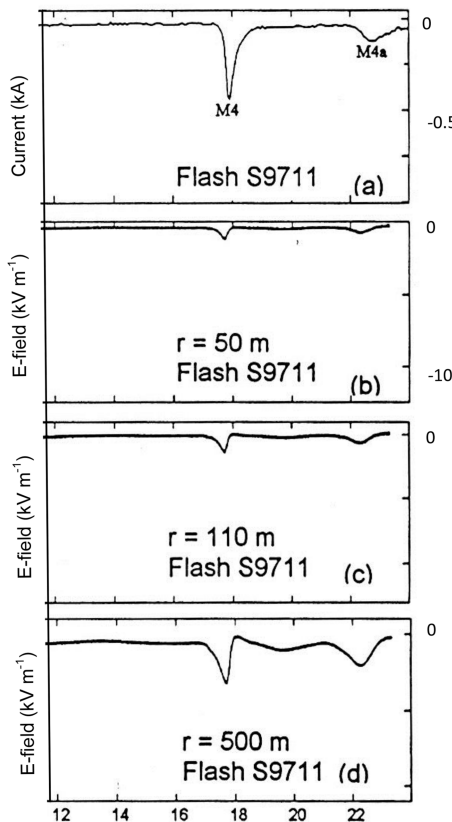


Figure 9.7. Current and electric-field records of an M-component. The electric-field record indicates an approaching negative charge (negative leader) prior to the surge of current in the channel-to-ground that follows the attachment. Note the beginning of the current pulse that occurs at the time of the negative peak in the *E*-field record at the moment of leader attachment to the grounded channel. Reproduced from Rakov *et al* (2001). Copyright 2001 by John Wiley Sons, Inc. Reprinted by permission of John Wiley & Sons, Inc.

record indicates the injection of a positive charge from the ground into the leader channel and, thus, to a newly formed branch. Analysis of the current and *E*-field records of the M-component clearly identifies the event producing the M-component to be the result of the attachment of the negatively charged leader to the conductive channel, similar to a leader–return stroke sequence from a leader’s attachment point, and provides no evidence to support the ‘guided-wave’ model by Rakov *et al* (1995).

The term *M-event* introduced in Shao *et al* (1995) and Mazur *et al* (1995), who studied CG flashes using interferometers and high-speed video systems, seems more appropriate and descriptive than the term ‘M-component’, because it implies a process, the *outcome* of which is the ‘M-component’.

The occurrence of an M-event can be verified with a high-speed video recording. Verification starts by searching for the branch of the positive leader that disappeared after current cutoff, and then proceeds by identifying the recoil leader that appears in

the traces of this previously existing branch. Then, when the recoil leader intercepts the luminous channel of the positive leader at the old branching point, we have found the M-event. An example of this search for an M-event in video images is demonstrated in figure 9.8.

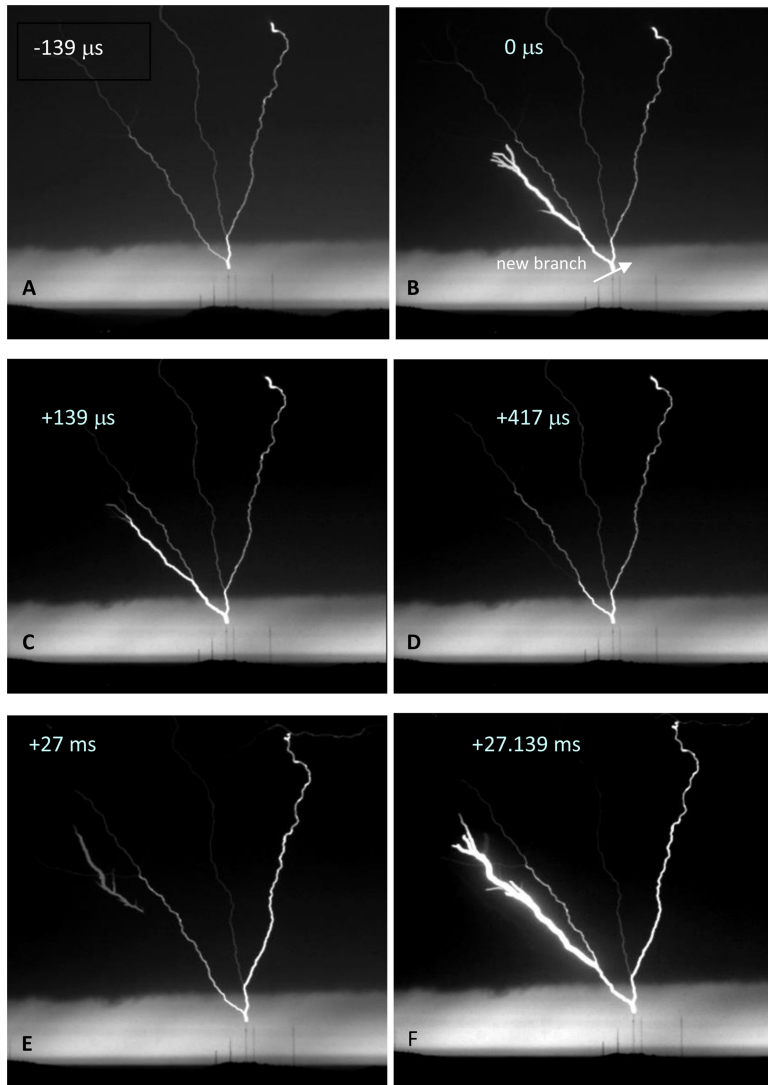


Figure 9.8. Development of a new branch in an upward leader from a TV tower in Rapid City, SD (frames A–D), and the recoil leader stages along the old path of the preceding branch (frames E–F). The images were obtained with a high-speed video system (7200 fps). The time interval between sequential frames is 139 μ s. Timing of the frames is from the moment of appearance of the new branch (marked as zero-time). (A) Upward leader before formation of a new branch, (B) a new branch forms, (C) the new branch penetrates the cloud, and (D) the new branch is cut off from the main channel of the upward leader. (E) The recoil leader appeared as a floating conductor 27 ms after the current cutoff seen in frame (D). (F) Attachment of the recoil leader to the branching point of the conducting leader's trunk connected to ground and formation of the M-component. Reprinted with permission from Mazur and Ruhnke (2011). Copyright 2011 Elsevier.

The first four-panel series of video images in figure 9.8 shows the formation of a new branch in the ascending upward positive leader, in frame (B) of the video sequence. The branch disappears visually 417 μs later, after the current cutoff, in frame (D). A recoil leader then appears along the path of the preceding branch, 27 ms after the current cutoff (frame (E)). The interception of the existing luminous channel of the upward leader by the recoil leader at the old branching point is seen in frame (F), as a pulse-type brightening of the recoil leader channel and the part of the main leader channel from the branching point to the ground. Note the difference in luminosity and, thus, in the current of the recoil leader, before and after the attachment. The newly established branch obtains ground potential from the leader channel connected to the ground, which leads to new positive breakdowns seen at the upper part of the new branch (frame (F) in figure 9.8).

This dynamic of M-event occurrence, based on high-speed video observations, confirms our interpretation of pulse-type brightening in the unbranched part of the upward leader channel, discussed in chapter 7, as the result of a recoil leader joining a conducting channel to the ground.

High-speed video records of recoil leaders and M-events in upward lightning triggered by a tall tower are provided in figures A.8 and A.9 in the appendix.

9.3 The electrostatic model of an M-event that produces an M-component

The simplified electrostatic model of an M-event (Mazur and Ruhnke 2011) is based on the bidirectional, zero-net-charge leader concept, an electrostatic model of the stepped leader–return stroke sequence before and following ground attachment (Mazur and Ruhnke 1998), and on the following assumptions and confirmed facts.

- A linearly increasing ambient potential and, thus, a constant ambient E -field. The charge distribution along the vertical conducting channel mirrors the ambient potential distribution (see figure 9.9).
- Charges associated with any leader channel are produced by corona streamers at the tip of the developing leader during the streamer–leader transition phase (Gallimberti *et al* 2002).
- The corona streamers form a corona envelope with a leader channel inside.

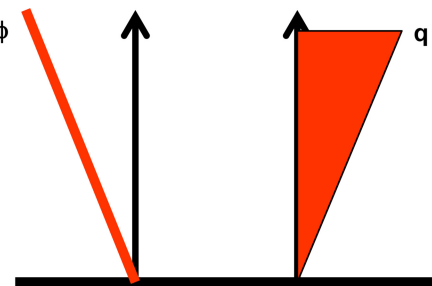


Figure 9.9. Vertical distribution of the ambient potential ϕ and of induced charges per unit length q for a conducting channel of an upward positive leader or a return stroke of a negative CG flash. Data from Kasemir (1986).

- The corona envelope contains static charges that decay with a relaxation-time constant much longer than the lifetime of lightning.
- The old branch channel, after the current cutoff, remains on ground potential, with charges distributed in accordance with ambient potential distribution, for much longer than the lifetime of lightning.
- The longitudinal electric field in the leader channel is ignored, because it is much smaller than the ambient electric field.
- The capacitance per unit length of the channel is assumed to be constant, and the capacitance end-effect is ignored.
- The two basic principles applied in developing the electrostatic model of an M-event are: the recoil and dart leaders are the same physical processes, both traversing previously existing leader channels; return strokes resulting from dart leaders that touch the ground in multi-stroke CG flashes are physically the same as those resulting from stepped leaders in single-stroke CG flashes.

9.3.1 The electrostatic model of a dart leader–return stroke sequence in CG flashes

Prior to touching the ground, the bidirectional and bipolar stepped leader has a negative potential of tens to hundreds of megavolts and induced dipole charges that reside in a corona envelope (figure 9.10(A)). When the leader touches the ground, uniformly distributed positive charges flow from the ground into the leader channel, bringing it to zero ground potential, with induced charges that now mirror the ambient potential distribution. Through this process, the bipolar distribution of induced charges on the stepped leader is transformed into a unipolar distribution of positive charge on the return-stroke channel, with a zero charge on the ground (figure 9.10(B)). The added positive charge at the upper tip of the channel may produce a sufficiently high E -field there to initiate new positive breakdowns, combined with an increased potential drop at the tip of the channel, which is now on ground potential. Almost inevitably, these two factors will lead to the renewal of positive-leader development that manifests itself as a continuing current, becoming *a component of each return-stroke process*, regardless of the continuing current's duration. Although the continuing-current flow in the channel ends eventually with the current cutoff, the charges in the corona envelope remain, maintaining for hundreds of milliseconds the same vertical distribution as had existed before current cutoff (figure 9.10(C)).

Now let us consider a dart leader approaching the ground. In the simplified physical model that describes electrostatically the dart leader's attachment to the ground, depicted in figure 9.11, the leader is a floating conductor in an ambient electric field, i.e. bidirectional, with a zero net charge, and with bipolar distribution of induced charges that mirror the ambient potential distribution along the channel's length (figure 9.11(A)). The difference in the dart leader's path toward the ground, i.e. along the remnants of the previous return-stroke channel, rather than in virgin air, explains an increased speed of leader propagation, which is on an order of magnitude higher than that of stepped leaders, but is lower than that of return

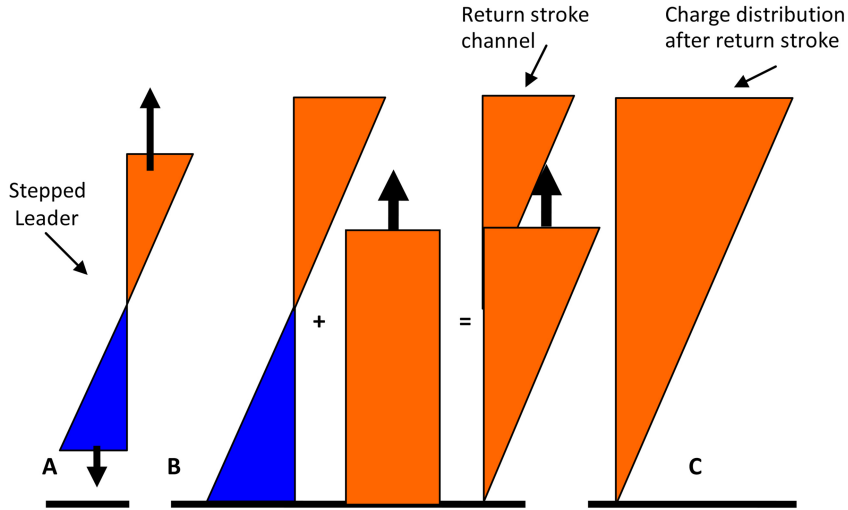


Figure 9.10. A simplified electrostatic charge representation of a stepped leader–return stroke sequence in a negative CG flash. Here, and also in figures 9.11 and 9.12, an abscissa is the charge density on the channels, and the ordinate is the height of the channels above ground. (A) Induced charges on a bidirectional and bipolar stepped leader with a strong negative potential. (B) Transition of charge distribution during the leader’s attachment to ground (at zero potential), with a uniform positive charge deposited to the leader channel by the return stroke current, constant along the channel. The resulting charge distribution is linear, with a zero charge at the ground, and mirrors the ambient potential distribution. (C) Charges along the previous return-stroke channel after it was cut off from the ground (no current, no light emission). The solid arrows indicate the upward movement of the uniform charge (return-stroke current) along the channel. The solid color represents established charges (blue = negative and red = positive charges). Reproduced from Mazur and Ruhnke (1998). Copyright 1998 by John Wiley Sons, Inc. Reprinted by permission of John Wiley & Sons, Inc.

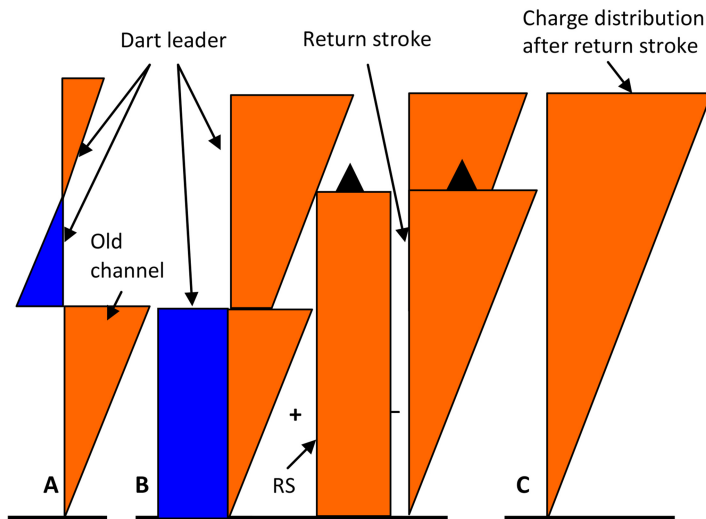


Figure 9.11. A simplified electrostatic charge representation of a dart leader–return stroke sequence in a negative CG flash. (A) A bidirectional and bipolar dart leader develops above the cutoff point, and propagates toward the ground. (B) Transition of charge distribution during the leader’s attachment to the ground zero potential, with a uniform positive charge deposited on the leader channel by the return-stroke current. (C) The final charge distribution of the subsequent return-stroke channel. Reprinted with permission from Mazur and Ruhnke (2011). Copyright 2011 Elsevier.

strokes. The higher speed of propagation indicates that the path to the ground is still sufficiently conductive to guide the dart leader.

The weakly conductive path of the dart leader is surrounded by space charges of the previous corona envelope. Neither charge relaxation, nor Coulomb forces, nor turbulence will significantly change the corona envelope over the lifetime of a lightning event. These space charges are shown in figure 9.11(A) as a positively charged region between the dart leader and ground. Because the old channel is still at ground potential, the dart leader, when it passes along the old channel, will have its induced negative charges reshaped into uniformly distributed charges. However, the upper part of the dart leader, above the old channel, still influenced by the ambient potential at that altitude, will have its charges distributed in a linear fashion (see figure 9.11(B)). Up to the instant of touching the ground, the requirement of a bipolar dart leader to have a zero net charge should be satisfied, but with a changed shape of charge distribution (compare the induced leader charges in figures 9.11(A) and (B)).

Upon touching the ground, the entire dart leader channel assumes a zero ground potential, starting from the ground upward (see figure 9.11(B)). Shifting the potential is accomplished by the uniform charges carried by the return stroke along the previous leader channel. Thus, the resulting charge distribution along the return-stroke channel will have a zero charge on the ground and a maximum positive charge at the top; this is similar to that which takes place in the stepped-leader attachment process to the ground (see figure 9.10(C)). By the end of the transformation, the charges on the subsequent return-stroke channel will be in equilibrium with the ambient potential distribution. The physical process of a recoil leader formation in the remnants of the previous leader channel is discussed in chapter 10.

9.3.2 The electrostatic model of an M-event

The simplified physical concept for dart leaders that touch the ground depicted in figure 9.11 is applicable also to recoil leaders that attach to the current-carrying main trunk of an upward positively charged leader. This process produces an M-component and is illustrated in figure 9.12.

After current cutoff in a branch of an upward leader, its former corona envelope remains charged (figure 9.12(A)). As soon as the recoil leader makes contact with the upward leader, current from the ground flows into the branch and, by adding a uniform net charge to the recoil-leader channel (figure 9.12(B)), brings the attached recoil leader to the near-zero potential of the current-carrying trunk of the upward leader (figure 9.12(C)).

This process transforms the bipolar charge distribution on the recoil leader channel into a unipolar charge distributed along the new branch made from the recoil leader. The additional positive charge at the upper tip of the new branch produces conditions for a new positive breakdown there, as well as elongations of the branch (see figure 9.8(F)). Now, the new branch and the upward leader are both in equilibrium with the environmental potential distribution. Also, the charge density of the new branch at the junction level becomes equal to that on the upward

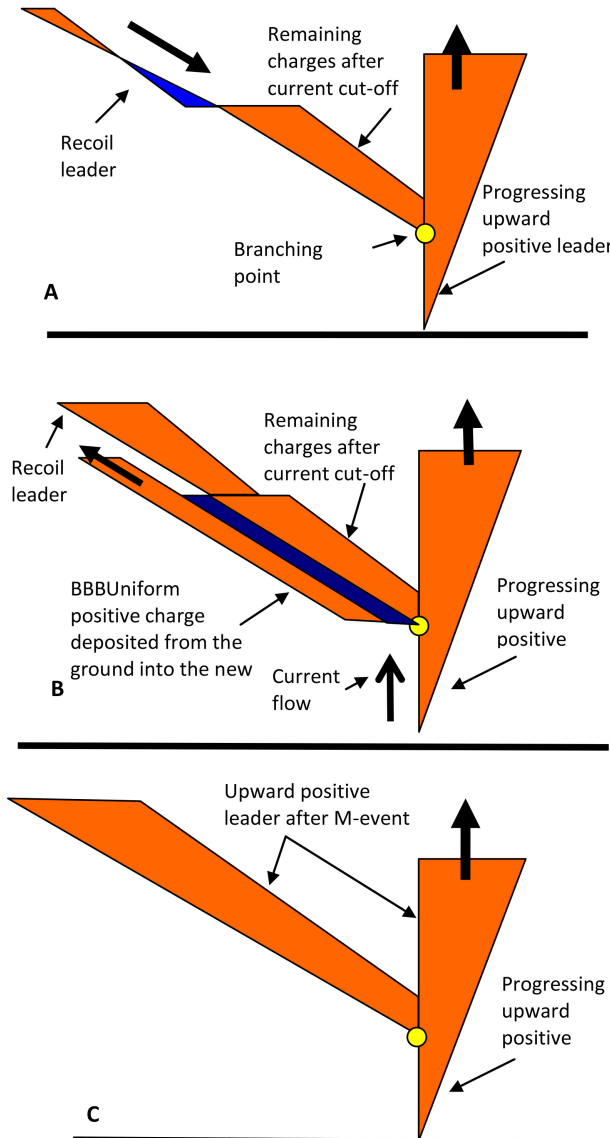


Figure 9.12. A simplified electrostatic charge representation of the attachment of a recoil leader to an upward positive-leader channel. (A) A bidirectional and bipolar recoil leader with zero net charge above the current cutoff point, and the residual charges along the previous upward-leader branch (no current, no light emission). (B) Transition of charge distribution during the recoil leader's attachment to the main channel that is at zero potential. The uniform positive charge is deposited to the new branch by the current flowing through part of the upward-leader channel (between the ground and the branching point) from the ground. The arrows indicate the direction of charge movement (current flow) into the added branch, formerly the recoil leader. (C) The final charge distribution of the upward leader with the new branch. Reprinted with permission from Mazur and Ruhnke (2011). Copyright 2011 Elsevier.

leader, at the level of the branching point. The current flow from the ground upward to the newly formed branch is the M-component, and it is actually ‘seen’ in video images as a brightening of the branch and the section of the main leader channel below the branching point (e.g. figure 9.8(F)).

It is important to note that, during the interception of the upward-leader channel by the recoil leader, the charge distribution on the trunk of the upward leader below the branching point does not change. This implies that a dE sensor on the ground near the leader channel will record a field change only from the charge changes on the new branch situated above the branching point.

A strong burst of radiation sometimes occurs when the recoil leader joins the primary channel, which indicates that the two channels had different electric potentials upon contact (Stock *et al* 2013).

9.4 The universal nature of M-events in lightning

To summarize, the sequence of processes that contribute to the occurrence of M-events consists of the following events: (1) branching of a positively charged leader; (2) current cutoff in a branch of the leader; (3) occurrence of a recoil leader along the path of the vanished branch; and (4) attachment of the recoil leader to a branching-point of the vanished branch on the conducting channel of the positive leader. The conditions that lead to the occurrence of M-events in negative CG flashes were identified in multi-stroke events (see figure 8.6). Recent observations (Visacro *et al* 2013) have detected M-events, both in current and E-field change records, also immediately following the first return stroke in a negative CG flash. Attributes of M-events, such as the pulse-type burst of luminosity in a conductive channel and a ‘hook’-type E-field change, were observed in both video and electric records during development of lightning flashes triggered by, and attached to, aircraft penetrating thunderstorms (see the examples of video records in figure 9.13).

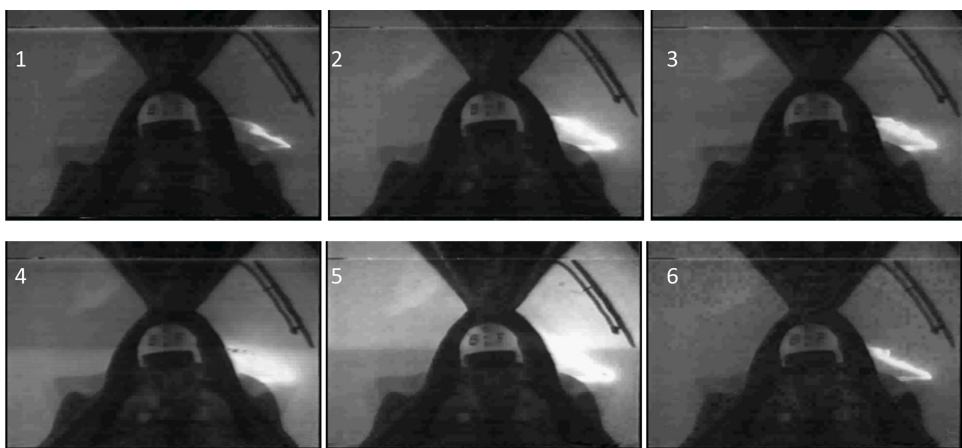


Figure 9.13. Sequence of video fields (17.5 ms apart) showing pulsing luminosity of the lightning channel attached to the NASA F-106B aircraft (aft view)—the indication of M-events. Reproduced from Mazur (1989). Copyright 1989 by John Wiley Sons, Inc. Reprinted by permission of John Wiley & Sons, Inc.

Most lightning flashes triggered by aircraft inside thunderstorms developed as regular IC flashes. Mazur and Moreau (1992) suggested that the pulse-type brightening of the attached lightning channel was the result of its interception by recoil leaders (then identified as ‘K-changes’). These observations provide additional evidence for the rather obvious conclusion that M-events are universal features of positively charged branching parts of lightning flashes, irrespective of their connection to ground, or of their occurrence inside the cloud.

M-events, however, do not occur in negatively charged branched leaders, such as the negatively charged parts of the bidirectional and bipolar lightning trees of IC and CG flashes, and upward triggered leaders of negative polarity. The reason for this is that no recoil leaders are produced in the branching structure of such flashes. A well-known fact about positive CG flashes (their return strokes are analogous to upward negative leaders) is that they do not have multiple return strokes, which are common in negative CG flashes. The current records of negative upward leaders started from tall towers (Heidler 2002) also show the absence of the current pulses that signify an M-event, and thus the absence of the recoil leaders that would produce them.

References

- Edens H E *et al* 2012 VHF lightning mapping observations of a triggered lightning flash *Geophys. Res. Lett.* **39** L19807
- Gallimberti I, Bacchigia G, Bondiou-Clergerie A and Lalande P 2002 Fundamental processes in long gap discharges *C. R. Phys.* **3** 1335–59
- Heidler F 2002 Lightning current measurements at the Peissenberg telecommunication tower *Proc. Int. Conf. on Grounding and Earthing, GROUND'2002 (November 4–7 Rio de Janeiro, Brazil)* pp 117–122
- Kasemir H W 1986 Model of lightning flashes triggered from the ground 1986 *Int. Aerospace and Ground Conf. on Lightning and Static Electricity (Dayton, OH)* p 39.I
- Malan D J and Schonland B F J 1947 Progressive lightning. Part 7. Directly correlated photographic and electrical studies of lightning from near thunderstorms *Proc. R. Soc. A* **191** 485–503
- Mazur V 1989 Triggered lightning strikes to aircraft and natural intracloud discharges *J. Geophys. Res.* **94** 331–25
- Mazur V and Moreau J-P 1992 Aircraft-triggered lightning: processes following strike initiation that affect aircraft *J. Aircraft* **29** 575–80
- Mazur V, Krehbiel P R and Shao X M 1995 Correlated high-speed video and radio interferometric observations of a cloud-to-ground lightning flash *J. Geophys. Res.* **100** 25731–53
- Mazur V and Ruhnke L H 1998 Model of electric charges in thunderstorms and associated lightning *J. Geophys. Res.* **100** 23299–308
- Mazur V 2002 Physical processes during development of lightning flashes *C.R. Phys.* **3** 1393–409
- Mazur V and Ruhnke L H 2011 Physical processes during development of upward leaders from tall structures *J. Electrostat.* **69** 97–110
- Mazur V, Ruhnke L H, Warner A and Orville R E 2013 Recoil leader formation and development *J. Electrostat.* **71** 763–8
- Ogawa T and Brook M 1964 The mechanism of the intracloud lightning discharge *J. Geophys. Res.* **69** 5141–50

- Rakov V A, Thottappillil R, Uman M A and Barker P P 1995 Mechanism of the lightning M component *J. Geophys. Res.* **100** 25701–10
- Rakov V A, Crawford D E, Rambo K J, Schnetzer G H and Uman M A 2001 M-component mode of charge transfer to ground in lightning discharges *J. Geophys. Res.* **106** 22817–31
- Saba M M F, Cummins K, Warner T, Krider E P, Campos L Z S, Ballarotti M G, Pinto Jr O and Fleenor S A 2008 Positive leader characteristics from high-speed video observations *Geophys. Res. Lett.* **35** L07802
- Shao X M, Krehbiel P R, Thomas R J and Rison W 1995 Radio interferometric observations of cloud-to-ground lightning phenomena in Florida *J. Geophys. Res.* **100** 2749–83
- Stock G, Akita M, Krehbiel P R, Rison W, Edens H E, Kawasaki Z and Stanley M A 2013 Continuous broadband digital interferometry of lightning using a generalized cross-correlation algorithm *J. Geophys. Res.* **119** 3134–65
- Visacro S, Araujo L, Guimaraes M and Murta Vale M H 2013 M-component currents of first return strokes in natural negative cloud-to-ground lightning *J. Geophys. Res.* **118** 12132–8

Principles of Lightning Physics

Vladislav Mazur

Chapter 10

The physical concept of recoil leader formation

10.1 The relationship between the internal electric field and current in lightning leaders

The assumption of the leader as a perfect and equipotential conductor, made in earlier, simplified computer-simulation models of leader development in a thundercloud (Mazur and Ruhnke 1998, Van der Velde and Montanya 2013), is only approximately valid for real-life leaders, and is not applicable for cooling leader channels. From initiation through decay, the leader channel is in a state of plasma, the features of which are very similar to those of a free-burning arc, with the current, I , and the internal longitudinal electric field, E_{int} , uniform along the channel, but changing in a wide range of values during the leader's lifetime. The potential ϕ at the tip of the leader is the product of the internal, longitudinal electric field $E_{\text{int}} = -\text{grad}\phi$ and the length of the channel, l . The value of E_{int} can be found in the E - I characteristic of a free-burning arc in the modified King's curve (see figure 2.4), which depicts a negative relationship between the $\text{grad}\phi$ and arc current I for the entire range of leader currents, from milliamperes to hundreds of amperes (Mazur and Ruhnke 2014). (From now on E_{int} will be used, rather than $\text{grad}\phi$.)

In the relationship between E and I in arcs, there is a time lag, or long response time, of several tens of milliseconds between the changes of the current I and the response of the E_{int} . An example of this effect is observed during a step-like application (switching on) of the 100 A current to a short laboratory arc (figure 2.2).

The similarity with a free-burning arc is most applicable to a unipolar leader, which is connected at one end to a current source. Therefore, we assume that unipolar leaders, like free-burning arcs, have a uniform current and potential gradient along their length, at any given moment of the leader-channel's development.

10.2 Current cutoff prior to the occurrence of recoil leaders

It is commonly understood in the lightning literature that the word ‘cutoff’ applied only to the current in the lightning channel, means the disruption of current flow, which is accompanied by the loss of the channel’s luminosity. This interpretation of current cutoff, however, lacks any quantitative description as it regards the current magnitude. Thus, not surprisingly, the questions of residual current and residual luminosity during current cutoff are still unsettled, and are frequently brought up in the literature (e.g. Ngin *et al* 2014).

For a unipolar leader to advance, the longitudinal E_{int} should be significantly smaller than the ambient E -field, and the potential difference at the leader tip between the leader potential and the ambient potential should be greater than a certain minimal threshold value. When the potential difference at the leader’s tip becomes equal to that threshold value, the propagation ceases, and the leader’s current cutoff begins. This type of termination of current, called the ‘death of the leader’ (see chapter 8), is most clearly visible in the development of single, unbranched leader channels, and also of individual branches in the branched leaders.

We define current cutoff as a process of an irreversible decline of the current in the lightning channel, rather than as an instantaneous act (drop-off), obviously accompanied by a decreasing, then disappearing, channel luminosity. Within a few tens of milliseconds, this process brings the current to the value of tens of milliamperes. This dynamic is seen in the current record of a multi-stroke negative CG flash (see figure 10.1), during the intervals between sequential return strokes. However, it takes several hundred milliseconds, if not a few seconds, to bring the current of the decaying return stroke to zero, evidence of which is seen in the record in figure 10.1, after the last return-stroke current pulse. So, the answer to the rhetorical questions in the title of the paper by Ngin *et al* (2014), ‘Does the lightning current go to zero between the ground strokes? Is there a current “cutoff”?’’, may be the following: because the full current cutoff process (down to zero) lasts significantly longer than the time intervals between return strokes, the current does not

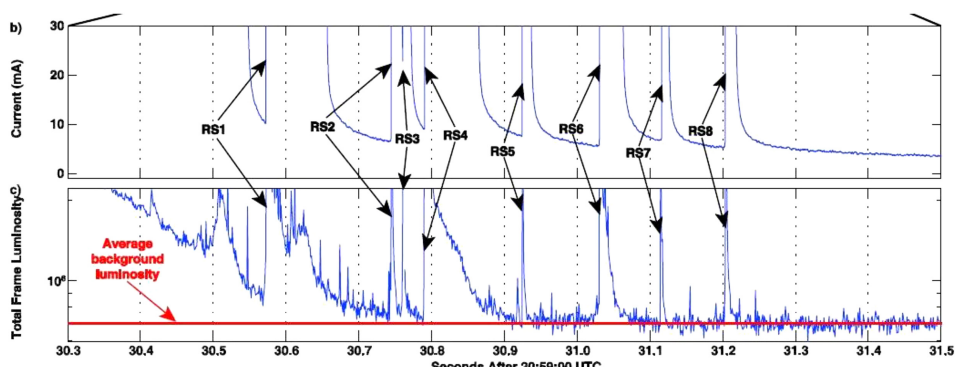


Figure 10.1. The log scale plot of current on a linear scale and the total frame-luminosity of a multi-stroke CG flash. The current did not drop below 5 mA between return strokes in this event. Reproduced from Ngin *et al* (2014). Copyright 2014 by John Wiley Sons, Inc. Reprinted by permission of John Wiley & Sons, Inc.

come to zero before it is interrupted (at the current level of a few millamps) by a dart leader that attaches to the ground, and starts the next return stroke. Thus, total current cutoff does not happen between return strokes, but rather occurs only after the final return stroke.

As the current cutoff process continues in the cooling channels of both the leaders and return strokes, the channels remain as charged plasma. The evidence of this is seen in the slowly decreasing (for hundreds of milliseconds) electric field produced by the cooling leader channel long after the current there has dropped to near-zero (see the example in figure 7.16); it is also evident in the residual ionization present in the cooling return-stroke channel prior to the occurrence of a dart leader (see figure 1.11). The E -field record in figure 7.16 may also serve as another illustration of the time-lag of the potential gradient behind the current change in the free-burning arc, as described in chapter 2. The presence of a small residual current (in millamps) during the cooling of the channel is evident from the current record after the last return stroke in figure 10.1.

In branched-leader channels, in addition to the phenomenon of the ‘death of the leader’ in each straight branch, the screening of branches exists within the branched structure, which affects the changing total current in its trunk (see chapter 8). In branched leaders of both polarities, the current in the leader trunk is affected by two processes: (1) the growth of upper branches, which contribute to increasing current, and (2) the screening effect from upper branches on the lower ones, which contributes to decreasing current. However, the total current in the leader’s trunk will not reach zero until all upper branches cease to propagate.

10.3 The development of recoil leaders

Recoil leaders are major players in almost all types of lightning flashes. Here is a summary of the known facts obtained from various observations related to recoil leaders, all of which should be addressed in any proposed physical model of recoil-leader formation.

- There is no observational evidence of ‘positive’ recoil leaders occurring in (1) negative leaders triggered by the rocket-and-wire technique (Kawasaki 2002), or (2) in return-stroke channels of positive CG flashes after the current cutoff, or (3) from the negative end of the lightning tree during the initial stage of the IC flash (Mazur 1989).
- An upward positively charged leader initiated by a tall structure exhibits a pulse-type luminosity produced by M-events, and thus, by recoil leaders, in a branched structure outside or within a cloud region. Evidence for this is presented in high-speed video observations in Mazur and Ruhnke (2011), and in Warner (2012), and also in observations with the LMA (e.g. Hill *et al* 2012 and Edens *et al* 2012).
- On the other hand, an unbranched upward positively charged leader that is initiated by a tall structure, and which dies off *without the ensuing dart leader* to ground, exhibits the type of slow-luminosity variation associated with

changing ambient potential distribution in the cloud regions. The evidence and analysis of this is presented in Mazur and Ruhnke (2011) and Mazur and Ruhnke (2014).

- Recoil leaders have been mistakenly perceived as negatively charged, unipolar leaders propagating along the path of a previous positively charged leader or return stroke of a negative CG flash towards the branching points, or towards the ground. This perception, which made no physical sense for an electrodeless discharge, has been disproved by high-speed video observation of a recoil leader (Mazur *et al* 2013) that showed the bidirectional development of a bipolar recoil leader occurring along an old branch of a positively charged leader.
- In branching leaders, recoil leaders do not occur while the positively charged branch is still visibly developing, but do so tens of milliseconds after the preceding branches become invisible. The evidence for this is obtained from LMA observations (Van der Velde and Montanya 2013) and high-speed video observations (Mazur and Ruhnke 2011).
- In branching leaders, recoil leaders do not originate at the tips of preceding branches. The suggestion that a recoil leader originates *near* the tip of the preceding positively charged branch (Van der Velde and Montanya 2013) confirms the observation that the positively charged part of the bidirectional recoil leader is much shorter than the negatively charged one, and thus, is closer to tip of the preceding positively charged branch (see figure 9.3).
- Electrostatics cannot explain and, thus, are not applicable to the process of transformation (cooling) of the leader channel after current cutoff, which lasts hundreds of milliseconds (Ruhnke 2014).
- The ‘negative resistance’ in the E - I relationship of free-burning arcs, and therefore, the arc’s features—a uniform current and a potential gradient (internal E -field) along the arc channel—are applicable to a unipolar leader channel. The assumption of a uniform current in the leader channel is more fitting for individual branches than for the trunk of the branching leader, because the current in the trunk of the growing leader is not always uniform (Mazur and Ruhnke 2014).
- There can be no further propagation of the leader after its tip reaches a region with a critical potential drop, a condition of the ‘death of the leader’.

The earlier hypothesis, of recoil-leader formation from the lower end of a developing positively charged leader (Mazur and Ruhnke 1993), was based on the assumption that a unipolar unbranched leader can continue to propagate after current cutoff from the ground. This is not the case, as we now know. Also, the purely electrostatic approach to recoil-leader formation used in that hypothesis cannot be applied to the state of transformation of the preceding leader channel after current cutoff.

An analysis of these listed observations leads us to the following conclusions, all of which should be considered and borne out by a conceptual model for recoil-leader formation:

1. Recoil leaders occur *only* in branching positively charged leaders (either inside or outside the cloud), which either follow return strokes that enter the cloud in negative CG flashes, are parts of IC flashes, or are initiated by a rocket-and-wire technique or tall ground structures.
2. The conditions for recoil-leader formation should exist in a single branch of a branched leader. The propagation and termination of this branch will be affected by the ‘screening effect’ from neighboring branches (Lalande and Mazur 2012), and current cutoff in the branch will occur as the ‘death of the leader’.
3. The conceptual model for the mechanism of recoil-leader formation should be based on an electro-dynamic (not electrostatic) approach that applies the similarities of lightning leaders to a free-burning arc.

10.4 A proposed conceptual model of recoil leader formation

Any branched leader consists of a number of individual branches that are separated in space, creating together a branched structure of a certain density. The conceptual model is applied to recoil-leader formation in a single branch that develops current cutoff, regardless of the leader’s polarity.

Recoil leaders, by their very nature as electrodeless discharges, are similar to leaders that are parts of IC and CG flashes (‘natural leaders’). The main difference between recoil leaders and these natural leaders lies in their origins: one (the recoil leader) occurs at a point on the existing cooling plasma channel, and the other (a natural leader) occurs in ‘virgin’ air. This difference in origins leads to the different types of paths of natural versus recoil leaders, and consequently, to differences in speed, current, luminosity, and the branching structures of the two leaders (absent in recoil leaders, present in natural ones). However, because of the similarity in the *nature* of recoil leaders and leaders of IC and CG flashes, it is reasonable to assume that the conditions for recoil-leader formation are similar to those in natural leaders. The remaining unknowns are the magnitudes of the ambient variables that constitute the initiation conditions, which may be different in each case.

We still do not know much about the electrical conditions during the initiation of natural leaders. It is well understood, however, that residual ionization in the cooling channel of the preceding positively charged leader, present for hundreds of milliseconds, would ease the formation of a recoil leader, e.g. by diminishing the ambient *E*-field needed for the initial electrical breakdown.

The current of the leader is proportional to the speed of its changing induced charges, dQ/dt , and the leader’s speed is affected by the potential drop at the leader tip, $\Delta\phi$. The empirical relationship $V(\text{m s}^{-1}) = 15 \Delta\phi^{0.5}$, suggested in Bazelyan and Raizer (2000), explains the effect of the potential drop on both the speed and electrical features of the propagating leader.

The usual development of any unipolar, single-channel leader starts with acceleration, during which the potential drop at the leader tip $\Delta\phi$ increases and then slows down, during which time the potential drop at the leader tip $\Delta\phi$ decreases

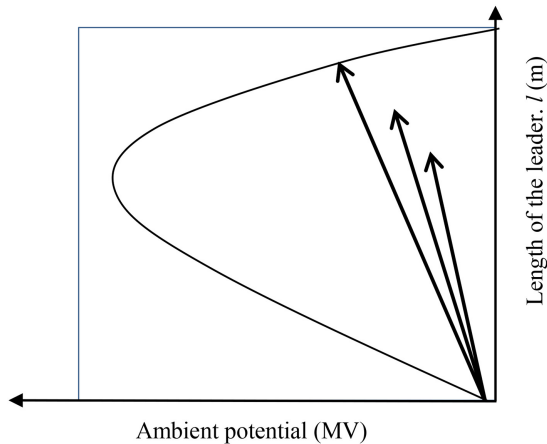


Figure 10.2. Conceptual sketch of the evolution of the potential of an ascending unipolar, positively charged leader at the slowing phase of its propagation. The potentials are marked by the sequence of arrows on a background of the vertical profile of the ambient potential distribution.

before reaching equilibrium with the ambient potential, and ends with the ‘death of the leader’-type current cutoff. The shape of the ambient potential distribution required to accommodate this development of a unipolar positively charged leader, regardless of the orientation of its propagation path, should look like the one shown in figure 10.2. The vertical scale in the figure is the length of the leader’s path, from the origin (e.g. a branching point) to the point of termination. The horizontal scale, for the case of the positively charged branch, is the ambient potential of negative values, starting either at a zero ground potential, in the case of a rocket-triggered upward leader, or at the potential of a branching point on the conductive trunk of the branched leader. The plot in figure 10.2 also illustrates the qualitative relationship between the ambient electrical environment and the propagating unipolar leader, before the termination of the leader. Similarly, the plot in figure 10.3 is used to illustrate the qualitative relationship between the ambient electrical environment and a recoil leader during cooling of the channel of the preceding leader.

From the ‘negative’ E - I relationship in the free-burning arc channel, one obtains the value of the potential gradient, $\text{grad}\phi = -E_{\text{int}}$, for a given leader’s current; both the current and the potential gradient are assumed to be uniform along the leader channel. Two factors affect the potential at the tip of the developing leader channel, which is $\phi = \text{grad}\phi l$: the potential increases with the length of the channel, l , and with the changing of the potential gradient, $\text{grad}\phi = -E_{\text{int}}$, as the result of the changing current of the leader. Therefore, the arrow representing the potential of the leader channel in figure 10.2 changes its length during propagation and changes its tilt toward a negative ambient potential, responding to the changes in leader current. The low end of the propagating leader channel remains at the initial potential value.

We assume that the process of the merging of the old leader channel into the ambient potential begins from the top of the cooling channel, where the cessation of propagation occurs, and that the merging continues downwards. This dynamic is

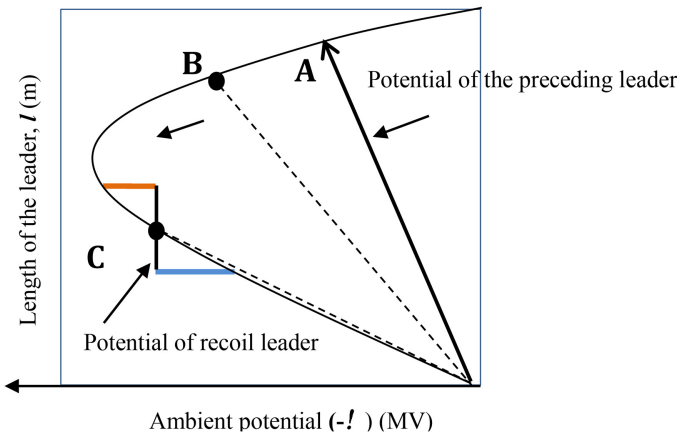


Figure 10.3. A conceptual sketch of the evolution of the potential of an old leader channel during its cooling stage, marked by the sequence of dashed lines that slide along the ambient potential line, from point A towards points B and then C, coinciding with the decreasing length of the cooling channel that merges with the ambient electric environment. Conditions for formation of a recoil leader occur at point C, where the ambient E -field is sufficient for initial electrical breakdown. The potential drops $\Delta\phi$ at the tips of the negatively and positively charged parts of the formed recoil leader are marked as blue and red lines, respectively.

depicted as the sliding of the tip of the cooling channel potential downwards along the curve of the ambient potential profile, while the length of the remaining (lower) part of the cooling channel decreases (see figure 10.3). If, or when, in the process of this evolution, the tip of the cooling channel reaches the region of the electrified cloud (a point on the ambient potential curve) with an ambient E -field sufficient to initiate electrical breakdown, this may become a condition for a streamer-leader transition followed by the formation of a bidirectional and bipolar recoil leader.

The development of a bipolar recoil leader in the conceptual model should be similar to that which is observed in recoil leaders in nature, i.e. with the negatively charged part of the leader moving towards the old channel origin and the positively charged part moving in the opposite direction (seen as moving upward). In the case of the ambient potential distribution depicted in figure 10.3, such a development may occur only if the formation of the recoil leader takes place at the lower slope of the ambient potential curve, e.g. at point C, and not earlier, at its upper slope, e.g. point B.

The negatively charged part of the bidirectional recoil leader has a ‘green light’ for propagation all the way to the branching point, because the potential drop at its tip will only increase with the leader’s approach to the branching point. The positively charged part of the bidirectional recoil leader will develop in the opposite direction, until its tip reaches the point of equal potential with the environment. (These dynamics of recoil-leader development are observed in the series of high-speed video frames in figure 9.4.) The duration of the cooling process from the beginning of the current cutoff (point A) in figure 10.3 until the initiation of the recoil leader (point C) could be in tens of milliseconds, depending on the ambient electrical environment.

The stages of recoil-leader development depicted in figure 10.3 are similar to those of natural leaders that start from the region with the highest ambient E -field, and which propagate with equal speeds (see figure 6.4), or have faster negative-leader and slower positive-leader speeds (Van der Velde and Montanya 2013). In essence, the possibility of recoil-leader formation is determined by the profile of the ambient potential along the cooling and still-ionized path of the preceding unipolar leader, and thus, by the presence of an ambient E -field required for the initial electrical breakdown for recoil-leader formation. In the absence of these conditions, recoil leaders would occur in every CG flash with a single return stroke, or in every case of an unbranched upward positive leader. This seems not to be the case at all.

10.4.1 Recoil leader formation and polarity asymmetry in branched leaders

Current cutoff is observed in branching leaders of both polarities and as parts of IC and CG flashes. Recoil leaders, however, are observed only in positively charged branching leaders, while overwhelming evidence points to the total absence of recoil leaders in negatively charged branching leaders, and consequently, in the return strokes of positive CG flashes, which have only a single return stroke. This evidence also suggests that the requirement for a suitable ambient potential distribution for the formation of recoil leaders is fulfilled only in positively charged branching leaders. Claims of more than a single return stroke in positive CG flashes lack the needed support of carefully analyzed observations that should confirm the occurrence of more than a single return stroke along the same channel to ground, or a commonality of origins for sequential return strokes. However, positive CG flashes with several channels to ground, separated by distances of tens of km from each other, have been observed in summer thunderstorms (Thomas 2001).

In search of an explanation for the observed difference in recoil-leader occurrence in branched leaders of the two polarities, we shall examine the polarity asymmetry in leaders of both polarities; this manifests itself in the leaders' speeds of propagation, and thus, in their currents, and also in the branching features of the two types of leaders. The spatial composition of the branching structure and the number and sizes of the branches would influence, by the screening effect, the exposure of individual branches to the ambient E -field and, thus, the branches' currents.

High-speed video observations of downward negatively charged leaders below the cloud base reveal a highly dense dendritic structure made of *small branches* (see the example in figure 10.4(A)). On the other hand, most downward positively charged leaders are made of single channels and, when branched, have a structure distinctly different from that found in negative leaders, with only a few individual *long branches* separated by large spaces (see figure 10.4(B)).

The same profound difference in the density of branches, their numbers, and their sizes between positive and negative leaders is observed inside the cloud, when we compare both the plain view and vertical profiles of the map of radiation sources of these leaders (figure 10.5).

The difference between positively and negatively charged leaders, in their speeds of propagation and also in their branching structures, apparently affects (1) the

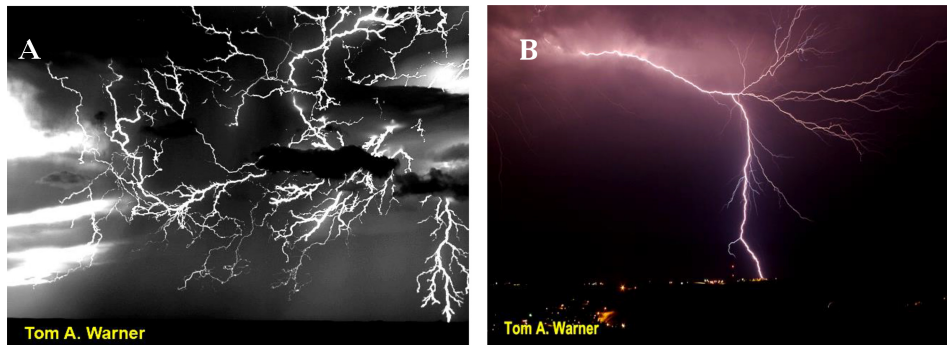


Figure 10.4. Time-compressed images from high-speed video observation of (A) branched negative leaders below the cloud base and (B) a branched downward positive leader of a positive CG flash. Courtesy of T A Warner.

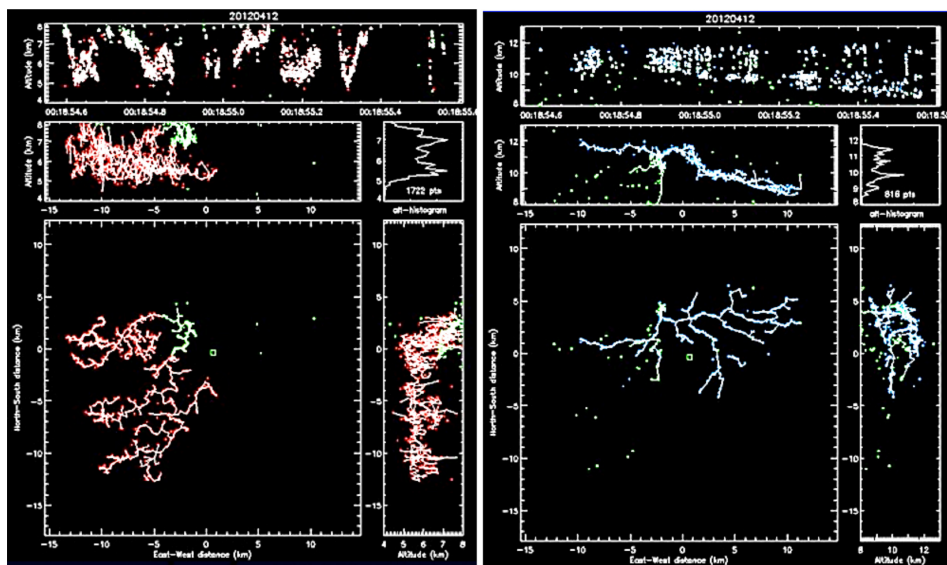


Figure 10.5. Radiation map of two parts—the region of negative breakdowns (left panel) and the region of positive breakdowns (right panel)—of an IC flash, obtained with the LMA system. The panels in the figure from top to bottom are: (1) altitude–time, (2) altitude–distance (east–west), (3) distance (north–south)—distance (east–west), and (4) distance (north–south)–altitude. Courtesy of P Krehbiel.

duration of the continuing current prior to the beginning of the current cutoff process (hundreds of milliseconds versus tens of milliseconds, respectively), (2) the magnitude of this current (hundreds of amperes versus a few kiloamperes, respectively), and (3) the rise- and drop-times of the continuing current (a few milliseconds versus tens of milliseconds, respectively) and the duration of the current cutoff process (Heidler 2002).

It is reasonable to assume that the ambient potential distribution in a *larger* spatial gap between *longer* branches of positively charged leaders is suitable for the formation of a recoil leader in the cooling channel of a preceding branch. On the other hand, the much higher number of *smaller* branches per unit volume in negatively charged leaders produces a significant reduction in the ambient *E*-field in the *smaller* spaces between shorter channels, making the *E*-field unsuitable for recoil-leader formation. This explains why the proposed model of recoil leader formation may not lead to the occurrence of recoil leaders in heavily branched negatively charged leaders. The conclusion that the highly dendritic structure of negative branching leaders prevents the formation of recoil leaders may seem intuitive, but this is perhaps the only conclusion that can properly explain why the proposed qualitative concept of recoil-leader formation, which is indifferent to the polarity of the preceding unipolar leader, actually works only in the cases of positively charged branched leaders.

10.5 Conclusion

The qualitative concept of recoil-leader formation has four essential components in its foundation.

- (1) It is based on the mechanism of the current cutoff process presented in Mazur and Ruhnke (2014), which is the ‘death of the leader’ in unbranched channels, plus an additional screening effect in branched channels.
- (2) It uses the analogy of a unipolar leader (a branch in a branched structure) to a free-burning arc with a uniform current and internal *E*-field.
- (3) It interprets the cooling of the preceding leaders during the current cutoff process as being similar to the transformation of current and potential gradient in a free-burning arc channel, which leads to the gradual merging of the cooling channel, starting from its tip, into the ambient environment.
- (4) It assumes that the conditions for the initiation and bidirectional, bipolar development of a recoil leader are qualitatively similar to those in natural lightning leaders, but require a lesser ambient *E*-field, due to the presence of the ionized media in the cooling channel of a preceding leader.

The absence of recoil leaders in branched negatively charged leaders, as well as the always-single incidence of return strokes in positive CG flashes, is interpreted as the effect of the dense branching structure of numerous small branches of these leaders, which prevents the ambient electric field from reaching the level necessary for initiation of an electrodeless discharge, such as a recoil leader.

References

- Bazelyan E and Raizer Yu 2000 *Lightning Physics and Lightning Protection* (Bristol: Institute of Physics Publishing)
- Edens H E *et al* 2012 VHF lightning mapping observations of a triggered lightning flash *Geophys. Res. Lett.* **39** L19807

- Heidler F 2002 Lightning current measurements at the Peissenberg telecommunication tower *Proc. Int. Conf. on Grounding and Earthing, GROUND'2002 (November 4–7, Rio de Janeiro, Brazil)* pp 117–22
- Hill J D, Pilkey J, Uman M A, Jordan D M, Biggerstaff M I, Hyland P, Rison W, Krehbiel P R and Blackeslee R 2012 Correlated lightning mapping array (LMA) and radar observations of the initial stages of Florida triggered lightning *Geophys. Res. Lett.* **39** L09807
- Kawasaki Z-I 2002 Personal communication
- Lalande P and Mazur V 2012 A physical model of branching in upward leaders *AerospaceLab J.* **5** AL05–7
- Mazur V 1989 Triggered lightning strikes to aircraft and natural intracloud discharges *J. Geophys. Res.* **94** 3311–25
- Mazur V and Ruhnke L H 1993 Common physical processes in natural and artificially triggered lightning *J. Geophys. Res.* **98** 12913–30
- Mazur V and Ruhnke L H 1998 Model of electric charges in thunderstorms and associated lightning *J. Geophys. Res.* **100** 23299–308
- Mazur V and Ruhnke L H 2011 Physical processes during development of upward leaders from tall structures *J. Electrostat.* **69** 97–110
- Mazur V, Ruhnke L H, Warner T A and Orville R E 2013 Recoil leader formation and development *J. Electrostat.* **71** 763–68
- Mazur V and Ruhnke L H 2014 The physical processes of current cutoff in lightning leaders *J. Geophys. Res.* **119** 2796–810
- Ngin T, Uman M A, Hill J D, Olsen R C, Pilkey J T, Gamerota W R and Jordan D M 2014 Does the lightning current go to zero between ground strokes? Is there a current ‘cutoff’? *Geophys. Res. Lett.* **41** 3266–73
- Petersen D A and Beasley W H 2014 High-speed video observations of a natural negative stepped leader and subsequent dart-stepped leader *J. Geophys. Res.* **118** 12110–9
- Ruhnke L H 2014 Analysis of electric fields and potentials on lightning channels *GROUND'2014 and 6th International Conference on Lightning Physics and Effects (Manaus, Brazil, May 2014)* p 1–6
- Thomas R 2001 Personal communication
- Van der Velde O and Montanya J 2013 Asymmetries in bidirectional leader development of lightning flashes *J. Geophys. Res.* **118** 13504–9
- Warner T A 2012 Observations of simultaneous upward lightning leaders from multiple tall structures *Atmos. Res.* **117** 45–54

Principles of Lightning Physics

Vladislav Mazur

Chapter 11

Some lightning protection issues viewed through the lens of lightning physics

The significant progress achieved in our understanding of lightning phenomena and lightning physics in the course of the last 30 years or so, which is the subject of this book, allows us to revisit in this chapter the justification for some established methods of lightning protection. Such a re-examination is particularly relevant to the very complex, multivariable interaction between lightning and those structures on and above ground which may be in need of protection. Additionally, recent lightning research has introduced some newly discovered, potentially hazardous features of lightning that were not previously considered in the designing of lightning protection.

11.1 Striking distance versus the parameters of downward leaders in lightning protection of ground installations

The main focus of lightning protection is on the prevention of lightning hazards to ground structures caused by CG lightning flashes. Therefore, understanding the physical processes that take place in the interaction between a downward leader of a CG flash and a ground structure is essential for determining the role of the parameters involved in these processes, and their effect on the probability of a lightning strike to the structure. The single parameter applied in the lightning protection for this type of interaction is the so-called ‘striking distance’. Striking distance is defined as the distance from the leader tip to the object on the ground, which would be struck by lightning when the electric field in the gap reaches a critical value of breakdown voltage. The following quotation from Uman (2008) mentions some problems in determining the striking distance: ‘The criterion for breakdown in long non-uniform air gaps, including lightning, is considerably more complex than can be described by a single parameter such as the critical electric field,

but such an approach has been generally used to compensate for our deficiency in understanding the physics of the attachment process and its variability.'

In lightning protection, the striking distance, d , is considered to be a function of the peak current, I_p , of the first return stroke of a CG flash: $d = AI_p^b$. As they are referred to in the literature, the values of the constants A and b in this formula are different in different studies. Indeed, observations of CG flashes show a general increase in striking distance with the increased peak current of return strokes. These observations, however, are based on a limited number of direct current measurements of return strokes made on a few selected ground installations (usually tall structures); furthermore, these measurements are affected by the local environmental conditions (climatological, topographical), which influence the development of thunderstorms and, therefore, the severity of CG flashes. As a result, the theoretical evaluations of striking distance, using the expression $d = AI_p^b$, suffer from an unacceptably large numerical spread. The use of this expression for a striking distance has been justified in view of the absence of any other practical way to estimate it, using a measurable parameter that would characterize a CG flash.

A computer-simulation study of the interaction between downward negative leaders and a tall structure (Mazur *et al* 2000) indicates that the peak current measurements on tall structures are biased toward powerful lightning flashes, because less-powerful CG flashes may miss attachment to a tall ground structure. Therefore, the value of the calculated striking distance will also be biased toward higher values.

The assumption that striking distance in lightning protection is indirectly based on the potential of the downward leader was stated in Young *et al* (1963). However, following the erroneous assumption that the leader potential is related to the velocity of the return stroke, which is related to the amplitude of the return stroke, striking distance became associated with the amplitude of the return stroke (Mousa 2016).

The two players that influence striking distance are the downward leader, with its polarity-dependent parameters, and the upward, so-called ‘connecting leader’, which is initiated from the ground structure in response to the approaching downward leader. The height and geometry of the structure affect the timing of initiation of the connecting leader and its dimensions. These factors, however, are not taken into consideration in the expression for the striking distance, d , which is a function of the peak return-stroke current only.

The return-stroke current, I , results from the attachment of the downward leader with the potential, Φ , to the ground, which is at zero potential; so, naturally, there is a relationship between the return-stroke current and the parameters of a downward leader. While the impedance of the downward-leader channel is $Z \sim 500 \Omega$, and the grounding impedance of the protected structure is in the tens of ohms (negligible in comparison with that of the leader), the return-stroke current would be $I = \Phi/Z$. An unprotected structure may have a much higher grounding impedance and, thus, will experience a return stroke of a lesser amplitude than a ‘protected’ structure, after attachment by a downward leader with the same potential Φ .

The length of the negative leader’s step, L_{st} , is determined by the expression $L_{st}(m) = \Phi/E_{st}$, where Φ is the potential at the tip of the leader, in kilovolts, and

$E_{st} = 750 \text{ kV m}^{-1}$ is the required electric field in the streamer-zone of the developing negative leader. This step length of the negative leader represents *the maximum value of the striking distance* before the leader's attachment to ground, or to a connecting leader from a ground structure. The actual striking distance to a ground structure, however, could be shorter than the preceding step of the downward leader. From a physics standpoint, it makes better sense to use the leader's potential, rather than the peak current of the first return stroke, to estimate striking distance. The reason the leader's potential is not yet used for this purpose, however, is that researchers lack the ability to measure it directly, unlike their ability to measure the current of a return stroke that is attached to an instrumented tower.

A method for estimating a lightning leader's potential, based on multi-station measurements of electric-field changes produced by the first return stroke in CG flashes, was proposed by Mazur and Ruhnke (2002). This approach utilizes remote measurements, is less intrusive than direct current measurements and, therefore, can be implemented in a variety of geographical locations and climatological conditions.

The electric-field change on the ground, dE_{RS} , at distance D from the return-stroke vertical channel of length Z , with the deposited charge per unit length, q , and the capacitance per unit length, c , is

$$dE_{RS} = -q/(2\pi\epsilon) \times [1/D - 1/Z^2]^{0.5} \quad (11.1)$$

If dE_{RS} is measured at various distances from a lightning ground attachment point by several 'slow antenna' sensors, the variables q and Z can be obtained by solving a system of equations (11.1) for several distances D . With the location of the attachment point of the return stroke channel relative to each 'slow antenna' station determined using the National Lightning Detection Network (NLDN) data, we need a minimum of two slow antenna stations to obtain the channel's vertical extent, Z , and the charge per unit length, q , of the return-stroke channel. For a vertical-leader channel, its actual length, L , is equal to Z .

With the charges distributed in the corona sheath surrounding the current-carrying core of the channel, the maximum radial E -fields in this region do not exceed the electrical breakdown E -field of 3 MV m^{-1} . Mazur and Ruhnke (2002) assumed that the capacitance per unit length of the channel during the return-stroke process is the same as during the leader stage, and is uniform. (This assumption, analyzed in Bazelyan and Raizer (2000, p 173), has been shown to be justifiable.) The capacitance per unit length, c , of the leader channel, approximated as a vertical, thin, long conductor over the ground, with diameter d and length L , is calculated using the formula from Meinke and Gundlach (1956):

$$c = 2\pi\epsilon/\ln(L/d) \quad (11.2)$$

The charge per unit length, q , deposited by the return stroke channel of capacitance per unit length, c , is

$$q = c\Phi \quad (11.3)$$

In order to determine the leader potential Φ using (11.3), we need also to assume an effective diameter, d , of the leader channel.

We arrive at the determination of the diameter, d , of a uniformly charged channel, which should be considered to be the average diameter of the channel during the return-stroke process:

$$d = q/\pi\epsilon_0 3 \times 10^6 \text{ (m)} \quad (11.4)$$

This method of calculating the leader potential Φ , and thus the length of the step of a negatively charged leader, may be implemented for obtaining statistically significant data for the last step-lengths of downward leaders, for a variety of environmental conditions that affect thunderstorms.

Admittedly, the issue of the degree of correlation between the leader's potential and the peak current of the return stroke has not been finally resolved. This correlation may be better estimated from a comparison of the direct measurements of the first return-stroke current at a tall structure (rather than current values from the NLDN data), and the leader-potential values calculated by using the described method of remote measurements of dE_{RS} at the tall structure's location.

The electro-geometric method in lightning protection uses the striking distance d as the radius of the so-called rolling sphere, within which lightning attachment to a ground structure may occur. The volume between the rolling sphere and the structure to be protected is considered to be safe from lightning attachment. The rolling-sphere method, however, cannot account either for the effect of the height of the structure, when the height is greater than the radius of the sphere, or for the presence of a connecting upward leader from the structure.

The deficiency of the rolling-sphere method in using striking distance lies in its weak relationship with the physical attributes of downward lightning leaders of CG flashes. Implementation of the method of calculation of the step-length of the downward negative stepped leader near the ground, described in this chapter, and using step-length as an estimator for the striking distance, could serve as an important refinement in the electro-geometric method.

11.2 A physical model of leader interaction with a ground structure

The models of lightning interaction with ground structures, also called leader-progression models (LPMs), play an important role in the verification of certain assumptions for the design of lightning protection systems. The LPM may help to interpret various behaviors of the downward and connecting leaders under different ambient electrical conditions. The LPM described in Dellera and Garbagnati (1990) attempted to incorporate knowledge of the discharge physics of leader development in long rod-plane gaps, by using the charge-simulation method. Mazur *et al* (2000) applied the same method in a three-dimensional computer model of the interaction between a downward negative stepped leader and a ground structure. This model incorporated the physical processes of the stepped and continuous progression of negative and positive leaders. The objective of the modeling was to determine the

dominant factors that affect development of a downward leader that started a few hundred meters above, and in close proximity to a ground structure (a 20 m tall mast).

In the model, the leader's diameter is the diameter of the envelope of induced charges formed around the thin conducting core. Because the progression of the leader is governed by its potential, the cases of a negative leader of 10 m in diameter with -40 MV potential, and of a leader of 2 m in diameter with -10 MV potential, were considered. The lengths of the downward leader's steps were calculated for each step, based on the magnitude of the leader's potential, the ambient potential distribution ahead of the leader's tip, and using a physically sound criterion for determining the direction of each step, with all parameters changing with the approaching ground. The same approach was implemented for determining the direction and extent of the positive leader in response to the changing ambient potential distribution produced by the approaching downward negatively charged leader.

The results of the modeling in Mazur *et al* (2000) indicated that the critical role in lightning attachment is played by the final jump of the stepping negative leader toward the ground structure, or toward the upward connecting leader (in the case of a stronger negative stepped leader). A weaker negative leader does not intercept the mast, but hits the ground near the mast, without an upward positive connecting leader having been initiated from the mast. This model showed clearly that the major factor in the lightning-attachment process is the potential of the downward leader. It is the downward leader's potential that determines the length of the leader step, and thus, the maximum length of the striking distance.

With the increasing potential Φ as the leader tip approaches the ground, the step length also increases. This trend has also been observed in laboratory-produced negative stepped leaders (Bacchigella *et al* 1994).

The model also indicated that the role of the connecting leader from the structure in the lightning-attachment process is basically secondary, and that the dynamic of the formation of the connecting leader changes with the height of the ground structure. In structures that are tens of meters in height, the connecting leader starts a fraction of a millisecond prior to the attachment, with its speed accelerating, and its rather short channel developing in a primarily vertical direction. In structures that are hundreds of meters in height, because of the enhancement of the E -field at the tip of these taller structures, the connecting leader would start earlier and would, therefore, develop a longer channel (see figure 11.1). The results of the physical model in Mazur *et al* (2000) contradicted the assumption made in LPM by Dellera and Garbagnati (1990) that the negative downward and positive upward leaders gradually converge toward each other.

The same three-dimensional modeling approach, applied to a downward stepped-leader interaction with a 30 m tall radar tower protected by a single lightning rod at the top (Mazur and Ruhnke 2001), has shown that a downward leader with a high potential will hit the lightning rod (see figure 11.2). However, a leader with a much lower potential, occurring at the same distance from the tower as the more powerful

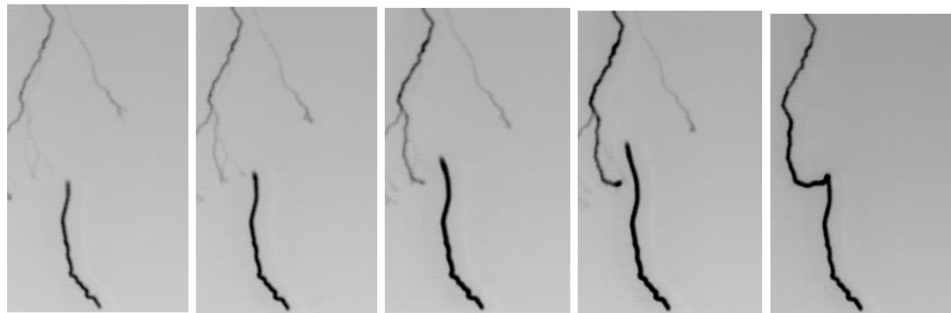


Figure 11.1. Sequence of high-speed video images (10 000 fps) of the lightning-attachment process to a 440 m tall building in Guangzhou, China. The timing of each frame is relative to the attachment time, assumed as zero. The upward connecting leader extended ~350 m above the top of the building, developing in a primarily vertical direction. The attachment jump-over is made by a branch of the downward stepped leader leader. Reproduced from Lu *et al* (2013). Copyright 2013 by John Wiley Sons, Inc. Reprinted by permission of John Wiley & Sons, Inc.

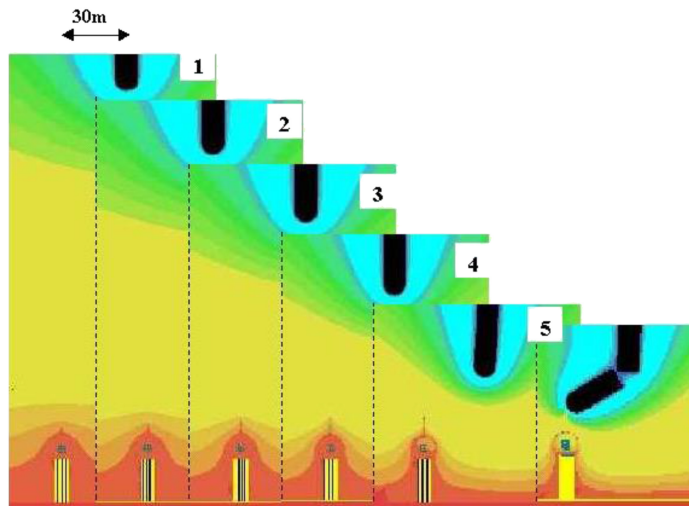


Figure 11.2. Progression of a negative stepped leader of a -40 MV potential towards a radar tower protected with a single vertical rod on top of the radome (superimposition of potential distribution plots in the $Y-Z$ plane). The ground distance between the leader and the lightning rod is 30 m. Step 6 is the jump-over toward the lightning rod on the radome, with a leader step of 38 m. Reprinted from Mazur and Ruhnke (2001).

leader, will completely miss the tower (see figure 11.3), or, when it is closer to the tower, at a distance of 15 m (placing it within the volume of the *cone of protection*), the leader with lower potential may miss the lightning rod and hit the side of the radome instead. The scenarios depicted are frequently observed in lightning interactions with tall structures (see figure 11.4). In the two cases illustrated in figures 11.2 and 11.4, negative leaders react to the presence of the tower by starting to turn toward it just one step before the final jump-over.

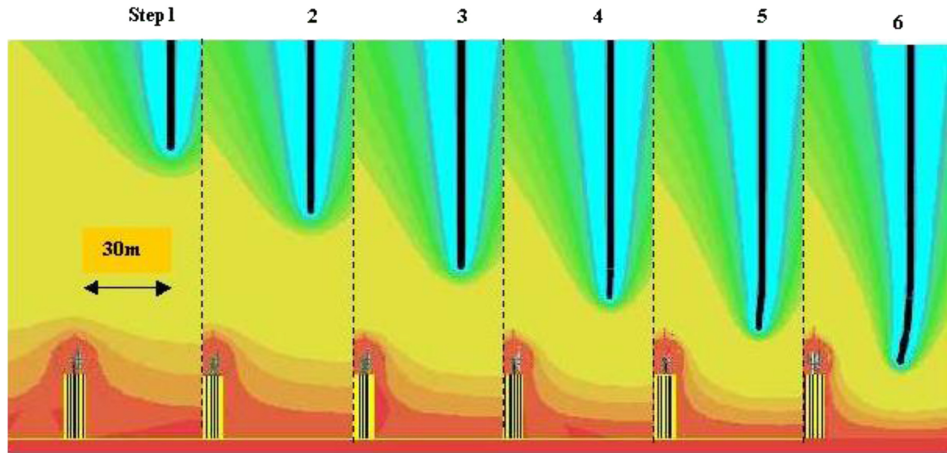


Figure 11.3. Progression of a downward leader of -10 MV potential towards the radome of the radar tower protected by a single vertical lightning rod. After step 4, the leaders had already missed each other, and the negative leader went to the ground. The ground distance between the leader and the lightning rod is 30 m. Reprinted from Mazur and Ruhnke (2001).



Figure 11.4. A CG lightning strike to the Washington Monument in Washington, DC (185 m tall). The connecting upward leader from the top of the monument did not connect with branches of the downward leader, and the lightning attachment occurred at the side of the monument. Courtesy of K Ambrose.

The test for any LPM should be how well the model replicates observed lightning interactions between ground structures and downward leaders of CG flashes. The computer-simulation model in Mazur and Ruhnke (2001), which followed the direction of the physical assessment of negative- and positive-leader development, produced results that passed this test.

11.3 On the hazardous effects of upward lightning to tall structures

All upward lightning flashes belong to the same category of structure-triggered flashes as flashes triggered by the rocket-and-wire techniques, or aircraft-triggered lightning. Obviously, tall structures are more susceptible to lightning strikes than short ones. However, extensive investigations into the nature of lightning attachments to such structures have taken place only during the last two decades. The data obtained show that the probability of upward lightning starting from towers is hundreds of times higher than the probability of strikes to tall towers by natural CG flashes (see chapter 7).

At this time, lightning-detection networks cannot detect upward positively charged leaders, which are the majority of upward lightning initiated at tall structures; therefore, systematically collected data for these flashes do not exist. In upward positively charged leaders, which are the initial (and often the only) stage of upward lightning, the high number of current pulses (M-events) is greater than the typical number of return strokes in multiple CG flashes, and the amplitudes of these pulses are in the range of those found in weak return strokes (Heidler 2002). This is equivalent to each upward leader being like a multiple CG flash with a dozen or more subsequent return strokes. The long-lasting (hundreds of milliseconds) continuing current, with its amplitudes of hundreds of amperes, presents serious fire and metal-melting hazards for any installation located on the tall structure's surface.

In upward negatively charged leaders, the continuing current lasts up to tens of milliseconds, and has amplitudes of tens of kiloamperes. However, the charge transfer by the continuing current for both positively and negatively charged leaders is comparable (Heidler 2002), as are the fire and metal-melting threats for both types of flashes. The fact that upward lightning is understood to be the predominant threat to tall structures demands that the lightning-protection community pay particular attention to the features of these flashes, which are in many ways different from those in CG flashes—the traditional source of lightning threat.

11.4 Sharp-tipped versus blunt-tipped lightning rods

A discussion in the lightning-protection community about which shape of lightning-rod tip is more efficient for attracting a downward-lightning leader has a long history. A conclusive analysis of the physics of the performance of lightning rods with tips of different curvatures was presented in Moore (1983). Experimental evidence of the effectiveness of the blunt versus sharp-pointed tip was obtained in the field experiments described in Moore *et al* (2000). The essence of the arguments for using a blunt-tipped lightning rod, rather than a sharp-tipped one, lies in their disparate abilities to produce a corona discharge, and to form a corona shield near the rod's tip. The curvature of the rod's tip affects the streamer-leader formation from the rod, creating a sort of ‘domino-effect’ of results: the sharper the tip of the rod, the greater the E -field enhancement at the tip, and the greater the corona current, and, thus, the greater the corona space charge near the tip that forms the corona shield, and the stronger the diminishing effect of this corona shield on the ambient E -field.

The issue of the so-called *corona-shielding* arose in designing the rocket-and-wire techniques for triggering lightning, where escaping the corona shield was dependent on a certain speed of the ascending rocket. In the case of a stationary tall structure, the triggering of upward leaders occurs as the result of breaking through the corona shield by the impulse-type electric-field change produced either by an approaching leader, or a return stroke that carries charges of the opposite polarity to that of the upward leader from the lightning rod.

Because of the absence of a space charge produced by the corona discharge in rods with blunt tips, a streamer from such a rod may start earlier than from the elements of a structure protected by a lightning rod with a sharp tip; so, in this case, a lightning rod with a blunt tip would do its job. A lightning rod with a sharp-pointed tip will require a much higher ambient E -field than a blunt-tipped rod to break through the corona shield, in order to initiate corona streamers from its tip; meanwhile, at a lower ambient E -field, corona streamers may start from elements of a structure that is supposed to be protected by a sharp-pointed lightning rod. In this scenario, a lightning rod with a sharp-pointed tip will only protect itself.

The difference in the performances of lightning rods with sharp-pointed versus blunt tips would be even more pronounced in tall vertical rods, because the higher the rod, the easier it is to achieve the critical electric field needed for propagation of the streamers.

11.5 Lightning protection of aircraft

Until about 30 years ago, lightning protection was never a serious worry for a flying aircraft made of a fully metallic body (the equivalent of a Faraday cage), as long as its body had no existing passage to allow a lightning current to progress to the fuel tank. The only non-metallic part on a contemporary commercial aircraft was a fiberglass radome covering the aircraft's navigational radar, which was effectively protected from lightning damage by the conducting diverter's strips. The diverter's strips formed a semi-open Faraday cage, which did not interfere with the aircraft's radar function. With the composite materials introduced in the 1980s to build certain parts of a modern aircraft, and the high sensitivity to lightning transients of the new low-voltage electronics used in the 'fly-by-wire' technology, the need arose to carefully evaluate the lightning hazards to these modern aircraft, prompting important, extensive research programs and investigations into lightning-aircraft interaction (see chapter 4). The main objective of all the in-flight programs on lightning-aircraft interaction has been to determine the critical values of the various parameters of lightning that affect the aircraft; the results of these investigations would be considered and utilized in the design and testing of the lightning protection of sensitive on-board electronic equipment and structures made of composite material.

The majority of lightning flashes triggered by an aircraft develop in the cloud as IC flashes, with the aircraft a part of the lightning channel. The current records of these flashes (see figure 4.7) have a DC-type continuing current of several hundreds of amperes lasting several hundreds of milliseconds, during which time the lightning

channel stays attached to the aircraft at two, often opposite, extremities (e.g. wing-tips and tail section), and is ‘dragged’ by the aircraft. A continuous current of the magnitude that dwells at an attachment-point for hundreds of milliseconds would melt the aluminum skin, or, in the case of a skin made of a composite material, would, by its intense heat, burst a large area of fiberglass layers. It has been learned that even the application of a layer of conducting mesh in the composite structure does not always provide effective protection for a skin made of composite material from such extensive damage, and repairs of this damage are expensive.

Aircraft-triggered lightning strikes occur in an electrified cloud, such as those found in active summer and winter thunderstorms, as well as in decaying thunderstorms and marginally electrified clouds that do not exhibit lightning activity. While an aircraft should, of course, avoid active thunderstorms, there are no existing remote methods of warning an aircraft about a marginally electrified cloud. An alternative is to identify such clouds by an onboard electric-field sensor, or by detecting the stage of the aircraft’s transformation into an electrical dipole; this stage precedes the initiation of a bidirectional leader from the aircraft.

When aircraft-triggered lightning develops as an IC type flash (usually at flying altitudes above 7 km), the current will have superimposed current pulses of M-events with amplitudes in a few tens of kilo-amperes, in addition to the DC-type current (Mazur 1993). When flying at altitudes below 7 km, the aircraft may initiate a bidirectional and bipolar leader, one part of which would propagate toward the ground and produce a CG flash with its return stroke striking the aircraft (Mazur *et al* 1990). (Video images of a multi-stroke CG flash triggered by an aircraft during takeoff are shown in figure 4.7.)

In lightning protection practice, the amplitude of the return strokes of the CG flashes is assessed from measurements on the ground, where this amplitude is at its maximum value. However, the return-stroke current diminishes with the increasing length of the lightning channel above the ground. The variation of the return-stroke’s current amplitude with altitude is inferred from the measurements of channel-luminosity that changes with height, because there is a strong positive correlation between return-stroke current and channel luminosity (Idone and Orville 1985). Judging from the rapid decrease in luminosity of return-stroke channels in time, at different heights above ground, it is to be expected that the return stroke’s peak amplitude will also be considerably smaller than that measured at the ground. The reasons for the diminishment of return-stroke current with height are the decreasing speed of propagation with height (Idone and Orville 1982) and the losses in the extended channel. These are the factors that bring the amplitude of the return stroke into the range of values of current pulses produced by M-events during lightning attachment to an aircraft; that is, into the range of tens of kiloamperes, rather than hundreds of kiloamperes, which is the maximum value measured in return strokes on the ground.

There are no statistically significant data for the current values of CG flashes triggered by aircraft, because gathering them is very difficult, and there are no dedicated efforts to address this issue. However, a consideration of their possible

amplitudes, as presented here, nevertheless represents a realistic picture of the lightning–aircraft interaction during a CG flash that affects an aircraft.

References

- Bacchigia G L, Gazzani A, Bernardi M, Gallimberti I and Bondiou A 1994 Theoretical modeling of the laboratory negative stepped leader *Proc. Int. Aerospace and Ground Conf. on Lightning and Static Electricity (Mannheim, Germany)* pp 13–22
- Bazelyan E and Raizer Yu 2000 *Lightning Physics and Lightning Protection* (Bristol: Institute of Physics Publishing)
- Dellera L and Garbagnati E 1990 Lightning stroke simulation by means of the leader progression model, 1. Description of the model and evaluation of exposure of free standing structure *IEEE Trans. Power Deliv.* **5** 2009–17
- Heidler F 2002 Lightning current measurements at the Peissenberg telecommunication tower *Proc. Int. Conf. on Grounding and Earthing, GROUND'2002 (November 4–7, Rio de Janeiro, Brazil)* pp 117–22
- Idone V R and Orville R E 1982 Lightning return stroke velocities in the Thunderstorm Research International Program (TRIP) *J. Geophys. Res.* **87** 4903–15
- Idone V P and Orville R E 1985 Correlated peak relative light intensity and peak current in triggered lightning subsequent return strokes *J. Geophys. Res.* **90** 6159–64
- Lu. W, Chen L, Ma Y, Rakov V A, Gao Y, Zhang Y, Yin Q and Zhang Y 2013 Lightning attachment process involving connection of the downward negative leader to the lateral surface of the upward connecting leader *Geophys. Res. Lett.* **40** 5531–5
- Mazur V, Fisher B D and Brown P W 1990 Multistroke cloud-to-ground strike to the NASA F-106B airplane *J. Geophys. Res.* **95** 5471–84
- Mazur V 1993 Lightning threat to aircraft: do we know all we need to know? *J. Aircraft* **30** 156–9
- Mazur V, Ruhnke L H, Bondiou-Clergerie A and Lalande P 2000 Computer simulation of a downward negative stepped leader and its interaction with a ground structure *J. Geophys. Res.* **105** 22361–9
- Mazur V and Ruhnke L H 2001 Evaluation of the lightning protection system at the WSR-88D radar sites *Final report, NOAA/National Severe Storms Laboratory*
- Mazur V and Ruhnke L H 2002 Determining leader potential in cloud-to-ground flashes *Geophys. Res. Lett.* **29** 1601
- Meinke H and Gundlach F W 1956 *Taschenbuch der Hochfrequenztechnik* (New York: Springer) p 52
- Moore C B 1983 Improved configurations of lightning rods and air terminals *J. Franklin Inst.* **315** 61–85
- Moore C B, Aulich G D and Rison W 2000 Measurement of lightning rod response to nearby strikes *Geophys. Res. Lett.* **11** 1487–90
- Mousa A 2016 Personal communication
- Uman M A 2008 *The Art and Science of Lightning Protection* (Cambridge: Cambridge University Press)
- Young F S, Clayton J M and Hileman A R 1963 Shielding of transmission lines *IEEE Trans. Power Apparatus Syst.* **S82** 132–54

Principles of Lightning Physics

Vladislav Mazur

Chapter 12

Lightning initiation—the most difficult issue of lightning physics

12.1 Hydrometeor theory of lightning initiation

The fundamental question of lightning physics, how lightning initiates inside thunderstorms, has remained unanswered, despite the tremendous progress achieved in recent years in lightning research that has led to an understanding of many other physical processes in lightning discharges. In researching this issue, there is no real possibility to obtain either *in situ* measurements of environmental and electrical characteristics in regions of the electrified cloud where lightning leaders form, or a realistic reproduction in a laboratory of the environmental conditions and processes of leader formation. Without these capabilities any suggested hypothesis would be just an unconfirmed speculation about factors and relationships contributing to this phenomenon. Nevertheless, the researching and testing of multiple assumptions relevant to lightning initiation has been proven to be relevant to the interpretation of various observations of the lightning initiation phenomenon and thus, to solving this mystery.

There are only two rather vague hypotheses that attempt to explain lightning initiation in thunderstorms. The first and oldest hypothesis, the ‘hydrometeor theory’, considers hydrometeors in the cloud region of a high electric field as the potential nuclei, from which a lightning leader emerges; this hypothesis, however, does not specify the entire mechanism of the leader initiation process. The hydrometeor theory seems intuitively logical, because the interaction between hydrometeors during storm development produces the electrification mechanism, and this mechanism generates space charges in the cloud and, thus, the ambient electric field necessary for the electrical breakdown. However, a confirmation of the hydrometeor theory of lightning initiation by means of *in situ* measurements does not seem realistic. Instead, lightning researchers during the last four decades have addressed, primarily in laboratory experiments, several issues associated with the

role of hydrometeors in lightning initiation. These experiments have been focused primarily on investigations of corona streamer formation on hydrometeors of different types, in conditions resembling those inside the cloud, which were reproduced in small environmental chambers (e.g. Griffiths and Latham 1974, Coquillat *et al* 1995, Petersen *et al* 2014). Griffiths and Latham (1974) concluded that the lowest temperature possible for streamer formation on a frozen particle, the so-called ‘reversal temperature’, is about -20°C . This meant that lightning initiation is impossible in the upper, coldest parts of thunderstorms. Later on, however, Latham (2003) expressed certain reservations about their earlier study, and suggested revisiting this issue in new settings of laboratory experiments.

Field observations of the locations in which lightning originates in storms, conducted with both the time-of-arrival technique and interferometers for mapping lightning-radiation sources (see, e.g., Proctor 1991, Shao and Krehbiel 1996), show that lightning initiation has actually been observed primarily in three thunderstorm regions, centered roughly at -10°C , -20°C , and -40°C . Two of these three regions have temperatures cooler than ‘reversal temperature’.

In laboratory investigations of streamer formation from simulated ice particles, Petersen *et al* (2006) and Petersen *et al* (2014) found that streamers from ice particles in laboratory experiments occur at temperatures as low as -38°C , basically confirming the findings from lightning-radiation source mapping referred to above.

Despite the differences in the environmental and electrical conditions in all three storm regions where most lightning flashes initiate, the common types of hydrometeors found there are ice particles, either graupel or hail, or ice crystals, or mixtures of these. Thunderstorm observations with dual-polarization radar have shown that in severe (lightning-producing) thunderstorms, hail particles prevail above the altitude of 5 km to the top; below that level, they are mixed with rain (Zrnic *et al* 2000). The overwhelming evidence from these studies points to ice particles as the most probable types of hydrometeors associated with lightning initiation in all regions of the storms. Still unknown is the mechanism by which a lightning leader emerges from a high electric field region that is populated by various ice particles.

The ability of corona streamers to start on individual hydrometeors in the ambient electric field is affected by the field-enhancement factor of a particle’s shape (e.g. for a spherical particle, this factor is 3) that magnifies the ambient electric field on the surface of the particle. However, hydrometeors with shapes that can create significant high field enhancements are rarely found among frozen hydrometeors. In order to create the multitude of streamers necessary for the streamer-leader transition, the electric field at the particle surface should be two orders of magnitude higher than the internal field of the particle (Lalande *et al* 2002). This condition cannot be met in ice particles; therefore, a streamer-leader transition started on a single ice particle would seem to be unrealistic.

Realization of such impossibility has led to the hypothesis by Nguyen and Michnovsky (1996) of the streamer-leader transition being a result of electrical interactions between hydrometeors in closely spaced clusters of such particles in a high electric field region. Indeed, hydrometeors in the cloud may appear in closely

spaced clusters of particles of similar sizes (e.g. ice crystals), or of mixed sizes (e.g. hail and graupel). Gardner *et al* (1985) reported, from airborne measurements in summer thunderstorms, that graupels ‘in sizes from $< 100 \mu\text{m}$ to $> 1 \text{ mm}$, are in total concentrations ranging from 2 to 40 L⁻¹.’ From measurements with a sailplane, at altitudes from 7 to 9 km and radar reflectivity from 20 to 45 dBZ, Dye *et al* (1986) reported that ‘as the cloud evolves to a mature stage of microphysical development, the total ice particle concentration can increase up to several hundred per liter.’ The observations by Gardner *et al* (1985) and Dye *et al* (1986) support the assumption of the existence of close clusters of hydrometeors in electrified clouds, although, to our knowledge, there are no *in situ* measurements of hydrometeor sizes and their concentration in the regions of lightning initiation in thunderstorms. To conduct such measurements would be far too dangerous for any flying platform with on-board sensors.

In order to test the effects of a dense array of hydrometeors on the process of leader formation in high-voltage laboratory experiments, researchers must consider two interrelated aspects of the hydrometeor theory. The first, the microphysical or environmental aspect, should answer the following questions. (1) What are the realistic sizes, types, and concentration of hydrometeors involved in lightning initiation? (2) What are the ambient electric fields required for leader initiation to occur in the ambient environmental conditions of thunderstorms? The second aspect of the hydrometeor theory, the electrical one, concerns the physical mechanism for transition from corona streamers, started either on a single hydrometeor, or on a group of hydrometeors, to a leader that subsequently becomes a lightning flash. An expectation that the interaction between particles in closely spaced clusters may occur in a lesser ambient electric field than that needed for electrical breakdown from a single particle, gave rise to the idea of an experiment in a uniform electric field in a high-voltage laboratory (Mazur *et al* 2015).

In this experiment, a laboratory simulation for the initiation of an electrodeless discharge from an array of particles has been created, by using an array of conducting particles (balls) in a high-voltage environment. Placed in an ambient *E*-field that was sufficient to start breakdown on a single conducting particle, the array of particles became a charged body, from which, predictably, the bidirectional and bipolar leader developed. The size of the array (the number of balls) affected both the duration of the discharge and the magnitude of the arc current to the electrodes. With each successively greater number of particles in the array, the duration of the discharge became shorter, and the current value increased. This first of this kind and rather limited experiment, however, was not able to isolate the influence of the *shape* of the array from its *size*, on the parameters of the discharge. Conducting additional experiments with arrays of simulated hydrometeors in a high-voltage facility, although overall quite complex, could be fruitful in uncovering the mechanism of streamer-leader transition from the cluster of particles in an ambient electric field. A computer simulation could be another venue for addressing the questions about the role of the dense cluster of hydrometeors of leader formation.

In trying to solve the mystery of lightning initiation by hydrometeors, the hypothesis that should to be tested is whether an array of particles can behave as the equivalent of a single large, weakly conductive and weakly charged body of corona streamers from the particles, which would have a total electric field enhancement factor significantly greater than that of any individual particle. This charged volume may serve as the nucleus from which a bidirectional, bipolar leader initiation in a strong ambient electric field may occur.

12.2 The runaway theory of lightning initiation

The second hypothesis of lightning initiation, introduced in Gurevich *et al* (1992) and Roussel-Dupre *et al* (1993), suggested that cosmic rays initiate a relativistic runaway electron avalanche breakdown (RREA) that somehow leads to the initiation of a lightning leader. This hypothesis was put forward as a possible explanation of the x-ray and gamma-ray emissions detected in thunderstorms by air- and balloon-borne measurements (Parks *et al* 1981, McCarthy and Parks 1985). However, observations of gamma-ray radiation in thunderstorms (Eack *et al* 1996, Moore *et al* 2001) and in a high-voltage laboratory (Kochkin *et al* 2015) suggest that this radiation, which may indicate the presence of runaway electrons, can be produced by lightning leaders approaching the ground and in the high-voltage laboratory, rather than being associated with the initiation phase of lightning.

The proponents of the ‘runaway electron theory’ of lightning initiation assumed that ‘at the onset of lightning, the RREA breakdown should generate a few-megahertz bipolar radio pulse lasting about $0.5\ \mu s$ ’ (Gurevich and Zybin 2005), which fits the description of the narrow bipolar events (NBEs) in thunderstorms. An NBE that is characterized by very strong VHF radiation and short-duration bipolar sferic waveforms was first reported in the literature in the 1980s (Le Vine 1980, Willett *et al* 1989).

The testing of the ‘runaway electrons theory’ of lightning initiation in a laboratory is unrealistic, because the runaway mechanism would require breakdown electric fields over distances of up to several kilometers in order to accelerate the electrons to the condition of a runaway avalanche. The same consideration makes doubtful the occurrence of RREA in rather small cloud regions (of a few hundreds of meters) where lightning leaders initiate.

The introduction of the ‘runaway electrons theory’ stimulated a powerful surge in the research of high-energy atmospheric physics conducted with complex field programs, and with the development of computer-simulated models. These research efforts resulted in tremendous progress towards understanding high-energy atmospheric phenomena (Dwyer and Uman 2014), but they have only confirmed a *consequential* relationship with the lightning processes, and characterized the runaway electron phenomenon as the end-result of lightning development, rather than as the cause of lightning occurrence. So far, there are no observational data to definitely support the involvement of any high-energy processes (runaway electrons, x-rays, or gamma rays) in lightning initiation. In spite of this, the attempt to keep this hypothesis alive continues, with it possibly being involved in explaining the

occurrence of high ambient electric field values in the regions of leader formation, as a part of the combination of two hypotheses. Petersen *et al* (2008) proposed a hybrid mechanism that involved RREAs providing the enhancement of the ambient electric field to a level sufficient for hydrometeor-initiated positive streamer formation from ice particles. Similarly, Dubinova *et al* (2015) attempted to combine the effects of the enhancement of the ambient electric field by elongated ice particles of centimeter size, and the presence of a sufficiently high number of free electrons provided by RREAs in air showers, as possibly leading to the formation of positive streamers from the ice particles.

12.3 Evidence supporting the hydrometeor theory of lightning initiation

If cosmic rays that energize the runaway electron processes are not involved in lightning initiation, then the only other processes that lead to lightning initiation must, of necessity, be related to hydrometeors. The convincing and conclusive evidence of the nature of lightning initiation as a process involving hydrometeors has been obtained quite recently by Rison *et al* (2016) from the analysis of observations of NBEs whose occurrence usually coincides with the initiation of IC flashes.

The nature of NBEs, as well as their relation to the stages of leader formation, continued to be puzzling for many years. A breakthrough came from the lucky occurrence of a small thunderstorm near the Langmuir Laboratory in New Mexico, close to an area with multiple observational systems ready for operation by a team of researchers from the New Mexico Institute of Mining and Technology who had been focusing on resolving the mystery of lightning initiation for years. A very meticulous and comprehensive analysis of remote measurements of NBEs from observations with a three-dimensional LMA, a high-speed broadband interferometer, and an electric field measuring system, combined with sferic computer simulations, produced convincing evidence for interpretation of the nature of NBEs and their role in lightning initiation. The following is a summary of the essential results of these remarkable observations and the analysis presented in Rison *et al* (2016).

- The NBE is a breakdown of positive polarity that occurs in a cloud between the upper positive and mid-level negative space charge region of the thunderstorm, and is directed downward.
- The NBE breakdown is characterized by currents of several tens of kiloamperes, but by a relatively small charge transfer, usually less than 1.0 C, and by the duration of a few μs . This observation has led to the following conclusion: the NBE is produced by a system made of a volume of positive streamers propagating with unusually high speed (10^7 m s^{-1}), thus resulting in current of huge amplitude that is spread over some cross-sectional area as a volume-current density. Therefore, the NBE breakdown *does not produce a conducting channel*, in contrast to the multitude of positive streamers that focus on the tip of a conducting leader channel, and forms a new part of the leader channel.

- The basic process of the positive breakdown associated with NBEs has been predicted by Griffiths and Phelps (1976), who showed, using a computer-simulated model based on laboratory studies of corona streamers, that *repeated and overlapping positive streamers* from hydrometeors will become self-intensifying in strong ambient electric fields. It is expected that the occurrence of positive breakdowns takes place prior to any stepped event produced by negative breakdowns, because the minimum breakdown electric field for positive streamers is much less than that for negative stepped breakdowns (about half).
- Observations of NBEs suggest that the conversion of some of the downward fast positive breakdown into slow positive leaders takes place as the NBE dies out.

The substantial difference between the positive corona streamers in the NBE and those in the corona streamer zone ahead of a developing positively charged leader is, first, in the volumes occupied by the corona streamers and, second, in the speeds of propagation of the streamer zone. The positively charged leader develops with a speed of $\sim 10^5 \text{ m s}^{-1}$, while the speed of NBEs exceeds 10^7 m s^{-1} . The combination of a huge volume with positive streamers, and the very high speed of their propagation, all within a microsecond's time interval, results in the current pulse of the NBEs having a peak current of tens of kiloamperes and a powerful VHF signal. On the other hand, positive corona streamers, ahead of the leaders, sum up their currents into a leader current (at the leader's tip) that does not exceed several hundreds of amperes. These streamers ahead of the leader develop continuously, which produces no radiation in VHF. Both types of positive breakdowns, in NBEs and in positively charged leaders, have low luminosity due to the spatial separation of individual streamers, each carrying a very low current, in microamperes.

Another known type of positive breakdown that produces strong radiation in VHF occurs when the return stroke of a negative CG flash reaches the upper (positively charged) tip of a bidirectional downward leader of a CG flash (Shao *et al* 1995). This brings the near-ground potential of the return stroke channel to the direct proximity of the much greater ambient cloud potential, leading to a very high electric field between the return stroke channel and the cloud environment, and to a powerful breakdown that is followed by formation of the new conducting channel of the positive leader. The development of this leader will be characterized by a slow positive breakdown in the streamer zone ahead of it. The transition in this case from powerful initial breakdown, radiating in VHF and detected with the lightning mapping system, into a conducting, positively charged leader, with radiation not detectable in VHF, is quite similar to the transition from NBEs into the conducting, positively charged leader channel observed by Rison *et al* (2016). While the positive breakdown ahead of the developing leader requires an ambient field of $\sim 500 \text{ kV m}^{-1}$, the ambient field that leads to a powerful breakdown at the upper tip of the return stroke reaching the cloud could be in tens of megavolts per meter.

When the positive steamer system of NBEs emerges from a volume of hydrometeors with an ambient E -field sufficient to produce positive breakdown, the charges remaining in this volume become negative, so the net charge of the total volume including NBEs is preserved (see the sketch in figure 12.1(a)). With repeated and overlapping progression of NBEs, the volume of their origin becomes more and more negatively charged, so the electric field at the edge of this volume increases to a value sufficient to produce a negative breakdown. This breakdown occurs as a sequence of stepped events well detected by the LMA as propagating upward (see figure 12.1(b)).

The negative breakdowns of stepping events are associated with successive episodes of the enhanced VHF and electric field perturbations registered by the interferometer and a fast antenna. Such occurrences are typical of the negative breakdowns at the beginning of IC (and CG) flashes, and are identified as ‘initial breakdown pulses’.

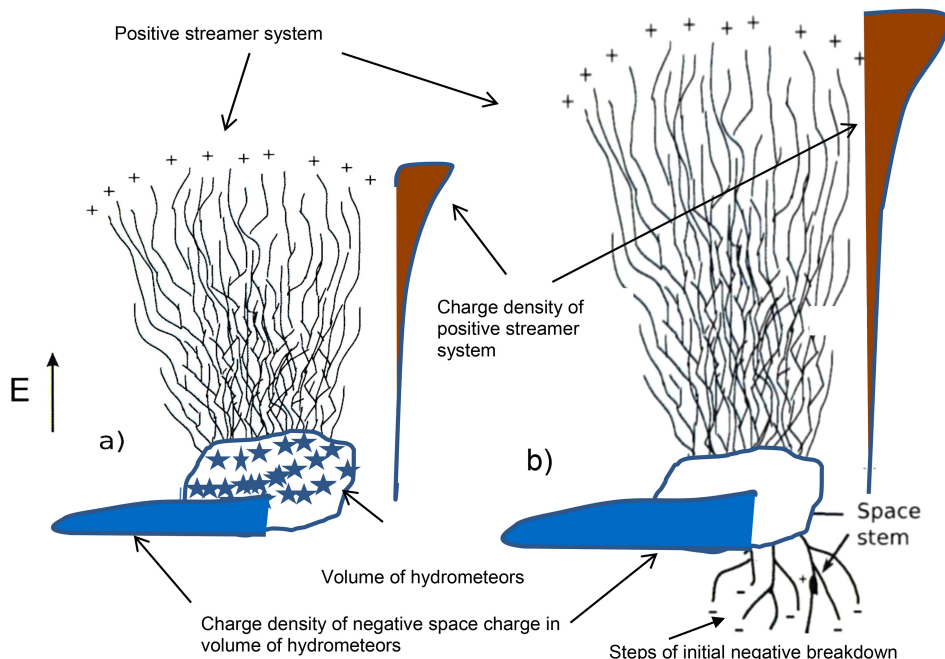


Figure 12.1. Hypothetical schematic of two stages of lightning leader initiation started by narrow bipolar events. (a) Formation of positive breakdown (NBEs) as a system of very fast positive streamers from a volume of hydrometeors. The charges of positive streamers are mainly at their tips. The origin of the extending positive streamer system while being depleted of positive charges becomes negatively charged. The net charge of the positive streamer system plus the volume of hydrometeors remains the same as before occurrence of NBEs due to conservation of the net charge in any electrodeless discharges. (b) Formation of the bidirectional and bipolar leader. With continuously developing positive breakdown by NBEs, and increasing charges of the positive streamer system, the negative charge in the volume of hydrometeors increases and the electric field at the edge of this volume reaches the level sufficient to start a negative breakdown identified as a stepped-type formation. The concept of this sketch was adapted from figure 8 in Petersen *et al* (2008), a hypothetical schematic of initial lightning leader formation from a single hydrometeor.

The fast positive breakdowns of the NBEs followed by the negative initial breakdown pulses initiate the formation of the electrodeless bidirectional leader in a region of a strong ambient electric field. Similar dynamics of leader formation, but occurring from a large nucleus such as an aircraft, takes place during triggered lightning by a flying aircraft (Mazur 1989). This similarity confirms authoritatively the validity of the concept of the bidirectional and bipolar leader, by Kasemir (1950), as the key mechanism of lightning leader development.

The observations of CG flashes by Rison *et al* (2016) also showed a remarkable resemblance of the lightning initiation processes there to those in IC flashes, with the only difference lying in the locations of space-charge regions in the thunderstorm for each type of flash and the directions of propagation of the positive breakdowns of NBEs (upward in CG flashes and downward in IC flashes). The results presented in Rison *et al* (2016) clearly indicate that it is possible that fast positive breakdown, occurring with a wide range of VHF strengths and sferic amplitudes, initiates all lightning flashes in storms.

Very importantly, the analysis of observations in Rison *et al* (2016) found *no evidence of the involvement of energetic electron avalanches in the leader initiation process*, either in the intensification of the electric field before NBEs, or in causing the NBEs themselves. The occurrences of short-duration precursor discharges in storms serve as sensitive detectors of locally strong electric field regions where NBEs may occur.

Positive breakdowns that produce NBEs appear within the boundary of the thundercloud, i.e. in the presence of hydrometeors, and because NBEs involve a huge number of fast positive streamers occupying a large volume, they cannot originate from a single hydrometeor. The unique results summarized here were obtained by means of remote sensing, without actual *in situ* measurements of the ambient electric field. They constitute the strongest evidence to date against the ‘runaway electrons theory’ of lightning initiation, confirming the validity of the hydrometeor theory of lightning initiation.

References

- Coquillat S, Chauzy S and Medale J C 1995 Micro discharges between ice particles *J. Geophys. Res.* **100** 14327–34
- Dubinova A, Rutjes C, Ebert U, Buitink S, Scholten O and Trinh T N G 2015 Prediction of lightning inception by large ice particles and extensive air showers *Phys. Rev. Lett.* **115** 015002
- Dye J E, Johnes J J, Winn W P, Cerni T A, Gardener B, Lamb D, Pitter R L, Hallett J and Saunders C P R 1986 Early electrification and precipitation development in a small isolated Montana cumulonimbus *J. Geophys. Res.* **91** 1231–247
- Dwyer J R and Uman M A 2014 The physics of lightning *Phys. Rep.* **534** 147–241
- Eack K B, Beasley W H, Rust W D, Marshall T C and Stolzenburg M 1996 Initial results from simultaneous observations of x-rays and electric fields in a thunderstorm *J. Geophys. Res.* **101** 29637–40
- Gardher B, Lame D, Pitter R L and Hallett J 1985 Measurements of initial potential gradient and particle charges in a Montana summer thunderstorm *J. Geophys. Res.* **90** 6079–86

- Griffiths R F and Latham J 1974 Electrical corona from ice hydrometeors *Q. J. R. Meteorol. Soc.* **100** 163–80
- Griffiths R F and Phelps C T 1976 A model of lightning initiation arising from positive corona streamer development *J. Geophys. Res.* **81** 3671–6
- Gurevich A V, Zybin K P and Roussel-Dupre R A 1992 Runaway electron mechanism of air breakdown and preconditioning during a thunderstorm *Phys. Lett. A* **165** 463–8
- Gurevich A V and Zybin May K P 2005 Runaway breakdown and the mysteries of lightning *Phys. Today* May 37–43
- Kasemir H W 1950 Qualitative Uebersicht ueber Potential-, Feld-, und Ladungsverhaltnisse bei einer Blitzentladung in der Gewitterwolke *Das Gewitter* ed H Israel (Leipzig: Akademische Verlagsgesellschaft)
- Mazur H and Ruhnke L H (ed) 2013 *Heinz Wolfram Kasemir: His Collected Works* (New York: Wiley) pp 398–411 (Engl. transl.)
- Kochkin P O, van Deursen A P J and Ebert U 2015 Experimental study on hard x-rays emitted from meter-scale negative discharges in air *J. Phys. D: Appl. Phys.* **40** 025205
- Lalande P, Bondiou-Clergerie A, Gallimberti I and Bacchigia G L 2002 Observations and modeling of lightning leaders *C. R. Physique* **3** 1375–92
- Latham J 2003 Personal communication
- Le Vine D M 1980 Sources of the strongest RP radiation from lightning *J. Geophys. Res.* **85** 4091–5
- McCarthy M and Parks G K 1985 Further observations of x-rays inside thunderstorms *Geophys. Res. Lett.* **12** 393–6
- Mazur V 1989 A physical model of lightning initiation on aircraft in thunderstorms *J. Geophys. Res.* **94** 3326–40
- Mazur V, Taylor C D and Petersen D A 2015 Simulating electrodeless discharge from a hydrometeor array *J. Geophys. Res.* **120** 10879–89
- Moore C B, Eack K B, Aulich G D and Rison W 2001 Energetic radiation associated with lightning stepped-leaders *Geophys. Res. Lett.* **28** 2141–4
- Nguyen M D and Michnovsky S 1996 On the initiation of lightning discharge in a cloud, 2. The lightning initiation on precipitation particles *J. Geophys. Res.* **101** 26675–80
- Parks G K, Mauk B, Spiger B and Chin J 1981 X-ray enhancements detected during thunderstorm and lightning activity *Geophys. Res. Lett.* **8** 1176–9
- Petersen D, Bailey M, Hallett J and Beasley W 2006 Laboratory investigation of positive streamer discharges from simulated ice hydrometeors *Q. J. R. Meteorol. Soc.* **132** 263–273
- Petersen D, Bailey M, Beasley W and Hallett J 2008 A brief review of the problem of lightning initiation and a hypothesis of initial lightning leader formation *J. Geophys. Res.* **113** D17205
- Petersen D, Bailey M, Hallett J and Beasley W 2014 Laboratory investigation of corona initiation by ice crystals and its importance to lightning *Q. J. R. Meteorol. Soc.* **141** 987–1478
- Proctor D E 1991 Regions where lightning flashes begin *J. Geophys. Res.* **96** 5099–112
- Rison W, Krehbiel P R, Stock M G, Edens H E, Shao X-M, Thomas R J, Stanley M A and Zhang Y 2016 Observations of narrow bipolar events reveal how lightning is initiated in thunderstorms *Nat. Commun.* **7** 10721
- Roussel-Dupre R A, Gurevich A V, Tunnell T and Milikh G M 1993 Kinetic theory of runaway air breakdown and the implications for lightning initiation *Los Alamos National Laboratory Report LA-12601-MS*
- Shao X M, Krehbiel P R, Thomas R R J and Rison W 1995 Radio interferometric observations of cloud-to-ground lightning phenomena in Florida *J. Geophys. Res.* **100** 2749–83

- Shao X M and Krehbiel P R 1996 The spatial and temporal development of intracloud lightning
J. Geophys. Res. **101** 26641–68
- Willett J C, Bailey J C and Krider E P 1989 A class of unusual lightning electric field waveforms
with very strong high-frequency radiation *J. Geophys. Res.* **94** 16255–67
- Zrnic D S, Ryzhkov A, Straka J, Liu Y and Vivekanandan J 2000 Testing a procedure for
automatic classification of hydrometeor types *J. Atmos. Oceanic Technol.* **18** 892–93

Appendix

Video images for selected chapters

Chapter 1



Figure A.1. The development of a positively-charged downward leader, recorded at a speed of 50 000 fps. Courtesy of Dan Petersen.

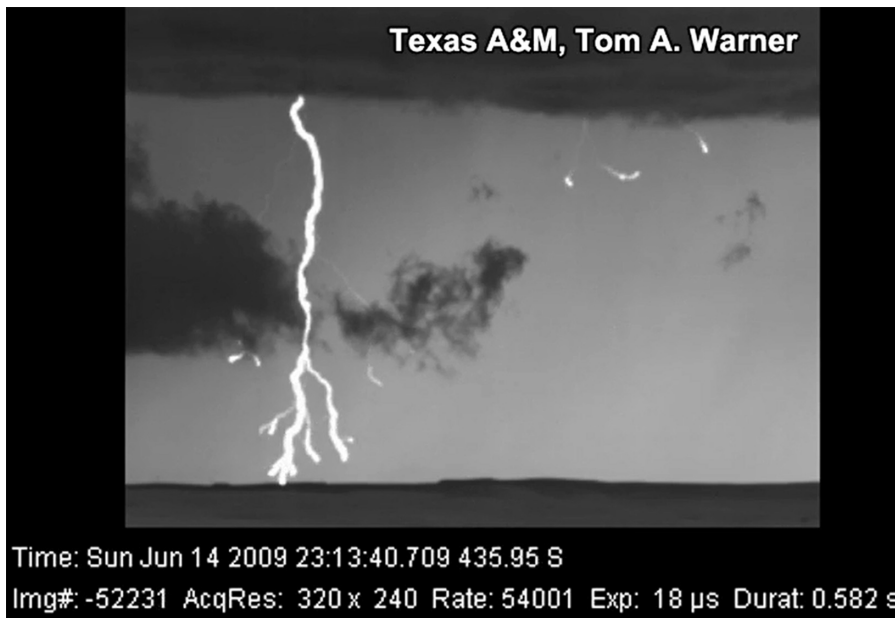


Figure A.2. The development of a negatively-charged downward leader, recorded at a speed of 54 000 fps. Courtesy of T A Warner.

Chapter 4

These four videos (courtesy of NASA) depict the development of a lightning strike triggered by the NASA F-106B research aircraft. The video images of this flash were recorded with four conventional video cameras: two cameras were installed in the cockpit, one behind the pilot, facing the nose boom; the other in front of the board engineer, facing aft. The third camera, mounted on the left wing, viewed the fuselage, including the nose boom. The fourth camera was placed on the top of the cockpit, looking upward, to obtain an image of the lightning channel at close range.



Figure A.3. Lightning initiates at the first attachment-point on the nose boom of the aircraft, and the channel sweeps aft along the cockpit, toward the vertical stabilizer. Courtesy of NASA.



Figure A.4. Lightning initiates at the second attachment point, on the right wing-tip, staying attached there, while the lightning channel sweeps aft from the first attachment-point, and becomes attached to the vertical stabilizer. Courtesy of NASA.



Figure A.5. Progression of the lightning channel along the fuselage from the first attachment-point at the nose boom, towards the tail. A reflection of the lightning channel is seen from the surface of the left wing. Courtesy of NASA.



Figure A.6. The lightning channel is seen at close range as it sweeps along the fuselage. The twisted rope-like structure of the channel is clearly visible. Courtesy of NASA.

Chapter 7

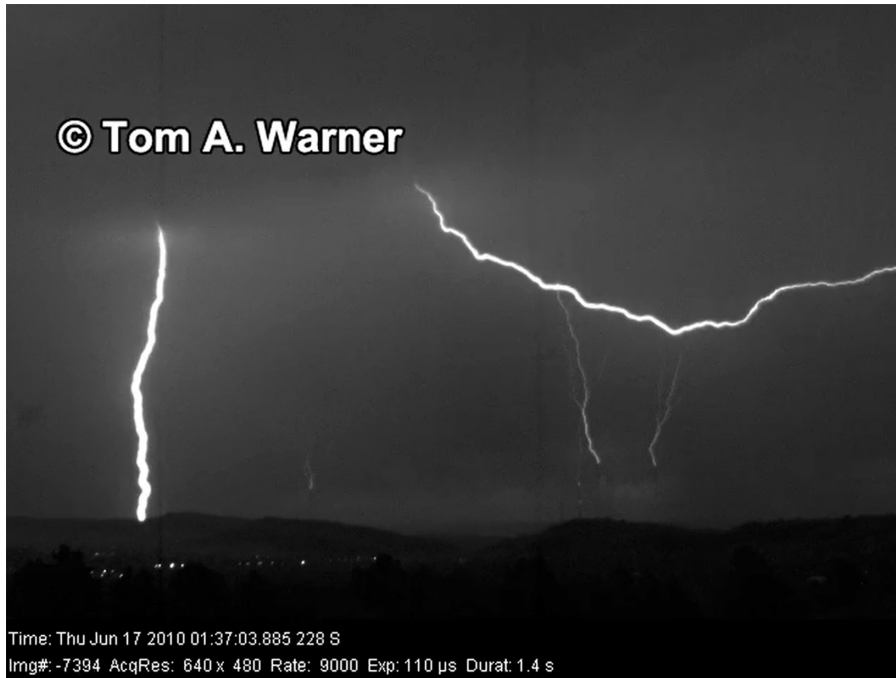


Figure A.7. Upward positive-charged leaders from three tall towers that were triggered by a positive CG flash nearby. A long positively-charged leader slowly passing the foreground is a part of the downward leader structure that produced the positive CG flash. Courtesy of T A Warner.

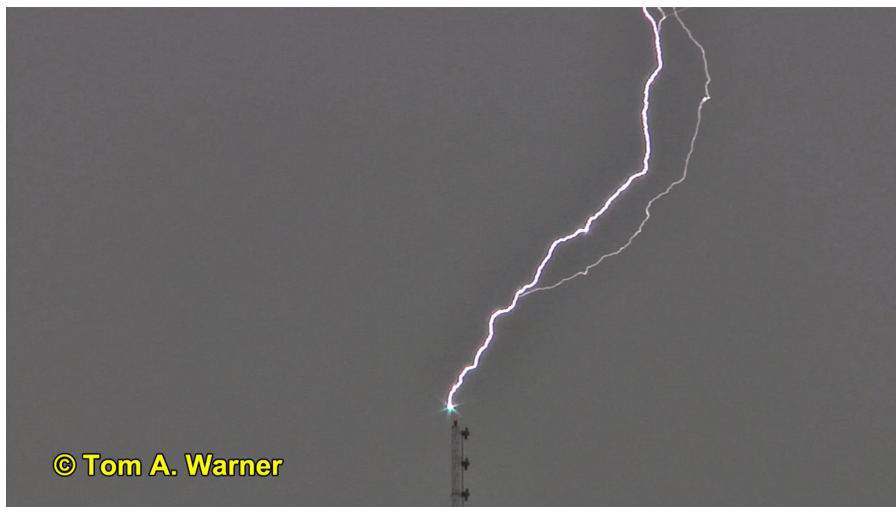


Figure A.8. A close-up high-speed video recording of the upward positively-charged leader from the top of a tall tower. Courtesy of T A Warner.

Chapter 8



Figure A.9. The unbranched positively-charged leader from a tall tower, triggered by a nearby positive CG flash. Notice the slowly-changing luminosity of the progressing channel, the nature of which is explained in section 7.6.2. Courtesy of T A Warner.

Chapter 9



Figure A.10. A high-speed video recording of an upward branching positively-charged lightning flash triggered by a tall tower. Courtesy of T A Warner.



Figure A.11. The same record as A.10, but with accumulated images showing the branching structure of the flash, with recoil leaders traveling towards the branching points. Courtesy of T A Warner.

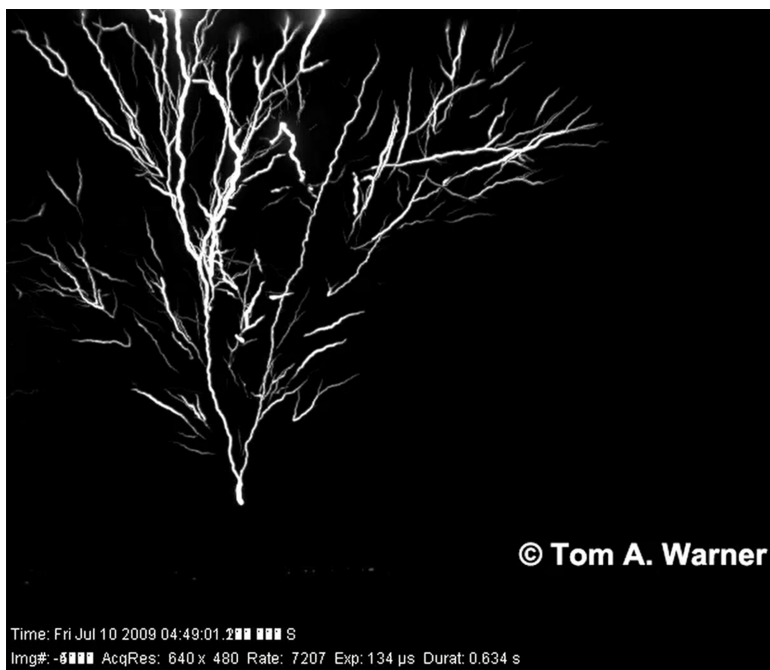


Figure A.12. Similar to figure A.10, showing the dynamics of the occurrence of recoil leaders. Courtesy of T A Warner.